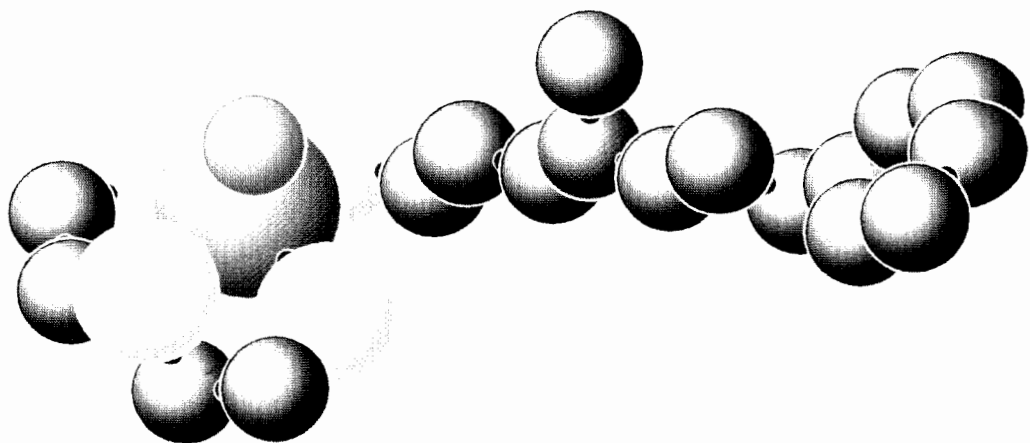


FZR-165

Archiv-Ex.:

**INSTITUTE OF BIOINORGANIC AND
RADIOPHARMACEUTICAL CHEMISTRY**



Annual Report 1996

Cover picture:

Space-filling model of a first serotonin receptor-binding technetium-99m molecule.

Forschungszentrum Rossendorf e. V.
Postfach 51 01 19; D-01314 Dresden
Bundesrepublik Deutschland
Telefon (03 51) 260 31 70
Telefax (03 51) 260 32 32
E-Mail johannsen@fz-rossendorf.de

FZR - 165
February 1997

Annual Report 1996

**Institute of Bioinorganic and
Radiopharmaceutical Chemistry**

Editor: B. Johannsen

Editorial staff: S. Seifert

FOREWORD

Research at the Institute of Bioinorganic and Radiopharmaceutical Chemistry of the Research Center Rossendorf Inc. is focused on radiotracers as molecular probes for diagnosis of disease. Derived from an awareness of the very important role modern nuclear medicine is playing, as expressed explicitly in the synonym *in vivo* biochemistry, this research effort has two main components:

- positron emission tomography (PET)
- technetium chemistry and radiopharmacology.

To make positron emission tomography available also in the eastern part of Germany, a PET center was established at Rossendorf. As envisaged in a contract signed in February 1995 between the Research Center Rossendorf and the Dresden University of Technology, the Institute is closely linked to the University Hospital in this PET center. A joint team of staff members from both the Institute and the Department of Nuclear Medicine with the University Hospital has been working at the Rossendorf PET Center.

To contribute to further exploitation of technetium-99m with its ideal nuclear properties for single photon emission tomography (SPECT), great commitment to interdisciplinary research into technetium tracers is required. The Institute's projects therefore address new approaches to tracer design.

The research activities of our Institute have been performed in three administratively classified groups. A PET tracer group is engaged in the chemistry and radiopharmacy of ^{11}C and ^{18}F compounds and in the setup of the PET center, which is jointly run by the Institute and the Clinic and Polyclinic of Nuclear Medicine at the University Hospital. A SPECT tracer group deals with the design, synthesis and chemical characterization of metal coordination compounds, primarily rhenium and technetium complexes. A biochemical group is working on SPECT and PET-relevant biochemical and biological projects. This includes the characterization and assessment of new compounds developed in the two synthetically oriented groups.

The annual report presented here covers the research activities of the Institute of Bioinorganic and Radiopharmaceutical Chemistry in 1996.

The achievements attained so far have only been possible because of the dedication and commitment of the permanent and temporary staff, the Ph.D. students and collaborators inside and outside the Rossendorf Research Center Inc. I would like to extend my thanks to all of them.

Bernd Johannsen

CONTENTS

I. RESEARCH REPORTS

1. Serotonin Receptor-Binding Technetium and Rhenium Complexes 1
 9. Synthesis and Characterization of Ligands Derived from Partial Structures of Ketanserin, Cisapride and MDL 72832
M. Scheunemann, H.-J. Pietzsch, H. Spies, P. Brust, B. Johannsen
2. Serotonin Receptor-Binding Technetium and Rhenium Complexes 5
 10. Synthesis and Characterization of Rhenium and Technetium Complexes Derived from Partial Structures of Ketanserin, Cisapride and MDL 72832
M. Scheunemann, H.-J. Pietzsch, H. Spies, P. Brust, B. Johannsen
3. Serotonin Receptor-Binding Technetium and Rhenium Complexes 9
 11. Affinity and Selectivity of Oxorhenium(V) Complexes Derived from Ketanserin, Cisapride and MDL 72832
H.-J. Pietzsch, M. Scheunemann, P. Brust, J. Wober, H. Spies, B. Johannsen
4. Serotonin Receptor-Binding Technetium and Rhenium Complexes 13
 12. Structural Modification of Receptor-Binding Technetium-99m Complexes in order to Improve Brain Uptake
B. Johannsen, R. Berger, P. Brust, H.-J. Pietzsch, M. Scheunemann, S. Seifert, H. Spies, R. Syhre
5. Serotonin Receptor-Binding Technetium and Rhenium Complexes 16
 13. No Carrier Added Preparations of "3+1" ^{99m}Tc Complexes
S. Seifert, H.-J. Pietzsch, M. Scheunemann, H. Spies, R. Syhre, B. Johannsen
6. Serotonin Receptor-Binding Technetium and Rhenium Complexes 23
 14. Distribution and Brain Uptake in Rats of Serotonin Receptor-Binding Oxotechnetium(V) Complexes at the c.a. (^{99m/99}Tc) and the n.c.a. (^{99m}Tc) Level
R. Syhre, H.-J. Pietzsch, M. Scheunemann, S. Seifert, H. Spies, B. Johannsen
7. Serotonin Receptor-Binding Technetium and Rhenium Complexes 32
 15. Synthesis and Characterization of Oxorhenium(V) Complexes with N-Functionalized Tridentate SNS Ligands
H.-J. Pietzsch, M. Scheunemann, R. Berger, H. Spies, B. Johannsen
8. Synthesis of Neutral Amine Group Bearing "3+1" Mixed-Ligand Complexes of Oxorhenium(V) 35

M. Friebe, M. Papadopoulos, S. Chiotellis, H. Spies, R. Berger, B. Johannsen
9. Preparation of Amine Group Bearing "3+1" Mixed-Ligand Oxotechnetium(V) complexes at the carrier added level 40

M. Friebe, M. Papadopoulos, E. Chiotellis, H. Spies, R. Berger, B. Johannsen
10. Lipophilicity and Ionization Properties of Some Amine-Bearing Technetium and Rhenium "3+1" Mixed-Ligand Chelates with Same Ligand Structure 43

R. Berger, M. Friebe, H.-J. Pietzsch, M. Scheunemann, B. Noll, T. Fietz, H. Spies, B. Johannsen
11. Retropare - a New Rhenium Complex as a Potential Ligand of the Dopamine Transporter 47

A. Hoepfing, H. Spies, B. Johannsen

12. Preparation and Structure of Neutral Oxo-Re(V)-Complexes with L-Cysteine Methyl Ester and D-Penicillamine Methyl Ester S. Kirsch, B. Noll, H. Spies, B. Johannsen, P. Leibnitz, D. Scheller	50
13. Formation of Mixed-Ligand Ester Complexes of Rhenium and Technetium with S/S/S-N or S-S/S-N Coordination S. Seifert, H. Spies	56
14. A Novel Amide Thioether Dithiolate Ligand Derived from Cysteine B. Noll, S. C. Hilger, P. Leibnitz, H. Spies, L. Dinkelborg, B. Johannsen	59
15. Novel Oxorhenium(V) Complexes with Cysteinylglycine and Glycylglycylcysteine: Preparation and Characterization in Solution S. Kirsch, R. Jankowsky, B. Noll, H. Spies, B. Johannsen, D. Scheller	62
16. Synthesis and Characterization of Technetium and Rhenium Oligoglycine Complexes and Technetium Tartrate R. Jankowsky, B. Noll, H. Spies, B. Johannsen	67
17. XAS Investigations on Tc and Re Complexes of Oligoglycine Ligands and Tc Tartrate R. Jankowsky, B. Noll, H. Spies, B. Johannsen	72
18. X-Ray Absorption Spectroscopy: A Valuable Tool for Structural Analysis of Tc and Re Complexes R. Jankowsky, B. Noll, H. Spies, T. Reich, H. Nitsche	76
19. Technetium and Rhenium Complexes with Thioether Ligands. 8. X-Ray Structures of Mononuclear Oxorhenium(V) Complexes with Bidentate Thioether and Dithiaalcohol Ligands M. Reisgys, H.-J. Pietzsch, H. Spies, P. Leibnitz	79
20. Rhenium and Technetium Carbonyl Complexes for the Labelling of Bioactive Molecules. 2. Tricarbonylrhenium(I) Complexes with Mono-, Bi- and Tridentate Thioether Ligands H.-J. Pietzsch, M. Reisgys, H. Spies, R. Alberto, U. Abram	82
21. Technetium and Rhenium Labelled Steroids. 1. First Synthesis of "3+1" Mixed-Ligand Oxorhenium(V) Complexes Bearing a Pendent Estradiol Moiety F. Wüst, H. Spies, D. Scheller, S. Machill	86
22. Technetium and Rhenium Labelled Steroids. 2. Oxorhenium(V) Complexes of 1-Mercapto-4-Methylestra-1,3,5(10)-trien-17-one F. Wüst, H. Spies, R. Beckert, S. Möller	91
23. Structure and Reactivity of a "3+1" Mixed-Ligand Rhenium Complex Containing Thiobenzoate as a Monodentate Ligand [ReO(SSS)(SC(O)Ph)] B. Noll, P. Leibnitz, St. Noll, R. M. Mahfouz, H. Spies	93
24. Nicotinamide Substituted Rhenium(V) Mixed-Ligand Complexes T. Kniess, H. Spies	96
25. Dihydropyridine Substituted Technetium(V) Mixed-Ligand Complexes T. Kniess, H. Spies	100
26. Note to Fast Hydrolysis of the Methyl Ester of MAG ₂ during Complexation with Tc/Re(V) Gluconate St. Noll, B. Noll, H. Spies	105

27. Synthesis of ^{186}Re Gluconate by Stannous Chloride Reduction of $^{186}\text{ReO}_4^-$ B. Noll, T. Kniess, H. Spies	106
28. Determination of Partition Coefficients for Coordination Compounds by Using the HPLC Column Nucleogel RP C_{18} 80-10 R. Berger, T. Fietz, M. Glaser, H. Spies	107
29. Investigations of Serotonin Receptor Subtypes on the Blood-Brain Barrier J. Wober, S. Matys, P. Brust	112
30. Comparison of a Microplate Assay with Conventional Binding Assay for the Screening of Potential Receptor Ligands J. Wober, P. Brust	120
31. Functional Expression of P-Glycoprotein in an Immortalized Rat Brain Endothelial Cell Line (RBE4) <i>in vitro</i> R. Bergmann, S. Matys, P. Brust	123
32. Different Response of Cerebral and Non Cerebral Endothelial Cells to Cytotoxic Hypoxia. B. Ahlemeyer, P. Brust, B. Johannsen	134
33. Studies on an HPLC Method to Assay the Concentrations of Amines in Brain Micro- dialysis Perfusates Based on Naphthalene-2,3-Dicarbaldehyde Derivatization and Fluorescence Detection G. Vorwieger, R. Bergmann, P. Brust, B. Johannsen	139
34. High-Affinity Binding of [^3H]Paroxetine to Caudate Nucleus and Microvessels from Porcine Brain P. Brust, R. Bergmann, B. Johannsen	143
35. Measurement of the Cerebral Uptake and Metabolism of L-6-[^{18}F] Fluoro-3,4-Dihydroxy-Phenylalanine in Newborn Piglets P. Brust, R. Bauer, R. Bergmann, B. Walter, J. Steinbach, F. Füchtner, E. Will, H. Linemann, M. Obert, U. Zwiener, B. Johannsen	148
36. High Yield Preparation of 6-[^{18}F]Fluoro-DOPA F. Füchtner, K. Günther, J. Steinbach, R. Lücke, R. Scholz, R. Hüller	153
37. Modified Access to the Thioester Precursor of [^{11}C](+)-McN-5652-Z J. Zessin, P. Brust, J. Steinbach	157
38. Substances Labelled in Metabolically Stable Positions: The Conversion of Pyrylium Salts with Nitro-[^{11}C]methane - a New Method for the Synthesis of n.c.a. ^{11}C -Ring-Labelled Nitroaromatics P. Mäding, J. Steinbach, H. Kasper	162
39. Substances Labelled in Metabolically Stable Positions: The Synthesis of Pyrylium salts as Precursors for ^{11}C -Ring Labelling of Nitrobenzenes P. Mäding, J. Steinbach, H. Kasper	166
40. Substances Labelled in Metabolically Stable Positions: The Synthesis of [$2\text{-}^{11}\text{C}$]1-Hydroxy-2-nitro-1-(2-nitrophenyl)ethane and [^{11}C]2-Dinitrostyrene J. Zessin, J. Steinbach	169
41. Substances Labelled in Metabolically Stable Positions: Synthesis of [$2\text{-}^{11}\text{C}$]Indole Starting with [^{11}C]2, -Dinitrostyrene J. Zessin, J. Steinbach	172

42. Electrophilic Fluorination: The Synthesis of [¹⁸ F]Caesium Fluoroxysulfate - A New Reagent for Electrophilic Labelling Chr. Fischer, K. Neubert, J. Steinbach	176
43. Electrophilic Fluorination: A New Access to ¹⁸ F-Labelled Compounds by [¹⁸ F]Caesium Fluoroxysulfate: 6-[¹⁸ F]Fluoro-DOPA as an Example Chr. Fischer, K. Neubert, J. Steinbach	177
44. Electrophilic Fluorination: A New Access to the Barnette-Reagents - N-Fluorination with Perchloryl Fluoride Chr. Fischer, J. Steinbach	179
45. Sulfamates of 3-Hydroxy-estra-1-3-5(10)-triene Derivatives J. Römer, J. Steinbach, H. Kasch	182
46. ¹³ C NMR Spectroscopic Characterization of Some Sulfamates of 3-Hydroxy-estra-1,3,5(10)-triene Derivatives J. Römer, J. Steinbach, D. Scheller	188
47. Synthesis of 16β-Bromo-3-methoxy-estra-1,3,5(10)-trien-17β-ol by a Novel One-Pot Reaction H. Kasch, U. Dintner, J. Römer, J. Steinbach	190
48. Further ¹³ C NMR Spectroscopic Proof of 16-F-Configuration in 16-Fluoro-estradiol Derivatives J. Römer, J. Steinbach, D. Scheller, H. Kasch	192
49. Improvements of the Rossendorf Radionuclide Transport System St. Preusche, F. Füchtner, H. Krug, J. Steinbach	193
50. Cerebral MRGluc and Perfusion Pattern of Patients with Myotonic Dystrophy B. Beuthien-Baumann, B. Kunath, J. Pinkert, U. Reuner, H. Linemann, M. Obert, E. Will, F. Füchtner, J. Steinbach, B. Johannsen, W.-G. Franke	195
51. Three-Compartment Model Software Tools to Analyze and Synthesize PET Data M. Obert, H. Linemann, E. Will	199
52. Application of the Fractal Concept of the Analysis of Positron Emission Tomography Investigations of Patients Suffering from Dystrophia Myotonia M. Obert, B. Beuthien-Baumann, E. Will, H. Linemann, B. Kunath	204
II. PUBLICATIONS, LECTURES AND TEACHING ACTIVITIES	207
III. SCIENTIFIC COOPERATION	213
IV. SEMINARS	216
V. ACKNOWLEDGEMENTS	217

I. RESEARCH REPORTS

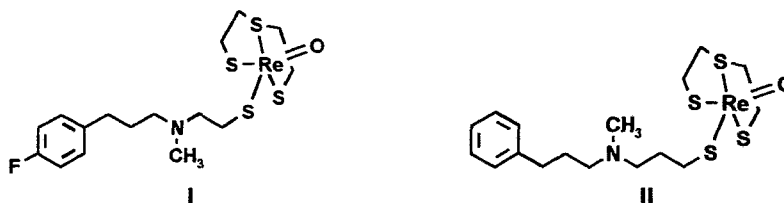
1. Serotonin Receptor-Binding Technetium and Rhenium Complexes

9. Synthesis and Characterization of Ligands Derived from Partial Structures of Ketanserin, Cisapride and MDL 72832

M. Scheunemann, H.-J. Pietzsch, H. Spies, P. Brust, B. Johannsen

Introduction

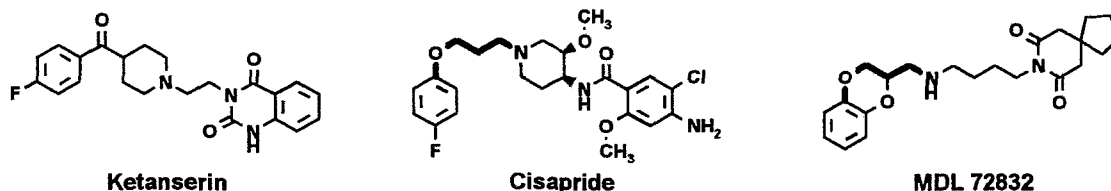
The design of both potent and selective receptor-binding technetium tracers has been a subject of intense efforts during the last eight years, especially in the field of brain receptor research [1]. As part of our ongoing programme of developing technetium and rhenium coordination compounds capable of binding to the 5-HT₂ receptor, we found that compounds I and II are potent ligands to the ketanserin binding sites with IC₅₀ values of 19 nM and 14 nM.



Thus, starting from these previously described compounds which contain single structural elements of the antagonist ketanserin [2] a novel series of structurally modified oxorhenium complexes as well as oxotechnetium complexes was constructed in order to expand our knowledge of the electronic and spatial factors necessary for affinity and selectivity at 5-HT_{2A} receptors.

In vitro, the usability of ^{99m}Tc complexes as brain imaging agents has been limited not only by their lack of selectivity, but also because of inadequate lipophilicity and molecule size leading to an unsatisfactory blood-brain transfer. It was hoped in particular that synthetic modifications originally intended to improve the HT_{2A} receptor selectivity would also allow access to new complex structures with increased blood-brain transfer.

We therefore extended this work by exploring other structures such as cisapride [3] and MDL 72832 [4]. Both compounds possess a 3-phenoxypropyl amine unit as an obvious structural similarity.



Among the variations made on these structures was replacement of the ring system bearing the amide structure by a small spacer, in most cases a propylene chain with a terminal thiol function.

Here we describe the synthesis and characterization of a novel series of monodentate thiol ligands derived from these three representative serotonin antagonists.

Experimental (Selected examples)

Method A:

1-(3-mercaptopropyl)-4-benzylpiperidine 11

A mixture of 1 (17.5 g, 0.1 mol), triethylamine (15.2 g, 0.15 mol), 1-bromo-3-chloro propane and toluene (75 ml) was heated to 60 - 65 °C for 8 h.

The cooled suspension was treated with an aqueous solution of NaHCO₃ (10 %, 50 ml) and the resulting two-phase mixture was stirred for 10 min. The organic layer was separated, dried (MgSO₄), filtered and evaporated. The crude product was purified by bulb to bulb distillation to give 20.1 g (80 %) of 1-(3-chloropropyl)-4-benzylpiperidine as an oil: $n_{D}^{22.6} = 1.5304$; ¹H NMR (300.13 MHz, CDCl₃; standard SiMe₄): δ_H 7.3 - 7.0 [m, 5H, Ar-H], 3.51 [t-like, J = 6.6 Hz, 2H, -CH₂Cl], 2.80 [m, 2H, piperidine: C2-H_{eq}, C6-H_{eq}], 2.47 [2H, piperidine: C2-H_{ax}, C6-H_{ax}], 2.37 [m, 2H, -CH₂-CH₂-CH₂Cl], 1.92 - 1.77 [m, 4H, PhCH₂CH, CH₂-CH₂-CH₂Cl], 1.59 - 1.54 [m, 2H, piperidine: C3-H_{eq}, C5-H_{eq}], 1.5 - 1.39 [m, 1H, piperidine: C4-H], 1.22 [m, 2H, piperidine: C3-H_{ax}, C5-H_{ax}].

A mixture of the intermediate chloride (5.04 g, 20 mmol), thiourea (1.85 g, 24.3 mmol), hydrogen chloride as a solution in ethanol (18 %, 4 g, 20 mmol) and 2-ethoxy ethanol (25 ml) was heated to 115 - 125 °C for 5 h. The resulting mixture was evaporated to an oily residue which was dissolved in water (40 ml). The aqueous solution was treated with NaOH (3.2 g, 80 mmol) and heated at 120 °C for 2 h. After cooling the pH was adjusted to ca. 8 with H₃PO₄ (6 N, 3.4 ml), and the resulting oil was extracted with methyl *tert*-butyl ether (3 × 15 ml). After evaporation the crude product was distilled to give 3.0 g (60 %) **11** as a colourless oil; b.p. 126 - 128 °C/6 Pa; $n_{D}^{26.0} = 1.5456$;

¹H NMR (300.13 MHz, CDCl₃; standard SiMe₄): δ_H 7.25 - 7.05 [m, 5H, Ar-H], 2.81 [m, 2H, piperidine: C2-H_{eq}, C6-H_{eq}], 2.47 [4H, CH₂SH, piperidine: C2-H_{ax}, C6-H_{ax}], 2.32 [m, 2H, -CH₂-CH₂-CH₂SH], 1.9 - 1.7 [m, 4H, PhCH₂CH, CH₂-CH₂-CH₂SH], 1.59 - 1.54 [m, 2H, piperidine: C3-H_{eq}, C5-H_{eq}], 1.5 - 1.39 [m, 2H, CH₂SH, pip.: C4-H], 1.22 [m, 2H, pip.: C3-H_{ax}, C5-H_{ax}].

¹³C NMR (75.475 MHz, CDCl₃; standard SiMe₄): δ_C 22.87, 31.20, 32.22, 37.95, 43.21, 54.00, 57.36, 125.73, 128.11, 129.09, 140.70.

0.265 g **11** free base (1.06 mmol) was transformed into the oxalate salt by treating a solution in 2-PROH with oxalic acid. It was recrystallized from MeOH/2-PROH mixtures: 0.302 g (84 %) **11**•oxalate; m.p. 139 °C.

Elemental analysis: (Found C, 60.18; H, 7.40; N, 4.09; S, 9.45, C₁₅H₂₃NS•C₂H₂O₄ requires C, 60.15; H, 7.42; N, 4.13; S, 9.44 %).

Method B:

(2RS)1-(3-phenoxypropyl)-2-(2-mercaptoethyl)piperidine **19**

An ethereal solution of hydrogen chloride (22 %, 3.1 g, 18.6 mmol) was added to a solution of **9** (4.9 g, 18.6 mmol) in chloroform (50 ml) was. The resultant homogeneous mixture was cooled to -30 °C and thionyl chloride (3.1 g, 26.1 mmol) was added in one portion. The mixture was allowed to warm to room temperature and then refluxed for 3 - 5 h. The solvent was removed *in vacuo* to give a viscous oil which was used without further purification.

The conversion of the chloride into the isothiuronium salt and its subsequent saponification to the desired thiol was carried out in the same manner as described for the preparation of **11**.

This procedure gives an oily residue which was finally purified by short-path distillation at 10 Pa to yield 3.5 g (68 %) **9** as a colourless oil; $n_{D}^{23.7} = 1.5473$.

¹H NMR (500.13 MHz, CDCl₃; standard SiMe₄): δ_H 1.26, 1.42, 1.48, 1.57 (4m, 7H, SH, piperidine: CH₂-3, CH₂-4, CH₂-5); 1.68 (dddd, J = 17.2, 9.7, 7.6, 5.45 Hz, 1H, -CH-HCH-CH₂-SH); 1.79 (dddd, J = 17.8, 10.1, 6.4, 4.0 Hz, 1H, -CH-HCH-CH₂-SH); 1.85 (m, 2H, -OCH₂-CH₂-CH₂-N); 2.19 (ddd, J = 11.8, 9.6, 3.3 Hz, 1H, PhO-CH₂-CH₂-HCH-N); 2.34 (m, 1H, piperidine: CH-2); 2.41 (ddd, J = 12.7, 9.8, 6.5 Hz, 1H, -CH₂-HCH-SH); 2.45 (m, 1H, PhO-CH₂-CH₂-HCH-N); 2.53 (ddd, J = 13.1, 10.0, 5.45 Hz, 1H, -CH₂-HCH-SH); 2.76 (m, 2H, piperidine: CH₂-6); 3.93 (t-like, J = 6.2 Hz, 2H, PhO-CH₂-6.85, 7.20 (2m, 5H, ArH).

¹³C NMR (75.475 MHz, CDCl₃; standard SiMe₄): δ_C 21.13; 23.20; 24.96; 26.10; 29.62; 35.71; 49.63, 51.24; 58.93; 65.94; 114.45; 120.50; 129.37; 158.91.

LRMS (Cl, *iso*-butane): m/z 280 (MH⁺, 100 %).

(E): m/z 218 (100 %), 98 (38 %), 279 (M⁺, 3 %).

HRMS 279.1693 (requires 279.1657).

Method C:

(2RS)2-mercaptomethyl-4-(3-phenylpropyl)morpholine **20**

Methansulphonyl chloride (2.2 g, 19.2 mmol) dissolved in methylenchloride (10 ml) at -5 °C was added drop by drop to a stirred mixture of **10** (2.82 g, 12 mmol) and triethylamine (2.43 g, 24 mmol) in methylene chloride (50 ml). The mixture was allowed to warm to room temperature and washed with H₂O (20 ml), 5 % aqueous NaHCO₃ solution (20 ml) and brine (20 ml). The organic layer was dried over MgSO₄, filtered and concentrated to give a yellowish viscous oil (4.7 g).

The crude material was dissolved in DMF (10 ml) and added to a solution of potassium thioacetate in DMF (15 ml) at 5 °C. The mixture was stirred and allowed to warm to room temperature and finally at 45 - 50 °C for 1 h. The mixture was partitioned between CH₂Cl₂ (60 ml) and 5 % aqueous NaHCO₃ solution (80 ml). The layers were separated, and the aqueous layer was extracted with CH₂Cl₂ (30 ml). The organic layers were combined, washed with 5 % aqueous NaHCO₃ solution (20 ml), 15 % aqueous NaCl solution (20 ml) and concentrated to a red oil (4.8 g).

A solution of this crude material in MeOH (12 ml) was cooled to 5 °C and saponified by dropwise addition of an aqueous NaOH solution (4N, 9 ml, 36 mmol). After 30 min the solvent was evaporated. The residue was dissolved in H₂O (20 ml), extracted with MTBE (8 ml), and the pH was adjusted to ca. 8 with H₃PO₄ (0.3N). The resulting oil was extracted with MTBE (3 × 10 ml) and dried over

MgSO₄. After filtration and evaporation the crude product was finally purified by short-path distillation at 10 Pa to yield 1.46 g (48 %) **20** as a slightly coloured oil; $n_{D}^{25.6} = 1.5454$.

¹H NMR (500.13 MHz, CDCl₃; standard SiMe₄): δ_H 7.29 - 7.17 [m, 5H, Ar-H], 3.88 [ddd, J = 11.4, 3.2, 1.7, 1H, morpholine: C6-H_{eq}], 3.67 [dt, J = 11.3, 2.5, 1H, morpholine: C6-H_{ax}], 3.56 [m, 1H, morpholine: C2-H], 2.87 [m, 1H, morpholine: C3-H_{eq}], 2.7 - 2.6, 2.5 [2m, 5H, morpholine: C3-H_{ax}, CH₂-5, PhCH₂-CH₂-CH₂-N], 2.36 [m, 2H, PhCH₂-], 2.1 [m, 1H, -CHHSH], 1.88 - 1.78 [m, 3H, -CHHSH, PhCH₂-CH₂-], 2.35 [1H, SH].

¹³C NMR (125.77 MHz, CDCl₃; standard SiMe₄): δ_C 27.41, 28.19, 33.46, 52.90, 57.24, 57.99, 66.78, 76.59, 125.72, 128.24, 128.31, 141.93.

LRMS (CI, iso-butane): m/z 252 (MH⁺, 100 %).

(EI): m/z 91 (100 %), 218 (28 %), 251 (M⁺, 8 %).

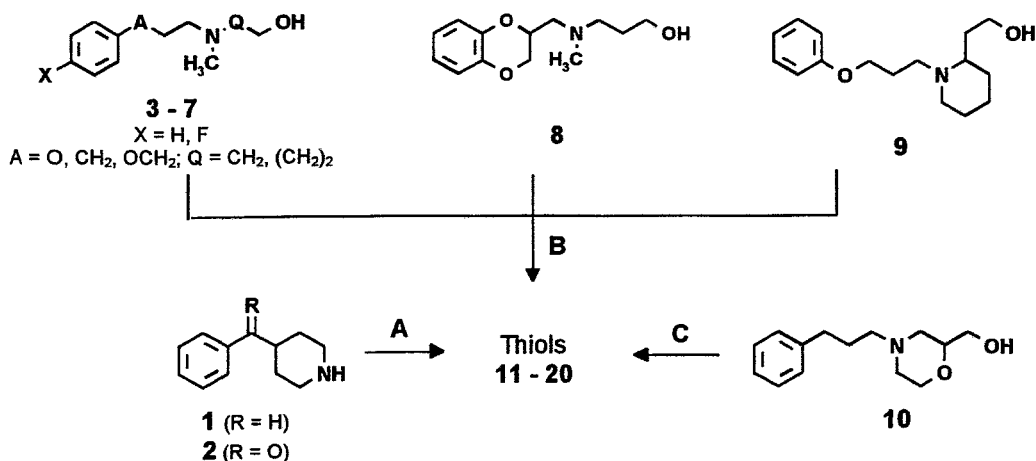
HRMS 251.1350 (requires 251.1344).

Results and Discussion

The target thiols were prepared by three different routes starting from commercially available amines **1** and **2** or aminoalcohols **3** - **10** (Scheme 1 and Table I).

The preparation of the aminoalcohols **3** - **9** is based on standard procedures similar to those described in our previous report [2]. In these are included the alkylation of the corresponding phenol: i.e. *p*-fluoro phenol, phenol and catechol with the appropriate halogenide or epichlorohydrine to give the aryloxy alkylhalide [5] or after chlorination (SOCl₂-pyridine), 2-chloromethyl-1,4-benzodioxane [6] as an intermediate.

Scheme 1: Synthesis of target thiols **11** - **20**



Method A: 1. Br(CH₂)₃Cl, base; 2. thiourea; 3. NaOH

Method B: 1. SOCl₂; 2. thiourea; 3. NaOH

Method C: 1. CH₃SO₂Cl, triethylamine, CH₂Cl₂; 2. CH₃COSK, DMF; 3. NaOH

Afterwards the halide intermediate was reacted either with 2-methylamino ethanol or with racemic 2-(2-hydroxyethyl) piperidine to give the aminoalcohols **3** and **9**. All other *N*-methyl derivatives were synthesized in a two-step procedure. First the starting halides were reacted with 3-aminopropanol to afford the secondary amines in good yield, then the secondary amines were converted to the tertiary amines **4** - **8** following the *Eschweiler-Clark Procedure*. The morpholine derivative **10** was synthesized from 3-phenylpropyl aminoethanol and *tert*-butyl glycidyl ether [7].

Thiols **11** and **12** were prepared in three steps from 4-benzyl piperidine (**1**) or 4-benzoyl piperidine (**2**) representing method A as depicted in scheme 1. Alkylation of **1** and **2** with 1-bromo-3-chloro propane at 60 - 80 °C in toluene in the presence of triethylamine (for the preparation of **11**) or K₂CO₃ (for the preparation of **12**) afforded the corresponding 3-chloropropyl amine. These compounds were converted to their isothiuronium salts by reaction with thiourea at elevated temperatures in ethanol or 2-ethoxy ethanol as a solvent. Finally, saponification of these isothiuronium salts with aqueous NaOH at 120 °C gave the desired thiols **11** and **12**.

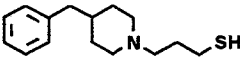
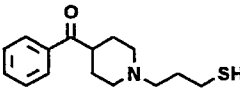
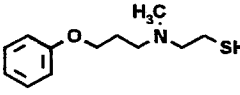
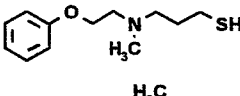
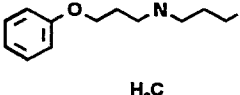
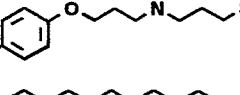
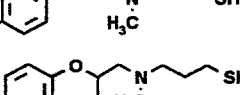
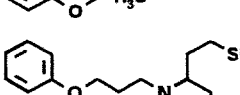
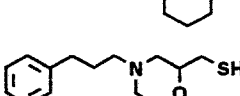
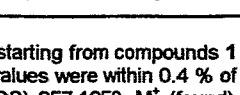
The ω -chloro alkylamine intermediates for the synthesis of **13** - **19** were obtained from the corresponding substituted aminoalcohols **3** - **9** by chlorination with thionyl chloride in chloroform

(Scheme 1: method B). The conversion of the chloride into the isothiuronium salt and its subsequent saponification to the desired thiol was carried out in the same manner as described for the preparation of **11** and **12**.

Method C (Scheme 1) was used for the preparation of the racemic morpholine derivative **20**. It consists of activation of the hydroxy group with methansulphonyl chloride and triethylamine at 0 °C in methylene chloride. Its nucleophilic substitution by means of potassium thioacetate in dimethyl formamide gave the *S*-acetyl-protected derivative of **20**. Finally the acetyl group was removed by treatment with diluted aqueous NaOH solution at 5 °C.

The thiols were purified by distillation (*Kugelrohr* or *Vigreux column*). In part they were converted to their crystalline oxalate salts. To our knowledge all target thiols were prepared for the first time. They are homogeneous on TLC and show satisfying high resolution mass spectra and correct elemental analyses (oxalate salts).

Table 1: Physicochemical properties of target thiols **11** - **20**

No.	Structure	Method	Yield [%] ^a	M.p.[°C] ^b	Analysis
11		A	48	139	C ₁₅ H ₂₃ NS • C ₂ H ₂ O ₄ ^d
12		A	36	140	C ₁₅ H ₂₁ NOS • C ₂ H ₂ O ₄ • ¼ H ₂ O ^d
13		B	74	oil ^c	C ₁₂ H ₁₉ NOS ^e
14		B	80	dec.	C ₁₂ H ₁₉ NOS • C ₂ H ₂ O ₄ ^d
15		B	66	dec.	C ₁₃ H ₂₁ NOS • C ₂ H ₂ O ₄ ^d
16		B	63	oil ^c	C ₁₃ H ₂₀ FNOS ^f
17		B	71	oil ^c	C ₁₃ H ₂₀ FNS ^g
18		B	74	103-104	C ₁₃ H ₁₉ NO ₂ S • C ₂ H ₂ O ₄ ^d
19		B	68	oil ^c	C ₁₆ H ₂₅ NOS ^h
20		C	48	oil ^c	C ₁₄ H ₂₁ NOS ⁱ

^a overall yield starting from compounds **1** - **10**, refers to isolated free base; ^b oxalate salt; ^c free base; ^d elemental analysis (C,H,N,S); experimental values were within 0.4 % of theoretical values; ^e M⁺ (calc. for C₁₂H₁₉NOS) 225.1187, M⁺ (found) 225.1200; ^f M⁺ (calc. for C₁₃H₂₀FNOS) 257.1250, M⁺ (found) 257.1245; ^g M⁺ (calc. for C₁₃H₂₂FNS) 241.1301, M⁺ (found) 241.1286; ^h M⁺ (calc. for C₁₆H₂₅NOS) 279.1657, M⁺ (found) 279.1693; ⁱ M⁺ (calc. for C₁₄H₂₁NOS) 251.1344, M⁺ (found) 251.1350.

References

- [1] a) Lever S. Z. and Wagner Jr. H. N. (1989) The status and future of technetium-99m radio-pharmaceuticals In *Technetium and Rhenium in Chemistry and Nuclear Medicine* (Ed. by Nicolini M. Bandoli G. and Mazzi U.) Cortina Intern., Verona, Vol. 3, pp. 649 - 660.

- b) Eisenhut M., Brandau W. and Mißfeld M. (1989) Synthesis and *in vivo* testing of a brombutyl substituted 1,2-dithia-5,9-diazacycloundecane: a versatile precursor for new ^{99m}Tc -bis(amino-ethanethiol) complexes *Nucl. Med. Biol.* **16**, 805-811.
- [2] Johannsen B., Scheunemann M., Spies H., Brust P., Wober J., Syhre R. and Pietzsch H.J. (1996) Technetium(V) and rhenium(V) complexes for 5-HT_{2A} serotonin receptor binding: structure-affinity considerations. *Nucl. Med. Biol.* **23**, 429-438.
- [3] Van Daele G. H. P., de Bruyn M. F. L., Sommen F. M., Janssen M., Van Nueten J. M., Schuurkes J. A. J., Niemegeers C. J. E. and Leysen J. E. (1996) Synthesis of cisapride, a gastrointestinal stimulant derived from cis-4-amino-3-methoxypiperidine. *Drug Dev. Res.* **8**, 225 - 232.
- [4] Hibert M. F., Gittos M. W., Middlemiss D. N., Mir A. K. and Fozard, J. R. (1988) Graphics computer-aided receptor mapping as a predictive tool for drug design: development of potent, selective and stereospecific ligands for the HT_{1A} receptor *J. Med. Chem.* **31**, 1087-1093.
- [5] a) Janssen Pharmaceutica N. V. Eur. Pat. Appl. 76530 (1983) [*Chem. Abstr.* **99**, 194812d].
b) Ihara Chemical Industry Co., Ltd. Japan. Kokai Tokyo Koho 59724 (1981) *Chem. Abstr.* **95**, 132471a.
- [6] Société des Usines Chimiques Rhône-Poulenc D.R.P. 615471 (1939) *Frtd.* **22**, 713-714.
- [7] Scheunemann M. (personal communication).

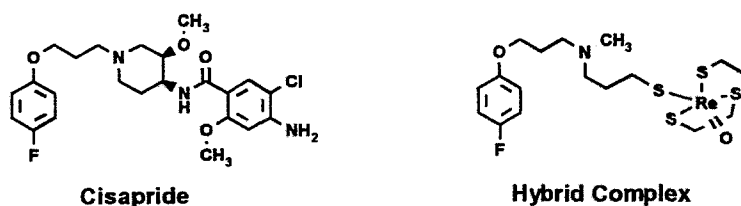
2. Serotonin Receptor-Binding Technetium and Rhenium Complexes

10. Synthesis and Characterization of Rhenium and Technetium Complexes Derived from Partial Structures of Ketanserin, Cisapride and MDL 72832

M. Scheunemann, H.-J. Pietzsch, H. Spies, P. Brust, B. Johannsen

Introduction

Previously we described the synthesis of several mixed-ligand oxorhenium(V) and oxotechnetium(V) complexes which show significant affinity to the 5-HT_{2A} receptor [1]. Based on these results, in order to improve both the affinity and selectivity to different subtypes of the 5-HT receptor, new hybrid molecules were to be developed starting from three serotonin receptor-binding substances, i.e. ketanserin and cisapride, which have affinity to the 5-HT_{2A} receptor, and MDL 72832, a highly affine and selective 5-HT_{1A} receptor antagonist [2].



After having described the synthesis of the corresponding monothiol ligands **11** - **20** [2], in this paper we are dealing with the synthesis and characterization of novel oxorhenium(V) and oxotechnetium(V) complexes obtained with these ligands according to the "3+1" concept.

Experimental (Selected examples)

(3-thiapentane-1,5-dithiolato)[3-N-(3-phenoxypropyl)-N-methylaminopropylthiolato]oxorhenium(V) **25**

A solution of **15** (45 mg, 0.188 mmol) in acetonitrile (0.5 ml) was added to a suspension of **21** [3] (58.2 mg, 0.15 mmol) in acetonitrile (6 ml). The colour of the mixture immediately turned from deep blue to red. After stirring for one hour at 22 °C the solvent was evaporated to give an oily residue. The raw material was partitioned between CHCl₃ (10 ml) and 5 % aqueous NaHCO₃ solution (8 ml). The organic layer was separated and concentrated to yield a crude product which was finally purified by passing it through a silica gel column with chloroform/MeOH (19:1) as eluent.

The eluate was evaporated to give 97 mg **25** (free base: 95 %) which was transformed into the oxalate salt by treating a solution in MeOH with oxalic acid. Crystallization was induced by cautious addition of MTBE to give 87 mg (85 %) **25**•oxalate as brown crystals; m.p. 147 - 150 °C.

IR absorption: ν/cm^{-1} (KBr) 960 s (Re=O).

¹H NMR (200.13 MHz, D₆-DMSO; standard SiMe₄): δ_{H} 9.75 [br, 1H, HOOC-COO], 7.4 - 7.2, 7.0 - 6.88 [2m, 5H, Ar-H], 4.32 [dd, J = 13.0, 4.3, S(C₂H₄)₂: 2H], 4.13 - 4.01 [m, 4H, PhOCH₂-CH₂-, S(C₂H₄)₂: 2H], 3.70 [m, 2H, -CH₂-CH₂-S], 3.21 - 2.98 [m, 6H, -CH₂-CH₂NH(CH₃)CH₂-].

The complexes are soluble in chloroform and acetonitrile, less soluble in MTBE and alcohols but insoluble in water and various alkanes.

All rhenium complexes were characterized by elemental analysis, infrared, proton and carbon NMR spectroscopy (Table 1). The IR spectra of all rhenium complexes show a strong and characteristic stretching vibration band in the 900 - 1000 cm^{-1} region indicating the $\text{Re}=\text{O}^{3+}$ core.

$^{99/99\text{m}}\text{Tc}$ complexes were also obtained by a two-step procedure starting with the reaction of the appropriate thiol as the monodentate ligand with $^{99/99\text{m}}\text{Tc}$ gluconate followed by addition of the tridentate chelator.

Table 1: Physicochemical properties of target oxorhenium(V) complexes 22 - 29

No.	Structure	Starting thiol	Yield [%] ^a	M.p. [°C] ^b	Analysis ^c
22		17	46	103 - 106	$\text{C}_{17}\text{H}_{27}\text{FReNOS}_4 \cdot \text{C}_2\text{H}_2\text{O}_4^{\text{d}}$
23		13	63		$\text{C}_{16}\text{H}_{26}\text{ReNO}_2\text{S}_4 \cdot \text{C}_2\text{H}_2\text{O}_4$
24		14	68	128 - 131	$\text{C}_{16}\text{H}_{26}\text{ReNO}_2\text{S}_4 \cdot \text{C}_2\text{H}_2\text{O}_4$
25		15	85	147 - 150	$\text{C}_{17}\text{H}_{28}\text{ReNO}_2\text{S}_4 \cdot \text{C}_2\text{H}_2\text{O}_4$
26		16	85	120 - 125	$\text{C}_{17}\text{H}_{27}\text{FReNO}_2\text{S}_4 \cdot \text{C}_2\text{H}_2\text{O}_4$
27		19	61	103 - 106	$\text{C}_{20}\text{H}_{32}\text{ReNO}_2\text{S}_4 \cdot \text{C}_2\text{H}_2\text{O}_4$
28		12	66	184 - 186	$\text{C}_{19}\text{H}_{28}\text{ReNO}_2\text{S}_4 \cdot \text{C}_2\text{H}_2\text{O}_4$
29		18	57	dec.	$\text{C}_{17}\text{H}_{26}\text{ReNO}_3\text{S}_4 \cdot \text{HCl}$

^a refers to isolated oxalate salt; ^b oxalate salt or hydrochloride; ^c elemental analysis (C,H,N,S): experimental values were within 0.4 % of theoretical values, unless stated otherwise; ^d $\text{C}_{17}\text{H}_{27}\text{FReNOS}_4 \cdot \text{C}_2\text{H}_2\text{O}_4$, calc: C, 33.32; H, 4.27; N, 2.05; S, 18.72
found: C, 33.44; H, 4.67; N, 2.14; S, 18.34 %.

An additional paper of this report describes the *in vitro* binding of some of the complexes to the serotonin 5-HT_{1A}, serotonin 5-HT_{2A} and dopamin D₂ receptor [4].

Acknowledgement

The authors thank Mrs. T. Brankoff for library research, Mrs. A. Rudolph, and Mrs. S. Machill for mass spectra and NMR support.

Financial support by Mallinckrodt Medical, Petten (The Netherlands) is gratefully acknowledged.

References

- [1] a) Johannsen B., Scheunemann M., Spies H., Brust P., Wober J., Syhre R. and Pietzsch H.-J. (1996) Technetium(V) and rhenium(V) complexes for 5-HT_{2A} serotonin receptor binding: structure-affinity considerations. *Nucl. Med. Biol.* **23**, 429-438.
b) Johannsen B., Berger R., Brust P., Pietzsch H.J., Scheunemann M., Seifert S., Spies H. and Syhre R. (1997) Structural modification of receptor-binding technetium-99m complexes in order to improve brain uptake. *Eur. J. Nucl. Med.*, in press.
- [2] Scheunemann M., Pietzsch H.-J., Spies H., Brust P. and Johannsen B. (1997) Serotonin receptor-binding technetium and rhenium complexes 9. Synthesis and characterization of ligands derived from partial structures of ketanserin, cisapride and MDL 72832. *This report*, pp. 1 - 5 and references cited therein.
- [3] Fietz T., Spies H., Pietzsch H.-J. and Leibnitz P. (1995) Synthesis and crystal structure of (3-thiapentane-1.5-dithiolato) chloro oxorhenium(V). *Inorg. Chim. Acta* **231**, 233-236.
- [4] Pietzsch H.-J., Scheunemann M., Brust P., Wober J., Spies H. and Johannsen B. (1997) Serotonin receptor-binding technetium and rhenium complexes 11. Affinity and selectivity of oxorhenium(V) complexes derived from ketanserin, cisapride and MDL 72832. *This report*, pp. 9 - 12.

3. Serotonin Receptor-Binding Technetium and Rhenium Complexes

11. Affinity and Selectivity of Oxorhenium(V) Complexes Derived from Ketanserin, Cisapride and MDL 72832

H.-J. Pietzsch, M. Scheunemann, P. Brust, J. Wober, H. Spies, B. Johannsen

Introduction

After having described the synthesis and characterization of oxorhenium(V) complexes bearing pharmacophores derived from ketanserin, cisapride and MDL 72832 [1, 2], we here summarize their affinities to the serotonin (5-HT_{1A}, 5-HT_{2A}) and dopamine (D₂) receptors, including the selectivity ratios.

Experimental

Rhenium complexes were synthesized and characterized as previously described [1 - 3].

Preparation of rat cortex and hippocampus

The rat brain cortices and hippocampi were homogenised with an Ultra-Turrax T25 in 10fold volumes of ice-cold tris/HCl buffer (50 mM, pH 7.6). The homogenate was centrifuged at 20,000 g for 10 min. The resulting pellet was resuspended and centrifuged at 20,000 for another 10 min. After repeating the same procedure the pellet was resuspended in 10 volumes of buffer and stored at -70 °C until used in the binding studies.

5-HT_{1A} and 5-HT_{2A} receptor-binding assay

To determine the IC₅₀ values for 5-HT_{2A} receptor, various concentrations of the complexes were incubated with tris/HCl buffer (50mM, pH 7.6) containing 0.12 nM [³H]ketanserin and about 20 µg/ml protein in a final volume of 5 ml.

Unspecific binding was determined by 1 µM mianserin. For determination of the IC₅₀ values for 5-HT_{1A} tris/HCl buffer (50mM, pH 7.4) was used containing 0.1 percent ascorbic acid, 2 mM CaCl₂, 0.13 nM [³H]-8-OH-DPAT, and about 20 µg/ml protein in a final volume of 5 ml. Unspecific binding was determined by 10 µM serotonin. The tests were incubated at 25 °C for 60 min (5-HT_{2A}) and for 120 min (5-HT_{1A}) [4, 5].

The binding assays were terminated by rapid filtration through GF/B glass fibre filters (Whatman). The filters were rapidly washed with four 4 ml portions of ice-cold buffer, transferred into 5 ml of scintillation fluid (Ultima-Gold, Packard) and analysed for radioactivity. The protein content of the membrane and cell suspensions was estimated according to the method of Lowry *et al.* [6].

D₂ receptor-binding assay

[³H]spiperone (684.5 GBq/mmol) was used as the radioligand. The binding assay was carried out in a final volume of 5 ml tris-HCl buffer, pH 7.4, containing 10 mM MgCl₂, 1 mM EDTA, 0.27 nM [³H]spiperone, 1 unit of cloned D₂ receptor and various concentrations of the rhenium or technetium complexes. The complexes were dissolved as described above. Nonspecific binding was defined as the amount of [³H]spiperone bound in the presence of 10 µM haloperidol and ranged from 8 percent to 12 percent of the total binding. Incubation, filtration and counting of the samples were the same as described above.

Results and Discussion

IC₅₀ data of *in vitro* binding affinity of the complexes for 5-HT_{1A}, 5-HT_{2A} and for D₂ receptors, as determined by their ability to displace [³H]-8-OH-DPAT, [³H]ketanserin and [³H]spiroperidol, are shown in Table 1.

For all complexes a moderate to high nanomolar affinity to the 5-HT_{2A} receptor is observed. Interestingly, the replacement of the standard ethylene spacer between the basic nitrogen atom and the coordinated sulphur atom in **1** by propylene units in **3**, **5** and **8 - 10** resulted in a considerable improvement in receptor binding. This effect suggests that a longer distance between the protonable nitrogen and the chelate unit allows the ligand to better conform to structural constraints imposed by the 5-HT_{2A} receptor. Fluorine substitution at the 4-position of the aromatic moiety increases the effect.

The D₂ affinity is more differentiated than the 5-HT_{2A} one. A significant loss in D₂ affinity accompanies the fluorine substitution at the 4-position of the phenyl ring, which was similiary observed for complex **4**, in which the nitrogen atom is an element of a piperidine ring system. This

result is remarkable because both compounds include structural features which are usually associated with strong 5-HT_{2A} receptor-binding agents.

Alterations in the immediate surroundings of the metal core were also sensitively recognized by different receptor types. This is shown by the exceptional binding profile of **11** and **12** within the second series of rhenium complexes. Replacing the small tridentate dithiol ligand in **1** by a more bulky Schiff base ligand to give **11** causes a complete shift in profile.

Replacement of the tridentate ligand by a tripodal one (complexes **13** and **14**) leads to a significant loss in 5-HT affinity. From these findings the Re=O core appears to be essential for serotonin receptor binding.

Table 1: Affinity to the serotonin (5-HT_{1A}/5-HT_{2A}) and dopamine (D₂) receptors and selectivity ratios of rhenium complexes (results are expressed as means ± SD). Complexes **1** - **4** and **11**, **12** were described previously [1]. For **13** and **14** see Glaser *et al.* [3]

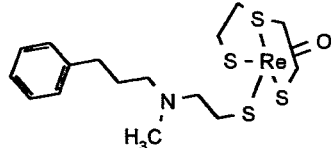
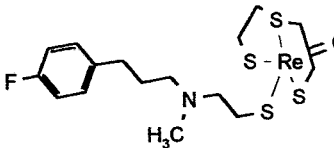
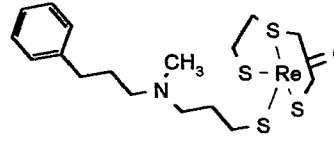
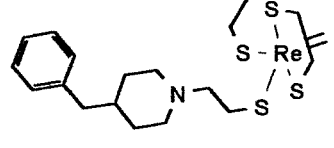
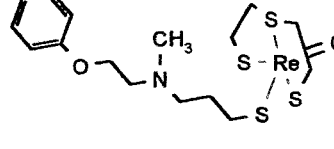
Complex	IC ₅₀ (nM)			Selectivity ratios			
	5-HT _{1A}	5-HT _{2A}	D ₂	5-HT _{1A} / 5-HT _{2A}	D ₂ / 5-HT _{2A}	D ₂ / 5-HT _{1A}	
	1	449±63	23.3±2.7	285±53	20	12	0.6
	2	665±106	20.3±1.7	903±160	33	45	1.4
	3	284±63	14.4±2.3	214±71	20	15	0.75
	4	245±38	25.3±1.9	833±49	10	33	3.4
	5	248±25	23.9±3.4	> 10 μM	10	417	40

Table 1 cont.

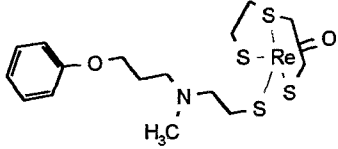
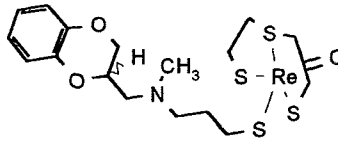
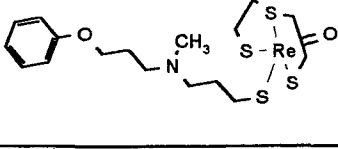
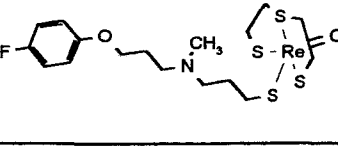
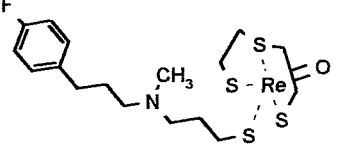
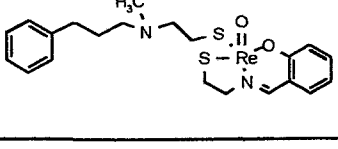
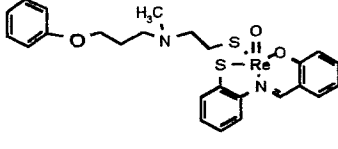
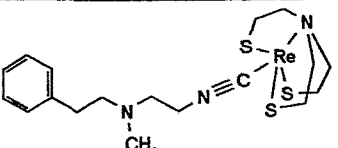
Complex	IC ₅₀ (nM)			Selectivity ratios			
	5-HT _{1A}	5-HT _{2A}	D ₂	5-HT _{1A} / 5-HT _{2A}	D ₂ / 5-HT _{2A}	D ₂ / 5-HT _{1A}	
	6	240±28	10.5±1.5	5118±949	23	512	21
	7	22.3±3.0	298±56	> 10 μM	0.07	34	454
	8	148±19	9.1±0.9	1016±82	16	112	7
	9	200±26	1.9±0.2	439±84	105	231	2
	10	326±45	2.2 ± 0.3	676±80	148	307	2
	11	780±154	1396±367	47±5	0.6	0.03	0.06
	12	481±51	60.8± 6.6	105±16	8	1.7	0.2
	13	ca. 500	352 ± 30	10000	1.4	28	20

Table 1 cont.

Complex	IC ₅₀ (nM)			Selectivity ratios			
	5-HT _{1A}	5-HT _{2A}	D ₂	5-HT _{1A} / 5-HT _{2A}	D ₂ / 5-HT _{2A}	D ₂ / 5-HT _{1A}	
	14	≈ 2000	≈ 130±35	>1000	16	8	0.5

References

- [1] Johannsen B., Scheunemann M., Spies H., Brust P., Wober J., Syhre R. and Pietzsch H.-J. (1996) Technetium(V) and rhenium(V) complexes for 5-HT_{2A} serotonin receptor binding: structure-affinity considerations. *Nucl. Med. Biol.* **23**, 429 - 438.
- [2] Scheunemann M., Pietzsch H.-J., Spies H., Brust P. and Johannsen B. (1996) Serotonin receptor-binding technetium and rhenium complexes. 9. Synthesis and characterization of ligands derived from partial structures of ketanserin, cisapride and MDL 72832. *This report*, pp. 1 - 5.
- [3] Glaser M. (1996) Tripodal-tetradentat/monodentat koordinierte Rheniumkomplexe mit Tris(2-thiolatoethyl)amin. *Thesis*, TU Dresden.
- [4] Hjorth S., Carlsson A., Lindberg P., Sanchez D., Wikström H., Arvidson L.E., Hacksell U. and Nilsson J. L. G. (1982) 8-Hydroxy-2-(di-n-propylamino)tetralin, 8-OH-DPAT, a potent and selective simplified ergot congener with central 5-HT receptor stimulating activity. *J. Neural. Transm.* **55**, 169.
- [5] Leysen J. E., Niemeegers C. J. E., Van Nueten J. M. and Laduron P. M. (1982) [3H]ketanserin (R41468), a selective ligand for serotonin₂ receptor binding sites. Binding properties, brain distribution, and functional role. *Molec. Pharmac.* **21**, 301 - 314.
- [6] Lowry O. H., Rosebrough N. J., Farr A. L. and Randall R. J. (1951) Protein measurement with the Folin phenol reagent. *J. Biol. Chem.* **193**, 265 - 275.

4. Serotonin Receptor-Binding Technetium and Rhenium Complexes

12. Structural Modification of Receptor-Binding Technetium-99m Complexes in order to Improve Brain Uptake

B. Johannsen, R. Berger, P. Brust, H.-J. Pietzsch, M. Scheunemann, S. Seifert, H. Spies, R. Syhre

Introduction

Low brain uptake is a generally accepted problem in developing ^{99m}Tc brain receptor imaging agents. For a class of potential 5-HT_{2A} receptor binding agents exemplified in Fig. 1, we tried to improve the original low brain uptake by modifying the lipophilic properties of the molecules, particularly by insertion of ether-oxygen and by lowering the apparent pK values [1].

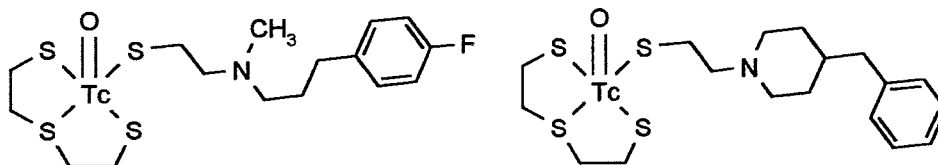


Fig. 1. Example of an 5-HT_{2A} receptor binding ^{99m}Tc complex designed according to the mixed-ligand (3+1), integrated approach [2, 3]

Experimental

Ligands and complexes

Monodentate thiol ligands containing ether-oxygen atoms were synthesized as described in Part 9 of our report [4].

Tc-99 complexes were prepared as previously reported [3]. To prepare n.c.a. ^{99m}Tc complexes, ligand exchange reactions starting from ^{99m}Tc gluconate or ^{99m}Tc ethylene glycolate were carried out [5].

Distribution coefficients

Log D were determined at pH 7.4 from the capacity factors log k values obtained by HPLC using a Perkin-Elmer HPLC Controller System equipped with a UV/VIS spectrometric detector (254 nm) and a Hamilton PRP-1 column (250 x 4.1 mm; 10 μm). As mobile phase an isocratic eluent (acetonitrile and 0.01 M phosphate or citrate buffer, 75:25, v/v) was applied with a flow rate of 1.5 ml/min. Aniline, benzene, and bromobenzene were used as internal standards.

Brain uptake

Animal experiments were carried out according to the relevant national regulations. 0.5 MBq of ^{99m}Tc complex was injected into the tail vein of 5 - 6 week old Wistar rats.

At 2 and 5 min p.i. the rats were sacrificed by heart puncture under ether anesthesia. Selected organs were isolated for weighing and counting [6].

Results and Discussion

A series of new ^{99m}Tc complexes 2 - 6, derived from the class of 5-HT_{2A} binding complexes illustrated in Fig. 2, were synthesized and characterized [4 - 7]. All the compounds contain an ether-oxygen atom which can be considered an isosteric replacement of a methylene group. Complex 6 contains an additional oxygen atom.

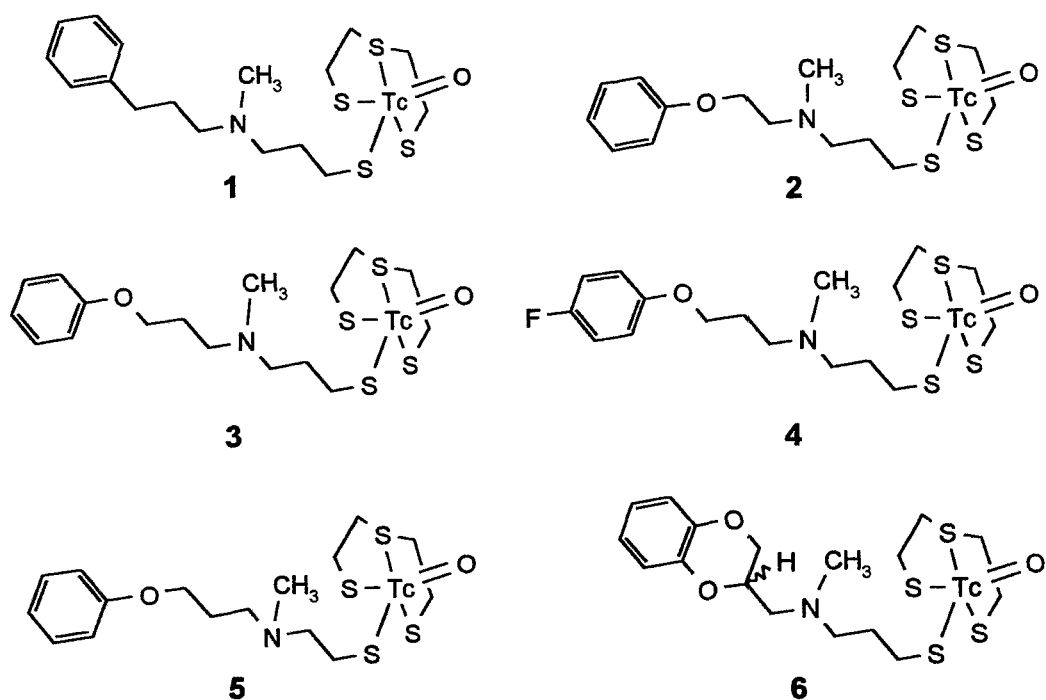


Fig.2: Receptor binding ^{99m}Tc complexes "functionalized" with ether-oxygen atoms [4].
For complex 1 see ref. [3]

Table 1 reveals that the ether-oxygen function in the technetium complex molecules has a profound effect on the pK_{HPLC} value, lipophilicity in terms of the distribution coefficient at pH 7.4, and brain uptake. The successful increase in brain uptake achieved by the structural modification is related to a decrease in the apparent pK value of the nitrogen which, in turn, increases the lipophilic portion of the tracer at physiological pH.

Table 1: Apparent pK_{HPLC} , $\log D$ and brain uptake (% ID/organ) in rats of receptor binding ^{99m}Tc complexes 1 - 6 (for complex 1 see ref. [3]).

	Complex no.					
	1	2	3	4	5	6
pK_{HPLC}	10.01	8.94	9.45	9.36	8.97	8.31
$\log D$	0.70	1.48	1.40	1.60	1.48	2.32
Brain uptake						
2 min*	0.52 ± 0.12	1.47 ± 0.11	0.57 ± 0.10	0.99 ± 0.18	1.01 ± 0.14	2.13
± 0.18						
Brain uptake						
5 min*	0.36 ± 0.07	0.94 ± 0.09	0.45 ± 0.06	0.78 ± 0.12	0.76 ± 0.06	1.31
± 0.14						

* Data shown are the mean \pm SEM of three rats

The relationship obtained between brain uptake in rats and pK value is shown in Fig. 3.

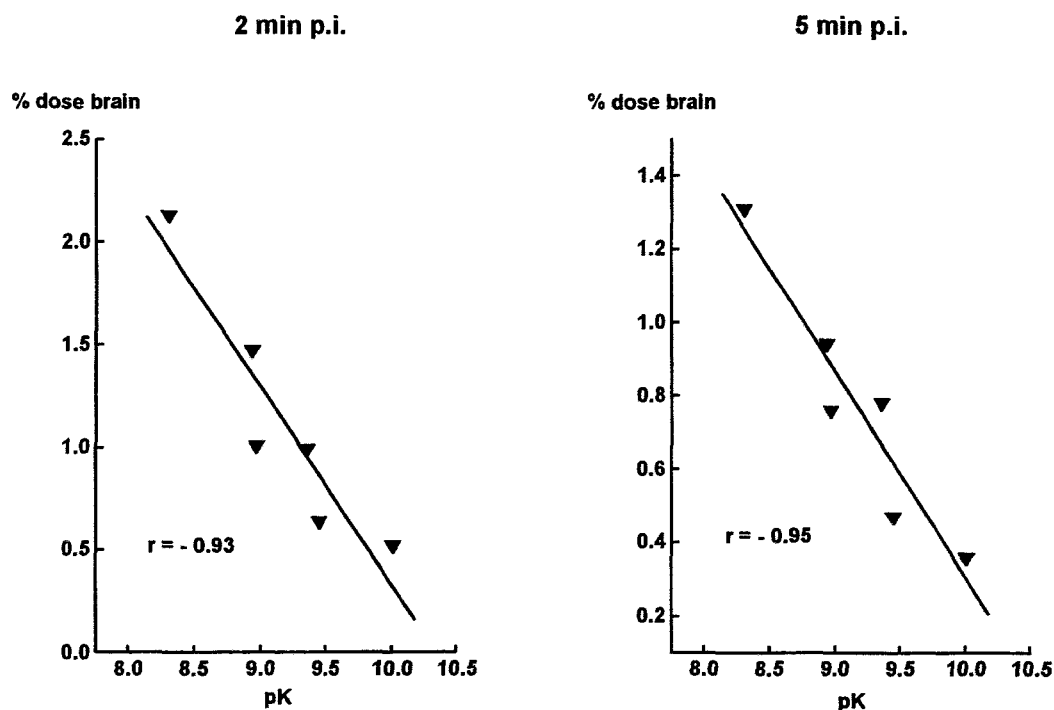


Fig. 3: Relationship of brain uptake in rats at 2 and 5 min. p. i. vs. apparent pK of the ^{99m}Tc complexes

It is a common assumption that there is a good correlation between blood-brain barrier penetration and lipid solubility of a drug, the latter being classically expressed as its partition coefficient between an organic solvent, such as octanol, and water. Other factors may also contribute, such as the molecular volume and charge of the drug, and the extent to which it makes hydrogen bonds. In order to define the factors responsible for the low uptake (up to 0.4 % in rats at 5 min p.i.) of our receptor binding ^{99m}Tc complexes of the type 1 and to elucidate whether modification of the molecular structure will lead to an increased brain uptake without loss of the high receptor binding affinity, the molecular size, lipophilicity and charge of the candidates were considered.

For CNS agents an optimum octanol/water partition coefficient ($\log P$) of around 2 ± 0.5 was found for various classes of compounds. Such a $\log P$ value, which is at the peak of a parabolic dependence of uptake, is also usually considered to be required for some types of neutral ^{99m}Tc chelates [8, 9]. However, for one class of ^{99m}Tc - N_2S_2 complexes containing an amide group, only a low brain uptake was reported, regardless of lipophilicity ($\log P$ from 0.56 to 1.75) [10].

In the neutral form, our complexes exhibit $\log P_{\text{HPLC}}$ values between 3.2 and 3.6, similar to ketanserin [3]. However, the protonable nitrogen atom as an essential constituent of the pharmacophore causes the technetium complexes to be almost completely ionized at the physiological pH. The proportion of ionizable technetium compounds which are neutral in solution is governed by the difference in pH of the solution and the pK of the molecule, according to the Henderson Hasselbalch equation. With ionizable molecules, the lipophilicity is better described by the distribution coefficient ($\log D$), i.e. the pK-corrected $\log P$ values. We suggest that an excessively high pK value is responsible for the low uptake of our technetium complexes. To test this hypothesis, apparent pK and $\log D$ values were determined and structural modifications, i.e. introduction of ether-oxygen atoms, performed in order to lower the pK value in the complex molecules. The results clearly demonstrate the usefulness of the hypothesis. The electronic effects of ether-oxygen two or three carbon atoms away from the protonable nitrogen in the ligand backbone are obviously strong enough to produce the desired decrease in pK value. Thus, the introduction of oxygen atoms proved to be a valuable tool in the design of certain ^{99m}Tc brain imaging agents. In view of the still relatively high pK values, the increase in brain uptake cannot be explained merely by a higher proportion of neutral, diffusible species. In this

respect, our class of technetium complexes resemble amphetamines, which show a high accumulation in the brain despite a low proportion of neutral species in the blood stream.

References

- [1] Johannsen B., Berger R., Brust P., Pietzsch H.J., Scheunemann M., Seifert S., Spies H. and Syhre R. (1997) Structural modification of receptor-binding technetium-99m complexes in order to improve brain uptake. *Eur. J. Nucl. Med.*, in press.
- [2] Johannsen B., Pietzsch H.-J., Scheunemann M., Spies H. and P. Brust (1996) Oxotechnetium(V) and oxorhenium(V) complexes as potential imaging agents for the serotonin receptor. *J. Nucl. Med.* **36**, 27P (abs.)
- [3] Johannsen B., Scheunemann M., Spies H., Brust P., Wober J., Syhre R. and Pietzsch H.J. (1996) Technetium(V) and rhenium(V) complexes for 5-HT_{2A} serotonin receptor binding: structure-affinity considerations. *Nucl. Med. Biol.* **23**, 429 - 438.
- [4] Scheunemann M., Pietzsch H.-J., Spies H., Brust P. and Johannsen B. (1996) Serotonin receptor-binding technetium and rhenium complexes. 10. Synthesis and characterization of rhenium and technetium complexes derived from partial structures of ketanserin, cisapride and MDL 72832. *This report*, pp. 5 - 8.
- [5] Seifert S., Pietzsch H.-J., Scheunemann M., Spies H., Syhre R. and Johannsen B. (1996) Serotonin receptor-binding technetium and rhenium complexes. 13. No carrier added preparations of "3+1" ^{99m}Tc complexes. *This report*, pp. 16 - 22.
- [6] Syhre R., Seifert S., Pietzsch H.-J., Scheunemann M., Spies H., Brust P. and Johannsen B. (1996) Serotonin receptor-binding technetium and rhenium complexes. 14. Distribution and brain uptake in rats of serotonin receptor-binding oxotechnetium(V) complexes at the c.a. (^{99m/99}Tc) and the n.c.a. (^{99m}Tc) level. *This report*, pp. 23 - 31.
- [7] Pietzsch H.-J., Scheunemann M., Brust P., Wober J., Spies H. and Johannsen B. (1996) Serotonin receptor-binding technetium and rhenium complexes. 11. Affinity and selectivity of oxorhenium(V) complexes derived from ketanserin, cisapride and MDL 72832. *This report*, pp. 9 - 12.
- [8] Eckelman W. C. (1995) Radiolabeling with technetium-99m to study high-capacity and low-capacity biochemical systems. *Eur. J. Nucl. Med.* **22**, 249 - 263.
- [9] Nowotnik D. P. (1992) Technetium-based brain perfusion agents. In: Nunn, A. (ed.) *Radiopharmaceuticals: chemistry and pharmacology*. New York: Marcel Dekker, pp. 37 - 95.
- [10] Oya S., Plössl K., Kung M. P., Stevenson D. A. and Kung H F. (1995) Small and neutral Tc^VO(III)N₂S₂ complexes for developing new brain imaging agents. *Eleventh International Symposium on Radiopharmaceutical Chemistry*, Vancouver; Abstracts 782 - 784.

5. Serotonin Receptor-Binding Technetium and Rhenium Complexes 13. No Carrier Added Preparations of "3+1" ^{99m}Tc Complexes

S. Seifert, H.-J. Pietzsch, M. Scheunemann, H. Spies, R. Syhre, B. Johannsen

Introduction

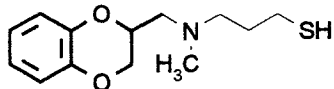
Oxotechnetium(V) complexes with tridentate dithiols "HS-C₂H₄-X-C₂H₄-SH" (X = S, O, N) and functionalized monodentate thiols, so-called "3+1" complexes of the general formula [MOL₁L₂] (L₁ = tridentate dithiol ligand, L₂ = monothiol ligand), play an important role in the development of receptor-binding technetium complexes [1, 2, 3]. While the preparation of these complexes at c.a. level (or with rhenium) is possible without any difficulties by stoichiometric ligand-exchange reaction starting with [TcOCl₄]⁻, Tc gluconate or [ReOCl₄]⁻, [ReOL₁Cl] and Re gluconate [4], the n.c.a. preparation generally results in a mixture of various partially unidentified complex compounds. Moreover, the prepared "3+1" complexes are not stable in the reaction solution containing an enormous ligand excess.

Furthermore, direct reduction of pertechnetate generator eluate in the ligand mixture solution leads to a lot of unknown products besides small amounts of the desired complex. Therefore, it was the aim of this work to find reaction conditions allowing reliable and reproducible preparation of "3+1" technetium complexes at n.c.a. level with yields and stabilities high enough for animal experiments.

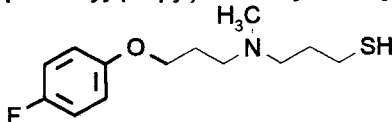
We studied the complexation reactions at n.c.a. level with the tridentate ligand L₁ = 3-thiapentane-1,5-dithiol (HS-(CH₂)₂-S-(CH₂)₂-SH) or, in one case, with 3-ethylaza-pentane-1,5-dithiol (HS-(CH₂)₂-

$N(C_2H_5)-(CH_2)_2-SH$) and a series of monodentate thiols L_2 , e.g. small ligands such as ethanethiol (C_2H_5SH), 2-propanethiol (C_3H_7SH), or larger monothiols like:

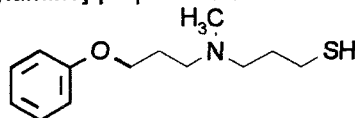
(2RS) 2-[N-(3-mercaptopropyl)-N-methyl-aminomethyl]-1,4-benzodioxane



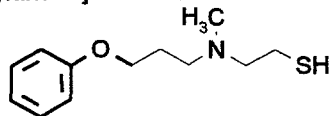
3-[N-(3-(4-fluorophenoxy)-propyl)-N-methylamino]-propanethiol



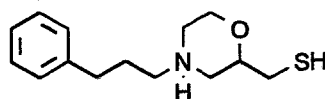
3-[N-(3-phenoxypropyl)-N-methylamino]-propanethiol



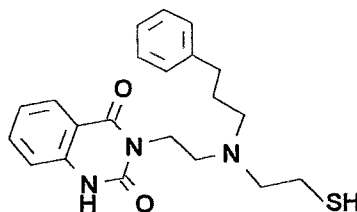
2-[N-(3-phenoxypropyl)-N-methylamino]-ethanethiol



(2RS) 2-mercaptomethyl-4-(3-phenylpropyl)morpholine



3-[2-(N-3-phenylpropyl-N-2-mercaptoethyl)-aminoethyl]-2,4-(1H,3H)-quinazolidione



The identity of the prepared n.c.a. complexes was examined by comparison of the chromatographic behaviour (TLC, HPLC) of these preparations with Re or ^{99}Tc reference complexes as well as organ distribution data of c.a. and n.c.a. Tc preparations.

Experimental

General

The tridentate ligand and both small thiols are commercial substances and were used without further purification. The other monothiols were prepared as described previously [5]. Pertechnetate generator eluate was obtained from a commercial $^{99}Mo/^{99m}Tc$ generator (Mallinckrodt). A 0.3 M aqueous solution of ammonium [^{99}Tc]pertechnetate was used for c.a. preparations. The comparative ^{99}Tc and Re substances were prepared according to the general procedure described in [2, 4].

N.c.a. preparations

In order to prepare n.c.a. ^{99m}Tc complexes **3 - 8**, ligand exchange reactions starting from ^{99m}Tc gluconate or ^{99m}Tc ethylene glycolate were carried out. Both precursor solutions were prepared by

gradual addition of 20 μ l stannous chloride solution (1.0 mg SnCl_2 dissolved in 10 ml ethanol) to an aqueous solution of [$^{99\text{m}}\text{Tc}$]pertechnetate eluate in an excess of sodium gluconate (10 mg) or ethylene glycol (10 μ l). 0.5 mg of the monodentate thiol ligand dissolved in ethanol was added to 1.0 ml of the precursor solution adjusted to pH 8 - 9 and 1.0 ml acetone or acetonitrile. 0.05 mg of the tridentate ligand dissolved in acetone was added after one minute and the formation of the desired mixed-ligand complex was completed by heating the reaction solution at 40 $^\circ\text{C}$ in a water bath for 15 - 20 minutes (yields: 80 - 90 %). For separation of byproducts and ligand excess the reaction solution was given onto a semi-preparative PRP-1 column (Hamilton, 305 x 7 mm, 10 μm , flow rate 2.0 ml/min) and eluted using a linear gradient system (t[min]/%A): (5/50), (10/100), (5/100) of acetonitrile (A)/water (B) with 0.1 % trifluoroacetic acid (pH 2). After adding 100 μ l propylene glycol and removing acetonitrile by vacuum evaporation, the separated neutralized complex fraction is stable for more than 8 h. For the preparation of complexes **1** and **2** only 0.2 mg of the monothiol ligand are added to the precursor solution. After addition of 0.1 mg of the tridentate ligand the reaction solution is heated to 60 $^\circ\text{C}$ for 1 h.

Analytical methods

TLC and HPLC analyses were used for the determination of the radiochemical purity and stability of the preparations.

TLC analyses were performed using silica gel strips (Silufol) developed with n-butanol/methanol/water/conc. ammonia (60/20/20/1) (method I) as well as methanol/0.1 N HCl (3/1) (method II) as solvents.

In addition to the above-mentioned conditions for separation of ligand excess (PRP-1, pH 2.0), HPLC analyses were mainly carried out with a Superspher 100 RP-18 column (250 x 4 mm) using an isocratic gradient mixture of 80 % methanol and 20 % 0.01 M phosphate buffer of pH 7.4 and a flow rate of 1.0 ml/min. The effluent from the column was monitored by UV absorbance at 254 nm for rhenium complexes or γ -detection for the $^{99\text{m}}\text{Tc}$ complexes. For the biological studies the solutions of the complexes were diluted with propylene glycol and sodium chloride for injection to adjust the desired radioactive concentration.

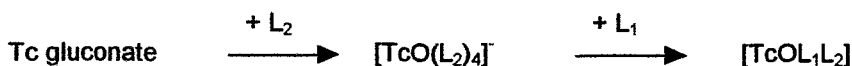
In vivo biodistribution in rats

The animal experiments were carried out according to the relevant national regulations. Organ distribution studies were performed on male Wistar rats (5 - 6 weeks old). 0.5 ml complex solution was injected into the tail vein. 1 - 120 min. p.i. the rats were sacrificed by heart puncture under ether anaesthesia. The selected organs were isolated for weighing and counting. The percentage dose/g values were computed from the percentage dose/organ values and the corresponding mean organ weights.

Results and Discussion

Preparation of n.c.a. complexes

As found for c.a. preparations, the complexation reaction to mixed-ligand "3+1" complexes proceeds with better yields when an excess of the monodentate ligand is added at first. After rapid formation of the Tc complex with only the monodentate ligand L_2 , the tridentate dithiol ligand L_1 is added and the "3+1" complex is formed in a slow reaction.



The formation of 1:4 complexes of technetium with sterically hindered or bulky monothiols is described in [6, 7]. A similar reaction should take place with the above-mentioned bulky ligands used for the formation of complexes **3** - **8**.

The formation of mixed-ligand complexes **3** - **8** listed in Table 1 from the intermediate technetium complexes represents a slow reaction (Fig. 1).

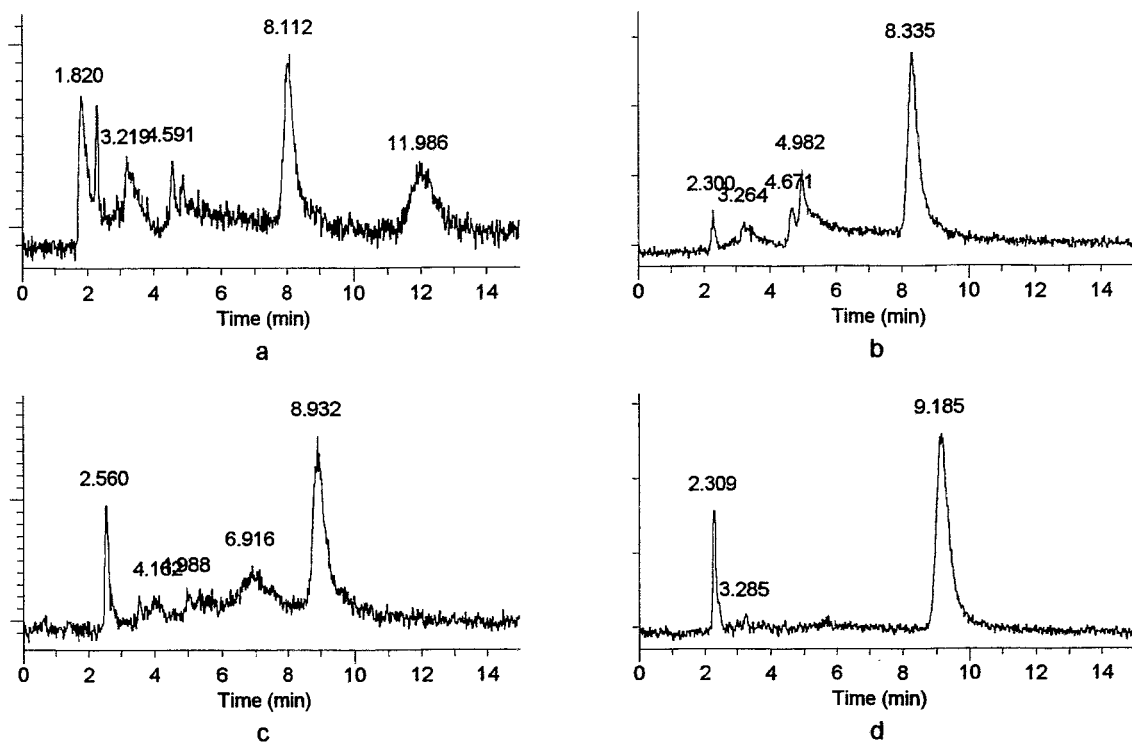


Fig. 1. HPLC analyses of formation of ^{99m}Tc complex 4 at room temperature. (Superspher RP-18, methanol/0.01 M phosphate buffer pH 7.4 (80/20), 1.0 ml/min) a: 5 min, b: 30 min, c: 80 min, d: 120 min after preparation

Without heating between two to three hours are needed for completion of the reaction depending on the ligand used. The successful formation of complex 7 is remarkable despite the voluminous monothiolato ligand.

Generally, the reaction is accelerated by careful heating. 15 - 20 minutes in a water bath at 40 °C is enough for yields of 80 - 90 % (Fig. 2). Heating over 40 °C results in a competing reaction, probably to complexes containing only the tridentate ligand. Similar reaction products were found when more than 1 mg of the tridentate ligand was added for preparing the "3+1" complex. That shows that the ligand concentration plays an important role concerning the course and kinetics of the reaction. Only microgram amounts are needed for the n.c.a. preparations. The use of milligram amounts of both ligands results in low yields of the desired complex and the formation of mostly unknown products. The best results were obtained with 0.5 - 0.2 mg of the monothiolato ligand and 0.05 - 0.02 mg of the tridentate ligand. The formation of complex 6 needs the smallest amounts.

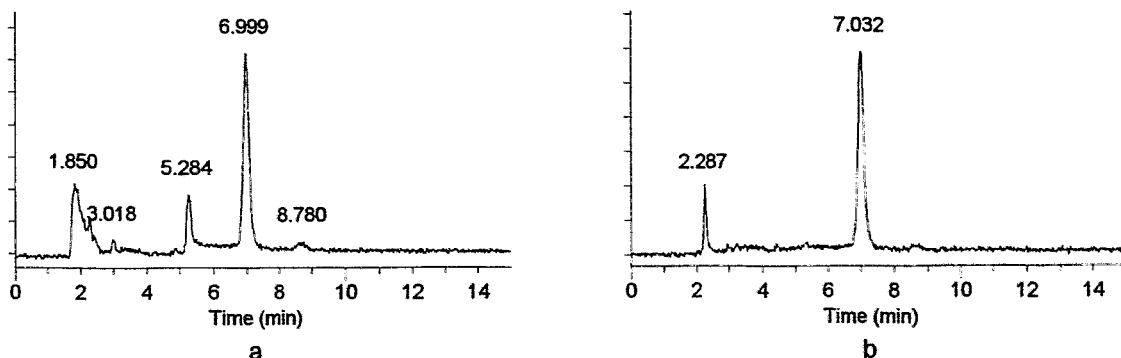


Fig. 2. HPLC analyses of formation of ^{99m}Tc complex 6 (Superspher RP-18, methanol/0.01 M phosphate buffer pH 7.4 (80/20), 1.0 ml/min) a: after 5 min, b: after 20 min heating at 40°C.

These low ligand quantities are also responsible for the relatively high stability of the complex preparations. While preparations with higher yields of ligands are unstable and undergo secondary reactions at higher temperatures or with time, the optimized preparations are stable for at least 2 h at room temperature, even without separation of the ligand excess. If the ligand excess is separated, e.g. by HPLC, the complex solutions are stable for more than 8 h.

It was found that the monothiols used for complexation change with time, probably by formation of disulphides. That results in a delay of reaction at room temperature. To accelerate the reaction, heating at 40 °C for 20 minutes is needed to obtain yields of 80 - 90 % of the desired complex.

Using freshly prepared monothiolato ligand, e.g. (2RS) 2-[N-(3-mercaptopropyl)-N-methylamino-methyl]-1,4-benzodioxane, for preparing complex 3 results in a yield of 73 % even after 5 minutes reaction time at room temperature. After 30 minutes the reaction is finished and yields of 75 - 90 % are obtained.

To protect the monothiol ligand, the very stable oxalate was formed and isolated as a white powder. This allows better storage and represents a first step to a "kit-like" preparation of the "3+1" complex.

For preparing the complex a certain content of sodium hydroxide has to be added to the reaction solution to deprotonate the nitrogen atom of the monothiolato ligand. Without adding NaOH the solution has a pH value of about 6, and only less than 10 % of the complex are formed.

The best yields were obtained by adding 100 µl 0.1 n NaOH to the ^{99m}Tc gluconate solution (pH = 11) and complexation with 0.3 - 0.5 mg oxalate of the monothiolato ligand and 0.05 mg of the tridentate HS-S-SH ligand. Without heating 3 h are needed to obtain more than 70 % of the desired complex. The same result is achieved by heating at 40 °C for at least 60 minutes (Fig. 3).

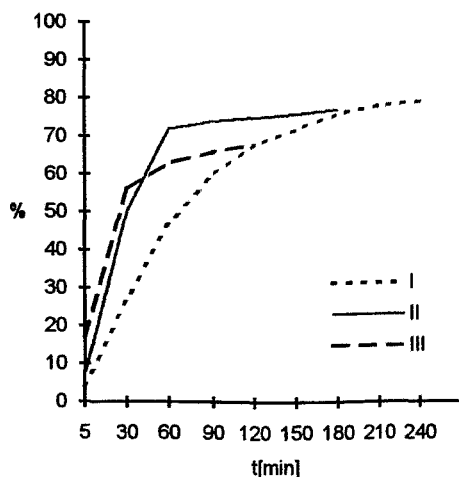


Fig. 3: Reaction conditions for preparing the "3+1" ^{99m}Tc complexes using the oxalate of the monothiolato ligand. I: 100 µl 0.1 n NaOH, 20 °C, pH 11, II: 100 µl 0.1 n NaOH, 40 °C, pH 11, III: 150 µl 0.1 n NaOH, 20 °C, pH 12.

The preparation of the ^{99m}Tc complexes 1 and 2 needs other reaction conditions. For instance, Tc gluconate reacts immediately with ethanethiol or 2-propanethiol to the intermediate complex. The exchange with the tridentate ligand using the same conditions as for complexes 3 - 8, however, proceeds very slowly at room temperature. 5 - 6 h reaction time results in yields of only 40 - 60 % of the mixed-ligand complex. It was found that a diminished monothiol ligand concentration of 0.2 mg and an increased content of 0.08 - 0.1 mg per vial of the S-S-S ligand lead to shorter reaction times of 1 - 2 h and higher yields of 80 - 90 %.

As already found for complexes 3 - 8 a higher temperature also accelerates the formation of the "3+1" complex. The optimum temperature for formation of complexes 1 and 2 was determined to be 60 °C. The stability of ^{99m}Tc complexes with thiols like ethanethiol or 2-propanethiol is probably higher than that of complexes with bulky ligands. The ligand exchange between these small monothiol ligands and the tridentate ligand proceeds therefore much slower.

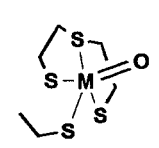
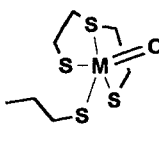
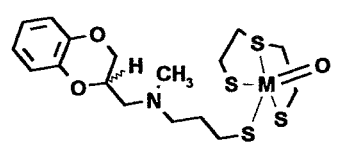
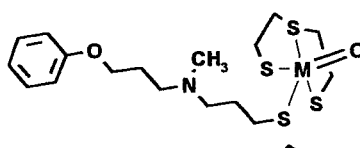
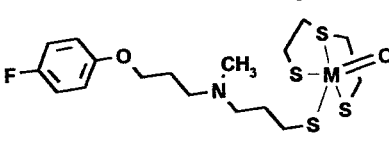
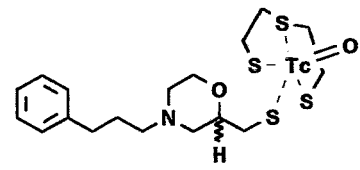
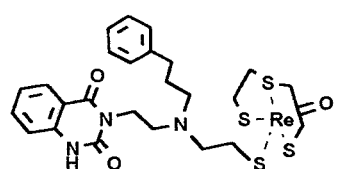
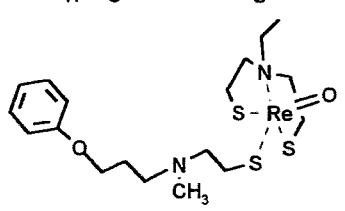
Reaction with the tridentate S-N-S ligand instead of the S-S-S ligand leads to complex 8. No significant differences were observed concerning the optimum parameters for the formation of the n.c.a. complex and the kinetics of complexation.

Chemical and biological evaluation of n.c.a. preparations

Two TLC methods were performed for identification of the ^{99m}Tc preparations. The R_f values of the n.c.a. complexes **3 - 8** determined with method I ($R_f = 0.6 - 0.7$) as well as method II ($R_f = 0.4 - 0.5$) are in accordance with the R_f values of the c.a. preparations.

The HPLC data obtained with an RP-18 and a PRP-1 column also show the identity of the n.c.a. and c.a. preparations (Table 1). In some cases rhenium complexes were also investigated. As expected, the same R_f values were obtained.

Table 1. Comparison of R_f values of n.c.a. and c.a. Tc complexes

Complex	No.	R_f value [min]			
		RP-18 n.c.a.	c.a.	PRP-1 (prep.) n.c.a. c.a.	
	1	2.3	2.4	-	8.4
	2	2.2	2.3	-	8.9
	3	7.7	7.8	9.3	9.4
	4	8.1	8.0	9.9	9.9
	5	9.8	9.7	9.9	9.7
	6	7.1	7.2	10.0	9.8
	7	7.5	7.6	10.6	10.7
	8	6.0	6.0	4.3	4.4

Organ distribution studies carried out with selected c.a. and n.c.a. technetium complexes also confirm the identity of preparations. In Table 2 the data for complexes 3, 5 and 6 are presented.

Table 2: Comparison of biodistribution data of c.a. and n.c.a. ^{99m}Tc complexes 5 min. p.i. in rats

Complex	Brain	\pm SEM	/g	\pm SEM	Blood	\pm SEM	Heart	\pm SEM	Lungs	\pm SEM
3										
c.a.	1,31	0,14	0,91	0,14	2,53	0,24	0,54	0,05	4,42	0,48
n.c.a.	1,08	0,25	0,83	0,16	2,88	0,40	0,47	0,04	3,92	0,53
5										
c.a.	0,84	0,03	0,56	0,05	6,66	0,62	1,20	0,08	6,02	1,45
n.c.a.	0,87	0,15	0,61	0,12	6,91	0,47	1,23	0,23	7,63	1,17
6										
c.a.	0,62	0,19	0,47	0,09	2,32	0,25	0,76	0,23	4,20	1,30
n.c.a.	0,68	0,05	0,54	0,02	2,27	0,22	0,65	0,08	4,17	0,65

References

- [1] Pietzsch H.-J., Spies H. and Hoffmann S. (1989) Lipophilic Tc complexes. VI. Neutral oxotechnetium(V) complexes with monothiol/tridentate dithiol coordination. *Inorg. Chim. Acta* **165**, 163 - 166.
- [2] Johannsen B, Pietzsch H.-J., Scheunemann M, Spies H and Brust P. (1995) Oxotechnetium(V) and oxorhenium(V) complexes as potential imaging agents for the serotonin receptor. *J. Nucl. Med.* **36**, 27P.
- [3] Johannsen B, Scheunemann M, Spies H, Brust P, Wober J, Syhre R and Pietzsch H.-J. (1996) Technetium(V) and rhenium(V) complexes for 5-HT_{2A} serotonin receptor binding: structure-affinity considerations. *Nucl. Med. Biol.* **23**, 429 - 438.
- [4] Spies H., Fietz Th., Pietzsch H.-J., Johannsen B., Leibnitz P., Reck, G., Scheller D. and Klostermann K. (1995) Neutral oxorhenium(V) complexes with tridentate and monodentate alkane- or arenethiolate coligands. *J. Chem. Soc., Dalton Trans.* 2277 - 2280.
- [5] Scheunemann M., Pietzsch H.-J., Spies H., Brust P. and Johannsen B. (1997) Serotonin receptor-binding technetium and rhenium complexes 9. Synthesis and characterization of ligands derived from partial structures of ketanserin, cisapride and MDL 72832. *This report*, pp. 1 - 5.
- [6] Davison A., de Vries N., Dewan J. and Jones A. (1986) Five coordinate complexes of technetium (III) and (V) with sterically hindered aryl thiolate ligands. *Inorg. Chim Acta* **120**, L15 - L16.
- [7] Hamor T., Hussain W., Jones C., McCleverty J. and Rothin A. (1988) The synthesis of technetium(V) complexes containing sterically bulky thiolate ligands. The molecular structure of tetrabutylammonium oxotetrakis(2,4,6-trimethylbenzenethiolato)technetate(V). *Inorg. Chim. Acta* **146**, 181 - 185.

6. Serotonin Receptor-Binding Technetium and Rhenium Complexes

14. Distribution and Brain Uptake in Rats of Serotonin Receptor-Binding Oxotechnetium(V) Complexes at the c.a. ($^{99m/99}\text{Tc}$) and the n.c.a. (^{99m}Tc) Level

R. Syhre, H.-J. Pietzsch, M. Scheunemann, S. Seifert, H. Spies, B. Johannsen

Introduction

Neutral lipophilic $^{99m/99}\text{Tc}$ oxotechnetium(V) complexes of various structures show affinity to serotonin receptors (5-HT_{2A}; 5-HT_{1A}) as determined by *in vitro* binding studies on rat cortex [1, 2, 3, 4, 5]. These complexes all contain a protonable nitrogen in the molecule, which might prevent brain uptake. As reported in [2, 6] the complexes studied are nevertheless able to cross the intact blood-brain barrier of the rat. However, the levels of the initial brain uptake were observed to be relatively low (0.2 - 0.5 % dose/organ at 2 min. p.i.). A slow washout from the brain and a retention into receptor-rich brain regions were found. A high and prolonged background activity in the blood stream was determined in biodistribution studies. This unfavourable characteristic may result from ionization at the blood pH 7.4 as well as from interaction of the complexes with plasma proteins and blood cells [7].

In the following we report the biodistribution of receptor-binding $^{99m/99}\text{Tc}$ oxotechnetium(V) complexes which have been modified to overcome the low brain uptake. Besides the protonable nitrogen these complexes contain ether-oxygen atom(s) in the side chain. This modification has a profound effect on lipophilicity parameters such as the distribution coefficient log D and the pK_a values [4, 8].

Experimental

Animal studies

Animal experiments were carried out according to the relevant national regulations.

The studies were performed on male Wistar rats (5 - 6 weeks old). 0.5 ml of the complex solution (propylene glycol / sodium chloride) were injected in the tail vein. 2 - 180 min. p.i. the rats were sacrificed by heart puncture under ether anaesthesia. The selected organs were isolated for weighing and counting. For the studies of brain regions the whole brain was removed, and cortex, caudate putamen hippocampus and cerebellum were dissected on an ice-cold glass plate, weighed and counted, and the percentage dose per gram was calculated.

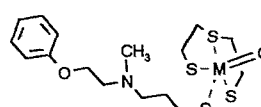
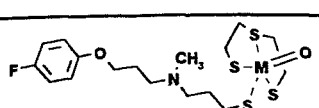
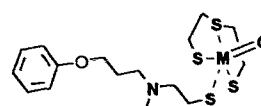
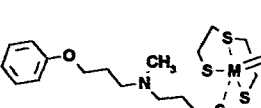
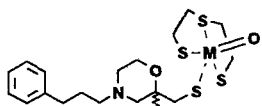
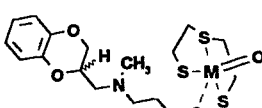
Binding on erythrocytes

After *in vivo* or *in vitro* incubation, red blood cells and plasma were separated by centrifugation of heparinized whole blood. The cells were washed plasma-free (sodium chloride for injection) and the radioactivity of the red cell fraction was counted and calculated.

Results and Discussion

The preparation and chemical characterization, the physicochemical characterization and the characterization of the biological *in vitro* behaviour of the ether-oxygen containing Tc-complexes have been described previously [10, 11]. The complexes under investigation are listed in Table 1.

Table 1: Structure of oxygen-containing oxotechnetium(V) complexes at the c.a. ($^{99m/99}\text{Tc}$) and n.c.a. (^{99m}Tc) level

Complex	Complex
<p>1</p> <p>M: $^{99m/99}\text{Tc}$</p> 	<p>4</p> <p>M: $^{99m/99}\text{Tc}$</p> 
<p>2</p> <p>M: $^{99m/99}\text{Tc}$</p> 	<p>4a</p> <p>M: ^{99m}Tc</p>
<p>3</p> <p>M: $^{99m/99}\text{Tc}$</p> 	<p>5</p> <p>M: $^{99m/99}\text{Tc}$</p> 
	<p>5a</p> <p>M: ^{99m}Tc</p>
	<p>6</p> <p>M: $^{99m/99}\text{Tc}$</p> 
	<p>6a</p> <p>M: ^{99m}Tc</p>

The results of the animal studies indicate that the ether-oxygen containing complexes are capable of crossing the blood-brain barrier. The distribution data show a successful increase in brain activity up to 2.1 % dose (complex 6) at 2 minutes p. i. and a prolonged retention in the rat brain within 10 - 120 min. post-injection of these new tracers (Fig. 1; Table 2).

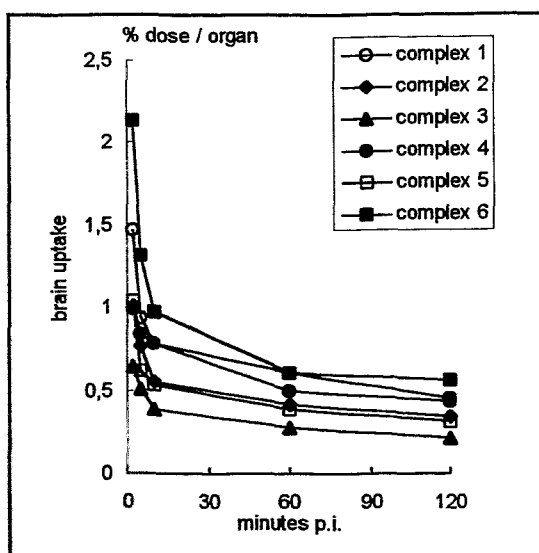


Fig.1: Time course of brain uptake in rats after injection of oxygen-containing complexes (mean values 2 - 120 minutes p.i.; n = 3 - 6)

The initial brain uptake of most of the complexes shows a good inverse correlation to the pK_a values of the complexes (Fig. 2). Interestingly, complex 5 (morpholinyl derivatives) does not fit into this correlation. Complex 5 displayed a significantly lower brain uptake than complex 6 despite similar lipophilicity parameters of both complexes [9]. This observation cannot yet be explained.

Another point of interest in the design of potential receptorbinding agents is the regional distribution in the brain, including target (receptor-rich) to nontarget (receptor-poor) ratios.

Table 2: Biodistribution of $^{99m/99}\text{Tc} / ^{99m}\text{Tc}$ oxotechnetium(V) complexes in rats
(mean % dose \pm SEM, n = 3 - 6)

Complex	Time min. p.i.	Brain			Blood			Heart			Lung			Kidney			Liver		
		%dose	\pm SEM	%dose/g	\pm SEM	%dose/g	\pm SEM	%dose	\pm SEM	%dose	\pm SEM	%dose	\pm SEM	%dose	\pm SEM	%dose	\pm SEM	%dose	\pm SEM
1	5	0.94	0.14	0.67	0.14	5.5	0.3	1.0	0.1	6.4	1.2	5.9	1.0	11.9	2.2				
	10	0.78	0.08	0.56	0.06	4.2	0.2	0.7	0.1	8.4	2.5	9.2	0.3	16.6	0.8				
	60	0.61	0.05	0.44	0.03	3.4	0.2	0.6	0.1	6.5	1.5	13.2	0.5	15.6	1.6				
2	5	0.76	0.05	0.53	0.05	5.9	0.2	1.4	0.2	10.0	0.9	6.0	0.9	6.8	2.1				
	10	0.55	0.04	0.37	0.01	4.9	0.3	0.9	0.2	8.4	1.1	9.2	1.7	13.4	2.6				
	60	0.41	0.08	0.30	0.06	3.3	0.3	0.7	0.0	7.8	0.9	15.4	0.5	18.2	2.4				
3	5	0.49	0.06	0.35	0.01	5.0	0.1	1.1	0.1	8.4	0.9	7.1	0.2	12.1	2.4				
	10	0.35	0.18	0.25	0.08	4.9	0.1	0.8	0.1	6.4	0.6	8.7	0.3	14.1	1.1				
	60	0.31	0.02	0.21	0.01	3.5	0.3	0.6	0.1	3.6	0.6	13.9	0.4	14.0	0.9				
4	5	0.84	0.03	0.56	0.05	6.7	0.6	1.2	0.1	6.0	1.5	7.6	0.8	10.8	0.8				
	10	0.78	0.11	0.57	0.08	6.1	0.5	1.0	0.2	6.6	0.5	8.3	1.0	12.3	0.1				
	60	0.50	0.14	0.36	0.13	5.3	1.0	0.6	0.1	3.6	0.6	13.5	0.7	14.8	1.0				
4a	5	0.87	0.15	0.61	0.12	7.0	0.6	1.2	0.2	7.6	1.2	6.5	0.6	10.9	1.4				
	10	0.69	0.09	0.52	0.08	4.9	0.6	0.9	0.1	6.7	1.6	8.5	0.5	12.8	0.9				
5	5	0.62	0.19	0.47	0.09	2.3	0.3	0.8	0.2	4.2	1.3	6.5	0.5	24.6	2.8				
	10	0.53	0.19	0.41	0.13	2.0	0.5	0.5	0.1	3.6	0.5	7.1	0.5	26.3	2.2				
	60	0.39	0.04	0.31	0.04	1.2	0.1	0.4	0.1	3.3	0.3	10.6	1.1	28.5	2.7				
5a	5	0.68	0.05	0.54	0.02	2.3	0.2	0.6	0.1	4.2	0.6	6.3	0.2	28.7	1.5				
	10	0.65	0.11	0.43	0.10	2.2	0.2	0.4	0.1	4.0	0.4	7.8	0.3	26.4	1.4				
6	5	1.31	0.14	0.91	0.14	2.5	0.2	0.5	0.1	4.4	0.5	6.0	0.4	19.8	0.4				
	10	0.97	0.11	0.70	0.05	2.1	0.3	0.5	0.1	3.6	0.7	8.3	1.2	24.4	1.3				
	60	0.61	0.05	0.48	0.05	1.7	0.2	0.4	0.1	3.4	0.6	11.7	1.5	33.3	0.4				
6a	5	1.08	0.25	0.83	0.16	2.2	0.4	0.5	0.1	3.9	0.5	6.4	0.7	26.4	3.6				
	10	0.85	0.04	0.63	0.01	2.1	0.2	0.5	0.1	3.1	0.2	8.2	0.3	31.0	1.3				

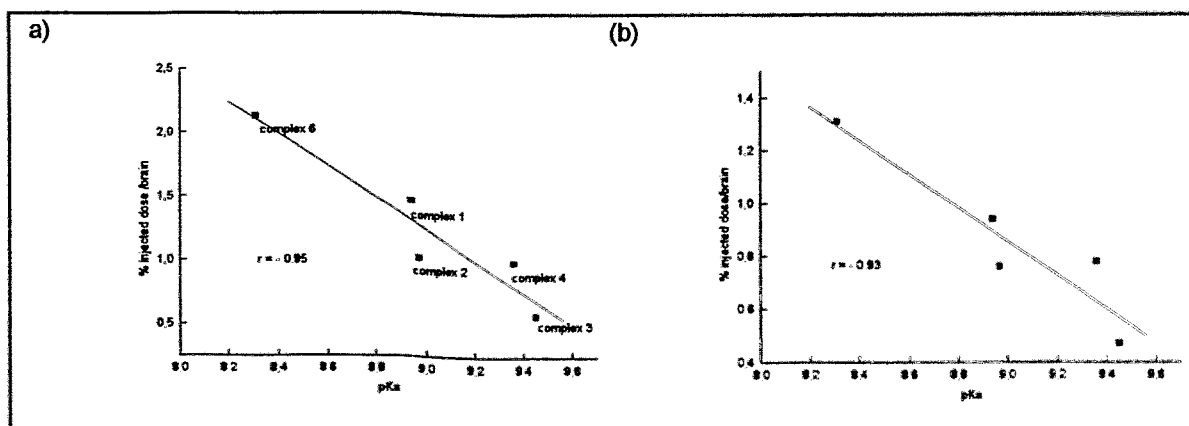


Fig. 2: Relationship of brain uptake in rats at 2 min (a) and 5 min (b) vs pKa values of the oxygen-containing complexes

Table 3: Calculated ratio of receptor-rich regions vs cerebellum 5 minutes after injection of the $^{99m/99}\text{Tc}$ complexes 1 - 6 in rats (% dose/g; n = 3 corrected by the blood activity portion in the regions according to Cremer [12])

Complex	Cortex/ cerebellum	Caudate putamen/ cerebellum	Hippocampus/ cerebellum
1	1.4	1.0	1.1
2	1.1	0.8	0.7
3	1.0	0.8	0.9
4	1.4	1.2	1.1
5	1.1	1.0	0.9
6	1.2	1.2	1.0

The ratios of regional brain uptake to cerebellum for complexes 1 - 6 at 5 minutes p.i. are listed. In Table 3. *In vitro*, complex 6 proved to be selective for 5-HT_{1A} receptor, the complexes 1 - 5 for the 5-HT_{2A} receptor [4, 5].

Table 4: Ratio of receptor-rich region and cerebellum 5 - 180 minutes after injection of the $^{99m/99}\text{Tc}$ complexes (column A) and ^{99m}Tc complexes (column B) in rats (% dose/g; n = 3)

Complex	Time p.i. [min]	Cortex/ cerebellum		Caudate putamen/ cerebellum		Hippocampus/ cerebellum	
		A	B	A	B	A	B
5	5	1.0	1.1	1.0	1.1	1.0	0.9
	10	1.3	1.3	1.2	1.2	0.9	1.2
	60	1.5	1.5	1.2	1.1	1.3	1.6
	120	1.5	1.3	1.2	1.1	1.1	1.4
	180	1.4	1.4	1.1	0.9	1.2	1.5
6	5	1.1	1.2	1.1	1.1	0.9	1.0
	10	1.3	1.5	1.2	1.1	1.2	1.2
	60	1.5	1.4	1.1	1.2	1.6	1.2
	120	1.3	1.4	1.1	1.3	1.4	1.3
	180	1.4	1.5	0.9	1.2	1.5	1.4

As shown in the preliminary studies, the unblocked *in vivo* distribution in rat brain exhibits remarkable heterogeneity with the moderate region to cerebellum ratios in the ranges of 0.7 - 1.4 at 5 minutes p.i..

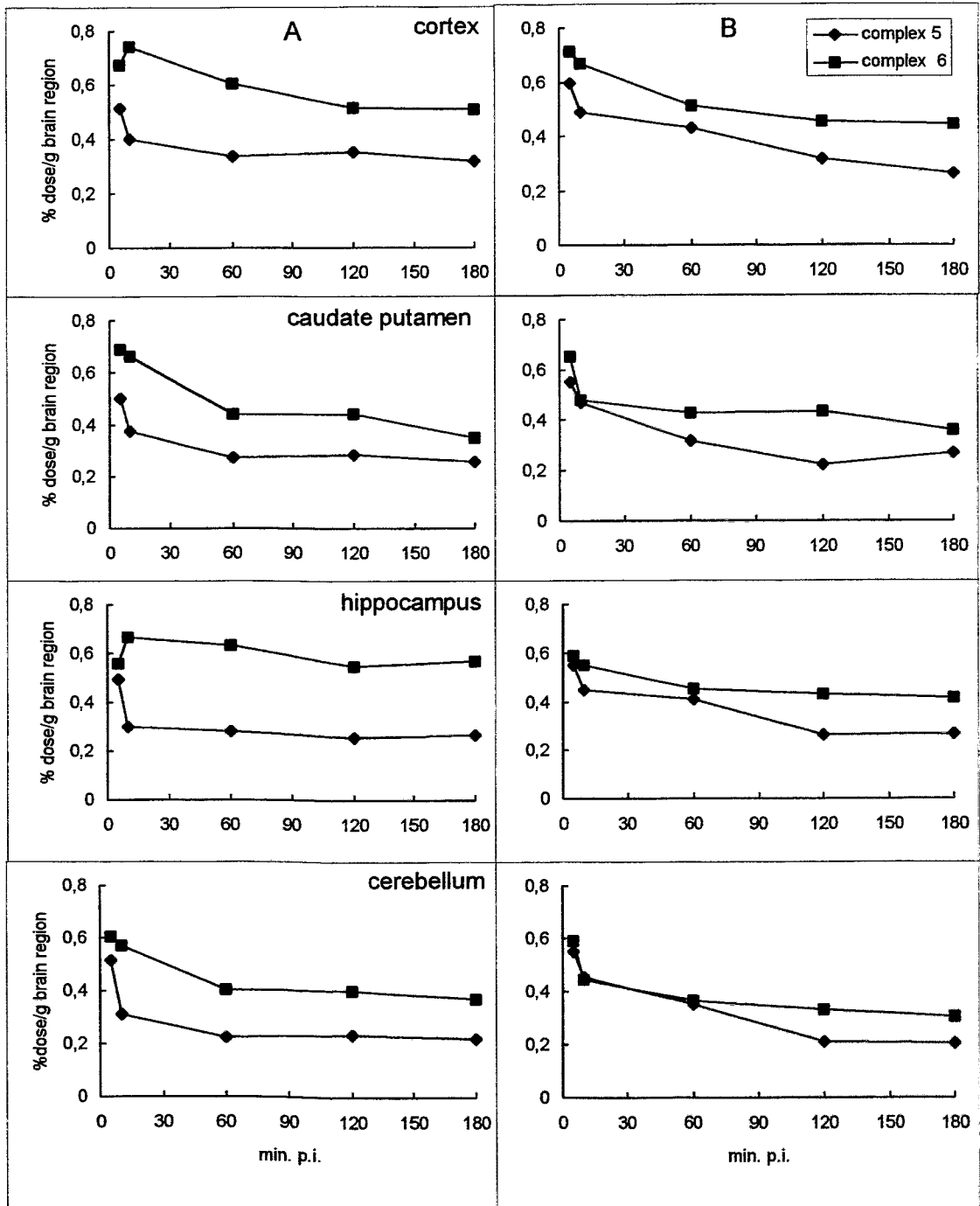


Fig. 3: Time course of radioactivity in various brain regions after injection of $^{99m/99}\text{Tc}$ complexes (A) and ^{99m}Tc complexes (B) in rats (mean values; $n = 3$)

For the complexes 5 and 6 the time course of radioactivity in selected brain regions (5 to 180' p.i.), especially in the cortex (frontal), the caudate putamen, the hippocampus and the cerebellum is demonstrated in Fig. 3A. The accumulation of radioactivity was highest in the brain regions at 5 min p.i. and declined gradually over the 180 min. period. The washout appears to be somewhat slower from the serotonin receptor-rich regions (cortex and hippocampus) compared with the other brain parts (caudate putamen; cerebellum). A moderate rise of the regional contrast ratio cortex/cerebellum

and hippocampus/cerebellum at 180 min after injection of these $^{99m/99}\text{Tc}$ complexes was observed (Table 4, column A).

These results suggest a long-term retention of the complexes in selected rat brain structures. In vivo receptorbinding as well as specific brain uptake in the regions of interest cannot be derived from the few results.

In Table 2 the results of the biodistribution of the $^{99m/99}\text{Tc}$ complexes (1 - 6) in the rat are summarized. The various complexes do not drastically differ in the distribution patterns in the peripheral tissue of lung, kidney, heart and liver. The enhanced activity in the lung was cleared very slow, while accumulation in the liver and kidney increased with time.

Unfortunately, the distribution data display a high blood activity and a slow blood clearance (Fig. 4; Table 2). About 70 % of the blood activity was always concentrated in the rat erythrocytes 5 min p.i. of the lipophilic complexes. *In vivo* the percentage bound to erythrocytes decreases slowly up to approx. 50 % at 120 min. p.i. (Table 5).

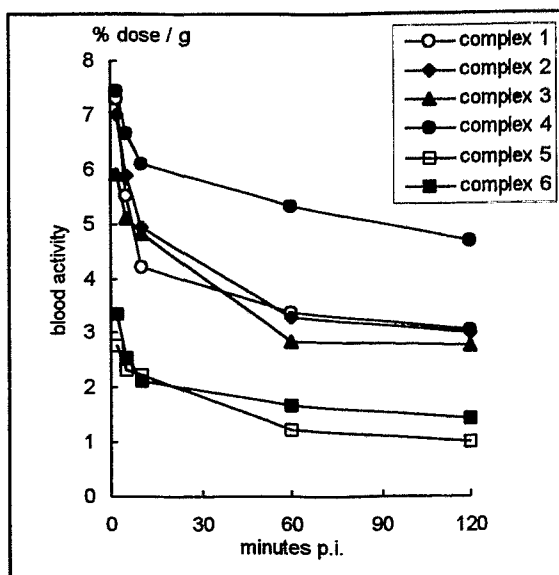


Fig. 4: Blood clearance curves of $^{99m/99}\text{Tc}$ complexes after injection in rats (mean values; n = 3 - 6)

The binding on erythrocytes as well as the elimination from the blood pool seem to correspond to the initial uptake and retention characteristics of the complexes in the liver. Especially complexes 5 and 6 show a relatively low blood activity (Fig. 4) and a correspondingly higher initial liver uptake (Table 2) compared the other oxygen-containing complexes under study.

Table 5: Radioactivity of erythrocytes after injection of oxygen-containing $^{99m/99}\text{Tc}$ complexes and ^{99m}Tc complex 6a in rats (mean % uptake \pm SEM ; n = 3 - 6)

Complex	Time of incubation	Radioactivity of erythrocytes
	[min.]	[% \pm SEM]
1	5	76 \pm 1
	120	56 \pm 2
2	5	78 \pm 2
	120	54 \pm 3
3	5	78 \pm 1
	120.	n.d.
4	5	72 \pm 2
	120	n.d.
5	5	76 \pm 2
	120	52 \pm 2
6	5	65 \pm 2
	120	47 \pm 1
6a	5	71 \pm 1
	120	50 \pm 1

Apparently, binding and retention of the oxygen-containing complexes in the peripheral organs and in the blood pool can be explained in the form of strong, unspecific binding on proteins of the rat plasma and tissues.

Table 6: *In vitro* binding to erythrocytes 5 minutes after incubation of $^{99m/99}\text{Tc}$ complexes in whole blood of different species (mean values \pm SEM ; n = 3 - 6)

Complex	Rat	Pig	Human
	% radioactivity \pm SEM	% radioactivity \pm SEM	% radioactivity \pm SEM
1	75 \pm 2	n.d.	37 \pm 2
5	69 \pm 2	24 \pm 2	15 \pm 3
6	70 \pm 3	28 \pm 1	20 \pm 2

For the interpretation of the biodistribution data it is important to note the species dependence of erythrocyte binding (Table 6; 5). The results discussed so far relate to c.a. $^{99m/99}\text{Tc}$ complexes. For further evaluation of the favourable uptake of the new oxygen-containing complexes in the rat brain it is necessary to compare the results with those obtained at the *no carrier added* level ^{99m}Tc . The identity of the complexes at both tracer levels was proved by HPLC [11], also the biological behaviour is similar as follows:

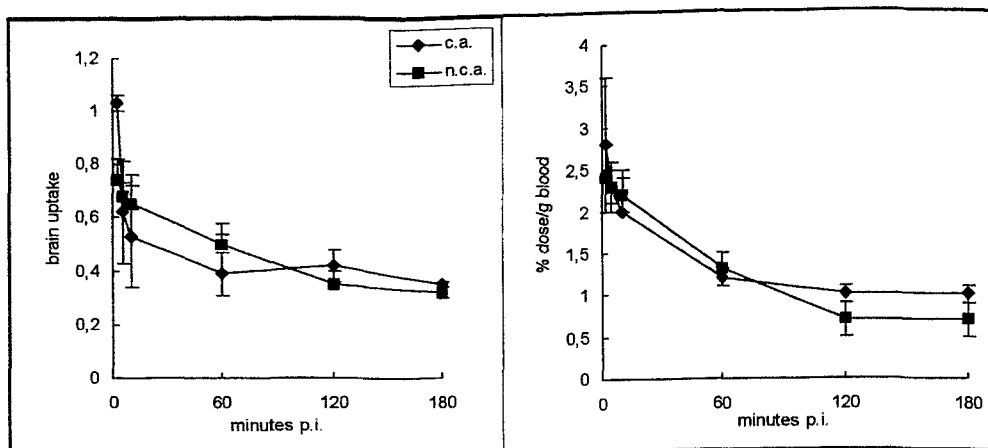


Fig. 5: Time course of distribution of $^{99m/99}\text{Tc}$ complexes **5** and ^{99m}Tc complexes **5a** compared in rats (mean % dose \pm SEM ; n = 3 - 6)

As shown in Table 2 and Fig. 5, similar distribution data were obtained at both tracer levels. The regional brain distribution (Fig. 3) as well as the target nontarget ratios (Table 4, column B) were found to be similar also for the c.a. and n.c.a. preparations of the complexes. The binding data to rat erythrocytes confirm the identity of the c.a. and the n.c.a. complexes (Table 5).

In summary, insertion of ether-oxygen in the complex structures dramatically improve the initial uptake in the rat brain. In all other aspects there is no significant difference in biodistribution compared with the corresponding oxygen-free, nitrogen-containing $^{99m/99}\text{Tc}$ complexes [6, 7].

These results indicate that the adjusted lipophilicity of the modified complexes shows an effect only on the initial brain uptake of the rat. The distribution pattern appears to be identical in *in vivo* behaviour for the carrier-added and no-carrier-added oxotechnetium(V) complexes.

References

- [1] Johannsen B., Pietzsch H.-J., Scheunemann M., Spies H. and Brust P. (1995) Oxotechnetium(V) and oxorhenium(V) complexes as potential imaging agents for the serotonin receptor. *J. Nucl. Med.* **36**, 27P (abs).
- [2] Johannsen B., Scheunemann M., Spies H., Brust P., Wober J., Syhre R. and Pietzsch H.-J. (1996) Technetium(V) and rhenium(V) complexes for 5-HT_{2A} serotonin receptor binding: structure-affinity considerations. *Nucl. Med. Biol.* **23**, 429 - 438.
- [3] Pietzsch H.-J., Scheunemann M., Fietz Th., Brust P., Spies H. and Johannsen B. (1995) Serotonin receptor-binding technetium and rhenium complexes. 5. Synthesis, characterization and biochemical evaluation of technetium and rhenium complexes derived from the 4-[p-fluorobenzoyl]-piperidine pharmacophore of ketanserin. *Annual Report 1995*, Institute of Bioinorganic and Radiopharmaceutical Chemistry, FZR-122, pp. 44 - 48.
- [4] Johannsen B., Pietzsch H.-J., Scheunemann M., Berger R., Spies H., Syhre R., Schenker Ch. and Brust P. (1996) Structural modification of serotonin receptor-binding technetium and rhenium complexes in order to improve receptor selectivity and blood-brain transfer. *J. Nucl. Med.* **37**, 17P.
- [5] Pietzsch H.-J., Scheunemann M., Brust P., Wober J., Spies H. and Johannsen B. (1996) Serotonin receptor-binding technetium and rhenium complexes. 11. Affinity and selectivity of oxorhenium(V) complexes derived from ketanserin, cisapride and MDL 72832. *This report*, pp. 9 - 12.
- [6] Syhre R., Berger R., Pietzsch H.-J., Scheunemann M., Spies H. and Johannsen B. (1995) Serotonin distribution and brain uptake in the rat of $^{99m/99}\text{Tc}$ oxotechnetium(V) complexes with affinity to the 5-HT₂ receptor. *Annual Report 1995*, Institute of Bioinorganic and Radiopharmaceutical Chemistry, FZR-122, pp.51 - 58.

- [7] Syhre R., Pietzsch H.-J., Scheunemann M., Spies H. and Johannsen B. (1995) Serotonin receptor-binding technetium and rhenium complexes. Binding characteristics of $^{99m/99}\text{Tc}$ oxotechnetium(V) complexes to erythrocytes of rats and humans. *Annual Report 1995*, Institute of Bioinorganic and Radiopharmaceutical Chemistry, FZR-122, pp.58 - 63.
- [8] Johannsen B., Berger R., Brust P., Pietzsch H.-J., Scheunemann M., Seifert S., Spies H. and Syhre R. (1997) Structural modification of receptor-binding technetium-99m complexes in order to improve brain uptake. *Eur. J. Nucl. Med.*, in press.
- [8] Johannsen B., Berger R., Brust P., Pietzsch H.-J., Scheunemann M., Seifert S., Spies H. and Syhre R. (1996) Serotonin receptor-binding technetium and rhenium complexes. 12. Structural modification of receptor-binding technetium-99m complexes in order to improve brain uptake. *This report*, pp. 13 - 16.
- [9] Berger R., Friebe M., Pietzsch H.-J., Scheunemann M., Noll B., Fietz Th., Spies H. and Johannsen B. (1996) Lipophilicity and ionization properties of some amine-bearing technetium and rhenium "3+1" mixed-ligand chelates with same ligand structure. *This report*, pp. 43 - 47.
- [10] Scheunemann M., Pietzsch H.-J., Spies H., Brust P. and Johannsen B. (1996) Serotonin receptor-binding technetium and rhenium complexes. 10. Synthesis and characterization of rhenium and technetium complexes derived from partial structures of ketanserin, cisapride and MDL 72832. *This report*, pp. 5 - 8.
- [11] Seifert S., Pietzsch H.-J., Scheunemann M., Spies H., Syhre R. and Johannsen B. (1996) Serotonin receptor-binding technetium and rhenium complexes. 13. No carrier added preparations of "3+1" ^{99m}Tc complexes. *This report*, pp. 17 - 22.
- [12] Cremer J. E. and Malcom P. S. (1983) Regional brain flow, blood volume, and haematocrit values in the adult rat. *J. Cerebr. Blood. Flow Metab.* 3, 254 - 256.

7. Serotonin Receptor-Binding Technetium and Rhenium Complexes

15. Synthesis and Characterization of Oxorhenium(V) Complexes with N-functionalized Tridentate SNS Ligands

H.-J. Pietzsch, M. Scheunemann, R. Berger, P. Brust, H. Spies, B. Johannsen

Introduction

We previously reported on mixed-ligand Tc and Re complexes that show substantial 5-HT₂ serotonin receptor binding. In this class of compounds the protonable nitrogen of the side-chain is a crucial structural feature, which is, on the one hand, an essential constituent for 5-HT₂ affinity but, on the other restricts the blood-brain transfer, depending on the nature and pK of the amine functionality [1]. After having described our efforts to improve the low brain uptake of the complexes by insertion of oxygen into the pharmacophore [2], we now report on a further way to influence the pK value of the nitrogen by changing the position of the pharmacophore portion with respect to the metal centre.

Experimental

pK values, partition and distribution coefficients were determined as previously described [3, 4] from the capacity factors log k values obtained by HPLC using a Perkin-Elmer HPLC Controller System equipped with a UV/VIS spectrometric detector (254 nm) and a Hamilton PRP-1 column (250 x 4.1 mm; 10 µm). As mobile phase an isocratic eluent (acetonitrile and 0.01 M phosphate or citrate buffer, 75:25, v/v) was applied with a flow rate of 1.5 ml/min. Aniline, benzene, and bromobenzene were used as internal standards.

General synthesis procedure for the tridentate ligands d - f

A solution of the appropriate amine a - c (0.1 mol) in 30 ml of dry toluene was mixed with a solution of ethylene sulphide (0.2 mol) in 10 ml of dry toluene and allowed to stand 6 h at ambient temperature (sealed tube, argon flushed). The reaction mixture was then heated to 110 °C for 10 h, cooled, and filtered to remove a small amount of polyethylene sulphide. The solvent was removed to give the raw product as a nearly colourless liquid.

The ligands were isolated as hydrochlorides and purified by recrystallization from ethanol/diethylether.

Yields: 65 - 70 %.

Elemental analysis:

d: (Found: C, 51.1; H, 8.0; N, 7.0; S, 16.0; Cl, 17.8, C₁₇H₃₂N₂S₂Cl₂ requires C, 49.9; H, 8.1; N, 6.8; S, 15.5; Cl, 18.0 %)

e: (Found: C, 53.6; H, 8.0; N, 6.6; S, 15.1; Cl, 16.7, C₁₉H₃₄N₂S₂Cl₂ requires C, 52.8; H, 7.7; N, 6.4; S, 14.8; Cl, 17.1 %)

f: (Found: C, 47.9; H, 7.5; N, 7.0; S, 16.0; Cl, 17.7, C₁₆H₃₀N₂OS₂Cl₂ requires C, 47.3; H, 7.2; N, 6.8; S, 16.3; Cl, 18.0 %)

General synthesis procedure for the complexes 1 - 4

A mixture of 0.3 mmol of the tridentate ligand d - f and 0.3 mmol of 4-methoxythiophenol (for 1, 3 and 4) or sodium methylthiolate (for 2) was added to a stirred suspension of [ReOCl₃(PPh₃)₂] (250 mg, 0.3 mmol) in 0.15 N sodium acetate/20 ml of methanol. The reaction mixture was refluxed for 45 min, at which time the metal precursor dissolved. The colour changed from greenish-yellow to greenish-brown. After cooling to ambient temperature, the mixture was diluted with 50 ml of dichloromethane and washed three times with 10 ml of water. The organic phase was separated from the mixture and dried over sodium sulphate. After evaporation of the solvent the product was isolated by column chromatography (silica gel, CHCl₃/methanol (90/10) as eluent).

Yields: 60 - 65 %.

Elemental analysis: 1: (Found: C, 43.3; H, 5.3; N, 4.2; S, 14.4, C₂₄H₃₅N₂O₂S₃Re requires C, 43.2; H, 5.0; N, 4.1; S, 14.3 %)

2: (Found: C, 37.7; H, 5.4; N, 4.9; S, 16.8, C₁₈H₃₁N₂OS₃Re requires C, 37.7; H, 5.5; N, 4.9; S, 16.6 %)

3: (Found: C, 45.2; H, 5.4; N, 4.1; S, 13.9, C₂₆H₃₇N₂O₂S₃Re requires C, 44.9; H, 5.7; N, 4.0; S, 14.0 %)

4: (Found: C, 39.7; H, 4.5; N, 3.7; S, 12.7, C₂₅H₃₄N₂O₇S₃Re requires C, 39.2; H, 4.6; N, 3.8; S, 12.4 %)

Results and Discussion

A series of novel mixed-ligand oxorhenium(V) complexes **1** - **4**, derived from the class of 5-HT_{2A} binding complexes, exemplified in Fig. 1, were synthesized and characterized.

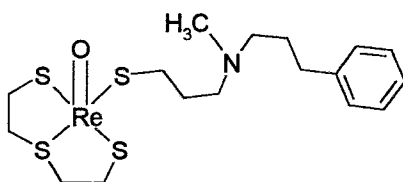


Fig. 1: Example of 5-HT_{2A} receptor-binding Re complex (**4**)

All the compounds differ from the original receptor-binding complexes in the position of the N-containing pharmacophore. In this respect the substances are comparable with the recently described analogous Tc and Re complexes [5, 6].

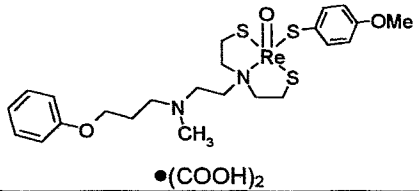
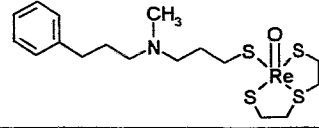
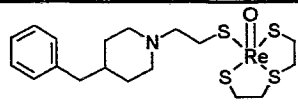
Table 1 reveals that the change in position of the N-containing pharmacophore portion in the complex molecule has a considerable effect on the pK value of the nitrogen (compare with complexes **5** and **6** in Table 1). The successful decrease in apparent pK value achieved by the structural modification is related to a significant increase in lipophilicity in terms of the distribution coefficient at pH 7.4.

Apart from the possibility of lowering the pK value by insertion of oxygen into the pharmacophore group [2], this finding presents a further way of influencing the pK value by modifying the coordination sphere.

Table 1: pK values, partition (P) and distribution (D) coefficients of N-functionalized Re chelates determined by HPLC

Complex	pK _{HPLC}	D _{HPLC} (pH 7.4)	P _{HPLC}	log P _{HPLC}	log D _{HPLC}	
	1	9.04	100	11900	4.08	2.00
	2	9.05	10	3500	3.54	1.00
	3	8.92	450	35500	4.55	2.65

Table 1 cont.

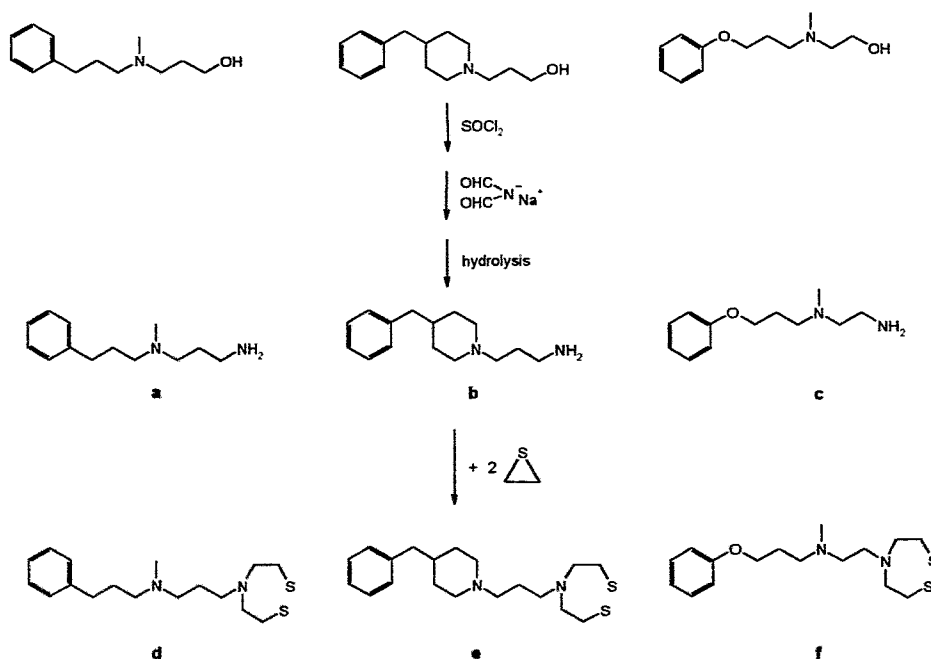
Complex	pK_{HPLC}	D_{HPLC} (pH 7.4)	P_{HPLC}	$\log P_{\text{HPLC}}$	$\log D_{\text{HPLC}}$
 •(COOH) ₂	4	7.21	9500	14340	4.16
	5 ref. [1]	10.08	5	3000	3.48
	6 ref. [1]	9.70	5	4150	3.62

Synthesis of the tridentate ligands

The general synthesis procedure is illustrated in Scheme 1. Starting from the appropriate amino alcohols [6], the primary amines **a** - **c** were prepared by standard procedures using thionyl chloride and sodium diformyl amide.

Subsequent addition of ethylene sulphide to **a**, **b** and **c** following a procedure described by Corbin *et al.* [7] yielded the tridentate ligands **d**, **e** and **f**. The products were isolated as hydrochlorides and purified by recrystallisation from ethanol/diethylether

Scheme 1: General synthesis procedure for the tridentate S, NR, S ligands **d** - **f** to form oxorhenium(V) complexes according to the [3+1] mixed ligand approach



Synthesis of the complexes 1 - 4

The oxorhenium(V) complexes 1 - 4 in Table 1 were prepared by ligand exchange reaction of $[\text{ReOCl}_3(\text{PPh}_3)_2]$ with equimolar amounts of the appropriate SNS ligand (c - f) and 4-methoxythiophenol (for 1, 3, 4) or sodium methylthiolate (for 2), following a modified procedure described by Papadopoulos *et al.* [5].

After column chromatography of the raw material only the *syn*-isomer (side-chain on the N-donor atom is directed to the oxygen of the $\text{Re}=\text{O}$ core) was isolated and investigated.

References

- [1] Johannsen B, Scheunemann M, Spies H, Brust P, Wober J, Syhre R and Pietzsch H.-J. (1996) Technetium(V) and rhenium(V) complexes for 5-HT_{2A} serotonin receptor binding: structure-affinity considerations. *Nucl. Med. Biol.* **23**, 429 - 438.
- [2] Johannsen B., Berger R., Brust P., Pietzsch H. J., Scheunemann M., Seifert S., Spies H. and Syhre R. (1997) Structural modification of receptor-binding technetium-99m complexes in order to improve brain uptake. *Eur. J. Nucl. Med.*, in press.
- [3] Berger R., Fietz Th., Glaser M., Spies H. and Johannsen B. (1995) Determination of partition coefficients for coordination compounds by using HPLC. *Annual Report 1995*, Institute of Bioinorganic and Radiopharmaceutical Chemistry, FZR-122, pp. 69 - 72.
- [4] Berger R., Scheunemann M., Pietzsch H.-J., Noll B., Noll St., Hoepfing A., Glaser M., Fietz Th., Spies H. and Johannsen B. (1995) pK_a value determinations by HPLC of some Tc and Re complexes containing an ionizable group. *Annual Report 1995*, Institute of Bioinorganic and Radiopharmaceutical Chemistry, FZR-122, pp. 73 - 79.
- [5] Mastrostamatis S. G., Papadopoulos M. S., Pirmettis I. C., Paschali E., Varvarigou A. D., Stassinopoulou C. I., Raptopoulou C. P., Terzis A. and Chiotellis E. (1994) Tridentate ligands containing the SNS donor atom set as a novel backbone for the development of technetium brain-imaging agents. *J. Med. Chem.* **37**, 3212 - 3218.
- [6] Papadopoulos M., Chiotellis S., Spies H., Friebe M., Berger R. and Johannsen B. (1995) Rhenium and technetium mixed-ligand chelates functionalized by amine groups 1. Rhenium complexes with *p*-substituted benzenethiols as monodentate ligands. *Annual Report 1995*, Institute of Bioinorganic and Radiopharmaceutical Chemistry, FZR-122, pp. 80 - 82.
- [7] Corbin J. L., Miller K. F., Wherland S., Bruce A. E. and Stiefel E. I. (1984) Preparation and properties of tripodal and linear tetradentate N,S-donor ligands and their complexes containing the MoO_2^{2+} core. *Inorg. Chim. Acta* **90**, 41 - 51.

8. Synthesis of Neutral Amine Group Bearing "3+1" Mixed-Ligand Oxorhenium(V) Complexes

M. Friebe, M. Papadopoulos¹, S. Chiotellis¹, H. Spies, R. Berger, B. Johannsen

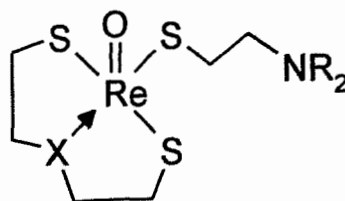
¹Institute of Radioisotopes and Radiodiagnostic Products of the National Center for Scientific Research "Demokritos", Athens (Greece)

Introduction

The synthesis of amine-group bearing rhenium complexes was performed in order to study the relationships between structural parameters such as lipophilicity or basicity (expressed in terms of log P and pK) and the brain uptake of oxometal(V) complexes (Re; Tc). The compounds shown in Scheme 1 are tertiary amine bearing mixed-ligand "3+1" complexes where the tertiary amine group is part of the monodentate ligand. The tridentate dithiolate ligand is variable with respect to the neutral donor group X. Tc complexes of this type have been the subject of earlier studies [1].

The first report informs on the preparation and characterization of a series of rhenium complexes where the tridentate ligand ($\text{HS}-\text{CH}_2\text{CH}_2-\text{X}-\text{CH}_2\text{CH}_2-\text{SH}$) contains O, S, or N-alkyl as the neutral donor group X, and the pendent amino group bears dimethyl, diethyl and di-n-butyl groups or is a piperidinyl or morpholinyl amine.

Scheme 1: General formula and numbering scheme of complexes $[ReO(SXS)(S-CH_2CH_2-NR_2)]$
(Pip = piperidine; Mo = morpholine)



NR ₂	X:	S	O	NMe	NEt	NBu
NMe ₂		1a	2a	3a	4a	5a
NEt ₂		1b	2b	3b	4b	5b
NBu ₂		1c	2c	3c	4c	5c
Pip		1d	2d	3d	4d	5d
Mo		1e	2e	3e	4e	5e

Experimental

Tetrabutylammonium tetrachlorooxorhenium(V), chloro(3-thiapentane-1,5-dithiolato)oxorhenium(V) and *trans*-monooxotrichlorobis(triphenylphosphine)rhenium(V) were obtained by the described procedures [2, 3, 4].

Preparation of $[MO(SXS)(S-CH_2CH_2-NR_2)]$ **1a** - **1e** (X = S) (general procedure)

A fourfold molar excess of NR₂-ethylene thiol (x mg, 0.3 mmol) in acetonitrile (2 ml) was added to a stirred and refluxed solution of chloro(3-thiapentane-1,5-dithiolato)oxorhenium(V) (29 mg, 74 μmol) in acetonitrile (4 ml). After a period of 30 minutes the reaction mixture was evaporated to dryness. The residue was dissolved in trichloromethane and purified by liquid chromatography over silica gel 60 with trichloromethane as the mobile phase (eluent: trichloromethane/methanol (19:1)) Complexes were precipitated as brown powder after the volume of the elution mixture had been reduced by evaporation. For **1a** and **1b**, the solvent was removed, the residue redissolved in dichloromethane, and - after adding methanol - the solution was slowly evaporated.

Preparation of $[MO(SXS)(S-CH_2CH_2-NR_2)]$ **2a** - **2e** (X = O) (general procedure)

Tetrabutylammonium tetrachlorooxorhenate(V) (87.9 mg, 0.15 mmol) was dissolved in trichloromethane (5 ml), stirred and cooled to 0 °C. A solution of 3-oxapentane-1,5-dithiol (20.5 mg, 0.15 mmol) and NR₂-ethylene thiol (0.20 mmol) in trichloromethane (2 ml) was added. After stirring for 30 minutes the reaction mixture was evaporated to dryness. The residue was dissolved in acetone reduced in volume by slow evaporation and the purple solid obtained was first washed with a small portion of methanol and then with ether (3 x 5ml). Complexes **2a**, **2c**, **2e** could not be obtained in a solid state.

Preparation of $[MO(SXS)(S-CH_2CH_2-NR_2)]$ **3a** - **3e**, **4a** - **4e**, **5a** - **5e** (X = N(-CH₃); N(-C₂H₅) and N(-C₄H₉)) (general procedure)

A mixture of the SNS ligand (0.2 mmol) and the monodentate ligand (0.2 mmol) in methanol (2 ml) was added to a stirred suspension of *trans*-monooxotrichlorobis(triphenylphosphine)rhenium(V) (166 mg, 0.2 mmol) in methanol (20 ml). The suspension was stirred and heated to 70 °C for 60 minutes by which time the greenish-yellow colour of the precursor compound had turned a dark greenish brown. After cooling to room temperature, the reaction mixture was diluted with dichloromethane and water/hydrochloric acid (pH ≈ 4) was added. The aqueous phase was reextracted with trichloromethane, the organic extract was separated and dried over sodium sulphate.

After purification by liquid chromatography over silica gel, first with trichloromethane and then with trichloromethane/methanol (19:1), the complexes were precipitated as green solids by slow evaporation of the mixtures: - trichloromethane/ethanol **4c**, **4d**, **5d**, **5e**¹

- trichloromethane/n-heptane **3a**, **3b**, **3d**, **3e**, **4e**

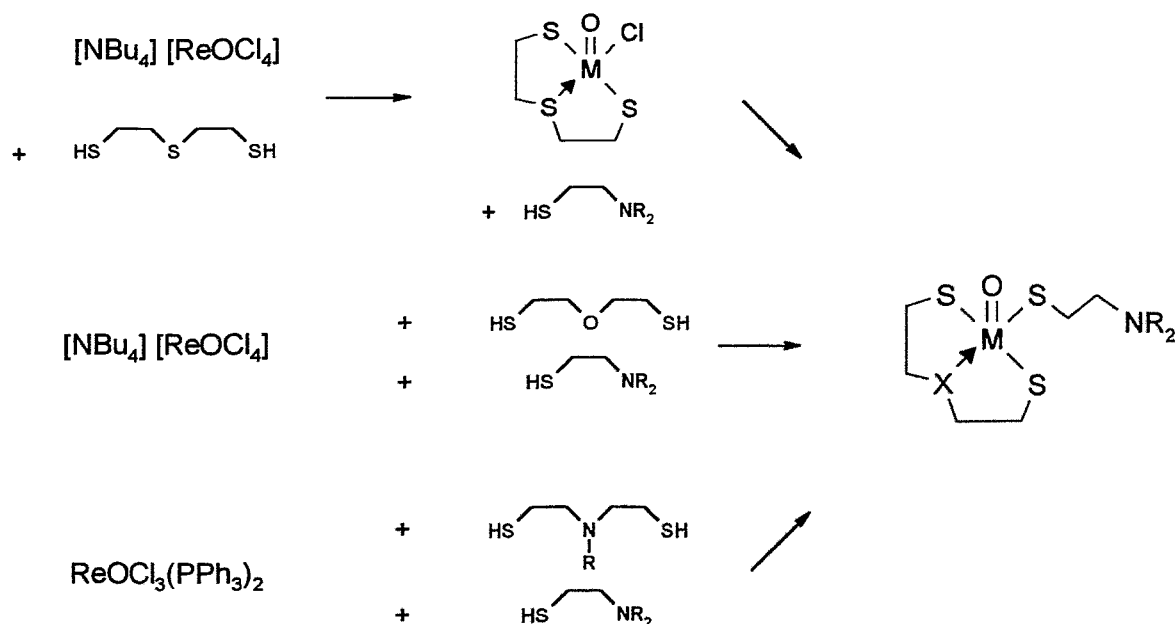
- diethylether/n-heptane **4a**, **4b**

Results and Discussion

The rhenium complexes containing SSS and SOS donors were obtained by reaction of tetrabutylammonium tetrachlorooxorhenium(V) [2, 5] with the tri- and monodentate ligands in a one-pot reaction [6, 7] (see Scheme 1). As an alternative route rhenium(V) complexes containing SSS donors were also synthesized using a two-step reaction by addition of an excess of the appropriate monodentate ligand to chloro(3-thiapentane-1,5-dithiolato)oxorhenium(V) as described by Fietz *et al.* [5, 3]. This procedure resulted in an increased yield. Analogous intermediates of the other tridentate ligands (X = O, N-R) with the chlorooxometal core are unknown and our efforts to prepare such stable precursors failed [6].

For preparation of the SNS-containing rhenium complexes transmonooxotrichlorobis(triphenylphosphine)rhenium(V) [4] was used as a precursor, yielding complexes **3a** - **3e**, **4a** - **4e** and **5a** - **5e** in the reaction with an equimolar mixture of tri- and monodentate ligands (see Scheme 2).

Scheme 2: Pathways to "3+1" oxorhenium(V) complexes



The yields of crystallized complexes for the various donor ligands differ considerably (9 - 62 % theor.). The best yields were achieved for SSS-containing complexes obtained by the two-step procedure. The crystallization tendency decreases with more lipophilic complexes.

The two precursors used for the synthesis differ in their reactivity, which should match that of the tridentate ligand. So we obtained pure stable products in higher yields with the tetrabutylammonium tetrachlorooxorhenium(V) precursor in the case of HSSSH and HSOSH ligands. For preparation of SNS-containing complexes the trans-monooxotrichlorobis(triphenylphosphine)rhenium(V) precursor gave the best yields.

All the resulting complexes were characterized by elemental analysis, IR spectroscopy, HPLC and melting point. Data are summarized in Table 1.

One of the compounds (**2d**) was examined by EXAFS to determine the structural parameters.

Table 1: Data of complexes [ReO(SXS)(S-CH₂-CH₂-NR₂)]

Complex No.	Molecular mass	M.p. [°C]	IR $\nu(\text{Re}=\text{O})$ [cm⁻¹]	Morphology
<u>1a</u>	458.7	169 - 172	965	brown needles
<u>1b</u>	486.7	104 - 144	965	brown needles
<u>1c</u>	542.9	-	-	redbrown needles
<u>1d</u>	498.8	-	962	brown powder
<u>1e</u>	500.7	207 - 220	968	brown powder
<u>2b</u>	470.7	123 - 125	974	purple powder
<u>2d</u>	482.7	144 - 146	976	purple powder
<u>3a</u>	455.7	124	952	green needles
<u>3b</u>	483.7	168 - 174	948	green needles
<u>3d</u>	495.7	201 - 210	948	green needles
<u>3e</u>	497.7	164	950	green compact crystals
<u>4a</u>	469.7	103 - 104	960	fine green needles
<u>4b</u>	497.8	92 - 94	952	fine green needles
<u>4c</u>	553.9	94 - 98	952	amorph green powder
<u>4d</u>	509.8	130 - 134	952	green compact crystals

Complex No.	Molecular mass	M.p. [°C]	IR $\nu(\text{Re}=\text{O})$ [cm ⁻¹]	Morphology
4e	511.7	170 - 173	948	green compact crystals
5a	497.8	-	-	green precipitate
5b	525.8	-	-	green precipitate
5d	537.8	-	952	green precipitate
5e	539.8	135 - 138	952	green powder/compact crystals

Correct elemental analyses were determined for all complexes with the exception for **1c** and **5a**, which contained impurities; and **2a**; **2c** and **2e**, which could not be obtained as solids. The infrared spectra (in KBr) of all rhenium complexes showed the expected Re=O stretch for the monooxo species in the range of 948 - 976 cm⁻¹ (Table 1).

EXAFS

The expected structure of compound **2d** was confirmed by the EXAFS investigations. Indeed an oxydation state of +V for rhenium could be evidenced by a short bound oxygen at 1.65 Å, typical for the Re=O core. The donor atoms of the first coordination shell were identified as three sulphur atoms with an average bond distance of about 2.27 Å (mercaptide sulphur atoms) and one oxygen atom with a bond distance of 2.06 Å, corresponding to an ether oxygen.

Table 2: Final fit

Coordination number	Atom	R [Å]	σ [Å ²] (Debye-Waller-factor)
1	O	1.65	0.001
1	O	2.06	0.002
3	S	2.27	0.002

Detailed description of the method will be published next time. I am grateful to R. Jankowsky for his help.

The rhenium complexes are soluble in trichloromethane, dichloromethane and acetone (**1a** - **5e**), slightly soluble in methanol and ethanol (**1a** - **5e**), and insoluble in ether (**1a** - **3e**, **4c** - **4e**), heptane (**1a** - **4e**) and water (**1a** - **5e**). Whereas all the compounds were found to be stable in the solid state and solution, decomposition was observed for complexes **2b** and **2d** when applied to a silica gel column and in the solute state.

References

- [1] Spies H., Syhre R. and Pietzsch H.-J. (1990) Radiopharmaceutical studies on technetium complexes with tridentate monodentate thiole ligands, *Plzen.lek.Sborn.*, **62**, 85 - 86.

- [2] Alberto R., Schibli R., Egli A., Schubiger P. A., Herrmann W. A., Artus G., Abram U. and Kaden T. A., (1995) Metal carbonyl synthesis XII. Low pressure carbonylation of $[\text{MOC}_4\text{L}]^-$ and $[\text{MO}_4]^-$: the technetium(I) and rhenium(I) complexes $[\text{NET}_4]_2[\text{MCl}_3(\text{CO})_3]$. *J. Organomet. Chem.* **493** 119 - 127.
- [3] Fietz Th., Spies H., Pietzsch H.-J. and Leibnitz P. (1995) Synthesis and molecular structure of chloro(3-thiapentane-1,5-dithiolato)oxorhenium(V), *Inorg. Chim. Acta* **231**, 233 - 236.
- [4] Johnson N. P., Lock C. J. and Wilkinson L. (1967) Complexes of rhenium(V) *Inorg. Synth.* **9**, 145.
- [5] Spies H., Fietz Th., Glaser M., Pietzsch H.-J. and Johannsen B. (1995) The "n+1" concept in the strategy of novel technetium and rhenium tracers. In: Nicolini M., Bandoli G., Mazzi U., *Technetium and Rhenium in Chemistry and Nuclear Medicine* **4**, p. 243, SGEditional Padova
- [6] Fietz Th. (1996) Oxorhenium(V)-Komplexe mit "3+1" Gemischtligandkoordination. *PhD Thesis*; TU Dresden, pp. 24 - 25.

9. Preparation of Amine Group Bearing "3+1" Mixed-Ligand Oxotechnetium(V) Complexes at the Carrier-Added Level

M. Friebe, M. Papadopoulos¹, E. Chiotellis¹, H. Spies, R. Berger, B. Johannsen

¹Institute of Radioisotopes and Radiodiagnostic Products of the National Center for Scientific Research "Demokritos", Athens (Greece)

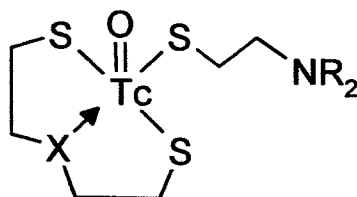
Introduction

Even in the early 1990s, neutral tertiary amine bearing "3+1" oxotechnetium(V) complexes were synthesized by Spies *et al.* [1] and Chiotellis *et al.* [2], and preliminary studies on the relationships between structural parameters and lipophilicity as well as basicity (expressed in terms of log P and pK) were carried out [1].

For some of these complexes a considerable brain uptake was found [2]. In order to obtain more information on the structure dependence of brain uptake it was necessary to make available and to study more technetium(V) complexes belonging to different classes of substances.

Here we describe the preparation and characterization of a series of oxotechnetium complexes at the c.a. level. Tri- and monodentate ligands and, therefore, the composition of the Tc complexes is analogous to the Re compounds described in the preceding article.

Scheme 1: General formula and numbering scheme of complexes $[\text{TcO}(\text{SXS})(\text{S}-\text{CH}_2\text{CH}_2-\text{NR}_2)]$



NR ₂	X:	S	O	NMe	Net	NBu
NMe ₂		1a	2a	3a	4a	5a
NEt ₂		1b	2b	3b	4b	5b
NBu ₂		1c	2c	3c	4c	5c
Pip		1d	2d	3d	4d	5d
Mo		1e	2e	3e	4e	5e

Experimental

Technetium-99/99m complexes

For radiolabelling a ⁹⁹Mo/^{99m}Tc generator "Ultra Techne Cow" (Mallinckrodt) was used.

A mixture of sodium [^{99m}Tc]pertechnetate (150 MBq in 1.0 ml of saline) and ammonium [⁹⁹Tc]pertechnetate (1.2 μmol in 0.12 ml of saline) was reduced by 0.12 ml of a stannous chloride solution (120 μmol in 0.1N hydrochloric acid) in the presence of 0.1 M sodium gluconate solution (1.6 ml) to give

Tc(V) gluconate. The purity of the precursor was analysed by thin layer chromatography over silica gel plates in acetone with a radioactivity detector. An activity peak at the starting range of the plate indicates complete reduction of pertechnetate.

Preparation of [TcO(SXS)(S-CH₂CH₂-NR₂)] 1a-5e

Tc(V) gluconate (1.2 μmol; 150 MBq in ≈2 ml) and a mixture of tridentate ligands (1.2 μmol) and monodentate ligands ¹(1.8 μmol) in ethanol (0.6 ml) were vortexed and kept at room temperature for 10 minutes. The colour of the mixture changes from colourless to yellow. The pH value of the solution was enhanced to 11 by 0.1 N sodium hydroxide² and dichloromethane (1 ml) was added quickly. The organic portion was separated and reextracted with water/hydrochloric acid (pH ≈ 4).

The purity of the complexes was analysed by thin layer chromatography over silica gel plates in methanol/0.1 N hydrochloric acid (4:1) with an activity detector. Three radioactive compounds were detected in the reaction mixture. After extraction one major peak (95 - 99 %) and impurities (< 5 %) were detected.

¹ an equimolar tri- and monodentate ligand mixture was used for complex 2d and 2e.

² the pH values of the complex solutions 2d ; 2e ; 4c ; 5d and 5e were enhanced to 8.5.

Results and Discussion

New [^{99/99m}Tc]technetium complexes were obtained in a two-step reaction, starting from pertechnetate via a ligand intermediate complex according to Scheme 1.

As the first step the precursor Tc(V) gluconate was prepared. The oxotechnetium complexes were obtained by a ligand exchange reaction of Tc(V) gluconate with a tridentate monodentate ligand mixture. The complexes were purified by extraction into the organic phase (dichloromethane), reextraction into an aqueous phase (pH = 4), and were not isolated at solid state. Radiochemical purity was determined by thin layer chromatography (Fig. 2) and HPLC.

R_f values for all technetium complexes were determined and are listed in Table 1.

In order to elucidate for the expected composition of the complexes, one representative was prepared as a crystalline technetium complex and the structure parameters were obtained by XRD.

Table 1: R_f data of complexes [TcO(SXS)(S-CH₂-CH₂-NR₂)] on silica gel plates in methanol/hydrochloric acid (4:1)

Complex No.	R _f value	Complex No.	R _f value	Complex No.	R _f value
<u>1a</u>	0.2	<u>2e</u>	0.	<u>4d</u>	0.2
<u>1b</u>	0.3	<u>3a</u>	0.3	<u>4e</u>	0.3
<u>1c</u>	0.5	<u>3b</u>	0.4	<u>5a</u>	0.3
<u>1d</u>	0.3	<u>3c</u>	0.6	<u>5b</u>	0.4
<u>1e</u>	0.3	<u>3d</u>	0.3	<u>5c</u>	0.7
<u>2a</u>	0.3	<u>3e</u>	0.3	<u>5d</u>	0.2
<u>2b</u>	0.4	<u>4a</u>	0.3	<u>5e</u>	0.2
<u>2c</u>	0.6	<u>4b</u>	0.4	-	-
<u>2d</u>	0.4	<u>4c</u>	-	-	-

The technetium complexes are stable for days in acidic/aqueous solution. Extraction from the reaction mixture in dichloromethane at pH 11 was not successful in any case, because of the relative instability of some complexes in alkaline solution. The yields after reextraction from dichloromethane in water/hydrochloric acid (pH 4) were different for the considered complexes. Best yields were obtained for **1a** - **1e** (about 70 % theor.).

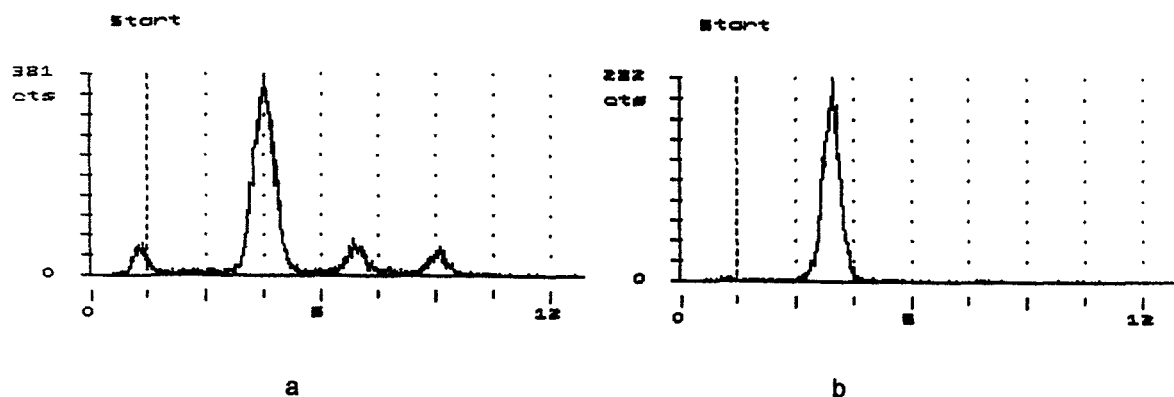


Fig. 1: TLC-pattern of complex **1b** before extraction (a) and after reextraction (b)

References

- [1] Spies H., Syhre R. and Pietzsch H.-J., (1990) Radiopharmaceutical studies on technetium complexes with tridentate/monodentate thiole ligands, *Plzen.lek. Sborn.* **62**, 85 - 86.
- [2] Mastrostamatis S. G., Papadopoulos M. S., Pirmettis I. C., Paschali E., Varvarigou A. D., Stassinopoulou C. I., Raptopoulou R., Terzis A. and Chiotellis E. (1994) Tridentate ligands containing the SNS donor atom set as a novel backbone for the development of technetium brain-imaging-agents. *J. Med. Chem.* **37**, 3212.

10. Lipophilicity and Ionization Properties of Some Amine-Bearing Technetium and Rhenium "3+1" Mixed-Ligand Chelates of the same Ligand Structure

R. Berger, M. Friebe, H.-J. Pietzsch, M. Scheunemann, B. Noll, T. Fietz, H. Spies, B. Johannsen

Introduction

In the design of brain (radio)pharmaceuticals special attention should be paid to lipophilicity and ionizability of the molecules. In the last ten years studies have been focused on ^{99m}Tc brain perfusion radiopharmaceuticals able to pass the blood-brain barrier and be accumulated within the brain. Neutral amino groups containing Tc complexes appear to be most favoured for this purpose.

Nowadays, research proceeds towards specific brain receptor binding ^{99m}Tc agents. Binding to the receptor site may require a positively charged nitrogen atom in the molecule, e.g. in 5-HT_{2A} receptor ligands. Such an essential constituent heavily affects the lipophilicity at physiological pH and hence diffusion through the BBB. For a better understanding of how physicochemical and structural properties such as (log) P and pK_a values of a Tc tracer influence its transport through the BBB, evaluation of the lipophilicity/pH relations of neutral, a protonable tertiary amine group containing "3+1" mixed-ligand Tc and analogous Re chelates has been aimed at.

Advances in reversed-phase high-performance liquid chromatography (RP-HPLC) and diverse publications on this topic [1 - 6] have encouraged us to use HPLC for the determination of both lipophilicity and ionizability of series of Tc/Re complexes.

The P and pK_a values were determined by means of lipophilicity/pH profiles [7].

Throughout this work all P values determined by RP-HPLC are notated as P_{HPLC} . The pK_a values are measured as pK_{HPLC} and after correction for the influence of organic solvent in the solution by means of the calibration curve (Fig. 1) they are given the denotation $pK_{a(c)}$.

Experimental

Experiments were performed and evaluated under almost the same conditions as described elsewhere in this Annual Report [8] for the determination of partition coefficients, i.e. with identical materials, reagent-grade chemicals, and methods. Samples were dissolved in a mixture of methanol/ acetonitrile or dimethyl sulphoxide (Re complexes: about 2 mg/ml, Tc complexes about 0.5 mg/ml). The determination of pK_{HPLC} involves the use of mobile phases of various pH values.

A PRP-1 column was used, and the elutions were carried out with a mixture of acetonitrile and buffers of definite pH values (volume ratio 3:1).

For a test series, buffers (frequently about ten or more) were employed to cover the pH range of about 2 to 10. The buffer components KH_2PO_4 and Na_2HPO_4 were completed by citric acid as well as 3-(cyclohexylamino)-1-propanesulphonic acid (CAPS) and a certain expansion of the pH range was achieved by adding either 0.1 M HCl or 0.1 M NaOH. Before each application the pH values of the eluents were measured after preparing the appropriate mixture of buffer and acetonitrile by using a glass electrode. At such a well defined pH value several samples with various chelates and the solution of reference substances were sequentially injected. Before injecting the first sample of a new eluent series with changed pH value, the time for equilibration of the column was at least 10 min at a flow rate of 2.5 ml/min [7].

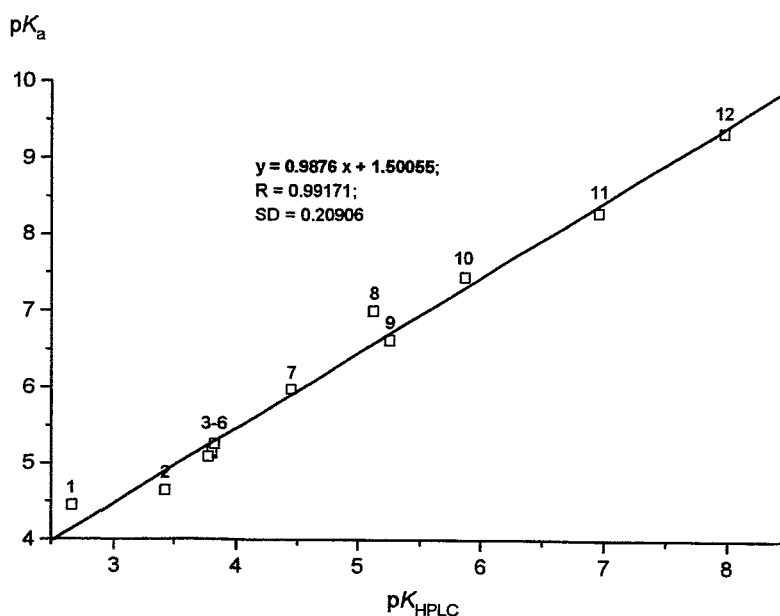
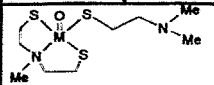
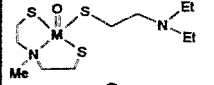
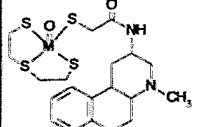
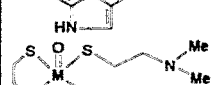
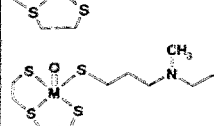


Fig. 1: Calibration curve pK_a/pK_{HPLC} using amines as standards, pK_a values for 12 amines were taken from [9]. (Found/literature): 1) *o*-toluidine (2.67/4.44), 2) aniline (3.43/4.63), 3) *p*-toluidine (3.78/5.08), 4) *N*-ethylaniline (3.81/5.12), 5) *N, N'*-dimethylaniline (3.81/5.15), 6) pyridine (3.83/5.25), 7) α -picoline (4.45/5.97), 8) 2,4-lutidine (5.13/6.99), 9) *N, N'*-diethylaniline (5.26/6.61), 10) collidine (5.87/7.43), 11) brucine (6.96/8.28), 12) benzylamine (7.98/9.33)

Results and Discussion

Table 1 summarizes the P_{HPLC} , $\log P_{HPLC}$ and $pK_{a(c)}$ values of several analogous neutral technetium and rhenium complexes as well as Tc/Re P_{HPLC} ratios.

Table 1: P_{HPLC} , $\log P_{HPLC}$ and $pK_{a(c)}$ values of several analogous neutral technetium ($M = Tc$) and rhenium complexes ($M = Re$) as well as Tc/Re P_{HPLC} ratios

No.	Complex structure	P_{HPLC}		$\log P_{HPLC}$		P_{HPLC} Tc/Re	$pK_{a(c)}$	
		Tc	Re	Tc	Re		Tc	Re
1		11	9	1.04	0.95	1.22	9.15	8.95
2		47	36	1.67	1.56	1.31	9.71	9.78
3		45	33	1.65	1.52	1.36	7.61	7.44
4		25	17	1.40	1.23	1.47	8.87	8.85
5		4450	3000	3.65	3.48	1.48	9.96	10.03

continued

Table 1: P_{HPLC} , $\log P_{\text{HPLC}}$ and pK_{HPLC} values of several analogous neutral technetium ($M = \text{Tc}$) and rhenium complexes ($M = \text{Re}$) as well as Tc/Re P_{HPLC} ratios (continued)

No.	Complex structure	P_{HPLC}		$\log P_{\text{HPLC}}$		P_{HPLC} Tc/Re	$pK_{\text{a(c)}}$	
		Tc	Re	Tc	Re		Tc	Re
6		21	14	1.32	1.15	1.50	9.05	9.13
7		1950	1300	3.29	3.11	1.50	9.52	9.52
8		2200	1460	3.34	3.16	1.51	9.58	9.58
9		3250	2115	3.51	3.33	1.52	9.93	10.20
10		23	15	1.36	1.18	1.53	7.20	7.23
11		7540	4750	3.88	3.68	1.59	9.91	10.03
12		6600	4150	3.82	3.62	1.59	9.67	9.66
13		3585	2230	3.55	3.35	1.61	9.39	9.52
14		4025	2500	3.60	3.40	1.61	9.47	9.58
15		133	78	2.12	1.89	1.70	9.51	9.65
16		123	72	2.09	1.86	1.71	9.15	9.05
17		112	65	2.05	1.81	1.72	7.37	7.46
18		26	15	1.41	1.16	1.73	7.17	7.25
19		14	8	1.15	0.90	1.75	7.17	7.16
20		313	178	2.50	2.25	1.76	8.99	9.25
21		32	17	1.51	1.23	1.88	8.98	8.83
22		120	63	2.08	1.80	1.90	9.59	9.79
23		137	71	2.14	1.85	1.93	9.51	9.56
24		308	158	2.49	2.20	1.95	9.42	9.43

continued

Table 1: P_{HPLC} , $\log P_{\text{HPLC}}$ and $pK_{\text{a(c)}}$ values of several analogous neutral technetium (M = Tc) and rhenium complexes (M = Re) as well as Tc/Re P_{HPLC} ratios (continued)

No.	Complex structure	P_{HPLC}		$\log P_{\text{HPLC}}$		P_{HPLC} Tc/Re	$pK_{\text{a(c)}}$	
		Tc	Re	Tc	Re		Tc	Re
25		154	79	2.19	1.89	1.95	9.50	9.47
26		622	310	2.79	2.49	2.01	9.76	9.92
27		8640	4270	3.94	3.63	2.02	9.68	9.87
28		1595	775	3.20	2.89	2.06	9.57	9.70
29		29	12	1.46	1.08	2.42	7.11	7.36
30		379	156	2.58	2.19	2.43	9.24	9.24

In Table 1, an always higher lipophilicity for the Tc complex can be deduced from the Tc/Re P_{HPLC} value pairs of the same ligand structure. A mean value of 1.72 results for the Tc/Re P_{HPLC} ratios. The mean difference between the lipophilicities of Tc and Re complexes is also demonstrated in Fig. 2, in which the $\log P_{\text{HPLC}}$ values of Tc on Re complexes are plotted. An almost parallel course of the linear regression function to the additional function $y = x$ can be observed.

Looking at the tridentate ligand parts of these complexes it can be seen that most of the complexes with an (SSS) chelate have lower Tc/Re P_{HPLC} ratios than (SN(R)S) chelates, exceptions are Nos. 1, 2, 5.

Considering the monodentate ligand parts of the complexes, a benzene ring in the ligand seems to have a less enhancing effect (Tc/Re P_{HPLC} ratio: 1.5 - 1.6) than piperidinyl or morpholinyl ligands (1.7 - 2.4).

An analogous difference between Re and Tc complexes has not been found for the $pK_{\text{a(c)}}$ values.

It is likely that Tc compounds compared to Re compounds have a higher lipophilicity as observed. However these results remain to be proven in detail.

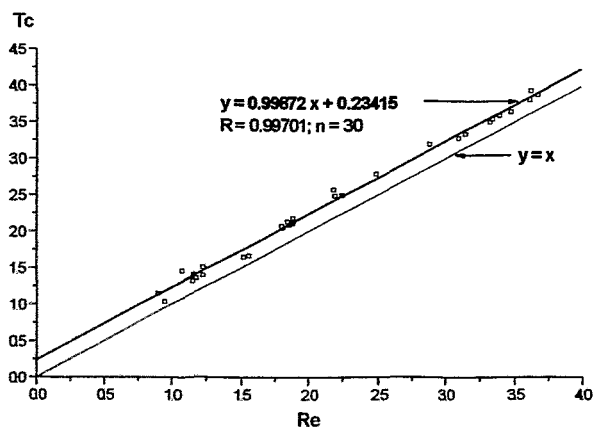


Fig. 2: A plot of the logarithm of $P_{\text{HPLC}}(\text{Tc})$ on $P_{\text{HPLC}}(\text{Re})$ values

Our systematic studies enable us to establish rules of thumb:

- 1) Replacement of the central heteroatom in the tridentate ligand increases P_{HPLC} in the rank order N-Me < N-Et ~ S ~ O < N-Bu. A similar dependence is not evident for the $pK_{\text{a(c)}}$ values.
- 2) Lengthening of the N-alkyl side chains in the monodentate ligand increases the $pK_{\text{a(c)}}$ as well as the P_{HPLC} values.
Apart from the morpholine derivatives the lipophilicity grows as expected with the number of the carbon atom in the amine group according to Mor ~ NMe₂ < NEt₂ < Pip < NBU₂.

References

- [1] Lee D. P. (1982) Reversed-phase HPLC from pH 1 to 13. *J. Chromatogr. Sci.* **20**, 203 - 208.
- [2] Rudzinski W. E., Bennett D. and Garica V. (1982) Retention of ionized solutes in reversed-phase high performance liquid chromatography. *J. Liq. Chromatogr.* **5**, 1295 - 1312.
- [3] Terada H. (1986) Determination of log P_{oct} by high-performance liquid chromatography, and its application in the study of quantitative structure-activity relationships. *Quant. Struct.-Act. Relat.* **5**, 81 - 88.
- [4] Miyake K., Kitaura F., Mizuno N. and Terada H. (1987) Determination of partition coefficient and acid dissociation constant by high-performance liquid chromatography on porous polymer gel as a stationary phase. *Chem. Pharm. Bull.* **35**, 377 - 388.
- [5] Stylli C. and Theobald A. E. (1987) Determination of ionisation constants of radiopharmaceuticals in mixed solvents. *Appl. Radiat. Isot.* **38**, 701 - 708.
- [6] Pagliara A., Khamis E., Trinh A., Carrupt P.-A., Tsai R.-S. and Testa, B. (1995) Structural properties governing retention mechanisms on RP-HPLC stationary phases used for lipophilicity measurements. *J. Liq. Chromatogr.* **18**, 1721 - 1745.
- [7] Berger R., Scheunemann M., Pietzsch H.-J., Noll B., Noll St., Hoeppling A., Glaser M., Fietz Th., Spies H. and Johannsen, B. (1995) pK_{a} value determinations by HPLC of some Tc and Re complexes containing an ionizable group. *Annual Report 1995*, Institute of Bioinorganic and Radiopharmaceutical Chemistry, FZR-122, pp. 73 - 79.
- [8] Berger R., Fietz Th., Glaser M. and Spies H. (1996) Determination of partition coefficients for coordination compounds by using the HPLC column NUCLEOGEL RP C₁₈ 80-10. *This report*, pp. 107 - 111.
- [9] Lide D. R. (ed.). (1992-1993) *CRC Handbook of Chemistry and Physics*, pp. 8 - 37. CRC Press, Tokyo.

11. Retropane - a New Rhenium Complex as a Potential Ligand for Labelling the Dopamine Transporter

A. Hoeppling, H. Spies

Introduction

Radiolabelled phenyltropanes as a class of ligands with a high affinity to the dopamine transporter offer many possibilities for nuclear medical diagnosis of dopamine-receptor-depending alterations of the brain. So far, ¹¹C, ¹⁸F, and ¹²³I-labelled β-CIT [1, 2] and IPT [3] have been proposed as PET and SPECT tracers for the diagnosis of Parkinson's disease.

Recently, some cocaine derivatives containing technetium or its congener rhenium [4, 5] have been published. They represent substituted phenyltropanes bearing a chelate moiety at the tropane nitrogen. Neumeyer [6] has recently reported on the attachment of a tetradentate N₂S₂ chelating unit to the β-CIT system by substitution of the methoxy group in the ester functionality.

We would like to report on the synthesis of the first rhenium complex, "retropane", alternatively derived from the basic skeleton of the tropane molecule modified at the C₃ position [7]. This contribution is part of our work to make available Tc tropane complexes with high affinities to dopamine transporters as potential radiopharmaceuticals.

Experimental

(3-thiapentane-1.5-dithiolato)(3-thiolato-propanoic acid trop-3α-yl-ester) oxorhenium(V)

34.4 mg (150 μmol) 3-thiopropanoic acid trop-3α-yl ester were added to a boiling solution of 38.9 mg (100 μmol) chloro(3-thiapentane-1,5-dithiolato)oxorhenium(V) in 5 ml acetonitrile while stirring. After adding 3 drops of triethylamine the mixture was refluxed for 5 minutes. The solvent was removed *in*

vacuo and the residue was purified by flash-chromatography using methanol/chloroform = 1:4 as an eluent.

The dark red oil obtained was crystallized as oxalic salt.

Yield: 28.6 mg (49 %, free base)

^1H NMR data: (500 MHz, CD_3OD): δ 2.13-2.15 (m, 4H), 2.32-2.36 (m, 2H), 2.43-2.47 (m, 2H), 2.52-2.57 (m, 2H), 2.85 (s, 3H, CH_3), 2.98 (t, $J = 6.85\text{Hz}$, 2H, CH_2), 3.13 (td, $J_1 = 13.65\text{ Hz}$, $J_2 = 2.78\text{Hz}$, 2H), 3.93 (bs, 2H), 4.06 (t, $J = 6.85\text{Hz}$, 2H, CH_2), 4.12 (dd, $J_1 = 10.74\text{ Hz}$, $J_2 = 3.37\text{ Hz}$, 2H), 4.37 (dd, $J_1 = 13\text{Hz}$, $J_2 = 4.77\text{Hz}$), 5.13 (t, $J = 4.6\text{Hz}$, 1H)

^{13}C NMR data: (125.77 MHz, CD_3OD): δ 24.89, 32.60, 36.03, 39.07, 39.46, 47.41, 48.49, 63.88, 65.63, 165.46, 172.97

Mass spectrum: m/z 582 (M^+ , 54.3 %), 583 (10.5), 584(100) $\text{M}^+ + 1$, 585(19), 586(17), 587(3), 588(1.4)

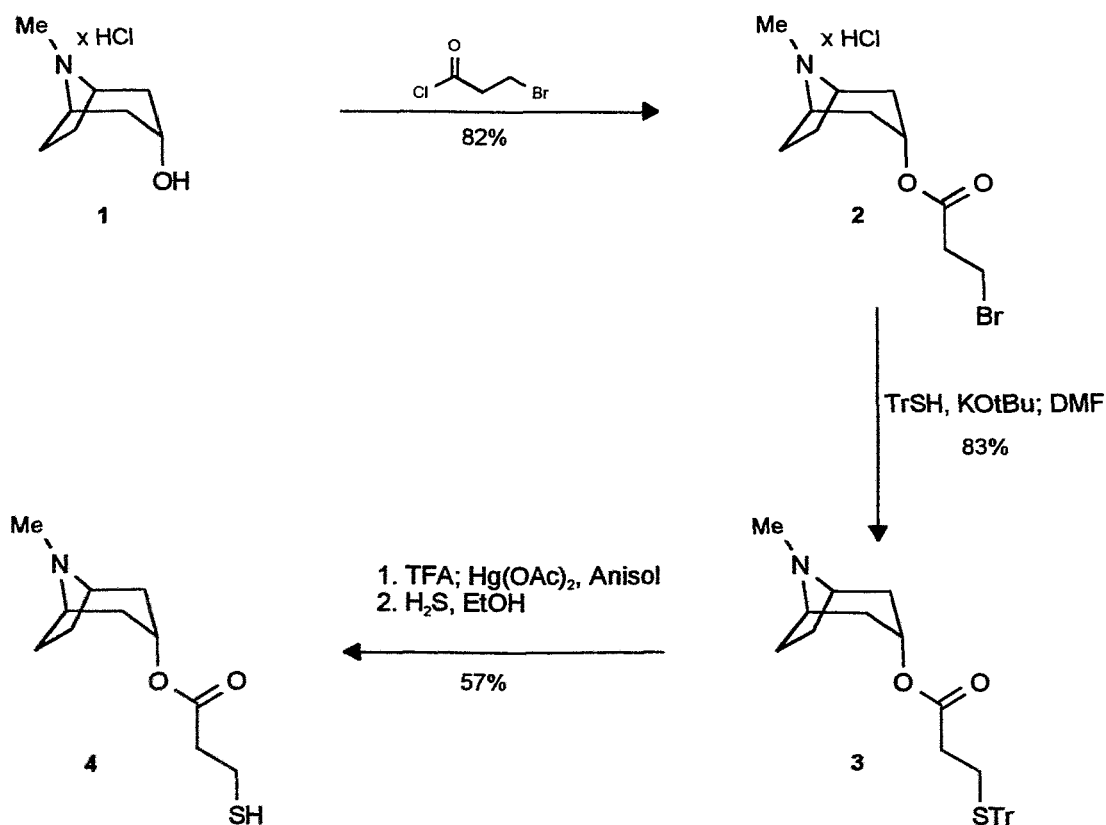
IR absorption (KBr): $\nu_{\text{max}}/\text{cm}^{-1}$ 960 (Re=O).

Elemental analysis (oxalate): (Found: C, 30.41; H, 4.33; N, 2.20; S, 17.92; $\text{C}_{17}\text{H}_{28}\text{NO}_7\text{S}_4\text{Re}$ requires C, 30.31; H, 4.19; N, 2.08; S, 19.00 %).

Results and Discussion

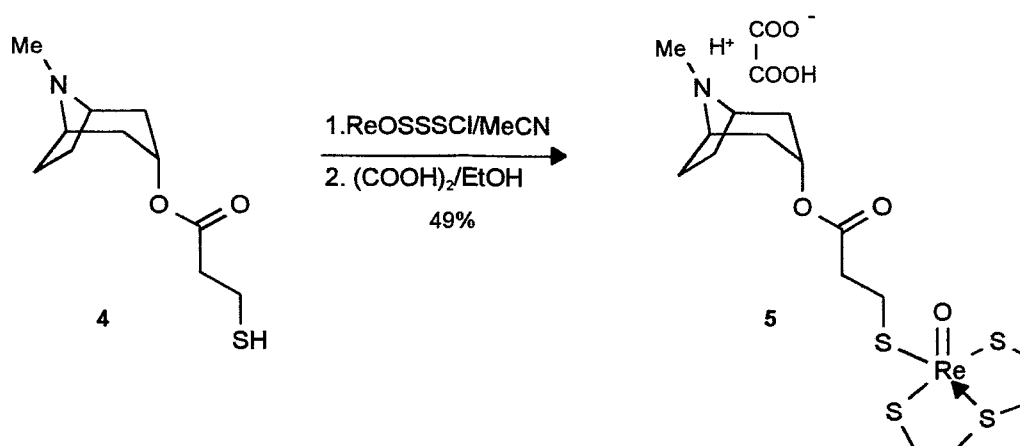
The introduction of a mercapto group was achieved in the form of ω -mercapto-substituted esters of tropanol. Starting from α -tropanol hydrochloride the 3-bromopropionic acid tropanyl ester was synthesized by a very simple procedure [8]. The resulting hydrochloric salt was reacted with triphenylmethanthiol in DMF to yield the S-protected mercaptan in a good yield. The deprotection of the mercapto group was accomplished by reacting the thiotritylated compound with mercury acetate in trifluoroacetic acid and cleaving the mercury-mercaptide with hydrogen sulphide.

Scheme 1:



The rhenium complex was obtained in a typical 3+1-reaction [9], in which the thiol as the monodentate ligand was reacted with $[\text{ReO}(\text{SSS})\text{Cl}]$.

Scheme 2:



To summarize, we were able to synthesize the first rhenium complex based on an O-substituted tropane derivative. Continuation of the work will refer to other esters of tropane, preparation of the congener technetium complexes and testing of the affinity to the dopamine transporter (DAT).

References

- [1] Boja J. W., Patel, A.; Carroll F. I., Rahman M. A., Philipp A., Kopajtic T. A. and Kuhar, M. J. (1991) 125I RTI-55: A potent ligand for dopamine transporters. *Europ. J. Pharmacol.* **194**, 133 - 134.
- [2] Neumeyer J. L., Wang S., Milius R. A., Baldwin R. M. Zea-Ponce Y., Hoffer P.B. Sybirska E., Al-Tikriti M. and Charney D. S. *et al.* (1991) [¹²³I]-2β-carbomethoxy-3β-(4-iodophenyl)tropane: a high-affinity SPECT (single photon emission computed tomography) radiotracer of monoamine re-uptake sites in brain. *J. Med. Chem.* **34**, 3144 - 3146.
- [3] Goodman M. M., Kung M.-P., Kabalka G. W., Kung H. F. and Switzer R. J. (1994) Synthesis and characterization of radioiodinated N-(3-iodopropen-1-yl)-2β-carbomethoxy-3β-(4-chlorophenyl)-tropanes: Potential dopamine reuptake site imaging agents. *J. Med. Chem.* **37**, 1535 - 1542.
- [4] Meegalla S., Ploessl K., Kung M.-P., Stevenson D. A., Liable-Sands L. M., Rheingold A. L. and Kung H. F. (1995) First example of a ^{99m}Tc complex as a dopamine transporter imaging agent. *J. Am. Chem. Soc.* **117**, 11037 - 11038.
- [5] Madras B. K., Jones A. G., Mahmood A., Zimmerman R. E., Garada B., Holman B. L., Davison A., Blundell P. and Meltzer P. C. (1996) Technepine: a high-affinity ⁹⁹technetium probe to label the dopamine transporter in brain by SPECT imaging. *Synapse (N. Y.)*, **22**, 239 - 246.
- [6] Tamagnan G., Gao Y. G., Baldwin R. M., Zoghbi, S. S. and Neumeyer, J. L. (1996) Synthesis of beta-CIT-BAT, a potential technetium-99m imaging ligand for dopamine transporter. *Tetrahedron Lett.* **37**, 4353 - 2556.
- [7] Hoepfing A., Spies H. and Johannsen B. (1996) Retropane - a new rhenium complex as a potential ligand to label the dopamine transporter. *Bioorg. Med. Chem. Lett.* **6**, 2871 - 2874.
- [8] Wolfenstein R. and Rolle J. (1908) Über halogensubstituierte Tropeine. *Chem. Ber.* **41**, 733 - 741.
- [9] Fietz Th., Spies H., Pietzsch H.-J. and Leibnitz P. (1995) Synthesis and molecular structure of chloro(3-thiapentane-1,5-dithiolato)oxorhenium (V). *Inorg. Chim. Acta* **231**, 233 - 236.

12. Preparation and Structure of Neutral Oxo-Re(V)-Complexes with L-Cysteine Methyl Ester and D-Penicillamine Methyl Ester

S. Kirsch, B. Noll, H. Spies, P. Leibnitz¹, D. Scheller², B. Johannsen

¹Bundesanstalt für Materialforschung, Berlin

²Institut für Analytische Chemie, Technische Universität Dresden

Introduction

In former studies [1] the neutral Re(V) complexes of penicillamine and cysteine were prepared by ligand exchange of Re(V) gluconate, and its crystal structure determined. The N- and S-atoms in the basal plane of the six-coordinate complex [ReO(-S-C(CH₃)₂-CH(COOH)-NH₂)-(-S-C(CH₃)₂-CH(COO)-NH₂-)] are cis coordinated, and one of the carboxyl groups is bound trans to the oxo group.

In order to obtain more information about the complexation behaviour of ligands of the 2(N,S,O) type, investigations were carried out in the following study into the penicillamine methyl ester and cysteine methyl ester moiety, where the O-donor is blocked.

Three different complexes were obtained with D-penicillamine methyl ester. Besides the two diester complexes [ReO(-S-C(CH₃)₂-CH(COOCH₃)-NH-)(-S-CH(-COOCH₃)-NH₂-)] (**2**) and [ReO(-S-C(CH₃)₂-CH(COOCH₃)-NH-)(-S-CH(-COOCH₃)-NH₂)-(H₂O)] (**3**) the mixed-ligand complex [ReO(-S-C(CH₃)₂-CH(COOCH₃)-NH₂)-(-S-CH(-COO-)-NH₂-)] (**1**) was formed, containing tridentate D-penicillamine, obviously generated upon coordination, and bidentate D-penicillamine methyl ester in a coordination geometry similar to that of the Re penicillamine complex. According to ¹H NMR studies in solution, (**2**) and (**3**) are surprisingly characterized by both a deprotonated and a neutral nitrogen donor atom in the ReO(NS)₂ system. This feature, usually attributed to complexes of [Tc=O]³⁺ and [Re=O]³⁺ with tetradentate aminethiols, is consistent with a neutral five-coordinate oxo metal complex of D-penicillamine methyl ester. In the case of L-cysteine methyl ester only the mixed-ligand complex [ReO(-S-CH₂-CH(COOCH₃)-NH₂)-(-S-CH(COO-)-NH₂-)] (**4**) with a similar structure to (**1**) could be isolated and its structure determined by X-ray analysis.

Experimental

[ReO(-S-C(CH₃)₂-CH(COOCH₃)-NH₂)-(-S-C(CH₃)₂-CH(-COO-)-NH₂-)] (**1**)

40 mg (0.2 mmol) of D-penicillamine methyl ester-HCl in 2 ml of water were added to 2 ml (0.1 mmol) Re gluconate solution. A reddish-brown residue was obtained, separated by filtration and redissolved in 2 - 3 ml of acetone. 3 ml of water were added and the solution was allowed to crystallize by slow evaporation at 25 °C.

Yield: 25 mg of dark violet needles suitable for X-ray analysis.

Elemental analysis: (Found: C, 25.28; H, 4.14; N, 5.48; S, 12.58 ReC₁₁H₂₁O₅N₂S₂ requires C, 26.00; H, 4.08; N, 5.39; S, 12.64 %).

IR absorptions: $\nu_{\max}/\text{cm}^{-1}$ (KBr) 976 (Re=O), 1732 (C=O-OCH₃) and 1624 (C=O, trans coordinated).

UV/VIS absorptions: λ_{\max}/nm (water) 345 with a shoulder at 290, 508.

Mass spectrum (DCI): m/z 512 (M^+ , 100%).

[ReO(-S-C(CH₃)₂-CH(COOCH₃)-NH₂)-(-S-C(CH₃)₂-CH(COOCH₃)-NH-)] (**2**) and

[ReO(-S-C(CH₃)₂-CH(COOCH₃)-NH₂)-(-S-C(CH₃)₂-CH(COOCH₃)-NH-)(H₂O)] (**3**).

40 mg (0.2 mmol) of D-penicillamine methyl ester-HCl in 2 ml of water were added to 2 ml (0.1 mmol) Re gluconate solution. The reddish-brown residue was filtered off and redissolved in 2 - 3 ml of acetone. The solution was purified by flash-chromatography on silica gel 60 in acetone. Two fractions can be isolated: (**2**) was obtained as a violet powder and (**3**) as light red powder, soluble in almost all organic solvents. The total yield of (**3**) depends on its contact time with water.

Analytical data for (**2**):

Elemental analysis: (Found: C, 27.37; H, 4.59; N, 5.32; S, 12.17 ReC₁₂H₂₃O₅N₂S₂ requires C, 28.03; H, 4.80; N, 5.10; S, 11.90 %).

IR absorptions: $\nu_{\max}/\text{cm}^{-1}$ (KBr) 940 (Re=O) and 1728s (C=O-OCH₃).

UV/VIS absorptions: λ_{\max}/nm (in CH₂Cl₂) 358, 523

Mass spectrum (FAB, neg.): m/z 525 (60%), 396 (20%), 183 (100%).

Analytical data for (**3**):

Elemental analysis: (Found: C, 26.32, H, 4.55, N, 5.10, S, 11.69 ReC₁₂H₂₃O₅N₂S₂(H₂O) requires C, 26.51, H, 4.63, N, 5.15, S, 11.79 %)

IR absorptions: $\nu_{\max}/\text{cm}^{-1}$ (KBr) 936 (Re=O) and 1728s (C=O, free ester).
 UV/VIS absorptions: λ_{\max}/nm (in CH_2Cl_2) 526, 350 with a small shoulder at 310.

$[\text{ReO}(-\text{S}-\text{C}(\text{CH}_3)_2-\text{CH}(\text{COOH})-\text{NH}_2)(-\text{S}-\text{C}(\text{CH}_3)_2-\text{CH}(-\text{COO}-)-\text{NH}_2)]$ (4)

34.33 mg (0.2 mmol) of L-cysteine methyl ester-HCl in 2 ml of water were added to 2 ml (0.1 mmol) Re gluconate solution. A dark brown residue was obtained after stirring for 45 min. The residue was separated by filtration and was washed twice with ethyl alcohol and ether.

After recrystallization in methyl alcohol dark brown crystals suitable for X-ray analysis were obtained.

Elemental analysis: (Found C, 18.46; H, 2.88; N, 6.15; S, 14.08, $\text{ReO}_5\text{C}_7\text{H}_{13}\text{N}_2\text{S}_2$ requires C, 18.63, H 2.82; N, 5.98; S, 13.95 %).

IR absorptions: $\nu_{\max}/\text{cm}^{-1}$ (KBr) $\nu(\text{C}=\text{O}-\text{OCH}_3)$ 1744 and $\nu(\text{C}=\text{O}-\text{O}, \text{trans})$ 1644 and $\nu(\text{Re}=\text{O})$ 976.

UV/VIS absorptions: λ_{\max}/nm (water) 345 with a shoulder at 290, 495.

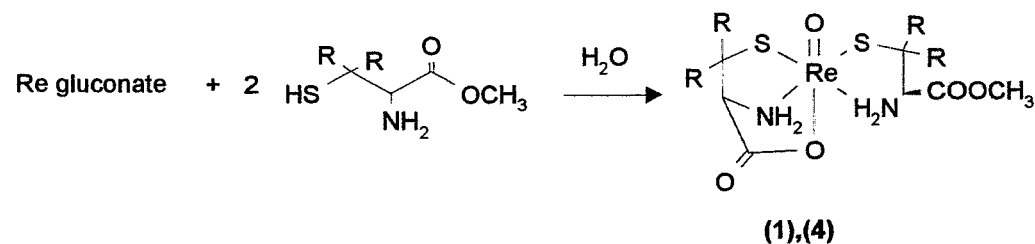
Mass spectrum (DCI neg.): m/z 456 (M^+ , 100%)

NMR data: δ_{H} (300 Mhz; solvent $\text{DMSO}-\text{D}_6$): 2.75 [1H, d], 3.13[1H, q], 3.5 [3H, T of fine structure], 3.72 [3H, s], 4.03 [1H, s], 6.11 [1H, d], 6.97 [1H, t], 7.63 [1H, d] and 7.86 [1H, d]

Results and Discussion

L-cysteine methyl ester and D-penicillamine methyl ester react with Re gluconate in acidified water according to Scheme 1.

Scheme 1: Reaction of Re gluconate with D-penicillamine methyl ester and L-cysteine methyl ester in acidified water resulting in the monoester complexes (1) and (4).



R = CH_3 for penicillamine methyl ester (1)

R = H for cysteine methyl ester (4)

Furthermore, another type of a neutral rhenium complex with D-penicillamine methyl ester as ligating moiety occurred (2 and 3) starting from rhenium gluconate. They were immediately extracted with organic solvents and isolated as powders after flash-chromatography on silica gel 60 in acetone.

When the products, without chromatographic separation, were allowed to react with water and then to crystallize, needles of complex (1) suitable for X-ray analysis were obtained. In Tables 1 and 2 selected bond distances and bond angles of (1) and (4) are compared.

The molecular structure of Re penicillamine methyl ester and cysteine methyl ester as ligating moiety resemble that of Re penicillamine at low pH [1]. One methyl group was saponified during complex formation in water to form the neutral monoester complexes (1, 4) with almost the same crystal structure. The S- and N-donor atoms are cis coordinated and the carboxyl group is involved in the complex formation trans to the Re-oxo-group. The structure comprises a distorted octahedron as shown in Figs. 1 and 2.

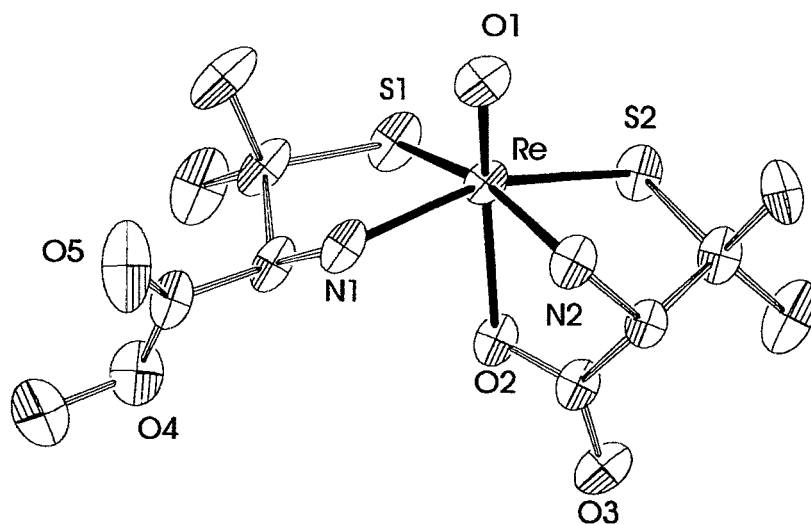


Fig.1: Crystal structure of Re penicillamine methyl ester determined by X-ray analysis

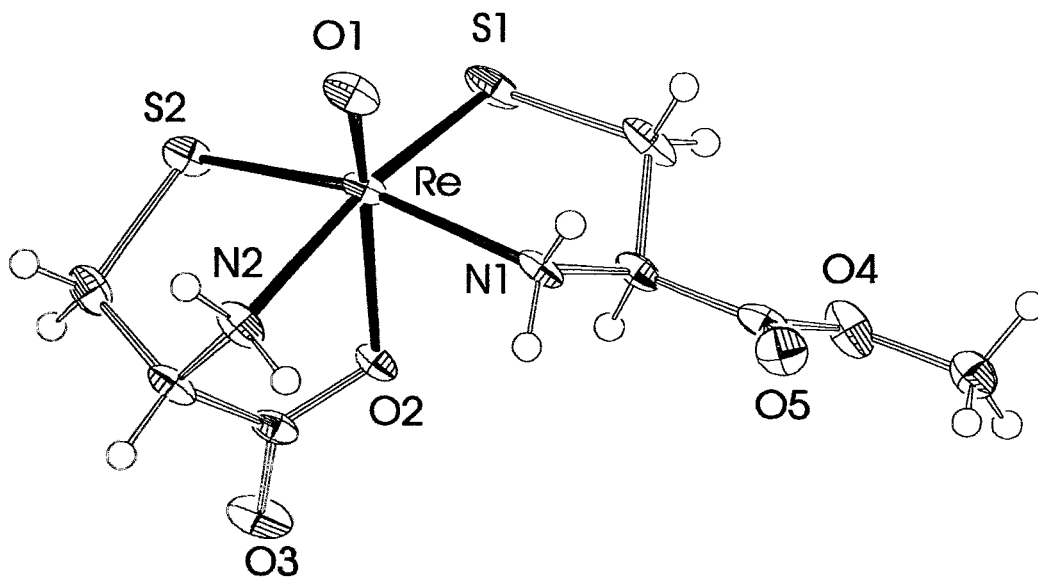


Fig.2: Crystal structure of Re cysteine methyl ester determined by X-ray analysis

Table 1: Comparison of selected bond distances of (1) and (4)

	Bond distances for	
	(1)	(4) [Å]
Re-O (1)	1.663 (5)	1.670 (4)
Re-N (2)	2.162 (6)	2.158 (4)
Re-O (2)	2.179 (4)	2.159 (4)
Re-N (1)	2.194 (6)	2.202 (5)
Re-S (2)	2.280 (2)	2.290 (14)
Re-S (1)	2.300 (2)	2.305 (14)

Table 2: Comparison of selected bond angles of (1) and (4)

	Bond angles of	
	(1)	(3) [deg]
O (1)-Re-N (2)	97.9 (2)	94.6 (2)
O (1)-Re-O (2)	157.9 (2)	157.3 (2)
N (2)-Re-O (2)	74.3 (2)	75.6 (2)
O (1)-Re-N (1)	90.2 (2)	90.8 (2)
N (2)-Re-N (1)	93.2 (2)	96.9 (2)
O (2)-Re-N (1)	70.1 (2)	70.5 (2)
O (1)-Re-S (2)	106.0 (2)	105.3 (2)
N (2)-Re-S (2)	83.1 (2)	82.23 (12)
O (2)-Re-S (2)	93.71 (13)	93.81 (11)
N (1)-Re-S (2)	163.8 (2)	163.8 (2)
O (1)-Re-S (1)	104.6 (2)	106.8 (2)
N (2)-Re-S (1)	157.3 (2)	158.59 (12)
O (2)-Re-S (1)	83.77 (12)	84.03 (11)
N (1)-Re-S (1)	84.6 (2)	82.22 (14)
S (2)-Re-S (1)	92.80 (7)	92.67 (6)

¹H NMR data

Re penicillamine methyl ester complexes were recorded in DMSO-D₆. In Table 3 the chemical shifts of (1) and (2) are compared. NMR data obtained for (4) are comparable to those of complex (1).

The postulated structure of (2) is shown in Fig. 3. In contrast to (1) with only one methoxy signal at $\delta = 3.81$ ppm two methoxy signals can be observed in the NMR spectrum of (2) with $\delta = 3.71$ ppm and $\delta = 3.79$ ppm. Furthermore, there are only three NH signals in the spectrum of (2): a triplet at 6.23 ppm, a doublet at 8.46 ppm and a singlet at 8.50 ppm in contrast to (1) with four NH signals belonging to the two protonated amine groups (NH₂). These facts prove that one amine group was deprotonated during complex formation of (2).

Table 3: ¹H NMR chemical shifts (δ in ppm) of (1), (2)

Re pen/penicillamine monomethylester (1)		Re penicillamine dimethylester (2)		Re penicillamine dimethylester - H ₂ O (3)	
				66.7 %	33.3%
1.29, s	CH ₃	0.91, s	CH ₃	0.91, s CH ₃	0.94, s CH ₃
1.48, s	CH ₃	1.05, s	CH ₃	1.05, s CH ₃	1.08, s CH ₃
1.68, s	CH ₃	1.69, s	CH ₃	1.69, s CH ₃	1.69, s CH ₃
1.89, s	CH ₃	1.93, s	CH ₃	1.93, s CH ₃	1.81, s CH ₃
3.10, dd	CH	3.47, dd	CH _Y	3.47, dd CH _Y	3.74, dd CH _Y
3.64, s	CH	3.91, s	CH _X	3.91, s CH _X	4.01, s CH _X
		3.71, s	OCH ₃	3.71, s OCH ₃	3.74, s OCH ₃
3.81, s	OCH ₃	3.79, s	OCH ₃	3.79, s OCH ₃	3.76, s OCH ₃
5.80, d	N(1)H				
6.79, t	N(2)H	6.23, t	N(2)H	6.23, t N(2)H	5.82, t N(2)H
7.60, d	N(2)H	8.46, d	N(2)H	8.46, d N(2)H	8.34, d N(2)H
7.75, d	N(1)H	8.50, s	N(1)H	8.50, s N(1)H	9.78, s N(1)H

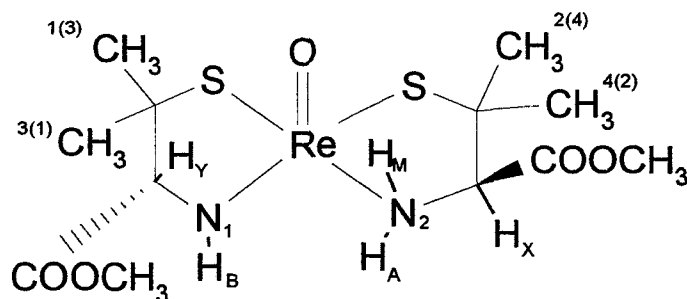


Fig. 3: Postulated structure of (2)

The magnetic anisotropy of the $\text{Re}=\text{O}$ core is responsible for the great differences in the chemical shifts of the NH_x and CH_3 groups. The nonequivalence of the four CH_3 and the two OCH_3 groups are caused by the chirality of the ligands and the asymmetry of the complex. For the same reason the two protons of the NH_2 group are chemically nonequivalent. For the $\text{N}_2\text{H}^{(\text{A})}$ group a pair of doublets is obtained at $\delta = 8.5$ ppm. Its coupling constant $^3J_{\text{HH}}$ with $\text{CH}^{(\text{X})}$ is relatively small (3.5 Hz) and therefore, with respect to the Karplus-Conroy curve, the dihedral angle between these protons must be nearly 50° . The coupling constants $^3J_{\text{HH}}$ of $\text{N}_2\text{H}^{(\text{M})}$ with $\text{CH}^{(\text{X})}$ and $^2J_{\text{HH}}$ for the two protons of the NH_2 group are of quite the same size, which causes a triplet at $\delta = 6.2$ ppm instead of the expected pair of doublets. Its coupling constant $^3J_{\text{HH}} = 12.5$ Hz is quite large. This fact indicates a dihedral angle of 180° between the $\text{N}_2\text{H}^{(\text{M})}$ and the $\text{CH}^{(\text{X})}$ proton.

Between the $\text{CH}^{(\text{Y})}$ group at $\delta = 3.9$ ppm and the neighboring deprotonated $\text{N}_1\text{H}^{(\text{B})}$ group at $\delta = 8.5$ ppm no coupling can be observed. These two signals are therefore not doublets, as expected, but singlets. Consequently the dihedral angle between these two protons must be nearly 90° .

In the 2D-NOESY-NMR spectrum of this complex cross peaks are obtained between $\text{N}_2\text{H}^{(\text{A})}$ and $\text{N}_2\text{H}^{(\text{M})}$. The last three cross peaks with CH_3 groups indicate that the $\text{CH}^{(\text{X})}$ group belongs to $\text{CH}_3^{(2)}$ and $\text{CH}_3^{(4)}$. $\text{CH}_3^{(1)}$ and $\text{CH}_3^{(3)}$ therefore belong to the deprotonated ligand.

For complex (3) we first recorded the ^1H NMR spectrum in CDCl_3 and found besides the expected CH and NH signals similar to complex (2) a water signal at 1.60 ppm integrating two protons. Therefore the trans position of complex (3) seems to be occupied with one molecule of water. This shows a great effect on the coordinatively bonded deprotonated N_1H group, which becomes apparent in the extremely shifted singlet at $\delta = 10.94$ ppm belonging to this proton. After the measurement CDCl_3 was evaporated and the residue was resolved in $\text{DMSO}-d_6$. The recorded spectrum shows a mixture of complex (2) and (3). Only about 33 % of the former complex (3) still exists with the extremely shifted N_1H group at $\delta = 9.77$ ppm. For the other 67 % the coordinated water in trans position is replaced by DMSO and the belonging chemical shifts are identical with those of complex (2). Thus, in coordinating solvents like DMSO or water a dynamical equilibrium seems to exist with varying replacement of solvent molecules in the trans position of these kind of complexes.

Conclusions

The studies on Re complexes of D-penicillamine methyl ester and L-cysteine methyl ester confirm a great tendency of 2(N,S) aminethiol ligands to form neutral Re oxocomplexes. Accordingly, in aprotic, non coordinating solvents such as CH_2Cl_2 one amine group in the 1:2 Re(V) oxocomplex (2) is deprotonated and thus contributes to the compensation of the positive charge at the Re-oxo-core. In the presence of coordinating solvents, the trans position is occupied with a solvent molecule, without any change of the NH/NH_2 coordination mode (3). In water, however, also an alternative form of the complex occurs, avoiding NH deprotonation. Unlike tetradentate DADT ligands, such as ethylenedi-L-cysteine diethyl ester (L,L-ECD) which form neutral species with the ester groups remaining intact [2], one of the ester group-bearing ligands in penicillamine methyl ester and cysteine methyl ester is hydrolyzed and assumes a higher denticity. The generated carboxyl group binds trans to the oxo ligand. The coordination geometry of the mixed-ligand complexes (1, 4) is similar to that of the known Tc and Re D-penicillamine complexes [1, 3]. It is evident that a NH_2/NH_2 coordination is preferred to the asymmetric NH/NH_2 coordination if charge compensation can be provided by an appropriate donor group, such as carboxyl that binds trans to the oxo group.

The whole reaction scheme and structures of the complexes are illustrated in Fig. 4.

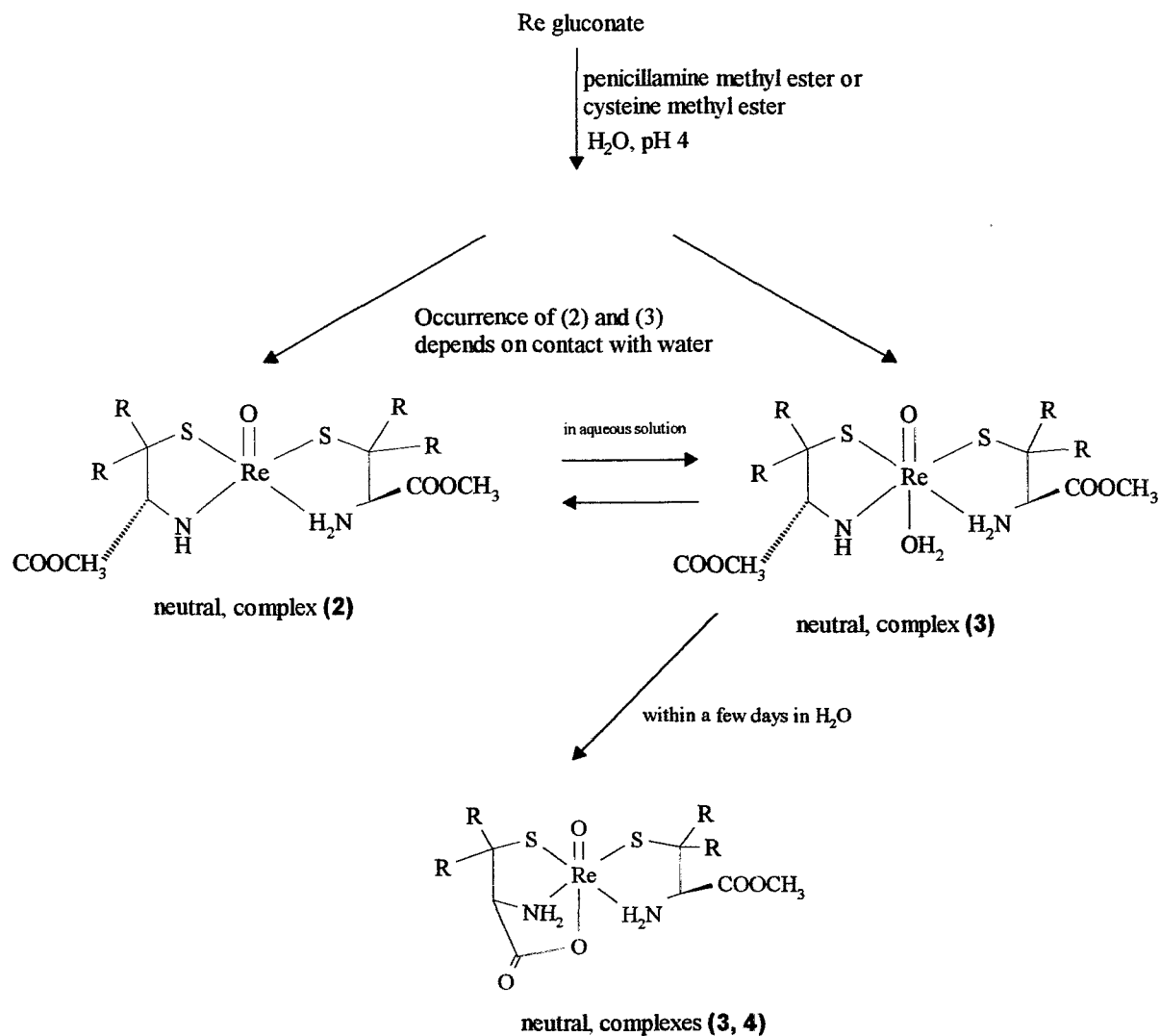


Fig. 4: Reaction scheme and structures of the obtained complexes

References

- [1] Kirsch S., Noll B., Scheller D., Klostermann K., Spies H. and Johannsen B. (1995) Preparation and characterization of rhenium(V) complexes with cysteine and its derivatives penicillamine and cysteamine, *Annual Report 1995*, Institute of Bioinorganic and Radiopharmaceutical Chemistry, FZR-122, pp. 110 - 114.
- [2] Marzilli L. G., Banaszcyk M. G., Hansen L., Kuklennyik Z., Cini R. and Taylor Jr. A. (1994) Deprotonation and denticity of chelate ligands. Rhenium(V) oxo analogues of technetium-99m radiopharmaceuticals containing N₂S₂ ligands, *Inorg. Chem.* **33**, 4850 - 4860.
- [3] Franklin K. J., Howard-Lock H. E. and Lock C. J. L. (1982) Preparation, spectroscopic properties, and structure of 1-oxo-2,3,6-(D-penicillaminato-N,S,O)-4,5-(D-penicillaminato-N,S) technetium(V), *Inorg. Chem.* **21**, 1941 - 1946.

13. Formation of Mixed-Ligand Ester Complexes of Rhenium and Technetium with S/S/S-N or S-S/S-N Coordination

S. Seifert, H. Spies

Introduction

A number of anionic S_4 coordinate rhenium and technetium complexes have been recently described [1, 2]. Substitution of a thiol donor atom by a nitrogen atom should make the resulting complexes neutral within a defined pH range. Such an NS_3 coordination can be achieved by combination of, for example, a dimercapto-succinic acid diethyl ester ligand ($DMSEt_2$) or two monomercaptoacetic acid ethyl ester ligands (MAEt) with cysteamine (CYSA), provided that the amine group of the cysteamine moiety is not deprotonated in the resulting complex. The formation of such mixed-ligand complexes is described as well as the transformation of complexation to the n.c.a. level of ^{99m}Tc .

Experimental

The precursor compounds $[ReO(gluc)_2]^-$ or $[ReOCl_4]^-$ were prepared for the formation of mixed-ligand rhenium complexes according to the well-known procedures.

In the case of complexes with monothiols and cysteamine, the mercaptocarboxylic acid or the ethyl ester complex was at first formed as described in [3]. The desired mixed-ligand complex was prepared in a following step by adding the stoichiometric quantity of cysteamine to the solution.

The preparation of rhenium complexes containing $DMSEt_2$ and cysteamine was carried out in a one-pot reaction with equimolar quantities of the ligands in aqueous/ethanolic or ethanolic/acetonic solutions by preparing at first the cysteine or cysteamine complex and then exchanging one CYS ligand for $DMSEt_2$.

The corresponding ^{99m}Tc complexes were obtained by stannous chloride reduction of pertechnetate in aqueous/acetonic ligand solutions. 1.2 mg CYSA and 0.05 mg $DMSEt_2$ were added to 1.0 ml pertechnetate eluate containing 7.0 mg $NaHCO_3$. The reduction proceeded with 0.01 ml of an ethanolic stannous chloride solution (1.0 - 2.0 mg/10 ml).

It is also possible to prepare the mixed-ligand ^{99m}Tc complex via ligand exchange starting with ^{99m}Tc gluconate and successively adding CYSA and $DMSEt_2$ in a similar way as described for the formation of n.c.a. "3+1" complexes [4].

The complexes were analysed in solution by thin layer chromatography (TLC), paper electrophoresis (PE), high performance liquid chromatography (HPLC) and some rhenium complexes also by mass spectrometry (MS).

TLC: Silufol/acetone

PE: acetonitrile/water (1.0 % $NaClO_4$) at pH 7.0 and 2.0 adjusted with $HClO_4$, 500 V

HPLC: PRP-1 (250 x 4.1 mm, 10 μm , flow rate 2.0 ml/min), acetonitrile (A)/20 mM phosphate buffer pH 7.4 (B), gradient 1.0, (t[min]/%A): (5/0), (10/50), (5/50), (1/75), (5/75)

MS: MAT 95 spectrometer (Finnigan), fast atom bombardment (FAB-MS) and chemical ionization (CI-MS)

Results and Discussion

Prior to the studies of mixed-ligand complexes involving the ligands cysteamine, cysteine and cysteine methyl ester, complexes of each of the ligands were only synthesized and analysed by HPLC. It was found that the rhenium cysteine methyl ester complex ($R_t = 11.2$ min) is immediately hydrolysed to the monoester complex ($R_t = 6.7$ min) and that in a following slower hydrolysis step the cysteine complex ($R_t = 2.1$ min) is formed. Considering this behaviour and the fact that no free carboxylate groups should be in the desired mixed-ligand complexes, cysteine ester does not appear to be suitable as a co-ligand. However, mono or dimercapto ligands containing one or two ester groups are suitable for this purpose.

The reactions of the rhenium complexes $[ReO(MAA)_2]^-$ and $[ReO(MAEt)_2MAA]^-$ (MAA = mercaptoacetic acid) with cysteine show, that cysteine is able to substitute a bidentately bound MAA ligand molecule and a mixed-ligand complex is formed according to the following route:



The same complex with a R_t value of 4.1 min is detected after reaction of $[\text{ReO}(\text{MAA})_2]^-$ with cysteine methyl ester and waiting for some hours while the ester complex hydrolyses to $[\text{ReO}(\text{CYS}/\text{MAA})]^-$. Initially cysteamine (CYSA) reacts with $[\text{ReO}(\text{MAA})_2]^-$ to form an anionic mixed-ligand complex. An excess of CYSA leads to complete substitution of MAA, and the Re-CYSA complex is formed accordingly ($R_t = 9.2$ min).

Using the ester complex $[\text{ReO}(\text{MAEt})_2\text{MAA}]^-$, ligand exchange with CYS or CYSA results in products which are stable in a phosphate buffer of pH 7.4 but can be hydrolysed by pig liver esterase (PLE). The hydrolysis products are the mixed-ligand mercapto acetic acid complexes $[\text{ReO}(\text{CYS}/\text{MAA})]^-$ and $[\text{ReO}(\text{CYSA}/\text{MAA})]^-$.

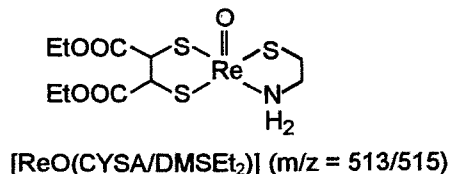
Electrophoresis studies show an anionic mobility at pH 7.0 for both ester complexes. The complex containing cysteamine moves only a very short distance at pH 2.0, possibly indicating the existence of a neutral compound in acidic solution.

Unfortunately, mass spectrometry failed for both ester complexes.

The mixed-ligand rhenium complexes containing DMSEt_2 and CYS or CYSA as ligands were prepared either by a stoichiometric ligand exchange in a one-pot reaction starting with $[\text{ReOCl}_4]^-$ or Re gluconate or by adding one equivalent of DMSEt_2 to the cysteine or cysteamine complex. The reaction mixture consisting of the mixed-ligand complex and the anionic complex $[\text{ReO}(\text{DMSEt}_2)_2]^-$ can be separated by HPLC. As found by HPLC, the mixed-ligand complexes are unstable and decompose mainly to the DMSEt_2 complex.

A neutral complex should be expected for the combination of a DMSEt_2 with a CYSA ligand. Actually, HPLC separation yields an anionic first fraction ($R_t = 10.8$ min) and a neutral second fraction ($R_t = 12.1$ min) as found by electrophoresis of the separated fractions and the reaction mixture at pH 7.0 and 2.0.

The fractions 1 and 2 were analysed by FAB-MS and CI-MS. The molecule ion peaks of the mixed-ligand complex $[\text{ReO}(\text{CYSA}/\text{DMSEt}_2)]$ and the complex $[\text{ReO}(\text{DMSEt}_2)_2]^-$ were detected by both methods.



The ($M-1$) value ($m/z = 512/514$) of the negative molecule ion was found with FAB^- -MS as well as CI^- -MS.

The corresponding ^{99m}Tc complex was prepared either by direct reduction of pertechnetate eluate in the ligand solution or by ligand exchange, starting with ^{99m}Tc gluconate.

The formation of the mixed-ligand complex by direct reduction of pertechnetate was monitored by TLC and HPLC. Three dominant peaks were detected in TLC:

peak I:	$R_f = 0-0.5$	^{99m}Tc cysteamine complex
peak II:	$R_f = 0.65$	mixed-ligand complex
peak III:	$R_f = 0.9$	$[\text{ReO}(\text{DMSEt}_2)_2]^-$

The product distribution changes with time. The start activity decreases with time while peaks II and III increase. On the other hand, peak II increases faster than peak III. Then the mixed-ligand complex decomposes mainly to the DMSEt_2 complex and other unknown species. The optimum quantities of ligands for direct reduction were determined to be in the range of 0.8 - 1.5 mg CYSA and 0.04 - 0.06 mg DMSEt_2 . The maximum yield of the desired complex is obtained at different times, depending on the quantity of cysteamine used for preparation. Fig. 1 shows the course of reaction for different contents of cysteamine in the reaction mixture.

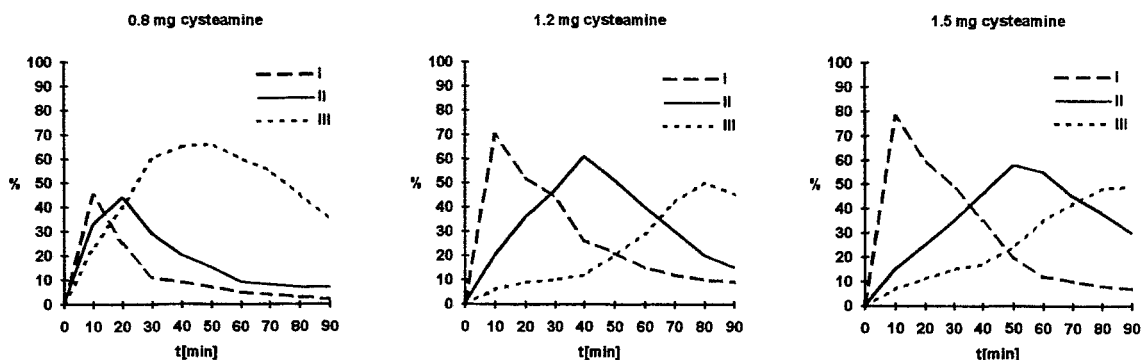


Fig. 1: Formation of $^{99m}\text{TcO}(\text{CYSA}/\text{DMSEt}_2)$ with 0.05 mg DMSEt_2 and 0.8 mg, 1.2 mg or 1.5 mg cysteamine as monitored by TLC.

The diagrams show that the cysteamine complex is mainly formed in a first fast step and that the DMSEt_2 attacks in a second step. It was observed that higher yields of cysteamine in the preparation delay the formation of the mixed-ligand complex. Amounts lower than 0.8 mg promote the formation of $^{99m}\text{TcO}(\text{DMSEt}_2)_2$.

To examine the stability of the ^{99m}Tc complex, the ligand excess was separated by HPLC. The complex fraction was re-injected at different times and analysed by TLC. It was found that the ^{99m}Tc complex decomposes within a few hours to $^{99m}\text{TcO}(\text{DMSEt}_2)_2$ and to the ^{99m}Tc cysteamine complex. After only 1 h about 50 % of the mixed-ligand complex could still be determined in the solution.

Attempts were made to improve the yield of mixed-ligand complex, using other preparation routes. For this reason the ligand exchange reaction starting with ^{99m}Tc gluconate was tested. This method led to satisfactory results in the preparation of "3+1" ^{99m}Tc complexes. Despite a variation of ligand quantities and reaction temperature, only less than 50 % of the desired complex were obtained.

To sum up, we were able to prove the formation of mixed-ligand complexes containing two mercaptocarboxylic ester ligands or a dimercaptocarboxylic ester or diester ligand in combination with a cysteine or cysteamine ligand. In the case of the combination $\text{CYSA}/\text{DMSEt}_2$ a neutral complex molecule is formed which might be of interest in the search for complexes which are able to cross the blood-brain barrier.

Acknowledgement

We thank Mrs. S. Machill of the Dresden University of Technology for performing mass spectrometric analyses.

References

- [1] Seifert S., Syhre R., Spies H. and Johannsen B. (1995) Enzymatic cleavage of technetium and rhenium complexes with DMSA ester ligands. In: *Technetium and Rhenium in Chemistry and Nuclear Medicine 4* (M. Nicolini, G. Bandoli, U. Mazzi Eds.) Padova, pp. 437 - 440.
- [2] Seifert S., Hoeping A., Klostermann K., Spies H. and Johannsen B. (1997) Preparation and characterization of novel mixed-ligand oxorhenium(V) and oxotechnetium(V) complexes bearing up to four ester groups. *Appl. Radiat. Isot.*, in press.
- [3] Seifert S., Syhre R., Spies H. and Johannsen B. (1997) Enzymatic hydrolysis of ester groups of mixed-ligand oxorhenium(V) and oxotechnetium(V) complexes. *Appl. Radiat. Isot.*, in press.
- [4] Seifert S., Pietzsch H.-J., Scheunemann M., Spies H., Syhre R. and Johannsen B. (1996) Serotonin receptor-binding technetium and rhenium complexes. 13. No carrier added preparations of "3+1" ^{99m}Tc complexes. *This report*, pp. 17 - 22.

14. A Novel Amide Thioether Dithiolate Ligand Derived from Cysteine

B. Noll, S. C. Hilger¹, P. Leibnitz², H. Spies, L. Dinkelborg¹, B. Johannsen

¹Schering AG Berlin, ²Bundesanstalt für Materialforschung und -prüfung Berlin

Efforts in the search for new chelators that are able both to coordinate radioactive metals and to bind the resulting complexes at biologically relevant anchor groups have been focused so far on tetradentate N₂S₂ ligands, N being an amide or amine functionality [1]. In the present paper we describe the synthesis of an alternative, cysteine-derived S,N,S,S ligand in which a nitrogen functionality in the above N₂S₂ ligands is substituted by a thioether group, as well as the formation of the corresponding oxorhenium(V) and oxotechnetium(V) complex.

Experimental

General

¹H NMR spectra were measured on a Bruker AC 400 (400 MHz), standard tetramethylsilane. IR spectra were measured by a Nicolet 710 spectrometer. The mass spectrum was recorded by a ZAB-E spectrometer, VG Analytical, Manchester (FAB Cs⁺ gun, 3-nitrobenzyl alcohol/glycerine/DMSO). The X-ray crystallographic data were obtained at 294 K on an Enraf-Nonius CAD-4 diffractometer, using graphite monochromated Mo-K α radiation ($\lambda = 0.71069 \text{ \AA}$) in the "Bundesanstalt für Materialforschung", Berlin.

Synthesis

2.5-dithiacyclohexanone

was prepared according to Larson *et al.* [2] by reaction of 48 ml (0.6 mol) chloroacetyl chloride with 51 ml (0.6 mol) 1.2-dimercaptoethane in 900 ml dichloromethane and 169 ml (1.2 mol) triethylamine. Yield: 52 g (65 %) of a yellow powder.

N-(5-mercapto-1-oxo-3-thia-pent-1-yl)-L-cysteine methylester (**1**)

6.7 g (50 mmol) 2.5-dithiacyclohexanone was added to a solution of 8.58 g (50 mmol) L-cysteine methyl ester hydrochloride and 13.86 ml (100 mmol) triethylamine in 250 ml dichloromethane. The mixture was stirred overnight at room temperature under an argon atmosphere. For working-up the mixture was treated with 300 ml 5 % aqueous citric acid solution, twice with 300 ml 1 % aqueous citric acid solution and with 300 ml saturated sodium hydrocarbonate solution. After drying of the organic phase with sodium sulphate, the solvent was removed in vacuo. The remaining yellow oil was purified by column chromatography (silica gel KG 60, 0.04 x 0.063 mm, Merck; eluent dichloromethane/methanol 99:1). Yield: 10.6 g (79 %) of a yellow powder. Melting point: 46 - 50 °C (from dichloromethane/methanol 99:1).

TLC (KG 60_{F254} Merck, eluent dichloromethane/methanol 95:5): R_f 0.75.

Elemental analysis: (Found: C, 35.90; H, 5.88, N, 5.11; S, 36.2; C₈H₁₅NO₃S₃ requires

C, 35.67; H, 5.61; N, 5.20; S, 35.70 %)

IR absorptions: $\nu_{\max}/\text{cm}^{-1}$ 3325 (NH), 2950 and 2940 (CH), 2580 and 2550 (SH), 1740 (COOMe), 1638 (amide-I), 1530 (amide-II).

¹H NMR: δ_{H} (400 MHz, solvent CDCl₃, standard SiMe₄) 1.42 (t, J = 10 Hz, 1H), 1.72 (t, J = 8 Hz, 1H), 2.75-2.81 (m, 2H), 2.85-2.90 (m, 2H), 2.97-3.12 (m, 2H), 3.32 (s, 2H), 3.81 (s, 3H), 4.85-4.91 (m, 1H), 7.59 (d, J = 8 Hz, broad, 1H).

Mass spectrum: m/z = 270 (M⁺+H, 35 %), 157 (13), 136 (17), 93 (10), 79 (100).

Rhenium complex [ReO(SNSS)] (**2**)

268 mg (1 mmol) of **1** in 4 ml MeOH was dropped into a solution of 725 mg (1 mmol) Ph₄As[ReOCl₄] in 15 ml chloroform and 4 ml MeOH (kept under nitrogen) and the mixture was stirred for 30 min. The brown precipitate formed was filtered off and washed with chloroform. Yield: 319 mg (0.7 mmol, 70 %). Recrystallization from isopropanol yields reddish-brown crystals. Melting point: 223 - 225 °C.

Elemental analysis: (Found: C, 20.80; H, 2.75; N, 3.16; S, 20.70; C₈H₁₂NO₄S₃Re requires

C, 20.51, H, 2.58; N, 2.99; S, 20.53 %)

IR absorptions (KBr): $\nu_{\max}/\text{cm}^{-1}$ 964 (ReO), 1740 (COOMe);

Labelling with technetium

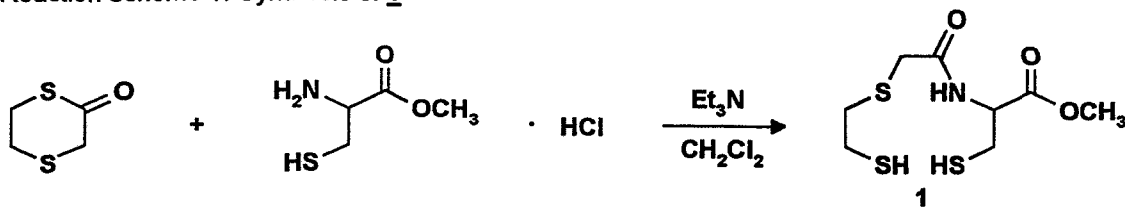
Compound **1** was complexed with technetium-99 by ligand exchange with Tc gluconate. $^{99/99m}\text{Tc}$ gluconate was prepared by addition of 100 μl 0.01 M stannous chloride solution (1×10^{-6} mol) in 0.1 M HCl to 100 μl 0.01 M potassium pertechnetate (1×10^{-6} mol) in 1 ml 0.1 M sodium gluconate solution and 100 μl ^{99m}Tc generator eluate.

50 μl stock solution containing 2.17 mg **1** dissolved in 400 μl 0.05 M NaOH are given to the $^{99/99m}\text{Tc}$ gluconate solution. After 30 min the exchange is complete.

Results and Discussion

The new ligand was obtained according to reaction scheme 1.

Reaction scheme 1: Synthesis of **1**



Reaction of the ligand with $[\text{ReOCl}_4]^-$ (Scheme 2) resulted in an oxorhenium complex which is uncharged because of the presence of the thioether group. The complex is stable on exposure to air and soluble in common organic solvents.

Reaction scheme 2: Formation of the rhenium complex **2**

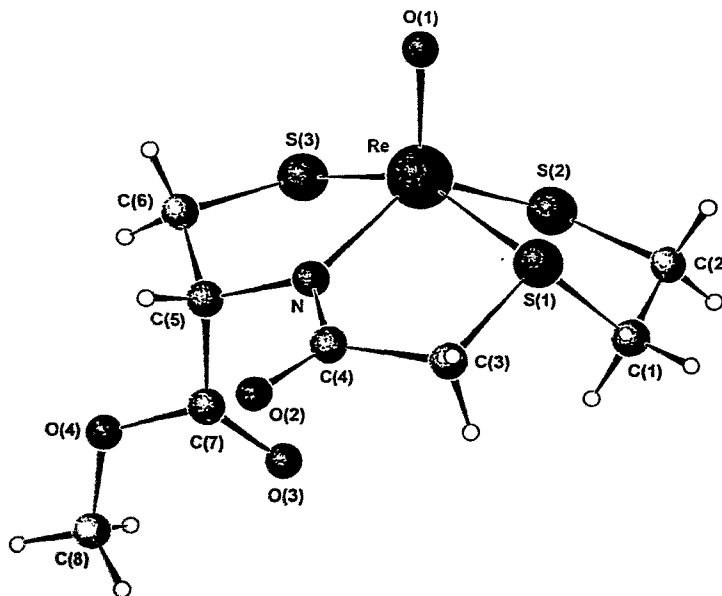
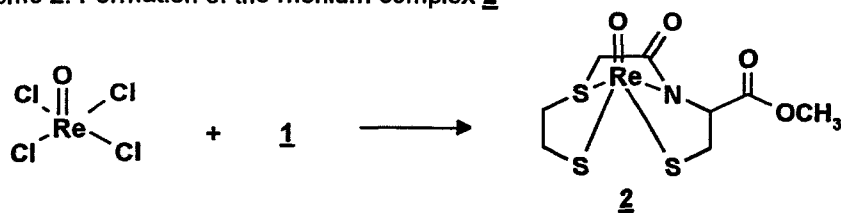


Fig. 1: POWDER CELL diagram of the molecular structure of **2**. Selected bond lengths [\AA] and angles [$^\circ$]: Re-O1 1.676(4), Re-N 1.991(4), Re-S1 2.359(2), Re-S2 2.266(2), Re-S3 2.290(2), C4-O2 1.201(7); O1-Re-N 117.8(2), O1-Re-S1 100.7(2), O1-Re-S2 115.0(2), O1-Re-S3 107.0(2).

Analytical data of **2** confirm the composition as a mono-ligand complex and a strong band in the infrared spectrum shows the presence of the ReO bond as expected for an oxorhenium(V) species. A single-crystal structure analysis revealed that the thioether sulphur is involved in coordination, possessing the equatorial plane together with the amide nitrogen and the two thiolate sulphur atoms to form a square-pyramidal arrangement at the central atom. Re-N_{amide} and Re-S distances are of the order generally found for these groups.

The formation of complexes with the radioactive technetium was accomplished by ligand substitution on Tc(V) gluconate at a concentration level of 1 mM and increasing molar ratios of ligand : Tc. Inspection of the reaction mixture after 30 min by HPLC and TLC shows complete conversion of the Tc(V) precursor into a complex component **3**. Three components being a small portion of Tc gluconate and two complexed species were observed in neutral media. The main product is extractable from the mixture by methylene chloride. The R_t value (14.0 min) of this radiochemically pure product is practically identical with that of the rhenium complex **2**.

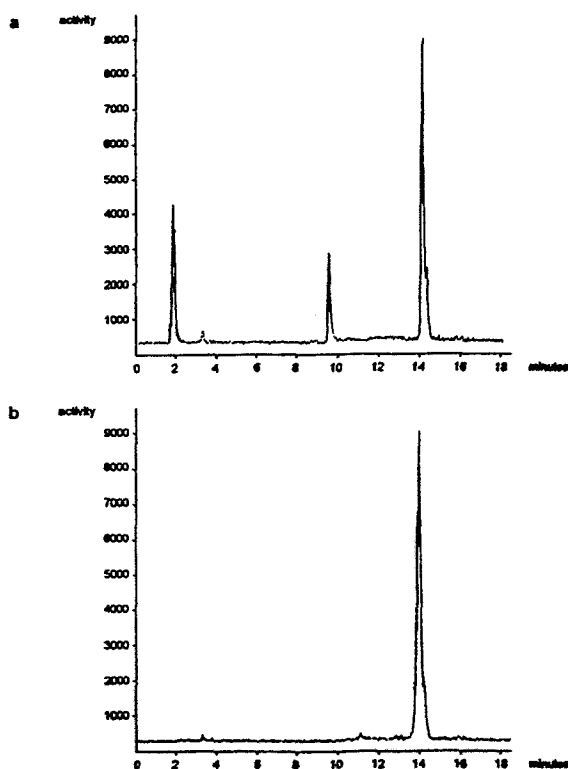


Fig. 2: Product pattern of the reaction of Tc gluconate with **1**,
(a): reaction mixture, (b): methylene chloride extract

The second component (R_t = 9.8 min) is assumed to be the free acid of **3** as deduced from its chromatographic properties and the non-extractability into organic solvents.

References

- [1] Johansen B. and Spies H. (1995) Technetium(V) chemistry as relevant to nuclear medicine, *Topics Curr.Chem.* **176**, 77 - 121.
- [2] Larsen J. and Lenor C. (1989) Synthesis of bis(ethylenedithio)tetrathiafulvalene (BEDT-TTF), *Synthesis*, 134.

15. Novel Oxorhenium(V) Complexes with Cysteinylglycine and Glycylglycylcysteine: Preparation and Characterization in Solution

S. Kirsch, R. Jankowsky, B. Noll, H. Spies, B. Johannsen, D. Scheller¹

¹Institut für Analytische Chemie, Technische Universität Dresden

Introduction

^{99m}Tc peptide complexes have aroused increasing interest in recent years. Direct labelling of peptides without a conjugated chelating moiety is possible because of the variety of potential donor groups present in peptides. An outstanding role in ligating technetium or its surrogate rhenium plays the sulphur atom of cysteine (Cys).

In the following work investigations were made into studying the complexation behaviour in solution of the sulphur-containing di- and tripeptides cysteinylglycine (CysGly) and glycylglycylcysteine (Gly₂Cys), (Fig. 1), with rhenium.

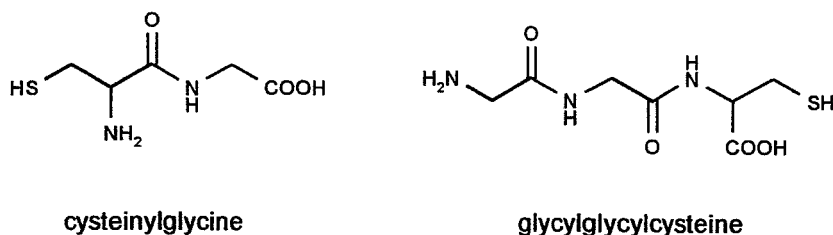


Fig. 1: Molecular formulas of the ligands CysGly and Gly₂Cys

Besides the thiol group, the amine, the amide and the carboxyl group are present in these molecules as potential ligating donors. In this report we are trying to answer the following questions:

- What kind of donating groups are involved in the complex formation?
- Does the complex formation depend on the pH?
- What is the structure of the complexes to be formed?

To determine the molecular structure of the complexes we carried out some EXAFS (extended absorption fine structure) studies in solution (at pH 2 - 3) and examined the complexation behaviour at various pH values (pH 2 - 12) by capillary electrophoresis.

Experimental

Methods

The influence of the molar ratio of the ligands on the occurrence of products was studied by HPLC (RP 18 column, Eurospher 100-C18, 25 cm, ID 4 mm, eluents: phosphate buffer pH 5.8, acetonitrile; gradient 0 → 90 % acetonitrile, 15 min, 1 ml/min).

Capillary electrophoresis (CE) was carried out on a fused silica gel capillary (ID = 50 μm, *l*_{eff} = 56 cm, extended light path, non-coated) at a voltage of 30 kV with the following buffer solutions pH 2.0 - 12.0:

pH 2.0 - 6.4: Citrate buffer SÖRENSEN (0.03 m)

pH 6.4 - 9.0: Borax-KH₂PO₄ buffer KOLTHOFF (0.015 m)

pH 9.0 - 12.0: Glycine buffer SÖRENSEN (0.03 m)

Components were detected by UV absorption at 200, 254, 350 and 450 nm. Acetone was used as a neutral marker and the tetraphenylarsonium cation as a +1 marker.

Synthesis of Re-CysGly and Re-Gly₂Cys

The Re complexes were prepared by ligand exchange, starting from the gluconate precursor with a molar ratio of 1 : 2 (Re : CysGly) and 1 : 1 (Re : Gly₂Cys). Both complexes were purified by HPLC (eluents: water acidified with 2 - 3 ml acetic acid/l = pH 2 - 3; acetonitrile; gradient: 5 min 100 % water; 7 min 0 → 70 % acetonitrile, 5 min 70 % acetonitrile; 5 min 100 % water) and lyophilized 5 times.

Results and Discussion

Re-CysGly

HPLC results show that only one Re-CysGly complex was formed irrespective of the addition of ligand. At a molar ratio of Re : peptide = 1 : 2 all Re gluconate was used up. A solid complex was obtained in a 40 % yield.

Analytical data for Re-CysGly:

Elemental analysis: (Found: C, 21.62; H, 3.08; N, 10.08; S, 11.54, $\text{ReC}_{10}\text{H}_{17}\text{O}_7\text{N}_4\text{S}_2$ requires C, 21.15; H, 3.10; N, 9.81; S, 11.21 %)

Mass spectrum (FAB, neg.): m/z 555 (100 %), 482 (80 %)

UV/VIS absorptions: $\lambda_{\text{max}}/\text{nm}$ (water) 493, 340 with a shoulder at 298.

IR absorptions: (KBr) $\nu_{\text{max}}/\text{cm}^{-1}$ 976 (Re=O) and several intensive overlapping absorptions from 1750 to 1550.

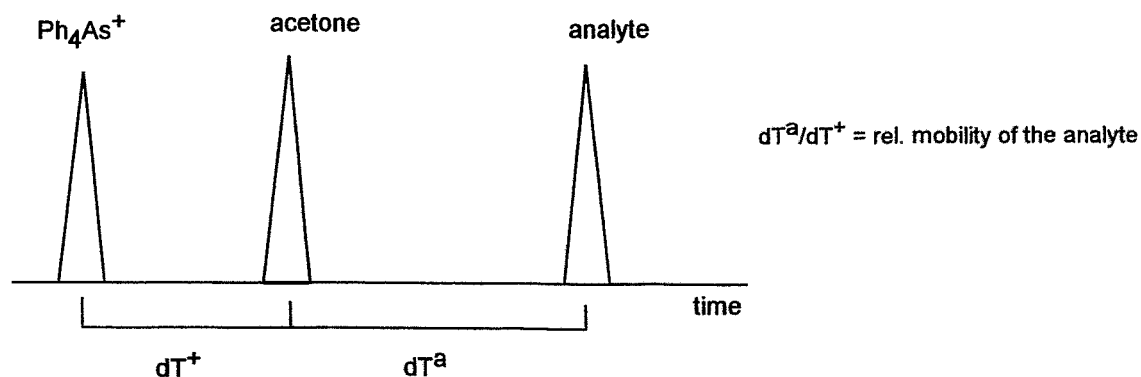
UV/VIS and IR data indicate a quite similar structure to that found for the Re cysteine complex [1] with two coordinating SH and amine groups.

Capillary electrophoresis

With the help of capillary electrophoresis it is possible to determine protonable groups in the Re-CysGly complex at different pH to learn more about the complexation behaviour in solution. An additional advantage of this method is that there is no need to isolate the received complex(es).

Analytical data were collected in buffer solutions from pH 2.5 to 11.6 in 0.4 pH units. To exclude the electroosmotic flow (EOF) a neutral marker was used (acetone). Furthermore we utilized a cationic +1 marker (Ph_4As^+) to determine the rel. mobility of the analyte, which consequently depends on its absolute charge, as follows: The time distance between +1 marker and neutral marker, dT^+ , as well as the distance between neutral marker and the analyte, dT^a , were determined according to scheme 1 and the ratio of dT^a to dT^+ (rel. mobility of the analyte) was pointed against the pH (Fig. 3). A rel. mobility < 0 indicates a cationic charge of the analyte, a rel. mobility = 0 a neutral complex and a rel. mobility > 0 an anionic charge.

Scheme 1: Determination of the rel. mobility of the analyte



In Fig. 2 Re-CysGly was compared with the free ligand CysGly. It is shown that the ligand possesses 3 protonable groups, which belong to COOH , NH_3^+ and SH but only 2 protonable groups exist in the complex ($\text{pK}_1 = 3.0$, $\text{pK}_2 = 5.9$). The rel. mobility (which is correlated to the absolute charge of the analyte) increases with the pH and seems to reach its maximum at $\text{pH} > 12$ (measurements above pH 12 were not possible because of the instability of the complex), which indicates an alteration in charge at the Re oxo core.

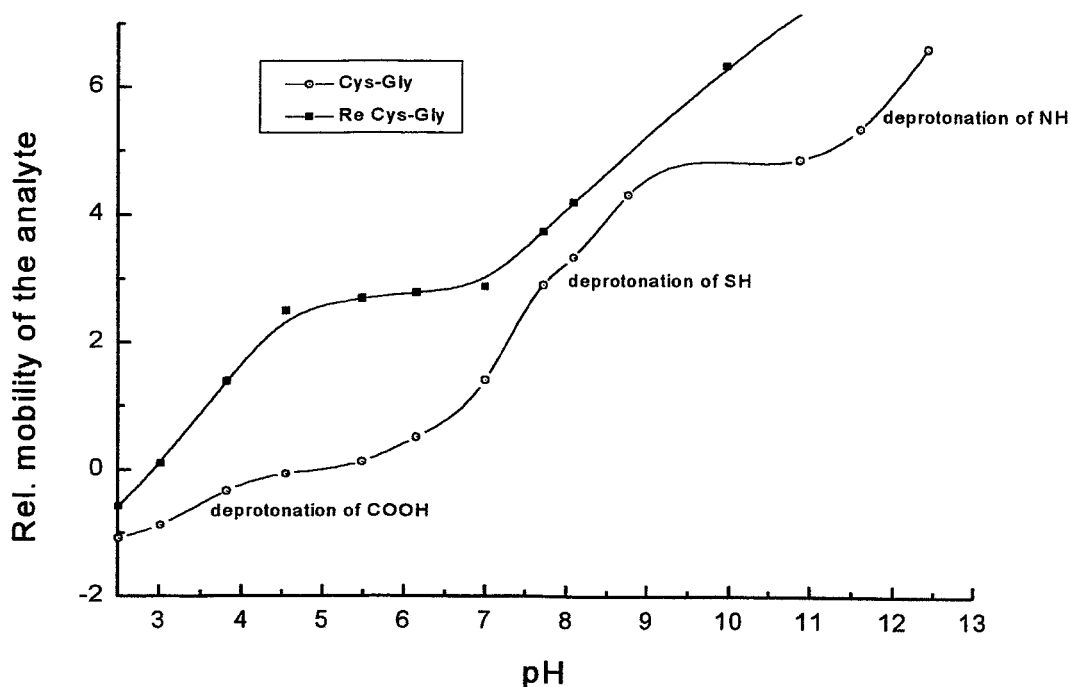


Fig. 2: Rel. mobility of Re-CysGly and CysGly depending on pH

Upon a pH value of 8 the UV spectrum of the detected Re complex changes (λ_{\max} 345 nm at pH < 8, λ_{\max} 290 nm at pH > 8) and this change is reversible with the pH. In Fig. 3 the postulated 1 : 2 Re complex is shown with its different forms depending on pH.

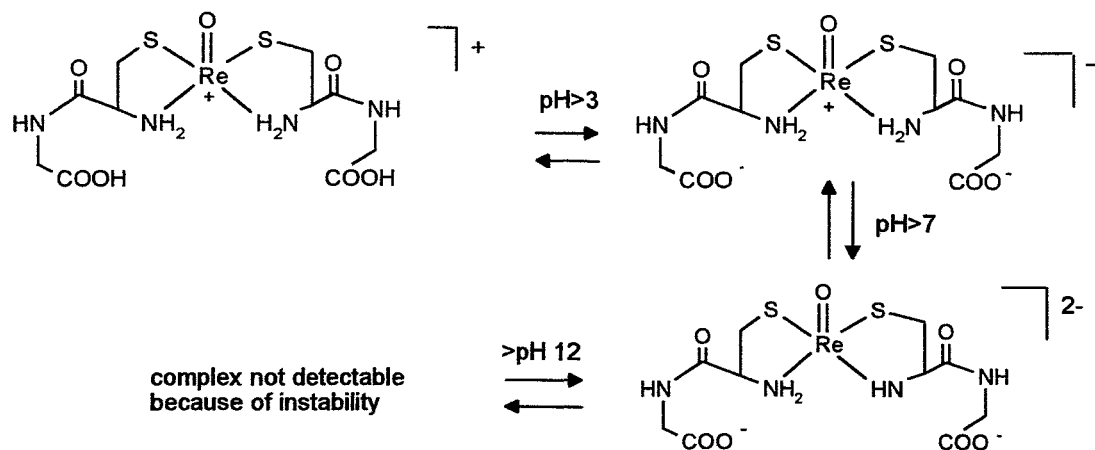


Fig. 3: Postulated 1 : 2 complex of Re-CysGly in solution with its different forms depending on pH

Re-Gly₂Cys

Capillary electrophoresis

Data from CE were collected as described above. HPLC results indicate a 1:1 complex. The rel. mobility of this Re-Gly₂Cys complex and the free ligand Gly₂Cys versus the pH is shown in Fig. 5. At a pH range < 4.5 the rel. mobility of the complex is 0 (neutral). Then the rel. mobility increases between pH 4.5 and 5.5 (anionic behaviour, deprotonation of COOH) and reaches a plateau. At a pH range > 8.5 the rel. mobility of the complex (and its absolute charge) increases again which could be

the result of deprotonation of the NH_2 group. No cationic complex is formed even at a low pH. In Fig. 4 the different forms depending on the pH of the postulated 1 : 1 complex are shown.

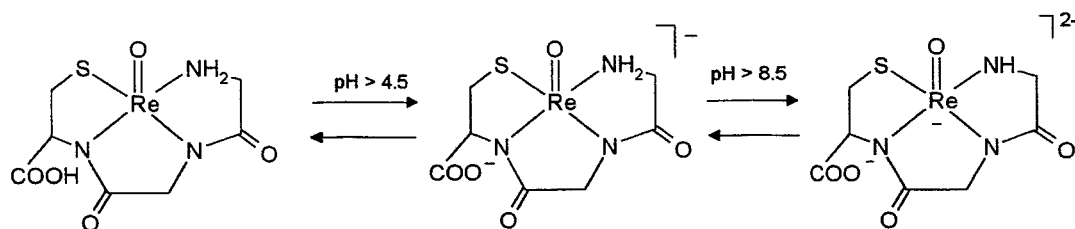


Fig. 4: Solution behaviour of the postulated $\text{Re-Gly}_2\text{Cys}$ complex

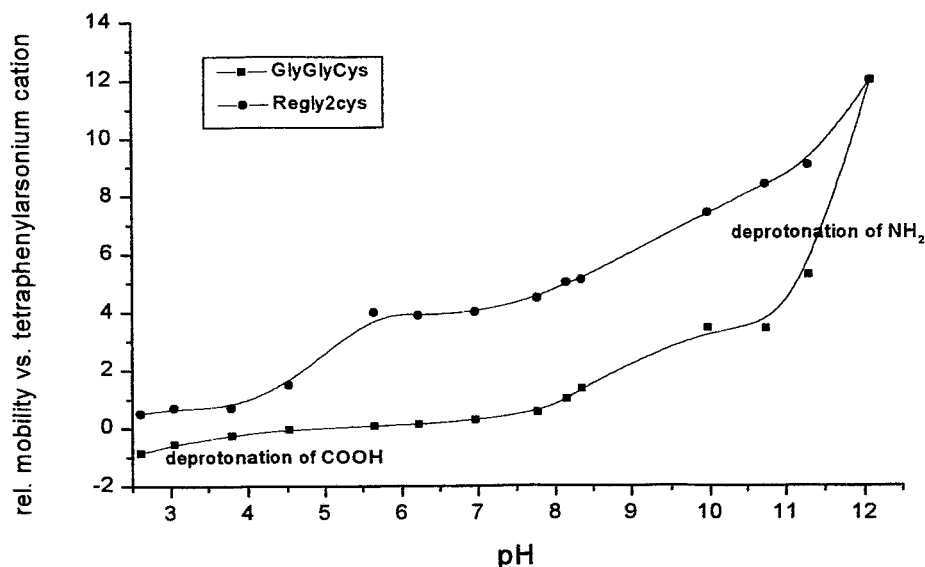


Fig. 5: Rel. mobility of $\text{Re-Gly}_2\text{Cys}$ and Gly_2Cys depending on pH

XAS measurements on $\text{Re-Gly}_2\text{Cys}$ and Re-CysGly

Rhenium L_{III} edge data were collected as described elsewhere [2]. Measurements were taken in aqueous solution, pH 2 - 3.

EXAFS investigations

In Fig. 6 and Table 1 EXAFS data for the two Re complexes are shown and the following characteristic features were found:

Both complexes possess the characteristic short bound oxygen atom at 1.69 Å.

In case of $\text{Re-Gly}_2\text{Cys}$ a SN_3 coordination was proven. Detection of protonated amine atoms, usually bound at a distance of 2.2 Å, is not possible because no discrimination can be made between coordination shells that differ in less than 0.15 Å. This fact is due to a limited K-range. Thus, Re is complexed by Gly_2Cys in a 1:1 complex.

Re-CysGly has a S_2N_2 coordination where the two amine nitrogen atoms are at a mean distance of 2.14 Å from each other. This is a typical short value for amine nitrogen atoms and therefore perhaps an indication of the partial deprotonation of one amine group. Further measurements at various pH values must be carried out to prove this postulation. However, for Re-CysGly a complex stoichiometry of 1:2 could be demonstrated by the S_2N_2 coordination.

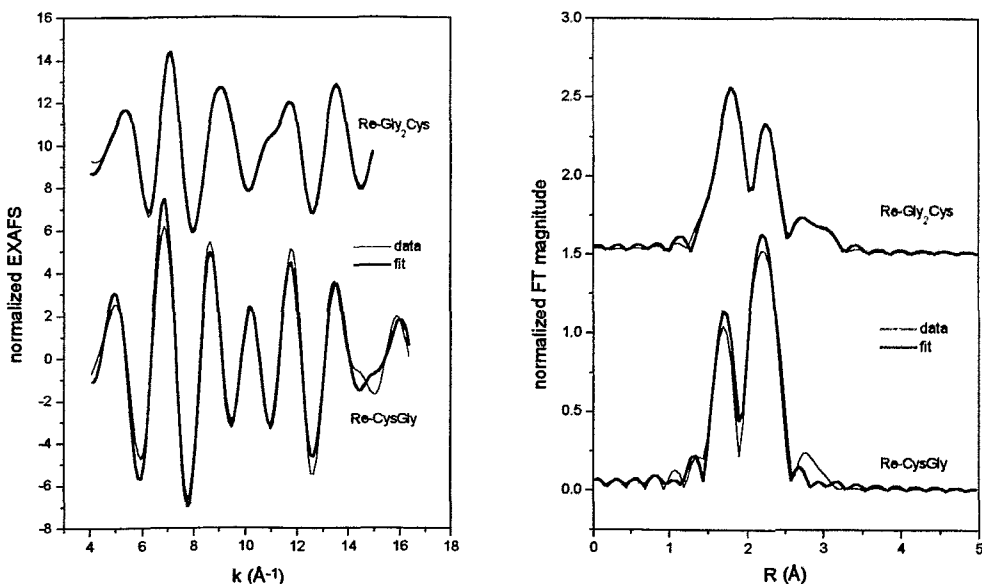


Fig. 6: EXAFS best fit data for Re-Gly₂Cys and Re-CysGly.

Table 1: EXAFS data for Re-Gly₂Cys and Re-CysGly

Complex	Backscattering atom	Coordination number	Distance to Re central atom (Å)	DEBYE-WELLER-factor
Re-Gly ₂ Cys	O (Re=O)	1	1.69	0.001
	N (amide/amine)	3	2.01	0.004
	S (mercapto)	1	2.27	0.002
Re-CysGly	O (Re=O)	1.3	1.69	0.001
	N (amine)	2	2.14	0.001
	S (mercapto)	2	2.33	0.002

Conclusions

The results obtained by EXAFS and capillary electrophoresis show that the tripeptide Gly₂Cys builds a 1 : 1 complex with Re (Fig. 4) and the dipeptide CysGly a 1:2 complex (Fig. 3) with a similar structure to that of Re-cysteine [1]. Furthermore, CE results prove that the charge changes with increasing pH, indicating that at pH > 2.5 the carboxyl groups are deprotonated. At pH > 8 another increase in charge is observed which could be caused by the deprotonation of an amine group. Thus, both types of complexes seem to exist in different forms, depending on pH.

References

- [1] Kirsch S., Noll B., Scheller D., Klostermann K., Spies H. and Johannsen B. (1995) Preparation and characterization of rhenium(V) complexes with cysteine and its derivatives penicillamine and cysteamine, *Annual Report 1995*, Institute of Bioinorganic and Radiopharmaceutical Chemistry, FZR-122, pp. 110 - 114.
- [2] Jankowsky R., Noll B., Spies H. and Johannsen B. (1996) XAS investigations on Tc and Re complexes of oligoglycine ligands and Tc tartrate. *This report*, pp. 72 - 76.

16. Synthesis and Characterization of Technetium and Rhenium Oligoglycine Complexes and Technetium Tartrate

R. Jankowsky, B. Noll, H. Spies, B. Johannsen

Introduction

Peptide molecules as technetium ligands have attracted increasing interest in nuclear medicine [1, 2]. To investigate the complexing properties of these ligands, systematic investigations into the complex structure of simple peptide complexes are necessary. Studies of sulphur-containing amino acids were therefore carried out by Kirsch [3]. More studies were required to find out about the complexing behaviour of sulphur-free peptides. Several assumptions were put forward concerning the structure of Tc oligoglycine complexes [4].

In the following study technetium and rhenium complexes of tri, tetra, penta and hexaglycine were synthesized and characterized. Capillary electrophoresis (CE) was applied as well as classical techniques like HPLC and elemental analysis.

Experimental

Synthesis of technetium tri, tetra, penta and hexaglycine

The complexes were synthesized by direct labelling procedure starting from $0.01 \text{ M } ^{99}\text{TcO}_4^-$ using sodium tartrate and SnCl_2 in alkaline solutions. The complex-forming reactions resulted in dark yellow solutions.

Synthesis of technetium tartrate

The synthesis procedure corresponds to the synthesis of Tc oligoglycine complexes, with the oligoglycine ligand omitted. The reaction yielded a dark red solution.

Synthesis of rhenium tetra-, penta- and hexaglycine

The synthesis was performed according to the Tc oligoglycine complexes and resulted in a brownish yellow solution.

HPLC separation of the Tc and Re Complexes

HPLC separation was carried out using an RP 18 semiprep. column with an aqueous acetic acid-acetonitrile gradient and radioactivity / UV 220 nm detection. Preparative separation was performed by collection of the fractions.

Elemental analysis of the Tc and Re complexes

The collected HPLC fractions were united and lyophilized 3 times to evaporate the HPLC eluent residues. The darkish powder obtained was analysed by a LECO CHNS elemental analysis device.

Infrared spectroscopy of Tc complexes

HPLC-isolated, lyophilized complexes were compressed into KBr pellets and measured on a CARL ZEISS JENA infrared spectrometer against air.

UV spectroscopy of Tc complexes

Lyophilized Tc complex powder was dissolved in water and measured on a CARL ZEISS JENA UV/VIS spectrometer against a water reference.

Capillary electrophoresis of Tc and Re complexes

Capillary electrophoresis was performed using a HEWLETT PACKARD device equipped with a diode array UV detection system. A non-coated fused silica capillary was used.

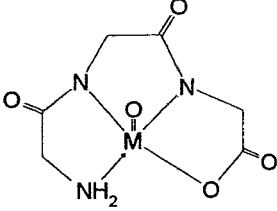
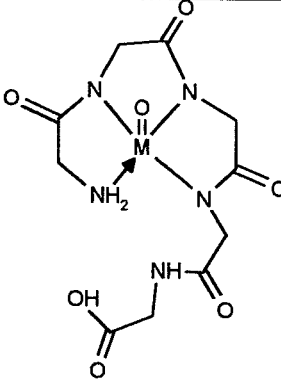
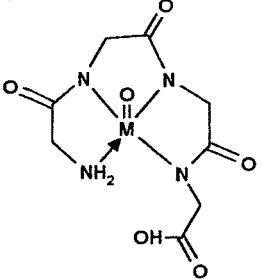
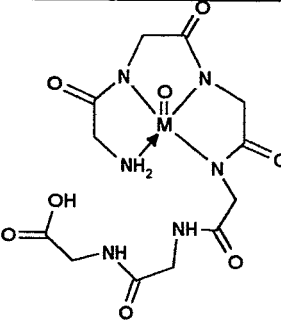
To study the Tc pentaglycine complex behaviour over the pH range, the following buffer systems were used:

- pH 2.0 - 6.4 citrate buffer SÖRENSEN (0.03 M)
- pH 6.4 - 9.0 borax- K_2HPO_4 buffer KOLTHOFF (0.015 M)
- pH 9.0 - 12.0 glycine buffer SÖRENSEN (0.03 M)

Results and Discussion

Complexes of the following structures were assumed to be obtained:

Table 1: Proposed complex structures (M = Re, Tc)

Complex	Proposed structure	Complex	Proposed structure
M-Gly ₃		M-Gly ₅	
M-Gly ₄		M-Gly ₆	

Technetium and rhenium show similar complexing properties to oligoglycine ligands. In both cases it was not possible to synthesize the complexes by common ligand exchange procedure starting from gluconate, glucoheptonate or citrate precursors because of only weak donor properties of the peptide ligand atoms. Furthermore, triglycine was not able to form a stable complex with rhenium. Table 2 shows the HPLC separation results.

Table 2: HPLC results

Complex	Retention time	Radiochemical yield
Tc-Gly ₃	10.5 min	95 %
Tc-Gly ₄	12.3 min	92 %
Tc-Gly ₅	11.6 min	91 %
Tc-Gly ₆	9.8 min	96 %
Tc-Tartrate	1.8 min	92 %
Re-Gly ₄	10.2 min	-
Re-Gly ₅	11.7 min	-
Re-Gly ₆	8.6 min	-

Collected fractions of technetium complexes possessed a yellow colour, whereas rhenium complexes turned red. Lyophilization of the HPLC-isolated technetium complexes produced brown powders, which resulted in a yellow solution when dissolved in water. Rhenium complexes obviously decomposed, because only a black powder was obtained giving a black suspension when dissolved. It is assumed that the rhenium complexes are not stable under the acidic separation conditions used. In the following elemental analysis results are given, with Re-Gly₆ excluded from elemental analysis because of its rapid decomposition after HPLC separation.

Tc-Gly₃: Found: C, 23.46; H, 3.10; N, 13.14, TcC₆H₈N₃O₅ requires C, 24.01; H, 2.69; N, 14.00 %.

Tc-Gly₄: Found: C, 27.21; H, 2.90; N, 16.54, TcC₈H₁₁N₄O₆ requires C, 26.90; H, 3.10; N, 15.69 %.

Tc-Gly₅: Found: C, 25.30; H, 2.98; N, 13.99, TcC₁₀H₁₄N₅O₇ requires C, 28.99; H, 3.41; N, 16.91 %.

Tc-Gly₆: Found: C, 27.92; H, 3.27; N, 15.71, TcC₁₂H₁₇N₆O₈ requires C, 30.58; H, 3.64; N, 17.83 %.

Re-Gly₄: Found: C, 19.99; H, 3.63; N, 12.99, ReC₈H₁₁N₄O₆ requires C, 21.57; H, 2.49; N, 12.58 %.

Re-Gly₅: Found: C, 21.71; H, 2.93; N, 11.61, TcC₁₀H₁₄N₅O₇ requires C, 23.90; H, 2.81; N, 13.94 %.

Roughly, all complexes show agreement as to the estimated atomic compositions. However, the complex formulas could not be clearly determined by elemental analysis.

The IR spectra showed no Tc=O absorption, which was estimated at wave numbers of around 950 cm⁻¹. The Tc complexes obviously decomposed by being compressed into KBr pellets.

As it was not possible to properly isolate the Re complexes, UV/VIS spectra could only be recorded of the Tc complexes. Fig. 1 shows the UV/VIS spectra of the Tc complexes.

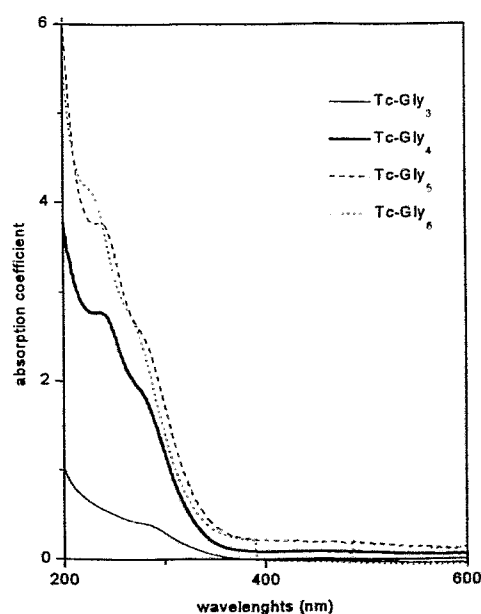


Fig. 1: UV/VIS spectra of the Tc complexes

All complexes investigated show similar UV absorption pattern, thus indicating similar atomic environments of the central atom.

Capillary electrophoresis monitoring of the Tc and Re complex-forming reactions also indicates similar relationships. At pH 2.5 all complexes are noncharged, at pH 7 and pH 9.3 they are negatively charged. Tc tartrate could not be detected in CE, possibly due to its decomposition in the electric field.

Except for Tc-Gly₃, these results support the structural assumptions shown in Table 1. In the case of Tc-Gly₃ a neutral complex was expected. Because of the negative charge found at the neutral pH

either a deprotonation of the coordinating amine group or an additional coordination of an OH⁻ group to the Tc core must have taken place.

To obtain more information about the complex behaviour over the pH range, the Tc pentaglycine complex was investigated, using a novel capillary electrophoresis method. A solution of Tc-Gly₅ containing tetraphenyl arsonium chloride and acetone was measured at buffer pH from 2.6 to 12.5. The migration times of the free ligand (Gly₅), the complex (Tc-Gly₅), the tetraphenyl arsonium chloride and acetone were detected. Identification of solution particles was performed, using the diode array detector UV fingerprint. Fig. 2 shows a capillary electropherogram of the Tc-Gly₅ sample at buffer pH 7.78.

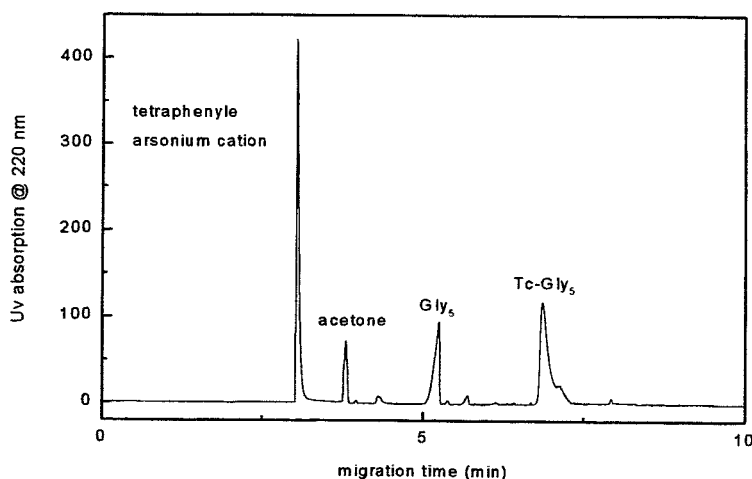


Fig. 2: Capillary electropherogram of Tc-Gly₅ sample

To exclude the electro-osmotic flow (EOF), which equally influences all particles in the analyte solution, the acetone migration time was set to 0. Assuming that the tetraphenyl arsonium cation's charge is +1 all over the pH range, the corrected migration time of this cation may serve as an internal standard. Migration time differences between analytes (Gly₅ and Tc-Gly₅) and acetone were divided by the migration time difference between the cation standard and acetone to give relative mobilities of the analytes. Relative mobilities of the analytes relate to the amount of protonable groups in the complex, i.e. every step in the resulting graph corresponds to one protonable group. Fig. 3 shows the results of the investigated Tc-Gly₅ complex.

The free Gly₅ ligand has two protonable groups, although the second (amino) step could not be properly detected because of its location at pH > 13. The first (carboxyl) group is detected at acidic pH below pH 3.

In the case of Tc-Gly₅ two significant steps were measured. The first step is situated at pH 5 and can be considered to be the free carboxyl group. The increase in relative mobility at high pH values can be explained both by a deprotonating amine group or a supplemental trans coordination of an OH⁻ group.

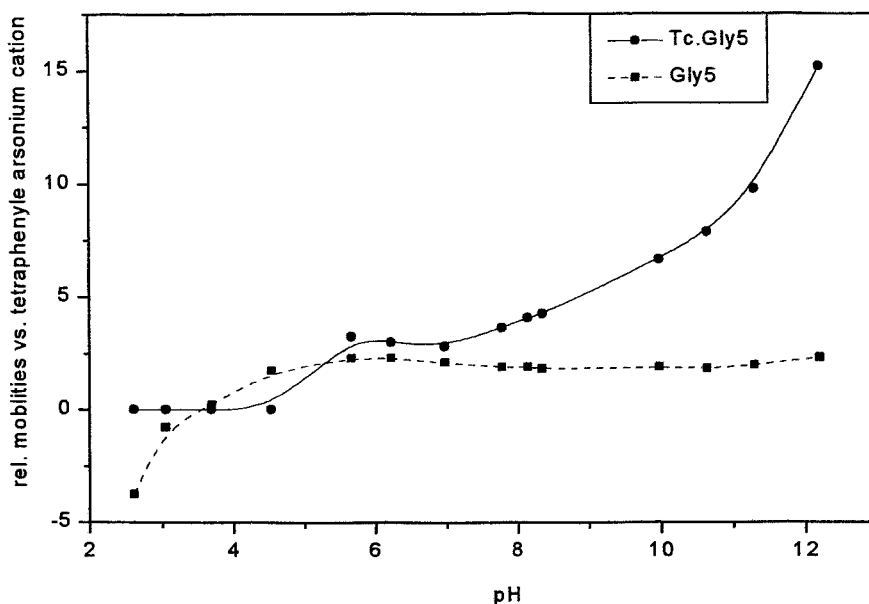


Fig. 3: Relative mobilities of Gly₅ and Tc-Gly₅

Conclusions

Except for Tc-Gly₃, the obtained analytical data support the above-mentioned structural assumptions. Tc-Gly₃ seems to coordinate either via the carboxylic group or via an OH⁻ group. Re complexes of oligoglycine ligands are not stable at neutral and acidic conditions.

References

- [1] Thakur M. L. (1995) Radiolabelled peptides: Now and the future. *Nucl. Med. Comm.* **16**, 724 - 732.
- [2] Fishman A. J., Babich J. W. and Strauss H. W. (1993) A ticket to ride: Peptide radiopharmaceuticals. *J. Nucl. Med.* **34**, 2253 - 2263.
- [3] Kirsch S., Noll B., Scheller D., Klostermann K., Leibnitz P., Spies H. and Johannsen B. (1995) Preparation and characterization of rhenium(V) complexes with cysteine and its derivatives penicillamine and cysteamine. *Annual Report 1995*, Institute of Bioinorganic and Radiopharmaceutical Chemistry, FZR-122, pp.110 - 114.
- [4] Vanbilloen H. P., De Roo M. J. and Verbruggen A. M. (1996) Complexes of technetium-99m with tetrapeptides containing one alanyl and three glycyl moieties. *Eur. J. Nucl. Med.* **23**, 40 - 48.

17. XAS Investigations on Tc and Re Complexes of Oligoglycine Ligands and Tc Tartrate

R. Jankowsky, B. Noll, H. Spies, B. Johannsen

Introduction

X-ray absorption measurements were employed to obtain more information about the Tc and Re complexes of oligoglycine ligands and Tc tartrate in solution. XAS is a well established technique in structural analysis of Tc complexes [1, 2] and has been shown to be a valuable tool in research on both metal peptide complexes [3] and radiopharmaceutically relevant complexes [4].

Because we were unable to obtain crystals, XAS was the method of choice to investigate the complex structures. Although XAS cannot provide structural parameters of the entire complex, important information on metal oxidation states and the metal environment was obtained.

Experimental

XAS measurements of the Tc and Re complexes

Technetium complex samples for XAS measurements were prepared by upscaled synthesis of the method described elsewhere [5] (60 μ l of 0.291 M $^{99}\text{TcO}_4^-$ in water were reacted) and lyophilization to a volume of 2.2 ml. Samples were filled into 2.2 ml EPPENDORF tubes under nitrogen heat sealed. The tubes were contained in a triple PE containment and immediately frozen at -10 °C.

Rhenium complexes were synthesized immediately before the measurements by mixing the reactants (using 1.4 mg NaReO_4) in 2.2 ml EPPENDORF tubes.

XAS data of the Tc complexes were collected at HASYLAB, Hamburg, at the bending magnet beamline X1.1 (ROEMO II monochromator). The DORIS III storage ring ran at 4.5 GeV with a positron current of 30 to 80 mA during measurements. Tc measurements were taken in transmission mode at room temperature, using ionization chambers against an aqueous KTcO_4 reference. An Si (311) double crystal monochromator was used to monochromatize the X-ray beam to the Tc K edge (21 044 eV). For energy calibration, the first maximum (pre-edge peak [2]) in reference spectra derivatives was set to 21 044 eV.

Rhenium measurements were taken at the Stanford Synchrotron Radiation Laboratory at beamline 2-3, which was equipped with a double crystal Si (220) monochromator. The SPEAR storage ring was operated with an electron current of 30 to 70 mA. A four-channel solid-state fluorescence detector was used to collect the Re L_{III} edge data. No reference sample data could be collected because the Re concentration was obviously too high. The software package EXAFSPAK [6] was used to process the data obtained. Energy calibration was performed using the first derivative method. In the case of Tc complexes, the first maximum in the reference spectrum derivative was defined as 21 044 eV. For Re complexes, the first maximum in the sample spectrum derivative was set at 10 535 eV. The theoretical phase and amplitude scattering functions were calculated with the program FEFF 5.05 [7]. Measurements of Tc-Gly₃ failed because of decomposition of the sample during transport.

Results

XAS measurements provided valuable structural results. The Tc oxidation states can be derived from the maximum of the spectra derivatives, as listed in Table 1. Because Tc +5 complexes do not possess the characteristic pre-edge peak as KTcO_4 complexes [2], edge energy determinations yielded a higher absorption edge energy for Tc +5 complexes than the KTcO_4 reference.

Table 1: XANES data of the Tc complexes

complex	position of derivative maximum (eV)
Tc-Gly ₄	21 053.8
Tc-Gly ₅	21 053.8
Tc-Gly ₆	21 054.47
Tc-Tartrate	21 053.44
Tc-N-methyl-MAG ₃	21 055.53

A Tc-MAG₃-derived complex (Tc-N-methyl-MAG₃) was used as a standard with a Tc oxidation state of +5. XANES data indicate the same oxidation state as the standard for all Tc complexes. It could be confirmed that tartrate is able to chelate Tc at an oxidation state of +5.

As there were no reference data for the Re measurement, no determinations of the Re oxidation state in the complexes were possible.

EXAFS analysis showed very similar patterns for the Tc-Gly_x complexes. Fig. 1 shows the Fourier filtered EXAFS [8] of the Tc complexes and their Fourier transforms.

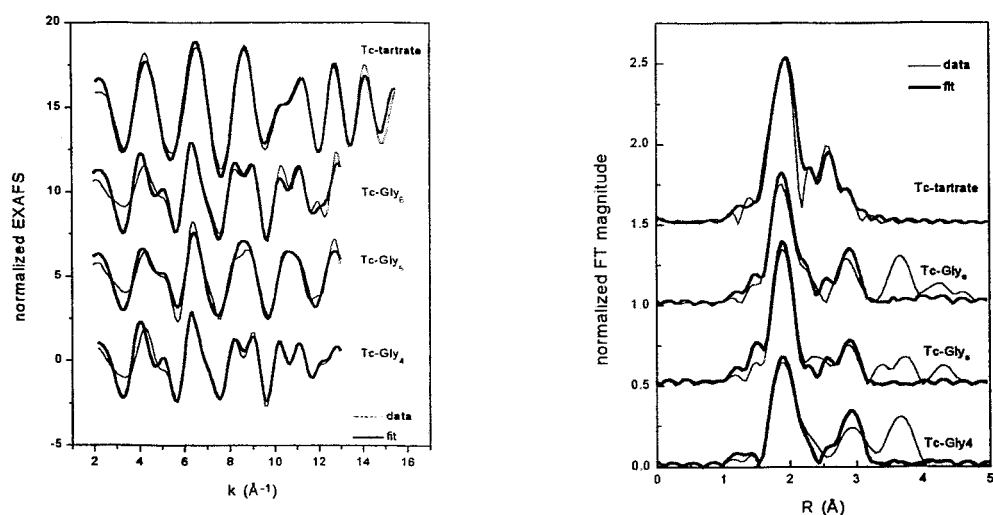


Fig. 1: EXAFS and Fourier transforms of the Tc complexes

In Table 2 best EXAFS fit results for the Tc complexes are listed.

Table 2: EXAFS fit results

Complex	Backscattering atom	Coordination number*	Distance to Tc central atom [Å]**	DEBYE-WALLER-factor
Tc-Gly ₄	O	0.75	1.67	0.003
	N	3.81	2.03	0.007
	Tc	1.12	2.86	0.009
Tc-Gly ₅	O	0.82	1.69	0.002
	N	4.32	2.07	0.008
	Tc	0.87	2.85	0.008
Tc-Gly ₆	O	0.66	1.68	0.002
	N	3.55	2.06	0.008
	Tc	1.07	2.82	0.009
Tc-tartrate***	O (Tc=O)	1	1.64	0.005
	O	5	1.99	0.006
	C	4	2.50	0.01

* Estimated uncertainty: 30 % ** Estimated uncertainty: 0.02 Å *** N were held constant during fit.

These data confirm the Tc oxidation state of +5 for all complexes. The Tc=O bond can be proved in all complexes. Furthermore, in all Gly_x complexes four nitrogen atoms with averaged bond lengths of around 2.05 Å could be detected. This averaged values are believed to represent 3 amide and 1 amine nitrogen atoms. This gives rise to the assumption, that the peptide N termini are involved in the metal complexation. Astonishingly, a distant technetium atom is detected at distances of around 2.85 Å at all complexes. A further coordination shell is visible at distances of around 4 Å, being

probably represented by the peptide backbone carbonyl oxygen atoms, which are detectable due to focussing multiple-scattering effects. These phenomena have to be further analyzed.

Tc tartrate was determined to have a short-bound oxygen atom at the Tc central atom and an additional O₅ coordination. Thus, a 1:2 complex stoichiometry and a *trans* coordination of a tartrate carboxylic oxygen can be assumed. The bridging carbons are located significantly closer to the Tc than in the Tc peptide complexes.

The two rhenium samples, Re-Gly₄ and Re-Gly₅, also showed very similar EXAFS and Fourier transforms, they are shown in Fig. 2.

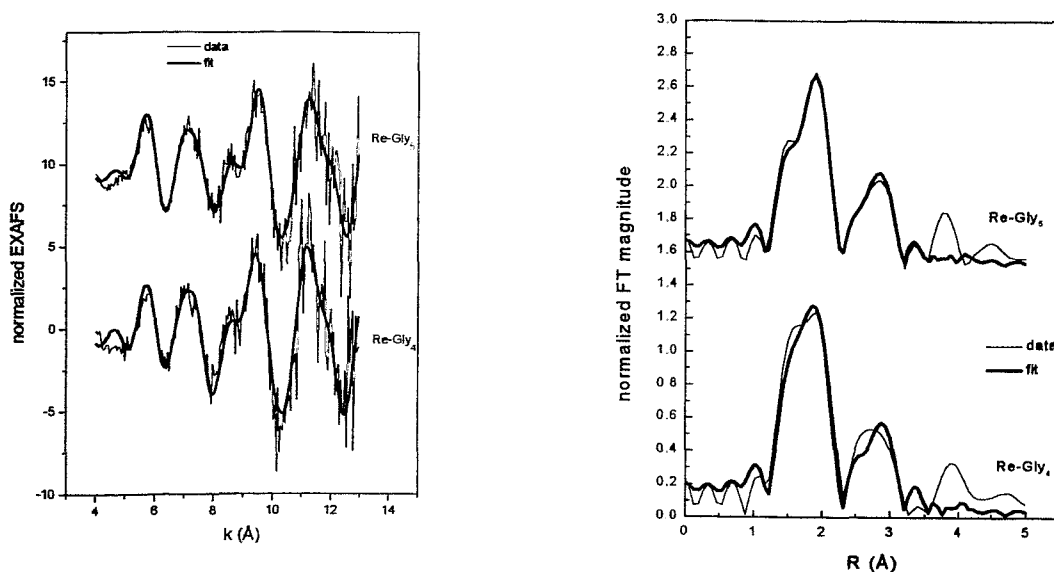


Fig. 2: EXAFS and Fourier transforms of Re-Gly₄ and Re-Gly₅

Table 3 shows the EXAFS best fit results for the Re complexes.

Table 3: EXAFS fit results for Re-Gly₄ and Re-Gly₅

Complex	Backscattering atom	Coordination number	Distance to Re central atom [Å]	DEBYE-WALLER-factor
Re-Gly ₄	O	1	1.70	0.002
	N	4	1.96	0.004
	Re	1	2.91	0.008
Re-Gly ₅	O	1	1.70	0.002
	N	4	1.98	0.005
	Re	1	2.92	0.009

The Re complexes show very similar fit results compared to the Tc fit results. Again, the +5 Re oxidation state could be proven by the detection of a short-bound oxygen atom. Four nitrogens are bound at averaged values of around 1.97 Å. Obviously, a deprotonation of the coordinating amine nitrogen atom takes place. A distant Re atom is detected at around 2.9 Å as well as a more distant coordination shell, again probably detectable due to multiple scattering effects.

Conclusions

Technetium and Rhenium are obviously complexed by sulphur-free oligopeptides in a complicated way. An involvement of the N termini in case of the Tc complexes could be shown. In case of Re, this unique evidence could not be obtained. The detected metal atoms at distances of under 3 Å give rise to the assumption, that the peptides cause a forming of dinuclear complexes. All complex EXAFS data have to be analyzed with regard to the detection of the distant metal atoms and possible multiple scattering effects in the future.

References

- [1] Almhamid I., Bryan J. C., Bucher J. C., Burell A. K., Edelstein N. M., Hudson E. A., Kaltsoyannis N., Lukens W. W., Shuh D., Nitsche H. and Reich T. (1995) Electronic and structural investigations of technetium compounds by X-ray absorption spectroscopy. *Inorg. Chem.* **34**, 193 - 198.
- [2] Allen P. G., Siemering G. S., Shuh D. K., Bucher J. J., Edelstein N. M., Langton C. A., Clark S. B., Reich T. and Denecke, M. A. (1996) Technetium speciation in cement waste forms determined by X-ray absorption fine structure spectroscopy. *Radiochim. Acta*, in press.
- [3] Foerster M., Brasack I., Duhme A.-K., Nolting H.-F. and Vahrenkamp H. (1996) Zinc complexes of oligopeptides containing histidine at both termini. *Chem. Ber.* **129**, 347 - 353.
- [4] Martin J. L., Yuan J., Lunte C. E., Elder R. C., Heineman W. R. and Deutsch E. (1989) Technetium diphosphonate skeletal imaging agents: EXAFS structural studies in aqueous solution. *Inorg. Chem.* **28**, 2899 - 2901.
- [5] Jankowsky R., Noll B., Spies H. and Johannsen B. (1996) Synthesis and characterization of technetium and rhenium oligoglycine complexes and technetium tartrate. *This report*, pp. 67 - 71.
- [6] George G. N. and Pickering I. J. (1995) EXAFSPAK, a suite of computer programs for analysis of X-ray absorption spectra. *Stanford Synchrotron Radiation Laboratory*, Stanford, CA.
- [7] Rehr J. J., Mustre de Leon J., Zabinsky S. and Albers R. C. (1991) Ab-initio curved wave X-ray absorption fine structure. *Phys. Rev. B* **44**, 4146.
- [8] Jankowsky R., Noll B., Spies H. and Johannsen B. (1996) X-ray absorption spectroscopy: A valuable tool for structural analysis of Tc and Re complexes. *This report*, pp. 76 - 78.

References

- [1] Almahamid I., Bryan J. C., Bucher J. C., Burell A. K., Edelstein N. M., Hudson E. A., Kaltsoyannis N., Lukens W. W., Shuh D., Nitsche H. and Reich T. (1995) Electronic and structural investigations of technetium compounds by X-ray absorption spectroscopy. *Inorg. Chem.* **34**, 193 - 198.
- [2] Allen P. G., Siemering G. S., Shuh D. K., Bucher J. J., Edelstein N. M., Langton C. A., Clark S. B., Reich T. and Denecke, M. A. (1996) Technetium speciation in cement waste forms determined by X-ray absorption fine structure spectroscopy. *Radiochim. Acta*, in press.
- [3] Foerster M., Brasack I., Duhme A.-K., Nolting H.-F. and Vahrenkamp H. (1996) Zinc complexes of oligopeptides containing histidine at both termini. *Chem. Ber.* **129**, 347 - 353.
- [4] Martin J. L., Yuan J., Lunte C. E., Elder R. C., Heineman W. R. and Deutsch E. (1989) Technetium diphosphonate skeletal imaging agents: EXAFS structural studies in aqueous solution. *Inorg. Chem.* **28**, 2899 - 2901.
- [5] Jankowsky R., Noll B., Spies H. and Johannsen B. (1996) Synthesis and characterization of technetium and rhenium oligoglycine complexes and technetium tartrate. *This report*, pp. 67 - 71.
- [6] George G. N. and Pickering I. J. (1995) EXAFSPAK, a suite of computer programs for analysis of X-ray absorption spectra. *Stanford Synchrotron Radiation Laboratory*, Stanford, CA.
- [7] Rehr J. J., Mustre de Leon J., Zabinsky S. and Albers R. C. (1991) Ab-initio curved wave X-ray absorption fine structure. *Phys. Rev. B* **44**, 4146.
- [8] Jankowsky R., Noll B., Spies H. and Johannsen B. (1996) X-ray absorption spectroscopy: A valuable tool for structural analysis of Tc and Re complexes. *This report*, pp. 76 - 78.

18. X-Ray Absorption Spectroscopy: a Valuable Tool for Structural Analysis of Tc and Re Complexes

R. Jankowsky, B. Noll, H. Spies, T. Reich, H. Nitsche

Introduction

X-ray absorption spectroscopy is a well-established tool in structural analysis of transition metals [1, 2]. Despite its unique ability to provide structural data of complexes in solution, only a few studies have so far been made on radiopharmaceutically interesting complexes containing Tc or Re [3, 4]. To emphasize the usefulness of the method, particularly for the third generation of ^{99m}Tc radiopharmaceuticals, a short evaluation of the XAS method will be given in the following.

Experimental

Data of Tc and Re complexes were collected at Stanford Synchrotron Radiation Laboratory, Stanford, CA, and at HASYLAB, Hamburg, as elsewhere described [5].

Results and Discussion

Several aspects of X-ray absorption spectroscopy should be discussed. First, there are some unique advantages provided by XAS.

Unlike XRD analysis, it is possible to determine the atomic environment of the central atom without availability of crystals. Thus, an *in situ* structural analysis can be performed. Complexes can be measured in reaction mixtures without any further purification, if a single metal species can be ensured. Amorphous and solid samples can be investigated as well, the latter prepared as a sample-Teflon or a sample-BN₃ pellet.

Concerning the data obtained, a lot of information is provided. It is possible to determine the central atom oxidation state by XANES (X-ray absorption near edge structure) measurements. For this a reference to a well known oxidation state is required. The energy absorption edge position correlates with the central atom oxidation state, thus the absorption spectra derivatives of both the reference and the samples have to be calculated and plotted as shown in Fig. 1 (Tc samples).

A MAG₃-derived complex with a known oxidation state of +5 was used as a reference. As can be seen, the absorption edge positions are the same, thus a +5 Tc oxidation state was concluded for all samples.

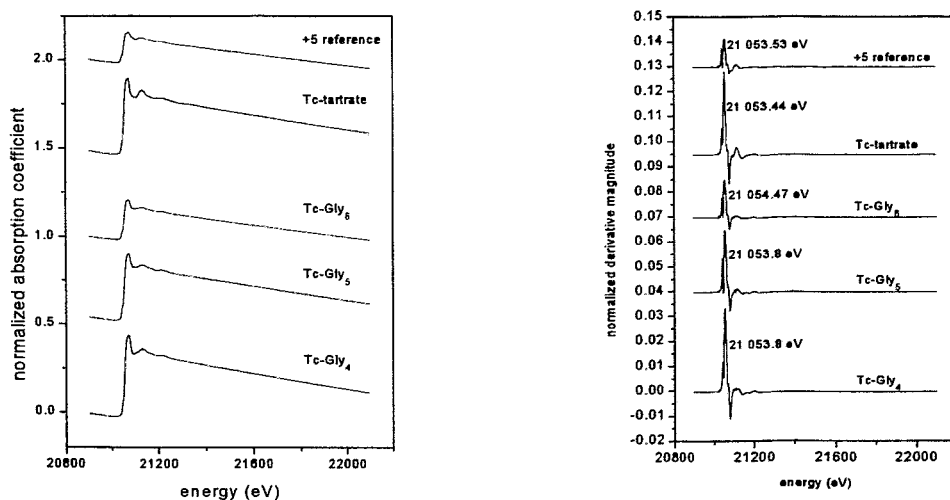


Fig. 1: XANES data processing (Ref.: Tc-N¹-methyl-MAG₃)

EXAFS measurements provide structural data about the atomic environment of the central atom, which are the atomic numbers of the backscattering atom, the coordination numbers and the DEBYE-WELLER factors as an expression of the thermal mobilities of the backscattering atoms. Furthermore, it is possible to distinguish between protonated and deprotonated nitrogen atoms via their distances to the central atom. Amine (protonated) nitrogen atoms usually are bonded at a distance of around 2.2 Å, while amide (deprotonated) nitrogen atoms are bound at around 2 Å. One of the most important characteristics of EXAFS is the ability to find out the complex stoichiometry. Taking the well-known ligand structure into consideration, the complex stoichiometry can be derived from the metal complexation mode, such as SN₃ or S₂N₂. Fig. 2 shows the EXAFS and the Fourier transform of both an SN₃ and an S₂N₂ coordination sphere.

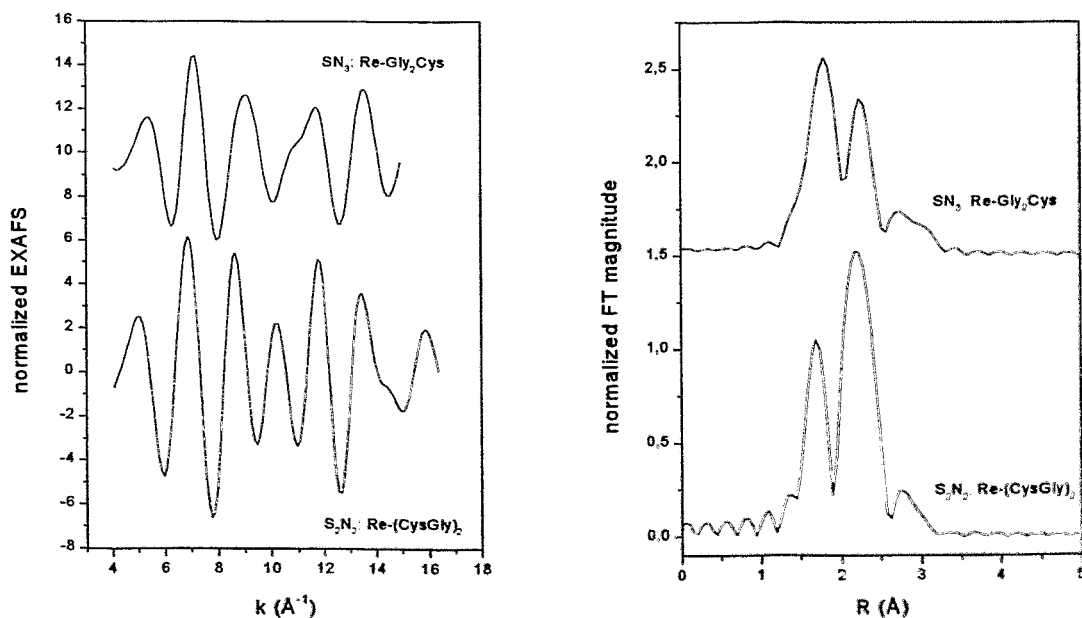


Fig. 2: EXAFS and Fourier transform of complexes with different coordination spheres: Re-Gly₂Cys and Re-(CysGly)₂

It can easily be seen that both the EXAFS and the Fourier transforms of the two peptide complexes differ significantly. Another advantage is the ability to detect intermolecular metal-metal distances, like Re-O-Re. Fig. 3 shows the EXAFS and the Fourier transform of a complex with an intermolecular Re-O-Re bridge (Re cysteamine).

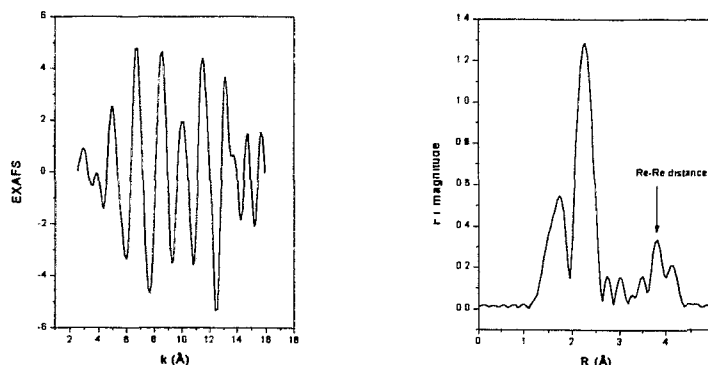


Fig. 3: EXAFS and Fourier transform of a Re-O-Re bridged complex (Re-cysteamine)

The Re-Re distance at a distance of 3.6 Å is indicated, which is also proved by X-ray powder diffraction analysis. Quick EXAFS measurements enable us to monitor complex-forming reactions in a time-resolved way. However, some drawbacks of XAS have to be mentioned.

The most important problem is that no distinction is possible between complexing atoms within the same PSE period, like oxygen and nitrogen or sulphur and phosphorus. The error in coordination numbers is up to 30 % for first and second coordination shells and up to 50 % for third and higher coordination shells. Thus, a proper identification of third and higher coordination shells- except distant metal-metal distances- will not be possible.

Depending on the recorded energy scan range and the data statistics, a resolution in distances of 0.1-0.17 Å will be obtained.

Conclusions

XAS has proved to be a very useful tool in structural analysis of Tc and Re complexes with insufficient crystallization properties. Though a good identification of the atomic environment of the central atom is possible, XAS results will not reach the possibilities in structural analysis that are provided by XRD analysis.

XAS results always have to be complemented by supplemental analytical techniques, such as electrophoresis or elemental analysis.

However, in the radiopharmaceutical chemistry of technetium and rhenium XAS measurements are believed to be an increasingly widely applied analytical method. In the future XAS measurements will be performed on a lot of Tc and Re complexes to obtain structural data regardless of the complex crystallization properties.

References

- [1] Almahamid I., Bryan J. C., Bucher J. C., Burell A. K., Edelstein N. M., Hudson E. A., Kaltsoyannis N., Lukens W. W., Shuh D., Nitsche H. and Reich T. (1995) Electronic and structural investigations of technetium compounds by X-ray absorption spectroscopy. *Inorg. Chem.* **34**, 193 - 198.
- [2] Allen P. G., Siemering G. S., Shuh D. K., Bucher J. J., Edelstein N. M., Langton C. A., Clark S. B., Reich T. and Denecke, M. A. (1996) Technetium speciation in cement waste forms determined by X-ray absorption fine structure spectroscopy. *Radiochim. Acta*, in press.
- [3] Martin J. L., Yuan J., Lunte C. E., Elder R. C., Heineman W. R. and Deutsch E. (1989) Technetium diphosphonate skeletal imaging agents: EXAFS structural studies in aqueous solution. *Inorg. Chem.* **28**, 2899 - 2901.
- [4] Elder R. C. and Eidsness M. K. (1987) Synchrotron X-ray studies of metal based drugs and metabolites. *Chem. Rev.* **87**, 1027 - 1046.
- [5] Jankowsky R., Noll B., Spies H. and Johannsen B. (1996) XAS investigations on Tc and Re complexes of oligoglycine ligands and Tc tartrate. *This report*, pp. 72 - 76.

19. Technetium and Rhenium Complexes with Thioether Ligands

8. X-Ray Structures of Mononuclear Oxorhenium(V) Complexes with Bidentate Thioether and Dithialcohol Ligands

M. Reisgys, H.-J. Pietzsch, H. Spies, P. Leibnitz¹
¹Bundesanstalt für Materialforschung Berlin

Introduction

We recently found a new simple way of synthesizing neutral rhenium complexes with S,S coordinating thioether ligands [1]. By reduction of ammonium perrhenate with concentrated hydrohalic acid followed by addition of the ligand in glacial acetic acid, the expected complexes (Fig. 1) were obtained in a one-pot reaction in a nearly quantitative yield.

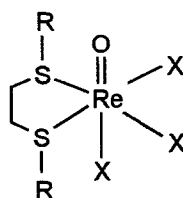
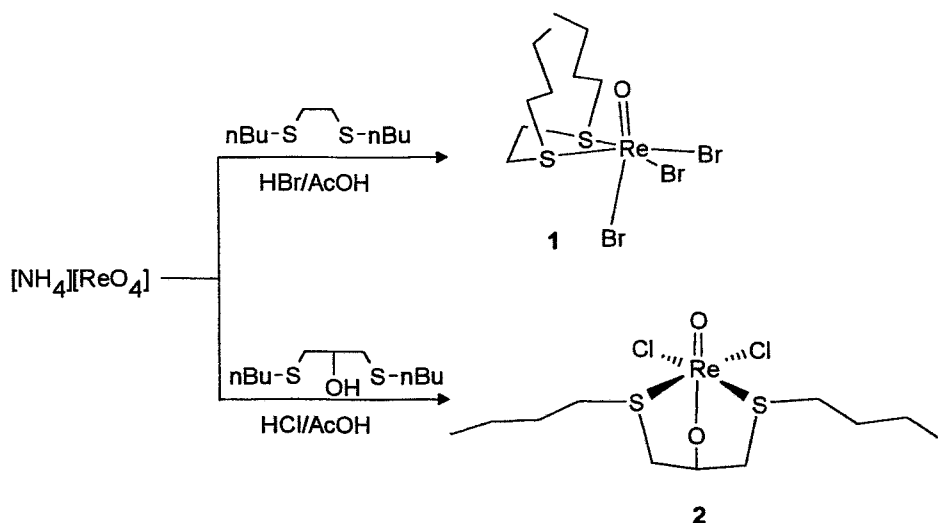


Fig. 1: General structure of the trihalo("SS")rhenium(V) complex (X = Cl, Br)

In this report we describe the X-ray structure of the tribromo("SS")rhenium(V) complex **1**. For the synthesis of this complex see ref. [1]. Further the thioether complex **2** with the S,O,S coordinating sequence was synthesized and characterized by X-ray analysis [2].



Experimental

Preparation of dichloro[5,9-dithiatridecan-7-olato-(S,O,S)]oxorhenium(V) **2**

To 40.2 mg (150 μmol) of NH_4ReO_4 , dissolved in 1.5 ml of concentrated HCl, 47.3 mg (200 μmol) of 5,9-dithiatridecan-7-ol [3], dissolved in 1 ml of glacial acetic acid, was added. After 20 min a violet precipitate was filtered off and washed three times with glacial acetic acid and following three times with diethyl ether.

Crystals for X-ray analysis could be obtained by recrystallization from CHCl_3 /diethyl ether.

Yield: (53 mg, 69 %).

M.p.: 128 - 129 $^\circ\text{C}$.

Elemental analysis: (Found: C 25.44; H 4.44; S 12.31; Cl 13.81, $\text{C}_{11}\text{H}_{23}\text{Cl}_2\text{O}_2\text{ReS}_2$ requires C 25.98, H 4.56, S 12.61, Cl 13.94 %)

IR absorptions: $\nu_{\text{max}}/\text{cm}^{-1}$ (KBr) 1040 (C-O), 960 (Re=O), 532 (Re-O).

Results and Discussion

Ammonium perrhenate, dissolved in concentrated hydrobromic acid, was added to a solution of 5,8-dithiadodecane in glacial acetic acid [1, 4]. **1** precipitates immediately as a yellowish green powder. Green crystals suitable for X-ray analysis were obtained by slow evaporation of the reaction solution. A strong vibration band at 976 cm^{-1} in the infrared spectrum of **1** can be assigned to the $[\text{Re}=\text{O}]^{5+}$ core [5]. The X-ray structure shows a distorted octahedral coordination sphere of the rhenium centre. The sulphurs of the ligand and two bromines form the equatorial plane, the oxygen and the third bromine are cis coordinated to the thioether ligand. In the crystal there is a statistical disorder of the n-butyl groups. This affects various positions of the carbons C(4), C(5), C(6), and C(10) of structure A (darker balls in Fig. 2) and C(4'), C(5'), C(6'), and C(10') of structure B (lighter balls). The mean probability for structure A and B lies at 49 and 51 %. Selected bond lengths and angles are summarized in Table 1.

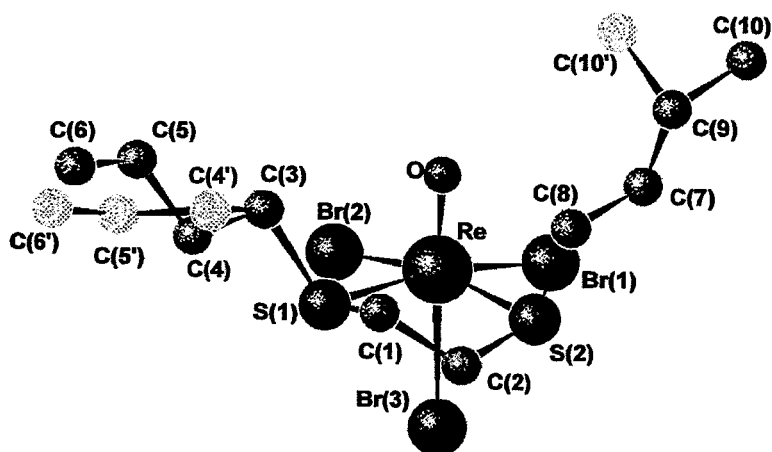


Fig. 2: The overlaid X-ray structures A (darker balls) and B (lighter balls) of complex **1**.

Table 1: Selected bond lengths and angles for compound **1** and **2**.

1					
Re-O	1.667 (5)	Re-S(1)	2.421 (2)	Re-S(2)	2.453 (3)
Re-Br(1)	2.4860 (14)	Re-Br(2)	2.490 (3)	Re-Br(3)	2.5969 (13)
Br(1)-Re-Br(2)	89.10 (6)	Br(1)-Re-S(2)	92.35 (7)	Br(3)-Re-S(1)	80.97 (7)
Br(1)-Re-Br(3)	87.93 (5)	Br(2)-Re-O	102.8 (2)	Br(3)-Re-S(2)	76.94 (8)
Br(2)-Re-Br(3)	90.83 (7)	Br(2)-Re-S(1)	90.11 (7)	O-Re-S(1)	90.2 (2)
Br(1)-Re-O	100.8 (2)	Br(2)-Re-S(2)	167.61 (6)	O-Re-S(2)	89.0 (2)
Br(1)-Re-S(1)	168.86 (7)	Br(3)-Re-O	163.8 (2)	S(1)-Re-S(2)	86.09 (7)
2					
Re-Cl(1)	2.370 (4)	Re-S(1)	2.482 (3)	Re-O(1)	1.692 (9)
Re-Cl(2)	2.363 (4)	Re-S(2)	2.462 (3)	Re-O(2)	1.953 (8)
Cl(1)-Re-Cl(2)	85.8 (2)	Cl(2)-Re-S(1)	170.26 (13)	S(1)-Re-O(1)	86.3 (3)
Cl(1)-Re-S(1)	93.04 (13)	Cl(2)-Re-S(2)	93.34 (13)	S(1)-Re-O(2)	77.7 (3)
Cl(1)-Re-S(2)	170.49 (13)	Cl(2)-Re-O(1)	92.7 (3)	S(2)-Re-O(1)	86.4 (3)
Cl(1)-Re-O(1)	93.3 (3)	Cl(2)-Re-O(2)	103.4 (4)	S(2)-Re-O(2)	77.3 (3)
Cl(1)-Re-O(2)	103.0 (3)	S(1)-Re-S(2)	86.21 (11)	O(1)-Re-O(2)	157.8 (4)

Reaction of $n\text{Bu-S-CH}_2\text{-CH(OH)-CH}_2\text{-S-nBu}$ in glacial acetic acid with ammoniumperrhenate in concentrated hydrochloric acid leads to the violet complex **2**. Violet crystals suitable for X-ray analysis could be obtained by slow evaporation of the reaction solution. A strong vibration band at 960 cm^{-1} in the infrared spectrum is characteristic for the O=Re-O moiety [6]. The main structure (Fig. 3) is defined by the bicyclo-[2,2,1]- $\text{ReC}_3\text{S}_2\text{O}$ unit. Because of the ring strain of this bicyclic compound the octahedral coordination sphere of the rhenium atom is distorted. All bond lengths and angles (Table 1) are in the normal range [7].

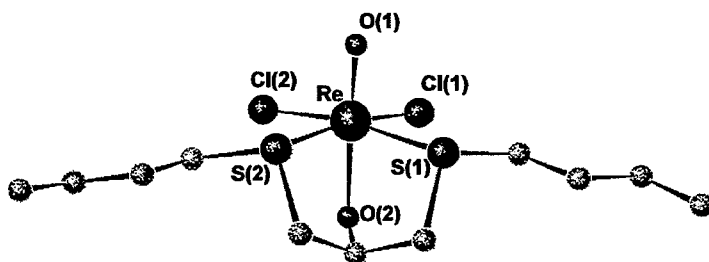


Fig. 3: X-ray structure of compound **2**

References

- [1] Reisgys M., Pietzsch H.-J., Spies H. and Leibnitz P. (1995) Technetium and rhenium complexes with thioether ligands 7. Mononuclear trichlorooxorhenium(V) complexes with bi- and tetradentate thioethers. *Annual Report 1995*, Institute of Bioinorganic and Radiopharmaceutical Chemistry, FZR-122, pp. 116 - 119.
- [2] Pietzsch H.-J., Reisgys M., Spies H., Leibnitz P. and Johannsen B. (1997) Technetium and rhenium complexes with thioether ligands, 5. Synthesis and structural characterization of neutral oxorhenium(V) complexes with tridentate dithioethers. *Chem. Ber.*, in press.
- [3] Reisgys M., Spies H., Johannsen B., Leibnitz P. and Pietzsch H.-J. (1997) Technetium and rhenium complexes with thioether ligands, 6. Synthesis and structural characterization of mixed-ligand oxorhenium(V) complexes containing bidentate dithioethers and monothiolato ligands. *Chem. Ber.*, in press.
- [4] Nicholson D. C., Rothstein E., Savelle R. W. and Whiteley R. (1953) The reactions of organic derivatives of elements capable of valency-shell expansion. Part V. A comparison of the near ultra-violet absorptions of unsaturated derivatives of nitrogen, phosphorus, and sulphur with those of their saturated analogues. *J. Chem. Soc.*, 4019 - 4025.
- [5] Kotegov K. V., Khakimov F. Kh., Konovalov L. V. and Kukushkin Y. N. (1974) Rhenium compounds with diethyl-ethylene-disulfide. *Zh. Obshch. Khim.* **44**, 2237 - 2240.
- [6] a) Pietzsch H.-J., Spies H., Leibnitz P. and Reck G. (1994) Technetium and rhenium complexes with thioether ligands -6. Oxorhenium(V) complexes derived from the potentially tetradentate ligand 1,8-dihydroxy-3,6-dithiaoctane. *Annual Report 1994*, Institute of Bioinorganic and Radiopharmaceutical Chemistry, FZR-73, pp 3 - 8.
b) Tisato F., Refosco F., Mazzi U., Bandoli G. and Nicolini M. (1987) Technetium(V) and rhenium(V) complexes with *N*-(2-mercaptophenyl)-salicylideneimine. Crystal structure of chloro(oxo)[*N*-(2-sulphidophenyl)-salicylideneimino-NOS]technetium(V). *J. Chem. Soc. Dalton Trans.* 1693 - 1699.
- [7] see ref. [2] and reports cited therein.

20. Rhenium and Technetium Carbonyl Complexes for the Labelling of Bioactive Molecules

2. Tricarbonylrhenium(I) Complexes with Mono-, Bi- and Tridentate Thioether Ligands

H.-J. Pietzsch, M. Reisgys, H. Spies, R. Alberto¹, U. Abram²

¹Paul-Scherrer-Institut Villigen (Switzerland), ²Institut für Anorganische Chemie Tübingen

Introduction

A new way for the synthesis of technetium and rhenium carbonyl complexes of the oxidation state +1 has recently been developed by Alberto *et al.* [1]. Starting from TcO_4^- or ReO_4^- tricarbonyl complexes of the main formula $[\text{MX}_3(\text{CO})_3]^{2-}$ (M = Tc, Re; X = Cl, Br) can be synthesized by reduction with borane under normal pressure of carbon monoxide and tetraalkylammonium halogenide in tetrahydrofuran. The characteristics of these carbonyl precursors for the design of radiopharmaceuticals are simple synthesis, easy complex formation with π -donor ligands, high stability of the complexes and the small volume of the coordination sphere.

In this report we introduce the synthesis and characterization of tricarbonyl complexes with mono-, bi- and tridentate thioether ligands. The structure of a dinuclear rhenium complex and a cationic complex with a tridentate thioether ligand could be obtained by X-ray analysis.

Experimental

Preparation of complex 1

A solution of 38 mg (260 μmol) di-n-butylsulphide in 1 ml methanol was added to 100 mg (130 μmol) $(\text{NEt}_4)_2[\text{ReBr}_3(\text{CO})_3]$ in 1 ml methanol under an inert atmosphere. After stirring for 1 h the solvent was removed by vacuum. The residue was taken up in dry THF and filtered. The solvent of the filtrate was reduced, and white microcrystals precipitated from the oil.

Yield: (83 mg, 91 %).

M.p.: 89 °C.

Elemental analysis: (Found: C, 32.23; H, 5.14; N, 1.98; S, 5.72, $\text{C}_{19}\text{H}_{38}\text{Br}_2\text{NO}_3\text{ReS}$ requires C, 32.30; H, 5.42; N, 1.98; S, 4.54 %).

IR absorptions: $\nu_{\text{max}}/\text{cm}^{-1}$ (KBr) 2960 (C-H), 2872 (C-H), 2008s (C-O), 1908s (C-O), 1872s (C-O), 1464, 1184.

Preparation of complex 2

A solution of 24 mg (130 μmol) 1,8-dihydroxy-3,6-dithiooctane in 1 ml methanol was added to 100 mg (130 μmol) $(\text{NEt}_4)_2[\text{ReBr}_3(\text{CO})_3]$ in 1 ml methanol under an inert atmosphere. After stirring for 1 h the solvent was removed by vacuum. The residue was taken up in dry THF and filtered. The solvent of the filtrate was reduced, and the remaining oil was washed with water and diethyl ether to obtain white microcrystals.

Yield: (55 mg, 80 %).

M.p.: 72 - 75 °C.

Elemental analysis: (Found: C, 20.47; H, 2.64; S, 11.99; Br, 14.98, $\text{C}_9\text{H}_{14}\text{BrO}_5\text{ReS}_2$ requires C, 20.30; H, 2.65; S, 12.04; Br, 15.01 %).

IR absorptions: $\nu_{\text{max}}/\text{cm}^{-1}$ (KBr) 3406 (O-H), 2926 (C-H), 2032s (C-O), 1942s (C-O), 1912s (C-O), 1508, 1410, 1208.

Preparation of complex 3

A solution of 51.3 mg (130 μmol) $(p\text{-MeOPhCH}_2\text{SCH}_2\text{CH}_2)_2\text{S}$ in 1 ml methanol was added to 100 mg (130 μmol) $(\text{NEt}_4)_2[\text{ReBr}_3(\text{CO})_3]$ in 1 ml methanol under an inert atmosphere. After stirring for 1 h the solvent was removed by vacuum. The residue was taken up in dry THF and filtered. The solvent of the filtrate was reduced, and the oil was washed with water and diethyl ether to obtain a white powder.

Yield: (64 mg, 67 %).

M.p.: 65 - 68 °C.

Elemental analysis: (Found: C, 37.36; H, 3.53; S, 13.03; Br, 10.08, $\text{C}_{23}\text{H}_{26}\text{BrO}_5\text{ReS}_3$ requires C, 37.09; H, 3.52; S, 12.91; Br, 10.73 %).

IR absorptions: $\nu_{\text{max}}/\text{cm}^{-1}$ (KBr) 2926 (C-H), 2030s (C-O), 1938s (C-O), 1898s (C-O), 1608, 1512, 1250.

Preparation of complex 4

A solution of 66 mg (390 μmol) AgNO_3 in water was added to a solution of 100 mg (130 μmol) $(\text{NEt}_4)_2[\text{ReBr}_3(\text{CO})_3]$ in 2 ml water. The immediately precipitating AgBr was filtered off, the solvent of the filtrate was removed by vacuum. The crystalline $(\text{NEt}_4)_2[\text{Re}(\text{NO}_3)_3(\text{CO})_3]$ was dissolved in 5ml tetrahydrofuran and a solution of 51 mg (130 μmol) $(p\text{-MeOPhCH}_2\text{SCH}_2\text{CH}_2)_2\text{S}$ in 2ml tetrahydrofuran was added. After 3 h the precipitate was filtered off and the filtrate was evaporated. The oil obtained was washed with diethyl ether and dried in vacuum. The beige powder was recrystallized in chloroform/n-hexane.

Yield: (56 mg, 59 %).

M.p.: 120 - 122 $^\circ\text{C}$.

Elemental analysis: (Found: C, 37.51; H, 3.68; N, 1.96; S, 13.25, $\text{C}_{23}\text{H}_{26}\text{NO}_8\text{ReS}_3$ requires C, 38.06; H, 3.47; N, 1.93; S, 13.25 %).

IR absorptions: $\nu_{\text{max}}/\text{cm}^{-1}$ (KBr) 2928 (C-H), 2040s (C-O), 1948s (C-O), 1612, 1512, 1252.

Preparation of complex 6

A solution of 19 mg (130 μmol) 3-thia-1-heptanthiol in 1 ml methanol was added to 100 mg (130 μmol) $(\text{NEt}_4)_2[\text{ReBr}_3(\text{CO})_3]$ in 1 ml methanol under an inert atmosphere. After stirring for 1 h the solvent was removed by vacuum. The residue was taken up in dry THF and filtered. The solvent of the filtrate was reduced, and the oil was washed with diethyl ether to obtain a nearly white powder. Recrystallization in chloroform/n-hexane produced crystals suitable for X-ray analysis.

Yield: (10 mg, 9 %).

M.p.: 123 - 125 $^\circ\text{C}$.

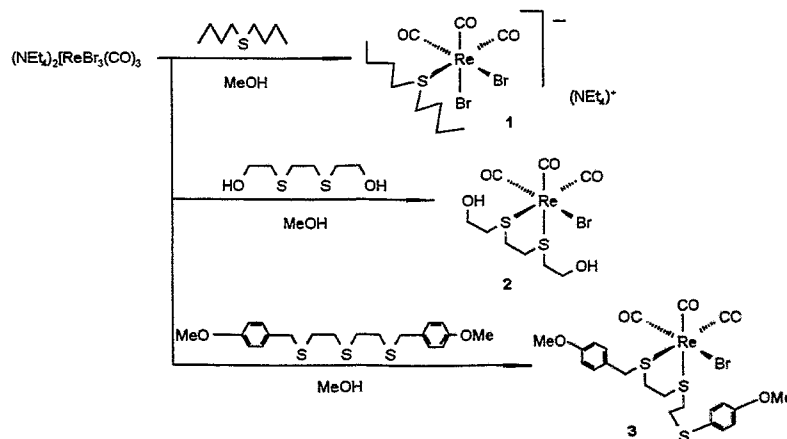
Elemental analysis: (Found: C, 25.56; H, 3.00; S, 14.60, $\text{C}_{18}\text{H}_{26}\text{O}_6\text{Re}_2\text{S}_4$ requires C, 25.28; H, 3.12; S, 15.28 %).

IR absorptions: $\nu_{\text{max}}/\text{cm}^{-1}$ (KBr) 2960 (C-H), 2016s (C-O), 1984s (C-O), 1920s (C-O), 1464, 1424.

Results and Discussion

Reaction of $(\text{NEt}_4)_2[\text{ReBr}_3(\text{CO})_3]$ with thioether ligands in methanol leads to different complexes.

Scheme 1:



Monothioether, such as di-n-butylsulfide, produces the anion complex 1, in which only one bromide is substituted by a ligand. Tetraethylammonium is the counterion.

Starting from a bidentate thioether two coordination positions of the rhenium will be occupied by sulphurs. The neutral complex 2 can be synthesised and characterized by infrared spectroscopy (2032 cm^{-1} , 1942 cm^{-1} , 1912 cm^{-1}) and elemental analysis. There are no signs of coordination of one of the hydroxyl groups. The tridentate ligand $(p\text{-MeOPhCH}_2\text{SCH}_2\text{CH}_2)_2\text{S}$ reacts in the same way. In comparison with 2 the infrared spectrum of 3 shows analogous bands in the CO stretching region (2030 cm^{-1} , 1938 cm^{-1} , 1898 cm^{-1}). This leads to the conclusion that only two sulphur atoms are coordinating, while one sulphur remains uncoordinated. The third coordination position is occupied by a bromide. In contrast, the reaction of $(\text{NEt}_4)_2[\text{Re}(\text{NO}_3)_3(\text{CO})_3]$ with the same ligand in tetrahydrofuran leads to complex 4 (Scheme 2). The X-ray structure (Fig. 1) shows an $[\text{S}_3(\text{CO})_3]$ coordination sphere

of the rhenium centre. The infrared data (2040 cm^{-1} , 1996 cm^{-1}) confirm the high symmetrical structure of 4.

Scheme 2:

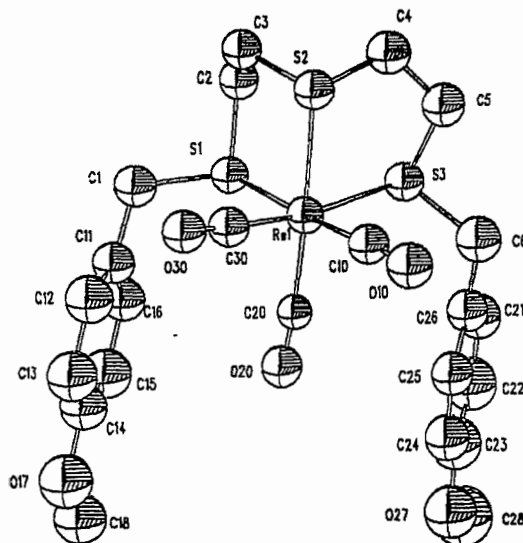
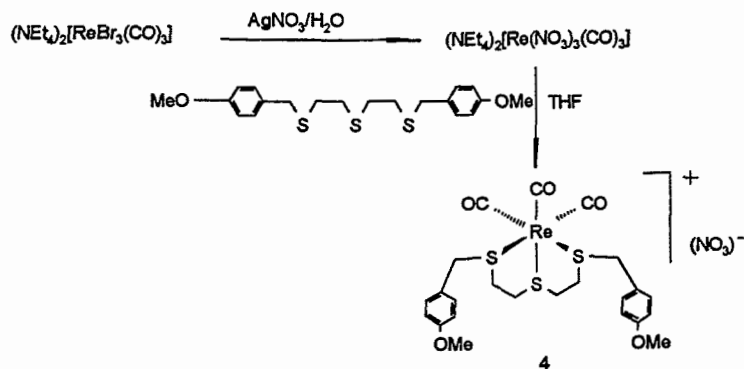


Fig. 1: X-ray structure of complex 4.

While the reaction of $(\text{NEt}_4)_2[\text{MX}_3(\text{CO})_3]$ ($\text{M} = \text{Re, Tc}$; $\text{X} = \text{Cl, Br}$) with thiols leads to anionic dirhenium complexes with three $\mu\text{-S}$ units (5, Scheme 3, [2, 3]), 3-thia-1-heptanthiol leads to a neutral dirhenium complex 6 with two $\mu\text{-S}$ atoms. Coordination of one thioether sulphur per rhenium forms a $[\text{ReS}(\text{CH}_2)_2\text{SReS}(\text{CH}_2)_2\text{S}]$ tricyclic compound in staircase conformation. The X-ray structure of 6 obtained is represented in Fig. 2.

Scheme 3:

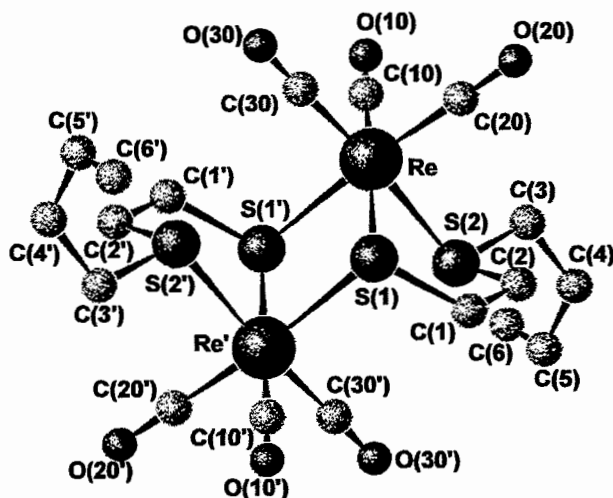
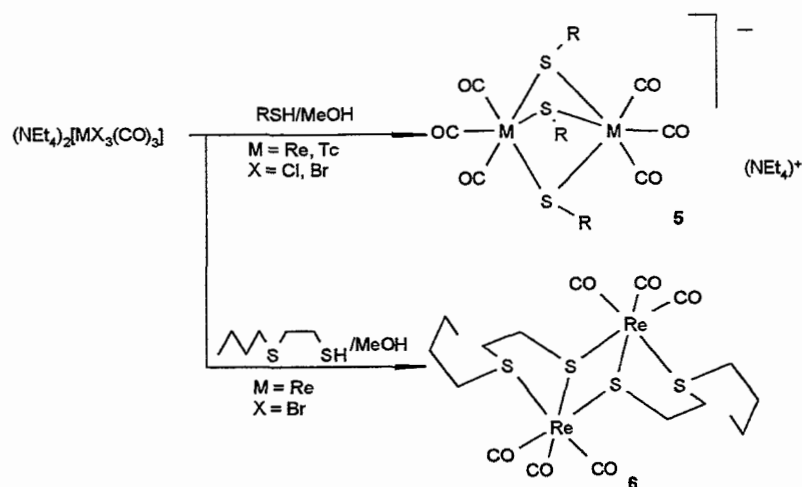


Fig. 2: Molecular structure of **6**.

The rhenium(I) tricarbonyl complexes presented demonstrate manifold ways of complex bonding starting from $(\text{NEt}_4)_2[\text{ReBr}_3(\text{CO})_3]$ with different thioether compounds. All complexes are stable in air and moisture as well as in organic solvents. We are now planning to assign the obtained results to the corresponding Tc-99 or Tc-99m tricarbonyl precursors.

References

- [1] Alberto R., Schibli R., Egli A., Schubiger P. A., Herrmann W. A., Artus G., Abram U. and Kaden T. A. (1995) Metal carbonyl syntheses XXII. Low pressure carbonylation of $[\text{MOC}_4]^-$ and $[\text{MO}_4]^-$: The technetium(I) and rhenium(I) complexes $(\text{NEt}_4)_2[\text{MCl}_3(\text{CO})_3]$. *J. Organomet. Chem.* **493**, 119-127.
- [2] Alberto R. (1996) personal communication.
- [3] Alberto R., Schibli R., Schubiger P. A., Abram U. and Kaden T. A. (1996) Reaction with the technetium and rhenium carbonyl complexes $(\text{NEt}_4)_2[\text{MX}_3(\text{CO})_3]$. Synthesis and structure of $[\text{Tc}(\text{CN-Bu})_3(\text{CO})_3](\text{NO}_3)$ and $(\text{NEt}_4)[\text{Tc}_2(\mu\text{-SCH}_2\text{CH}_2\text{OH})_3(\text{CO})_6]$. *Polyhedron* **15**, 1079 - 1089.

21. Technetium and Rhenium Labelled Steroids

1. First Synthesis of "3+1" Mixed-Ligand Oxorhenium(V) Complexes Bearing a Pendant Estradiol Moiety

F. Wüst, H. Spies, D. Scheller¹, S. Machill¹

¹ TU Dresden, Institut für Analytische Chemie

Introduction

The introduction of technetium into steroid hormones by coupling it to the complete molecule or by the construction of Tc-steroid mimics open a promising route to receptor-binding technetium-99m radiotracers which are potentially able to image hormone-depending tumors [1, 2].

In order to investigate the possibilities for labelling steroids with the readily available radionuclide technetium-99m, a number of attempts have been made to combine steroids with metal cores. Especially the Katzenellenbogen group [3, 4, 5] developed various metal-labelled steroids with a high receptor-binding affinity.

In extension of our current research which aims for at technetium tracers reactive *in vivo*, efforts are being made to explore results in the coordination chemistry of mixed-ligand "3+1"-complexes for the design of steroid complexes of both technetium and rhenium. The latter element is involved in our investigations as an inactive surrogate for the radioactive technetium. The principle of preparing mixed-ligand complexes in which small-sized chelate units are bound to steroids has been applied to thiocholesterol as a substituent in an earlier work [6].

The present article describes some first investigations of the chemistry of estradiol-rhenium complexes, starting from easily available 2-substituted estradiol derivatives.

¹³C NMR spectroscopy was used to elucidate the structure of the synthesized steroid compounds.

Experimental

1. General

Solvents and reagents were purchased from the following commercial sources: Sigma, Fluka and Aldrich. THF and DMF were dried and distilled prior to use. The reagents were used as received.

¹³C NMR spectra were recorded at 75 MHz with an MSL Bruker spectrometer using BB decoupling and APT method for assignment. 30° pulses and a repetition time of 2 s were applied. The digital resolution was 1 Hz (0.013 ppm). All spectra were indirectly calibrated using the solvent peak of CDCl₃ at 77.0 ppm.

2. Synthesis

2-thiomethyl-estra-1,3,5(10)-triene-3,17β-diol **7** (Fig. 1)

The synthesis commenced by protecting 3,17β-estradiol **1** with MOMCl by a modification of the general procedure of Stork and Takahashi [7] to give MOM ether **2**. Deprotonation of **2** with *s*-BuLi and quenching the intermediate carbanion with DMF gave exclusively the 2-formyl product **3** in a 87 % yield. Reduction of **3** with NaBH₄ in MeOH led to the alcohol **4** which was converted with thioacetic acid under Mitsunobu conditions [8] to the thioester **5**. Cleavage of the MOM-protecting groups with dilute HCl and subsequent saponification of the thioester **6** by sodium methoxide gave the desired thiol **7** in a total yield of 25 % related to 3,17β-estradiol **1**.

(3-thiapentane-1,5-dithiolato)(3,17β-estradiol-2-thiomethylato)oxorhenium(V) **9** (Fig. 2)

36.5 mg (94 μmol) chloro(3-thiapentane-1,5-dithiolato)oxorhenium(V) **8** [9] were dissolved in 4 ml hot acetonitrile while stirring. At 80 °C 61 mg (192 μmol) of the thiol **7** dissolved in 4 ml acetonitrile were added slowly, followed by addition of one drop of triethylamine. The colour of the mixture changed immediately from dark blue to red. The red mixture was stirred at 80 °C for 30 min. Afterwards it was evaporated to dryness. The residue was purified by passing through a silica gel column with chloroform : methanol (5:1) as eluent. After evaporation of the eluate 28 mg (35 %) of a light brown solid were obtained.

Melting point: 186 - 188 °C (decomposition)

IR absorption $\nu_{\max}/\text{cm}^{-1}$ (KBr) 960 cm^{-1} (Re=O)

MS (FAB positive): 693(68.1), 694(16.2), 695(100) M+1+Na⁺, 696(21.9), 697(20.9) 698(4.8)

Elemental analysis: (Found C, 39.99; H, 5.14; S, 19.00; C₂₃H₃₃O₃ReS₄ requires C, 41.11; H, 4.95; S, 19.08 %)

(3-oxapentane-1,5-dithiolato)(3,17 β -estradiol-2-thiomethylato)oxorhenium(V) 12 (Fig. 3)

103 mg (175 μ mol) tetra-*n*-butylammonium-tetrachlorooxorhenate(V) **10** [10] were dissolved in 2 ml EtOH and cooled to 0 °C. At this temperature 61 mg (191 μ mol) thiol **7** and 21 μ l (175 μ mol) 3-oxapentane-1,5-dithiol **11** in 2 ml chloroform were added while stirring. Stirring the mixture at 0 °C was continued for two hours. During this time a light brown solid was formed. The solid was separated and washed with chloroform. After drying 56 mg (49 %) of complex **12** were obtained.

Melting point: 170 - 171 °C (decomposition)

IR absorption $\nu_{\text{max}}/\text{cm}^{-1}$ (KBr) 952 cm^{-1} (Re=O)

MS (FAB positive): 677(69.5), 678(14.3), 679(100) $\text{M}+1+\text{Na}^+$, 680(20), 681(15,3)

Elemental analysis: (Found C, 40.69; H, 5.10; S, 14.33; $\text{C}_{23}\text{H}_{33}\text{O}_4\text{ReS}_3$ requires C, 42.12; H, 5.07; S, 14.66 %)

Remark: The elemental analysis was performed on a LECO CHNS 932 elemental analyser. The differences in the carbon value are caused by technical problems.

Results and Discussion

Binding of metals at the steroid moiety requires the presence of a suitable donor group. For technetium and rhenium at the oxidation state (V) a mercaptide sulphur is the preferred group to provide stable binding of the metal.

Introduction of a thiol group into the steroid molecule is therefore the key step in the reaction sequence (Fig. 1) and succeeded via forming a thiolacetate using the Mitsunobu reaction starting from the corresponding alcohol. This reaction appeared to be an ideal method for introducing a sulphur moiety in a high yield under mild conditions into primary hydroxyl groups containing molecules.

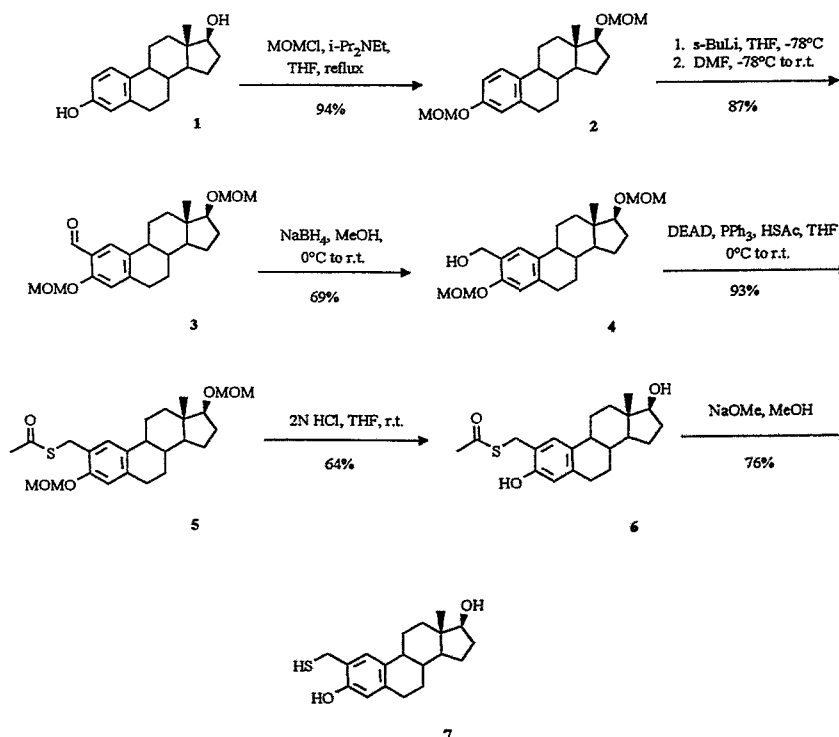
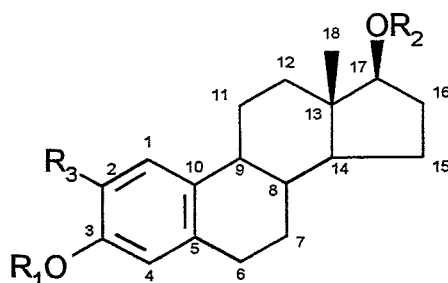


Fig. 1: Reaction sequence for the synthesis of monothiol **7**

^{13}C NMR spectroscopy as a suitable tool for structure elucidation of steroids [11] was used for characterizing synthesized steroid compounds (Fig. 1). The chemical shifts of the carbon atoms of steroids **2** - **7** are listed in Table 1. The spectra confirm the structure of all prepared estradiol derivatives. The chemical modifications in position 2 of the steroid skeleton could be proved by observation of the new signals of the introduced substituents and the characteristic changes of the chemical shifts of the aromatic carbon atoms due to the substituent effects. Successful introduction and cleavage of the MOM-protecting group in positions 3 and 17β could be observed in the same way.

Table 1: Chemical shifts (in ppm) of the carbon atoms of steroids **2** - **7**



Steroid	R ₁	R ₂	R ₃
2	CH ₃ OCH ₂	CH ₃ OCH ₂	H
3	CH ₃ OCH ₂	CH ₃ OCH ₂	CHO
4	CH ₃ OCH ₂	CH ₃ OCH ₂	CH ₂ OH
5	CH ₃ OCH ₂	CH ₃ OCH ₂	CH ₂ SCOCH ₃
6	H	H	CH ₂ SCOCH ₃
7	H	H	CH ₂ SH

Carbon atom	2	3	4	5	6	7
1	126,3	125,3	126,3	128,4	127,6	126,3
2	113,7	123,2	127,2	123,6	121,1	123,9
3	155,0	157,4	153,0	152,7	151,9	151,7
4	116,2	114,9	114,6	114,0	117,2	116,6
5	138,0	146,4	137,7	137,5	132,9	132,9
6	29,7	30,4	29,7	29,7	29,3 ^{m)}	29,3
7	27,2	26,8	27,2	27,1	27,1	27,1
8	38,5	38,2	38,5	38,5	38,7	38,7
9	44,0	43,9	44,0	43,9	43,8	43,8
10	134,0	134,4	134,0	133,9	138,3	137,7
11	26,2	26,1	26,3	26,2	26,3	26,3
12	37,2	37,0	37,2	37,2	36,6	36,6
13	43,0	42,9	43,0	43,0	43,2	43,2
14	50,0	49,9	49,9	49,9	50,0	50,0
15	23,0	23,0	23,1	23,0	23,1	23,1
16	28,0	28,0	28,1	28,1	30,6	30,6
17	86,6	86,4	86,5	86,6	81,9	81,9
18	11,7	11,7	11,7	11,7	11,0	11,0
CHO		189,6				
CH ₂ OH			62,0			
CH ₂ SCOCH ₃				28,6	29,2 ^{m)}	
CH ₂ SCOCH ₃				195,8	200,3	
CH ₂ SCOCH ₃				30,4	30,2	
CH ₂ SH						25,08
CH ₃ OCH ₂ ⁿ⁾	55,9 / 55,1	56,4 / 55,2	56,2 / 55,2	56,1 / 55,1		
CH ₃ OCH ₂ ⁿ⁾	94,4 / 96,0	94,5 / 96,0	94,7 / 96,0	94,2 / 96,0		

ⁿ⁾ 1st value position 3 / 2nd value position 17

^{m)} probable assignment

Starting from the monothiol **7**, two new rhenium "3+1" complexes bearing a receptor binding molecule were synthesized.

The complex formation occurs according to the "3+1" concept [12] with two different rhenium precursors in a 35 % and 49 % yield (Fig. 2 and Fig. 3). The complexes differ with respect to the neutral donor atom in the tridentate ligand part, which is S for **9** and O for **12**.

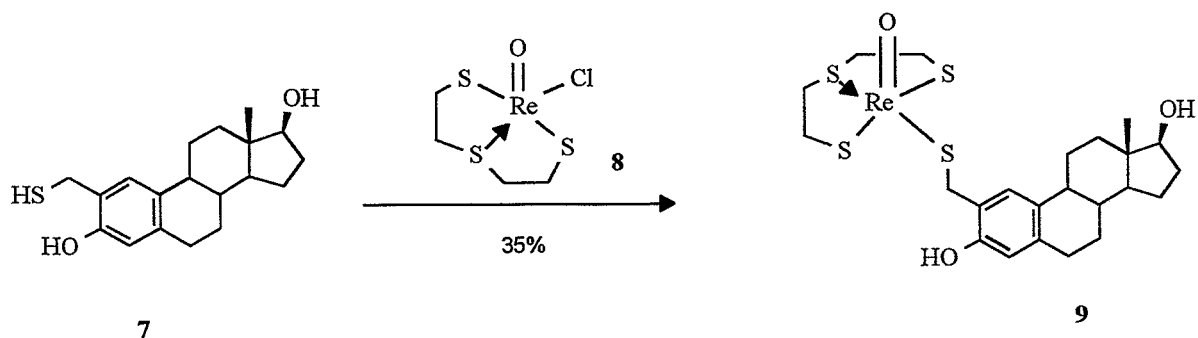


Fig. 2: Reaction of monothiol **7** with rhenium precursor **8**

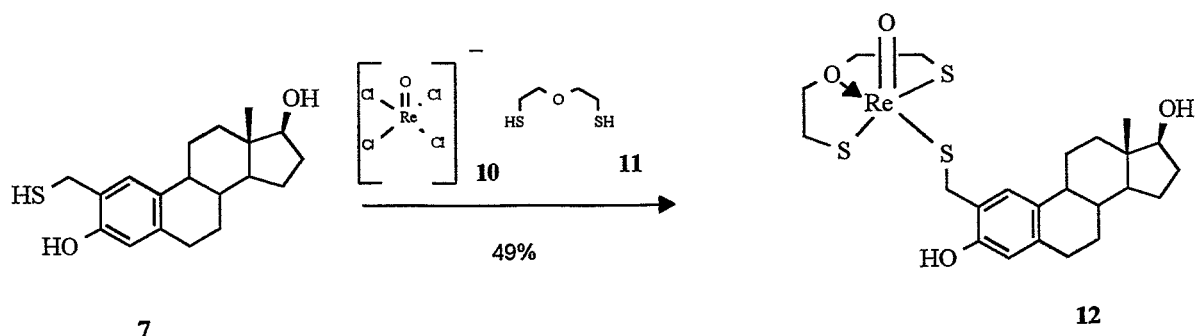


Fig. 3: Reaction of monothiol **7** with rhenium precursor **10**

The resulting complexes are light brown solids soluble in DMSO of a reddish-brown colour. In general the one-pot method of forming complexes like **12** starting from the tetrachlorooxorhenate(V) **10** as a precursor should produce lower yields compared with the two-pot method (Fig. 2) [9]. The lower yield of complex **9** is due to its chromatographic purification. The experiments show that the mixed-ligand concept can be applied to biologically important steroid compounds, such as 3,17 β -estradiol **1**. In further investigations we want to study the influence of the chelating group on various positions of the steroid molecule of biological interest, like 17 α , 7 α or 11 β . Furthermore, efforts in the construction of steroid mimic chelating groups according to the mixed-ligand concept should be a beneficial route for designing potential estrogen receptor-binding technetium-based radiotracers.

References

- [1] Katzenellenbogen J. A., Heiman D. F., Carlson K. E. and Lloyd J. E. (1982) *In vivo* and *in vitro* steroid receptor assays in the design of estrogen pharmaceuticals in *Receptor Binding Radiotracers* (W. C. Eckelman, Ed.), Vol. 1, Chapter 6, pp 93 - 126, CRC Press, Boca Raton, FL.
- [2] Katzenellenbogen J. A. (1995) Designing steroid receptor-based radiotracers to image breast and prostate tumors. *J. Nucl. Med.* **36** (6) Suppl., 8S - 13S.
- [3] DiZio J. P., Anderson C. J., Davison A., Ehrhardt G. J., Carlson K. E., Welch M. J. and Katzenellenbogen J. A. (1992) Technetium- and rhenium-labeled progestins: Synthesis, receptor

- binding and *in vivo* distribution of a 11 β -substituted progestin labeled with technetium-99 and rhenium-186. *J. Nucl. Med.* **33** (4), 558 - 569.
- [4] DiZio J. P., Fiaschi R., Davison A., Jones A. G. and Katzenellenbogen J. A. (1991) Progestin-rhenium complexes: Metal-labeled steroids with high receptor affinity, potential receptor-directed agents for diagnostic imaging or therapy. *Bioconj. Chem.* **2**, 353 - 366.
- [5] O'Neil J. P., Carlson K. E., Anderson C. J., Welch M. J. and Katzenellenbogen J. A. (1994) Progestin radiopharmaceuticals labeled with technetium and rhenium: Synthesis, binding affinity, and *in vivo* distribution of a new progestin N₂S₂-metal conjugate. *Bioconj. Chem.* **5**, 182 - 193.
- [6] Spies H. and Johannsen B. (1995) Functionalization of technetium complexes to make them active *in vivo*. *Analyst* **120**, 775 - 777.
- [7] Stork G. and Takahashi T. (1977) Chiral synthesis of prostaglandins (PGE₁) from D-glycer-aldehyde. *J. Am. Chem. Soc.* **99**, 1275 -1276.
- [8] Mitsunobu O. (1981) The use of diethyl azodicarboxylate and triphenylphosphine in synthesis and transformation of natural products. *Synthesis* 1 - 28.
- [9] Fietz T., Spies H., Pietzsch H.-J. and Leibnitz P. (1995) Synthesis and crystal structure of (3-thiapentane-1.5-dithiolato)chlorooxorhenium(V). *Inorg. Chim. Acta* **321**, 233 - 236.
- [10] Alberto R., Schibli R., Egli A., Schubiger P. A., Herrmann W. A., Artus G. M, Abram U. and Kaden T. A. (1995) Metal carbonyl syntheses XXII. Low pressure carbonylation of [MOCl₄]⁻ and [MO₄]⁻ technetium(I) and rhenium(I) complexes [NEt₃]₂[MCl₃(CO₃)]. *J. Organomet. Chem.* **493**, 119 - 127.
- [11] Blunt J. W. and Stothers J. B. (1977) ¹³C NMR spectra of steroids - a survey and commentary. *Org. Magn. Reson.* **9**, 439.
- [12] Pietzsch H.-J., Spies H. and Hoffmann S. (1989) Lipophilic technetium complexes VI. Neutral oxotechnetium(V) complexes with monothiole/tridentate dithiole coordination. *Inorg. Chim. Acta* **165**, 163 - 166.

22. Technetium and Rhenium Labelled Steroids

2. Oxorhenium(V) Complexes of 1-Mercapto-4-methylestra-1,3,5(10)-trien-17-one

F. Wüst, H. Spies, R. Beckert¹, S. Möller¹

¹Friedrich-Schiller-Universität Jena, Institut für Organische und Makromolekulare Chemie

Introduction

The rearrangement of 3-thioxo- $\Delta^{1,4}$ -steroids offers a new approach to mercapto functionalized steroids [1]. The dithion-thiophenol rearrangement (Fig. 1) of 3-thioxoandrosta-1,4-dien-17-one **1** in an aprotic solvent in the presence of an acid catalyst results in 1-mercapto-4-methylestra-1,3,5(10)-trien-17-one **2** suitable for forming mixed-ligand "3+1"-complexes. The mercapto functionalized steroid compound **2** was synthesized by the group of Prof. Beckert at Jena university.

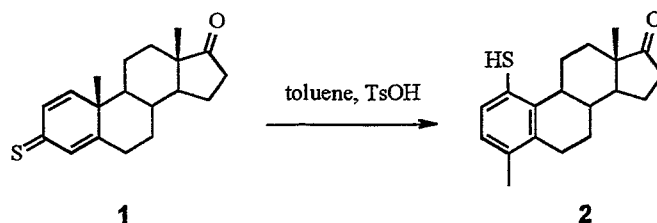


Fig. 1 Dithion-thiophenol rearrangement

Experimental

(3-thiapentane-1,5-dithiolato)(1-mercapto-4-methylestra-1,3,5(10)-trien-17-one)oxorhenium(V) **3**
39 mg (100 μ mol) chloro(3-thiapentane-1,5-dithiolato)oxorhenium(V) **5** [2] were dissolved in 4 ml hot acetonitrile while stirring. At 80 °C 61 mg (200 μ mol) of the thiol **2** dissolved in 4 ml acetonitrile were added. The colour of the mixture changed from dark blue to red while stirring and heating at 80 °C for 2 h. Afterwards it was evaporated to dryness and the residue was redissolved in chloroform. The red solution was worked up by chromatography on a silica gel column with chloroform/methanol (5:1) as an eluent. Slow evaporation of the eluate yielded 29 mg (44 %) of reddish brown crystals.

Melting point: 244 - 246 °C

IR absorption $\nu_{\max}/\text{cm}^{-1}$ (KBr) 960 (Re=O)

Elemental analysis: (Found C, 41.78; H, 4.58; S, 18.94; $\text{C}_{23}\text{H}_{31}\text{O}_2\text{ReS}_4$ requires C, 42.24; H, 4.78; S, 19.61 %).

(3-oxapentane-1,5-dithiolato)(1-mercapto-4-methylestra-1,3,5(10)-trien-17-one)oxorhenium(V) **4**
66.8 mg (114 μ mol) tetra-n-butylammonium-tetrachlorooxorhenate(V) **6** [3] were dissolved in 2 ml EtOH and cooled to 0 °C. At this temperature 37.6 mg (125 μ mol) thiol **2** and 13.6 μ l (114 μ mol) 3-oxapentane-1,5-dithiol **7** in 2 ml chloroform were added while stirring. The colour of the mixture changed to red. The mixture was stirred at 0 °C for another two hours. During this time a solid was formed. Evaporation of the solution and redissolving of the residue in chloroform yielded a red solution, which was purified by being passed through a silica gel column with chloroform / methanol (5:1). Slow evaporation of the eluate yielded 26 mg (36 %) of brown crystals.

Melting point: 211 - 215 °C

IR absorptions: $\nu_{\max}/\text{cm}^{-1}$ (KBr) 952, 968 (Re=O)

Elemental analysis: (Found C, 42.97; H, 5.09; S, 13.94; $\text{C}_{23}\text{H}_{31}\text{O}_3\text{ReS}_3$ requires C, 43.31; H, 4.90; S, 15.08 %).

Results and Discussion

The steroid thiol **2** is readily available by rearrangement of the corresponding 3-thioxo- $\Delta^{1,4}$ -steroids. These steroid compounds were obtained by a method developed by Beckert *et al.* [4]. This method involves the regioselective thionation of 3-oxo-1,4-dien steroids using Lawesson's reagent. With steroid thiol **2** two rhenium "3+1" complexes were synthesized with the appropriate rhenium precursors **5** and **6**. The complexes **3** and **4** were obtained in 44 % and 36 % yield (Fig. 2).

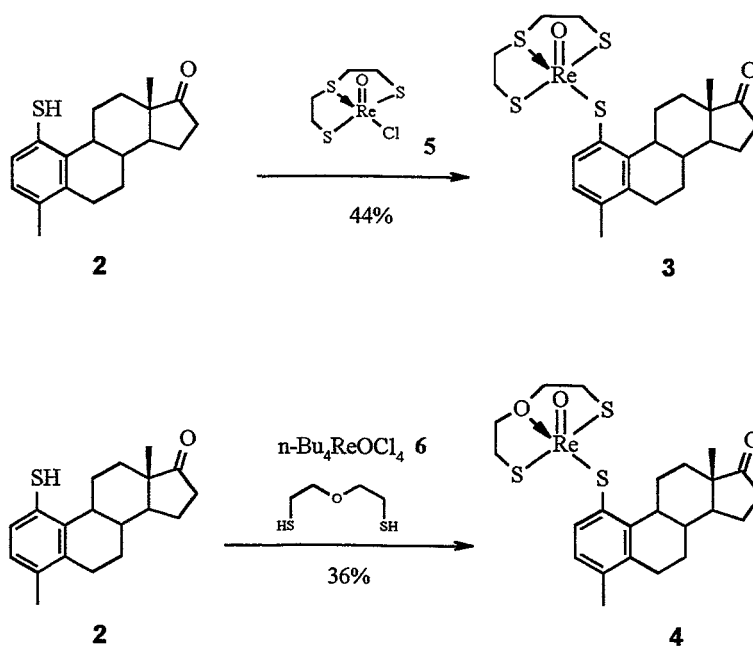


Fig. 2: Complex formation of monothiol 2

Complex formation by exchange of the Re-Cl bond in 5 with thiol 2 requires heating for 2 hours due to the sterical requirements of thiol steroid 2. Using the more reactive rhenium precursor 6, the complex formation according to the "3+1"-concept occurs immediately at 0 °C.

The complexes 3 and 4 were characterized by elemental analysis and ir-spectroscopy. In the ir-spectrum of complex 4 two strong bands of the same intensity in the range of the Re=O absorption at 952 cm^{-1} and 960 cm^{-1} were unexpectedly observed. Complex 3 only shows one strong band at 960 cm^{-1} . The reasons for giving two strong absorption bands for complex 4 with S-O-S coordination in the tridentate ligand part instead of the expected single one as in complex 3 with S-S-S coordination are not yet known. Further characterization of the well crystallized compounds 3 and 4 by X-ray crystal structure determination is intended.

Recently we reported two new oxorhenium(V) complexes with functionalized estradiol [5]. In the complexes the chelate unit was bound via a mercaptomethyl group to the steroid molecule. The present work describes labelling of the chelate directly to the steroid without any carbon spacer.

References

- [1] Möller S., Weiß D. and Beckert R. (1995) Umlagerung von 3-Thioxo- $\Delta^{1,4}$ -steroiden, ein neuer Zugang zu Steroidthiolen. *Liebigs Ann.*, 1397-1399.
- [2] Fietz T., Spies H., Pietzsch H.-J. and Leibnitz P. (1995) Synthesis and crystal structure of (3-thiapentane-1.5-dithiolato)chlorooxorhenium(V). *Inorg. Chim. Acta* **321**, 233 - 236.
- [3] Alberto R., Schibli R., Egli A., Schubiger P. A., Herrmann W. A., Artus G. M, Abram U. and Kaden T. A. (1995) Metal carbonyl syntheses XXII. Low pressure carbonylation of $[\text{MOCl}_4]^-$ and $[\text{MO}_4]^-$ technetium(I) and rhenium(I) complexes $[\text{NEt}_2][\text{MCl}_3(\text{CO}_3)]$. *J. Organomet. Chem.* **493**, 119 - 127.
- [4] Weiß D., Gaudig U., Beckert R. (1992) Eine neue Methode zur Herstellung von gekreuzt-konjugierten 3-Thioxosteroiden. *Synthesis*, 751 - 752.
- [5] Wüst F., Spies H. and Johannsen B. (1996) Synthesis of "3+1" mixed-ligand oxorhenium(V) complexes containing modified 3,17 β -estradiol. *Bioorg. Med. Chem. Lett.* **6**, 2729 - 2734.

23. Structure and Reactivity of a "3+1" Mixed-Ligand Rhenium Complex Containing Thiobenzoate as a Monodentate Ligand [ReO(SSS)(SC(O)Ph)]

B. Noll, P. Leibnitz¹, St. Noll, R. M. Mahfouz², H. Spies

¹Bundesanstalt für Materialforschung, ²Assiut University, Egypt

Introduction

"3+1" rhenium complexes with aliphatic or aromatic thiols as monodentate ligands are well known as compounds having a relatively stable S₄ coordination sphere [1] and subsequent reactions at pendent-substituted groups may be successfully carried out without any alteration of the coordination sphere. In this article we report on the synthesis and molecular structure of a rhenium complex with thiobenzoic acid as a co-ligand [ReO(SSS)(SBz)]. This compound is expected to have some potential as a synthon for the complexes [ReO(SSS)SR], provided hydrolysis of the benzoylic group will lead to a [ReO(SSS)S] intermediate. Preliminary experiments were carried out to cleave the S - CO bond.

Experimental

Polarographic measurements were carried out under an argon atmosphere with a DC/AC polarograph (GWP 673, tastpolarography 5 mV steps, droptime 1 s, potential range from 0.0 mV to -1600 mV). X-ray data were collected at room temperature (296 K) with an ENRAF NONIUS CAD 4 diffractometer, graphite monochromatized Mo K α radiation (A = 0.71073).

Synthesis of [(S-thiobenzoylato)(3-thiapentanedithiolato-1.5)]oxorhenium(V) [ReO(SSS)(SBz)] 1

96 mg [ReO(SSS)Cl] complex (0.25 mmol) is dissolved in 10 ml acetonitrile while stirring and warming. 60 μ l thiobenzoic acid (0.50 mmol) is dissolved in 2 ml methanol and then neutralized by adding about 400 μ l 1.25 M NaOCH₃ solution. This solution is added to the Re precursor while stirring. All manipulations were performed under argon or nitrogen. The colour of the reaction solution changed from blue to dark red. After 2 hours the solution is gently heated (40 - 50 °C) and the volume is halved in a stream of nitrogen (argon). The grey precipitate is separated by filtration. The filtrate is evaporated to dryness and the residue is extracted with ether.

After evaporation of the ether the residue is dissolved in acetonitrile. Reddish-brown crystals are received. Yield: (87 mg, 71 %).

M.p.: 203 - 203 °C (from ethanol)

Elemental analysis: (Found: C, 26.94; H, 2.67; S, 26.08, C₁₁H₁₃O₂S₄ requires C, 26.59; H, 2.62; S, 25.93 %)

IR absorptions: $\nu_{\max}/\text{cm}^{-1}$ 1648 (CO) and 976 (ReO)

Synthesis of [(methoxy)(3-thiapentanedithiolato-1.5)]oxorhenium(V) [ReO(SSS)(OMe)] 2

73.8 mg 1 (0.15 mmol) are dissolved in 10 ml acetonitrile while warming (about 50 °C) and stirring. 200 μ l 1.13 M NaOCH₃ (0.23 mmol) are dropped into the solution, the colour changes from purple to brown, and after two hours a brown precipitate is separated, extracted with ether and dried in vacuum. Yield: (29 mg, 67 %).

M.p.: 168 - 173 °C (from acetonitrile)

Elemental analysis: (Found: C, 16.14; H, 2.76; S, 25.16, C₅H₁₁O₂S₃Re requires C, 15.58; H, 2.88; S, 24.95 %)

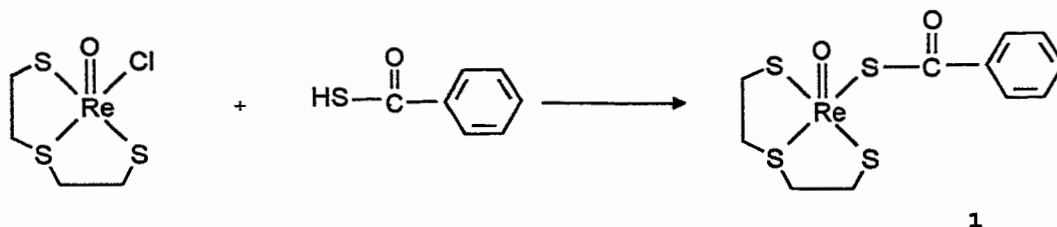
IR absorptions: $\nu_{\max}/\text{cm}^{-1}$ 960 (ReO)

Saponification studies of 1

7.1 mg 1 (15 μ mol) are dissolved in 8.0 ml supporting electrolyte. A 0.1 M Bu₄N[PF₆] solution in acetonitrile was used as supporting electrolyte. 1.13 M sodium methylate was added step by step (5 μ mol at a time) and polarograms were recorded.

Results and Discussion

The complex $[ReO(SSS)(SBz)]$ **1** was obtained as a pure, crystalline compound by reaction of thiobenzoic acid with $(ReO(SSS)Cl)$ according to Fig. 1.



The structure of **1** was determined by X-ray crystallography and is shown in Fig. 2.

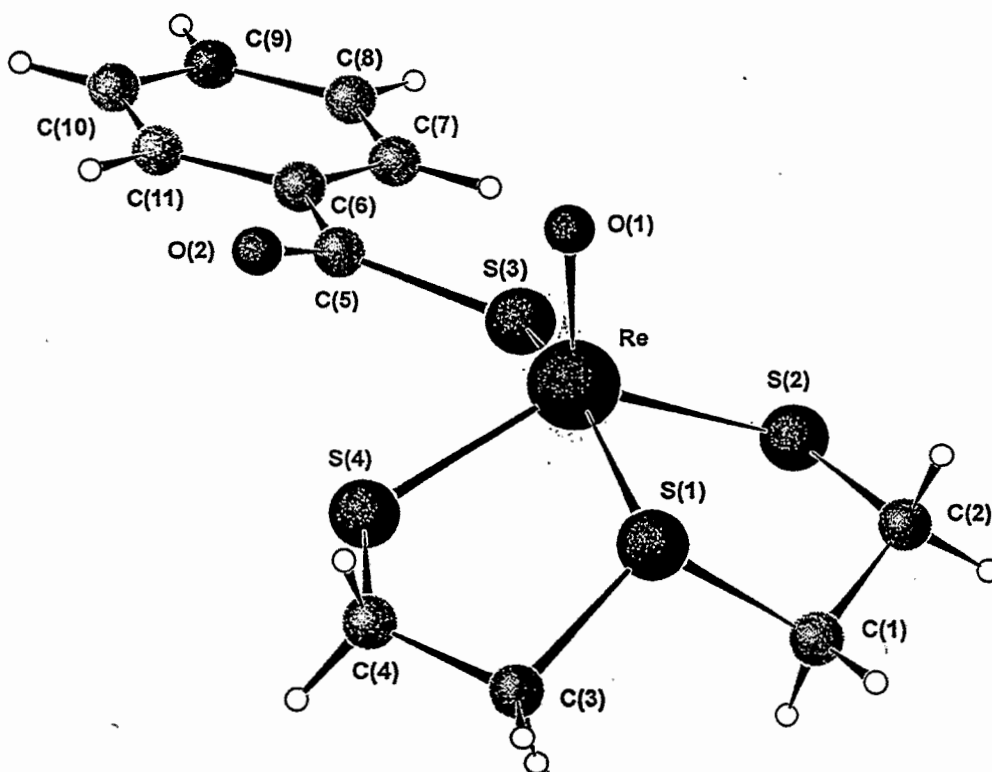


Fig.2: Molecular structure of **1**

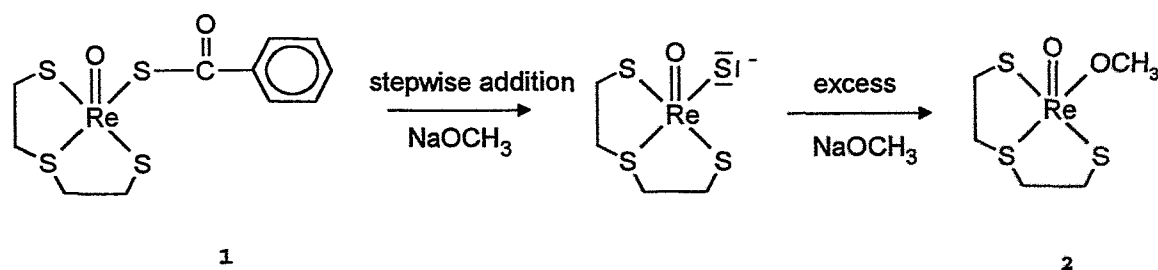
The crystal system was found to be orthorhombic, with a space group: $P2(1)2(1)2(1)$, $Z = 4$, $R = 2.9\%$. Selected bond lengths and angles are listed in Table 1. The structure of the tridentate/monodentate complex is related to $[ReO(S_3)(SR)]$, where $R = -CH_2C_6H_5$ [1].

Table 1: Selected bond lengths and angles of **1**

Bond lengths[X]			
Re-O (1)	1.682(4)	Re-S (3)	2.351(2)
Re-S (1)	2.348(2)	Re-S (4)	2.276(2)
Re-S (2)	2.293(2)		
Bond angles [°]			
O(1)-Re-S(4)	115.9(2)	O(1)-Re-S(3)	103.8(2)
O(1)-Re-S(2)	114.9(2)	O(1)-Re-S(1)	102.0(2)
S(4)-Re-S(2)	129.17(7)	S(2)-Re-S(1)	84.36(6)
S(2)-Re-S(3)	80.36(6)	S(4)-Re-S(1)	83.65(6)
S(4)-Re-S(3)	89.59(6)		

The saponification of the monodentate benzoic mercapto ester bound to the ReOSSS core by stepwise addition of sodium methylate was polarographically controlled. The increase in the anodic step with a half wave potential at -480 mV indicates the presence of the free mercapto group located at the Re core. The cathodic step at -1030 mV assigned to the redox step of the carboxylic group decreases at the same time. From these results the existence of the [ReO(SSS)S] intermediate can be assumed.

Using a molar excess of sodium methylate a brown precipitate **2** was separated by filtration. There is some evidence that substitution of the negatively charged sulphur by methylate occurred and the complex **2** has the composition [ReO(SSS)(OMe)] (elemental analysis and infrared spectra). However, this assumption has to be confirmed by further analytical investigations, and studies of nucleophilic substitution reactions at a postulated S⁻ centre will be carried out.



References

- [1] Spies H., Fietz Th., Pietzsch H., Johannsen B., Leibnitz P., Reck G., Scheller D. and Klostermann K. (1995) Neutral oxorhenium(V) complexes with tridentate dithiolates and monodentate alkane- or arene-thiolate coligands. *J. Chem. Soc., Dalton Trans.* 2277.

24. Nicotinamide-Substituted Rhenium(V) Mixed-Ligand Complexes

T. Kniess, H. Spies

Introduction

The radiopharmaceutical research aims at present at tracers whose ultimate distribution is determined by specific biochemical or receptor-binding interactions [1]. One of the challenging tasks is the development of radiotracers able to indicate and to image certain redox processes.

Bodor and co-workers used the NAD^+/NADH equilibrium as a model to develop a redox delivery system to move polar drugs through the blood-brain barrier [2 - 5]. Prompted by this work, we looked for potentialities of this principle for the design of new rhenium and technetium compounds. To our knowledge such types of chelates suitable for coupling to a pyridinium salt or a dihydropyridine moiety - both of which are constituents of the NAD^+/NADH redox pair - are so far unknown.

In this paper we report the synthesis of rhenium chelates bearing either a pyridinium or a dihydropyridine functionality as potential metal-based redox-active tracers. Nicotinamide was converted into the N-(2-mercaptoethyl) derivative which directly or after quaternization to the 3-(2-mercaptoethyl-carbamoyl)-1-methylpyridinium as a monodentate ligand binds to an oxometal core. The remaining coordination sites were occupied by the tridentate bis(2-mercaptoethyl)-sulphide (HSSH) resulting in neutral "3+1" mixed-ligand complexes [6].

Experimental

General

Melting points were obtained on a Boetius apparatus and were uncorrected. Infrared spectra were determined on a Specord M 80 spectrophotometer and UV-VIS spectra provided by a Specord M 40 spectrometer (Carl Zeiss Jena). The NMR spectra were recorded on an FT-Spectrometer DC 300 (Bruker) in deuterated chloroform or dimethyl sulphoxide with tetramethyl silane as the internal standard. Elemental analyses were performed on a LECO CHNS932 Elemental Analyser.

Materials and methods

Methyl nicotinate, ethanolamine, thionyl chloride, bis(mercaptoethyl)sulphide and sodium dithionite were obtained from FLUKA. $\text{Na}_3\text{PO}_3\text{S} \times 12\text{H}_2\text{O}$ was synthesized according to a literature procedure [7]. Methyl iodide was obtained from RIEDEL de HAEN. The precursor chloro(3-thiapentane-1,5-dithiolato)oxo-rhenium(V) was prepared according to the literature [8].

Preparation of 3(2-hydroxyethyl-carbamoyl)pyridine (2). 41.1 g (0.3 mol) methyl nicotinate **1** were heated with 18.3 g (0.3 mol) ethanolamine to a temperature of 150 - 160 °C and the resulting methanol was collected by distillation. After 3 hours the heating was removed and the product solidified as a yellowish mass. Recrystallization from 1,2-dichloroethane gave the pure substance but the crude product was used for the next step.

Yield: 49.8 g (98 %); melting point: 82 - 86 °C.

Elemental analysis: (Found: C, 57.79; H, 5.97; N, 16.49, $\text{C}_8\text{H}_{10}\text{N}_2\text{O}_2$ requires C, 57.83; H, 6.02; N, 16.86 %).

^1H NMR data: δ_{H} (200.13 MHz; solvent CDCl_3) 3.62 (2H, q), 3.82 (1H, s), 3.83 (2H, t), 7.25 (1H, s), 7.38 (1H, m), 8.13 (1H, d), 8.66 (1H, d), 8.99 (1H, s).

Preparation of 3(2-chlor-ethyl-carbamoyl)pyridine (3). 49 g (0.295 mol) **2** were dissolved in 200 ml chloroform and cooled to 0 °C. 42.8 g (0.36 mol) thionyl chloride were dropped into the solution, while stirring vigorously (glass stirrer), the mixture was warmed up to room temperature and then refluxed four hours until the oily product solidified. 200 ml water and 45 g NaHCO_3 were added in portions after cooling. The organic layer was separated and the residue extracted two times with 200 ml chloroform. The unified organic solutions were dried over MgSO_4 and evaporated. The resulting product was purified by column chromatography on aluminium oxide with chloroform/acetone (1:1) as the eluent to yield **3** as white needles.

Yield: 25 g (45 %); melting point: 89 - 91 °C.

Elemental analysis: (Found: C, 51.82; H, 4.92; N, 14.91; Cl, 18.61, $\text{C}_8\text{H}_9\text{ClN}_2\text{O}$ requires C, 52.03; H, 4.87; N, 15.17; Cl, 19.24 %)

^1H NMR data: δ_{H} (200.13 MHz; solvent CDCl_3) 3.66 (2H, q), 3.77 (2H, t), 7.02 (1H, s), 7.33 (1H, m), 8.08 (1H, d), 8.66 (1H, d), 8.95 (1H, s).

Preparation of 3(2-mercaptoethyl-carbamoyl)pyridine (4): 3.7 g (20 mmol) **3** were dissolved in 20 ml water and stirred with a solution of 15.8 g (40 mmol) $\text{Na}_3\text{PO}_3\text{S} \times 12 \text{H}_2\text{O}$ in 150 ml water for 7 hours at 40 - 50 °C. After cooling to room temperature the pH was adjusted to 4.0 by adding 3.5 % HCl. The mixture was allowed to stand overnight and then extracted with CH_2Cl_2 (4 x 100 ml). The organic layer was dried over MgSO_4 and evaporated. Purification by column chromatography on silica gel with acetone/chloroform (6:1) yielded **4** as white crystals.

Yield: 1.8 g (48 %); melting point: 96 - 98 °C.

Elemental analysis: (Found: C, 52.57; H, 5.58; N, 15.12; S, 16.93, $\text{C}_8\text{H}_{10}\text{N}_2\text{OS}$ requires C, 52.74; H, 5.49; N, 15.38; S, 17.58 %)

^{13}C NMR data: $\delta_{\text{C-13}}$ (75.475 Mhz; solvent DMSO-d_6) 23.32 (CH_2), 42.80 (CH_2), 123.60 (C_{ar}), 129.89 (C_{ar}), 135.10 (C_{ar}), 148.38 (C_{ar}), 151.95 (C_{ar}), 165.00 (CO).

Preparation of 3(2-mercaptoethyl-carbamoyl)-1-methyl-pyridiniumiodide (5): 370 mg (2.03 mmol) **4** in 35 ml p.a. acetone were refluxed with 6.0 g (40 mmol) methyl iodide for 20 minutes. After cooling the mixture was concentrated by evaporation up to 5 ml and stored overnight at -18 °C. The resulting yellow needles were separated. The product **5** was pure enough to be used without further purification.

Yield: 490 mg (74 %); melting point: 102 - 104 °C.

Elemental analysis: (Found: C, 33.46; H, 3.83; N, 8.52; I, 38.37; S, 9.59, $\text{C}_9\text{H}_{13}\text{N}_2\text{IOS}$ requires C, 33.33; H, 4.01; N, 8.64; I, 39.19; S, 9.87 %)

^{13}C NMR data: $\delta_{\text{C-13}}$ (125.70 MHz; solvent DMSO-d_6) 23.07 (CH_2), 42.91 (CH_2), 48.24 (CH_3), 127.34 (C_{ar}), 133.19 (C_{ar}), 142.66 (C_{ar}), 145.43 (C_{ar}), 147.16 (C_{ar}), 161.39 (CO).

Preparation of (3-pyridinyl-ethylcarbamoyl-thiolato)-(3-thiapentane-1,5-dithiolato)oxorhenium(V) (6): 1.06 g (2.7 mmol) chloro(3-thiapentane-1,5-dithiolato)oxorhenium(V) were dissolved in 60 ml boiling acetonitrile. 0.975 g (5.4 mmol) **4** in 20 ml acetonitrile was dropped to this solution and the mixture was refluxed for one hour. The solid product was separated, dried and purified by column chromatography (Al_2O_3 , methanol). The eluate was concentrated to half its original volume and allowed to stand overnight at -18 °C. The product **6** crystallized as fine red needles.

Yield: 1.03 g (71 %); melting point: 186 - 188 °C.

Elemental analysis: (Found: C, 26.43; H, 3.02; N, 5.13; S, 23.40, $\text{C}_{12}\text{H}_{17}\text{N}_2\text{O}_2\text{S}_4\text{Re}$ requires C, 26.91; H, 3.17; N, 5.23; S, 23.92 %)

^{13}C NMR data: $\delta_{\text{C-13}}$ (75.475 MHz; solvent DMSO-d_6) 35.41 (CH_2), 42.42 (CH_2), 43.13 ($2 \times \text{CH}_2$), 45.61 ($2 \times \text{CH}_2$), 123.56 (C_{ar}), 129.95 (C_{ar}), 135.08 (C_{ar}), 148.44 (C_{ar}), 151.69 (C_{ar}), 164.62 (CO).

IR absorptions: $\nu_{\text{max}}/\text{cm}^{-1}$ (KBr) 960 (Re=O); 1664 (C=O).

Preparation of (1-methyl-3-pyridinyl-ethylcarbamoyl-thiolato)-(3-thiapentane-1,5-dithiolato)-oxorhenium(V)iodide (7):

Route A: 535 mg (1mmol) **6** were refluxed with 1.42 g (10 mmol) methyl iodide in 150 ml p.a. acetone. After 4 hours the solution was nearly discoloured and a light red product had separated. It was filtered and recrystallized from methanol to yield **7**.

Yield: 336 mg (50 %); melting point: 197 - 198 °C.

Route B: 83 mg (211 μmol) chloro(3-thiapentane-1,5-dithiolato)oxorhenium(V) were refluxed in 5 ml acetonitrile. 137 mg (422 μmol) **5** in 2 ml acetonitrile were added and the mixture was refluxed for 30 minutes. The solution was concentrated to 3 ml and after cooling 3 ml diethyl ether were added to the mixture. The solid product was separated and recrystallized.

Yield: 86 mg (60 %); melting point: 198 - 200 °C.

Elemental analysis: (Found: C, 22.86; H, 2.81; N, 4.08; I, 16.84; S, 18.65, $\text{C}_{13}\text{H}_{20}\text{N}_2\text{IO}_2\text{S}_4\text{Re}$ requires C: 23.04, H: 2.95, N: 4.13, I: 18.75, S: 18.90 %).

^1H NMR data: δ_{H} (500.13 Mhz, solvent DMSO-d_6) 2.26 (2H, m), 3.04 (2H, t), 3.68 (2H, q), 3.87 (2H, t), 4.08 (2H, q), 4.32 (2H, d), 4.39 (3H, s), 8.24 (1H, t), 8.89 (1H, d), 9.10 (1H, d), 9.34 (1H, t), 9.41 (1H, s).

IR absorptions: $\nu_{\text{max}}/\text{cm}^{-1}$ (KBr) 960 (Re=O); 1668 (C=O).

Results and Discussion

The synthesis of 3(2-mercaptoethyl-carbamoyl)-1-methylpyridine **4** is associated, as the literature shows, with some difficulties and by-products [9, 10]. We decided to start from the methyl nicotinate **1** which was heated with ethanolamine at 150 °C to relieve methanol and form 3(2-hydroxyethyl-carbamoyl)pyridine **2** (Fig. 1).

Treatment of the hydroxyl group with thionyl chloride leads to the 3(2-chlor-ethyl-carbamoyl)pyridine **3**. The introduction of the thiol group resulted in reacting **3** with sodium thiophosphate dodecahydrate in aqueous solution by modification of a literature procedure [11]. Acid hydrolysis of the phosphoric acid thioester supplied the free thiol **4** in high purity.

Thiol **4** was methylated with excess methyl iodide. Alkylation of sulphur could be prevented by application of an inert solvent.

Both thiolates **4** and **5** were reacted with the precursor chloro(3-thiapentane-1,5-dithiolato)oxo-rhenium(V) according to the "3+1" principle [6]. In this way the new rhenium mixed-ligand complexes **6** and **7** were obtained. Complex **7** can also be obtained by direct methylation of the complex **6** with excess methyl iodide in acetone (route A).

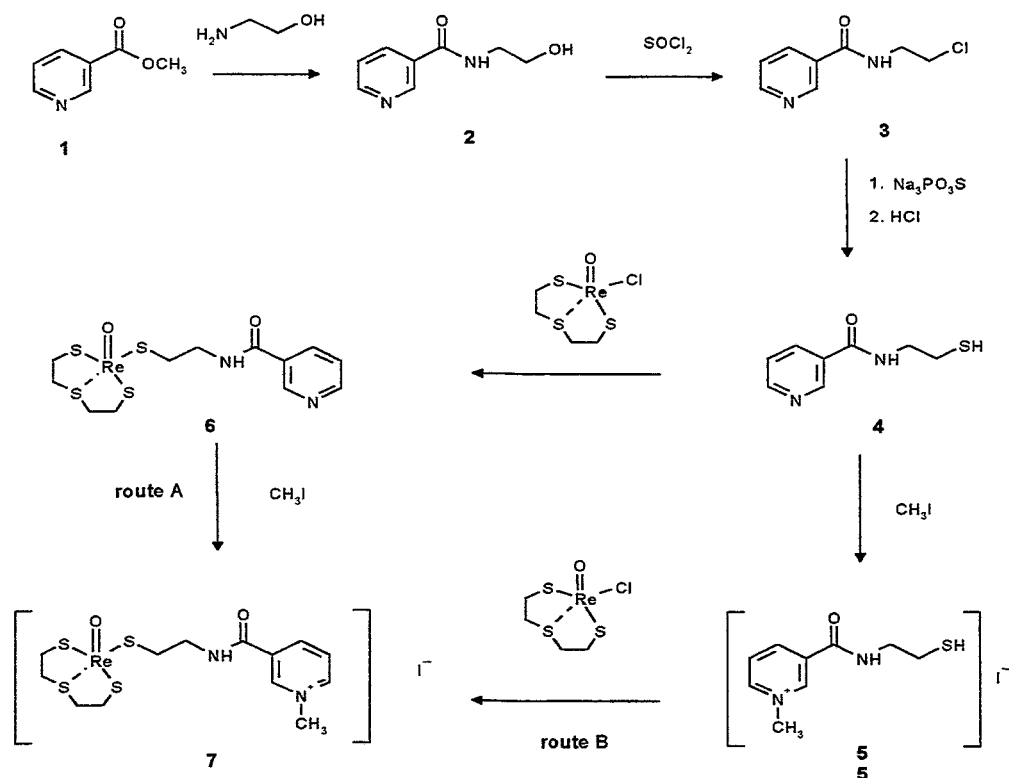


Fig. 1: Reaction pathway for preparation of nicotinamide-substituted Re-complexes **6** and **7**

The most convenient method of generating dihydropyridines from pyridinium salts is reduction with sodium dithionite in alkaline solution [12, 13]. In this way it should be possible to reduce the pyridinium salt "3+1" complex **7** with $\text{Na}_2\text{S}_2\text{O}_4$ to the 1,4-dihydropyridine derivative. Because of the oxidation sensitivity of the dihydropyridines it is difficult to detect them analytically. Nevertheless, a significant identifying mark is the characteristic absorption in UV-VIS spectrometry at about 360 nm [2, 14]. By stirring **7** in alkaline aqueous medium with $\text{Na}_2\text{S}_2\text{O}_4$ a brick-red solid was separated (decomposition 105 - 115 °C). Attempts at purification resulted in a viscous red substance. Fig. 2 shows the UV-VIS spectrum of complex **7** and the alteration of the spectrum after reduction to the dihydropyridine. A new band at 299.3 nm appeared and the absorption at 366 nm increased. The latter may serve as an indication for the existence of a dihydropyridine complex.

Further investigations on the preparation and stability of dihydropyridines have been carried out with the technetium complexes and will be published in a subsequent paper.

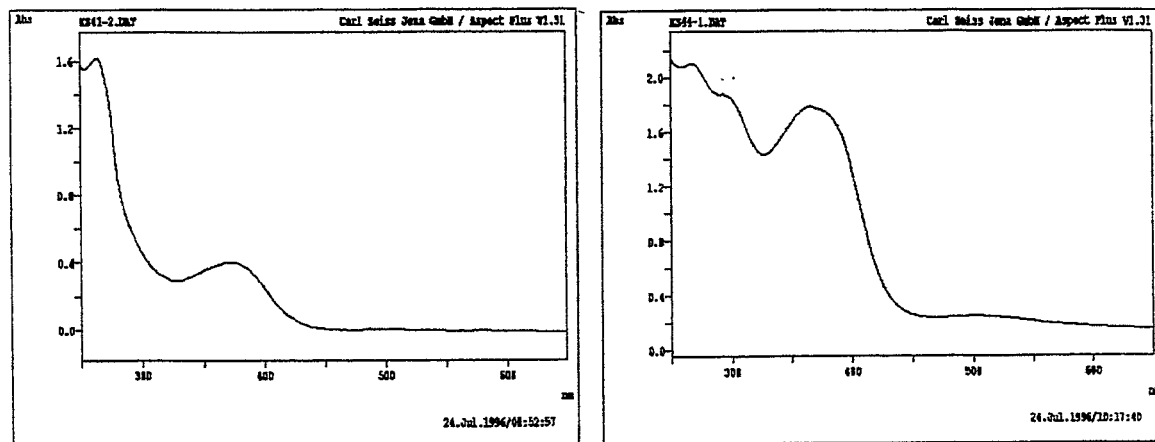


Fig. 2. UV-VIS spectrum of complex 7 in water and after reduction with $\text{Na}_2\text{S}_2\text{O}_4$

References

- [1] Jurisson S., Bernig D., Jia W. and Ma D. (1993) Coordination compounds in nuclear medicine. *Chem. Rev.* **93**, 1137 - 1156.
- [2] Bodor N. and Farag H. H. (1984) Brain specific, sustained delivery of testosterone, using a redox chemical delivery system. *J. Pharm. Sci.* **73**, 385 - 389.
- [3] Bodor N. and Abdelalim A. M. (1985) Novel redox carriers for brain-specific chemical delivery systems. *J. Pharm. Sci.* **74**, 241 - 245.
- [4] Simpkins J. W., Bodor N. and Enz A. (1985) Direct evidence for brain-specific release of dopamine from a redox delivery system. *J. Pharm. Sci.* **74**, 1033 - 1036.
- [5] Pop E., Brewster E. M., Prokai-Tatrai K. and Bodor N. (1994) Novel redox derivatives of tryptophan. *Heterocycles* **38**, 2051 - 2064.
- [6] Spies H., Fietz T., Pietzsch H. J., Johannsen B., Leibnitz P., Reck G., Scheller D. and Klostermann K. (1995) Neutral oxorhenium(V) complexes with tridentate dithiolates and monodentate alkane- or arene-thiolate coligands. *J. Chem. Soc. Dalton Trans.*, 2277 - 2280.
- [7] Brauer G. (1975-1981) *Handbuch Präp. Anorg. Chem.*, 3rd edn., Ferdinand Enke Verlag, 1, 552.
- [8] Fietz T., Spies H., Pietzsch H. J. and Leibnitz P. (1995) Synthesis and molecular structure of chloro-(3-thiapentane-1,5-dithiolato)-oxorhenium(V). *Inorg. Chem. Acta* **231**, 233 - 236.
- [9] Cavazza C. (1975) Nikotinsäure-mercaptoamid und seine Salze. *Ger. Offen* **2,339,815**, (CA **80**, 133273).
- [10] Su Z. F., Noll St. and Spies H. (1994) Synthesis of N(2-mercaptoethyl)nicotinamides. *Annual Report 1994*, Institute of Bioinorganic and Radiopharmaceutical Chemistry, FZR-73, 75 - 78.
- [11] Bieniarz C. and Cornwell M. J. (1993) A facile, high yielding method for the conversion of halides to mercaptans. *Tetrah. Lett.* **34**, 939 - 942.
- [12] Lovesey A. C. and Ross W. C. (1969) Potential coenzyme inhibitors. Reduction of 4-methylnicotinamide derivatives by sodium dithionite and sodium borohydride. *J. Chem. Soc. (B)*, 192 - 194.
- [13] Blankenhorn G. and Moore E. G. (1980) Sulfoxylate ion, the hydride donor in dithionite-dependent reduction of NAD^+ analogues. *J. Am. Chem. Soc.* **102**, 1092 - 1098.
- [14] Lehninger A. L., Nelson D. L. and Cox M. M. (1994) *Prinzipien der Biochemie*. 2nd edn., Spektrum Akadem. Verlag, Heidelberg, p. 458.

25. Dihydropyridine-Substituted Technetium(V) Mixed-Ligand Complexes

T. Kniess, H. Spies

Introduction

In researching redox-active Tc-99m radiotracers based on the pyridinium salt/dihydropyridine system we described the synthesis of 3(2-mercaptoethyl-carbamoyl)-1-methyl-pyridinium-iodide **1** and the preparation of corresponding rhenium(V) mixed-ligand complexes [1]. In this paper the formation of the analogous technetium complexes starting from $^{99/99m}\text{Tc}$ gluconate is reported. The reduction of pyridinium to the dihydropyridine group with sodium dithionite is documented for the free ligand and for the complex. UV-VIS spectrometric investigations were carried out concerning the characterization and the stability of the dihydropyridines.

Experimental

General

UV-VIS spectra were determined on a Specord M 40 spectrometer (Carl Zeiss Jena). The radioscaner was a TRACEMASTER 20 (Berthold).

NaHCO_3 , $\text{Na}_2\text{S}_2\text{O}_4$, sodium gluconate and bis(mercaptoethyl)sulphide were obtained from FLUKA. 3(2-mercaptoethyl-carbamoyl)-1-methyl-pyridiniumiodide **1** was synthesized according to the preceding report [1]. Stannous chloride dihydrate was obtained from ALDRICH. Sodium pertechnetate in saline solution was eluted from a $^{99}\text{Mo}/^{99m}\text{Tc}$ generator purchased from MALLINCKRODT.

Thin-layer chromatography (TLC) was performed on silufol plates (KAVALIER). The RP-18 glass-backed plates were obtained from MERCK.

Preparation of 3(2-mercaptoethyl-carbamoyl)-1-methyl-1,4-dihydropyridine (4): 9.75 mg (30 μmol) **1** and 15 mg (180 μmol) NaHCO_3 were dissolved in 2 ml water. The mixture was cooled to almost 0°C and 10.5 mg (60 μmol) $\text{Na}_2\text{S}_2\text{O}_4$ were added so that the solution turned light orange. When the reduction was finished after 15 minutes, the nearly colourless dihydropyridine solution was used for further reactions.

UV-VIS data: λ_{max} 361.8 nm

Radiolabelling with $^{99/99m}\text{Tc}$

(1-methyl-3-pyridinylethylcarbamoyl-thiolato)-(3-thiapentane-1,5-dithiolato)oxotechnetium(V)iodide (3): 1 μmol $^{99}\text{TcO}_4^-$ and (5-10 MBq) $^{99m}\text{TcO}_4^-$ in 1 ml 0.1 M sodium gluconate was diluted with 1 ml 0.9 % NaCl and then reduced with 100 μl freshly prepared 0.01 M stannous chloride dihydrate in 0.1 M HCl. 1.95 mg (6 μmol) **1** in 200 μl water were added to this $^{99/99m}\text{Tc(V)}$ gluconate solution. 1.0 ml acetone was given to the yellow complex and then 0.3 mg (2 μmol) bis(mercaptoethyl)sulphide in 300 μl acetone. The reaction process was controlled by TLC (RP18 plates, butanol/acetic acid/water = 2:1:1). **3** was determined as a peak with $R_f = 0.54$ in 73 % radiochemical purity.

[1-methyl-3-(1,4)dihydropyridinyl-ethylcarbamoyl-thiolato]-(3-thiapentane-1,5-dithiolato)oxotechnetium(V) (6):

1 μmol (5-10 MBq) $^{99/99m}\text{Tc(V)}$ gluconate prepared as above was reacted with 1 ml of dihydropyridine solution (containing 15 μmol **4**). After 5 minutes 1 ml acetone and 0.3 mg (2 μmol) bis(mercaptoethyl)sulphide in 300 μl acetone were added. The reaction was observed by UV-VIS spectroscopy.

Results and Discussion

The reaction pattern for the synthesis of the nicotinamide-substituted $^{99/99m}\text{Tc}$ mixed-ligand complexes is visible in Fig. 1. The pyridinium salt **1** was reacted with $^{99/99m}\text{Tc}$ gluconate to the supposed intermediate **2**. In a second step the tridentate ligand bis(2-mercaptoethyl)sulphide (HSSSH) was added. Three monodentate ligands were thereby replaced and the complex **3** was formed.

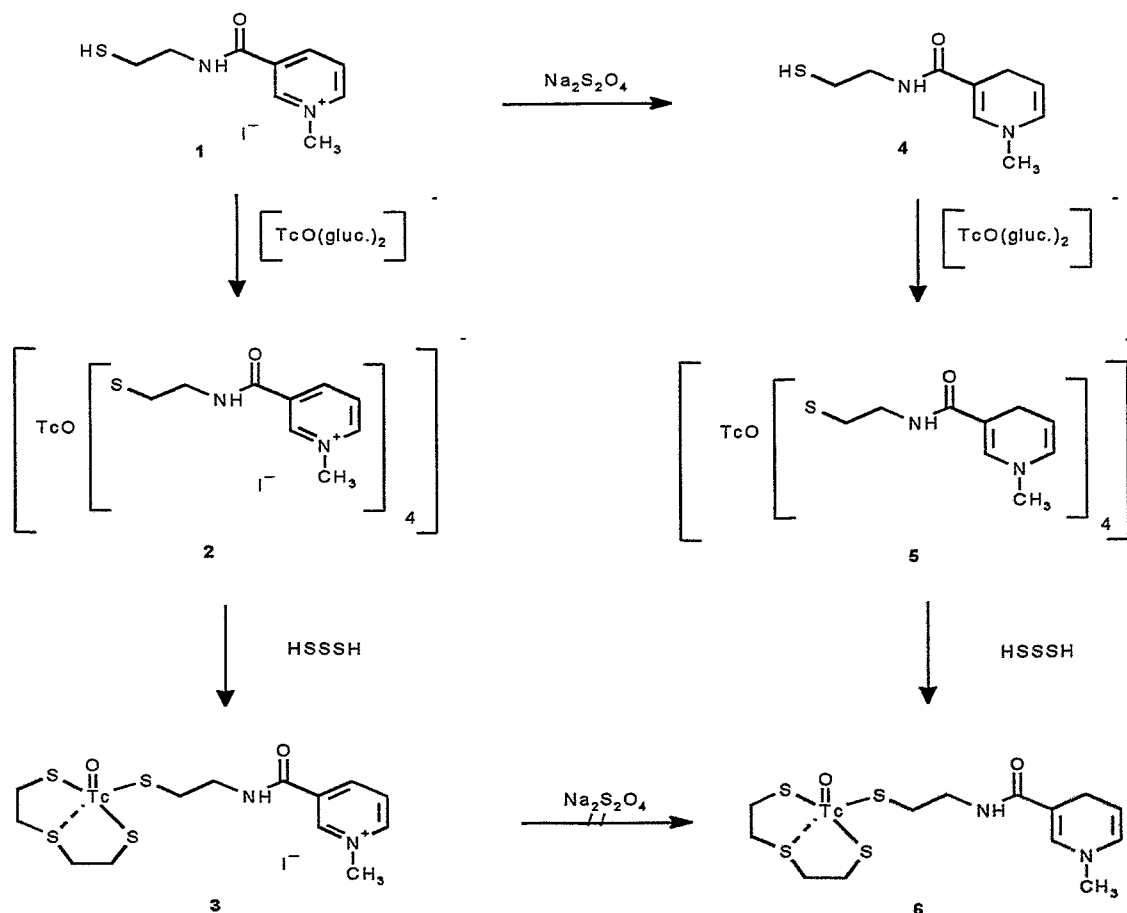


Fig. 1: Reaction pathway for preparation of pyridinium salt and dihydropyridine-substituted Tc complexes **3** and **4**

The progress of the reaction was observed by TLC. Fig. 2 shows typical thin layer chromatograms. In the first step after reaction of **1** with $^{99/99m}\text{Tc}$ gluconate the intermediate **2** is detectable with unreacted sodium gluconate near the start. When the tridentate HSSSH was added, the peak of complex **2** disappeared and the new '3+1' complex **3** was found as the major product. An investigation of **3** by capillary electrophoresis proved that **3** is a cationic complex.

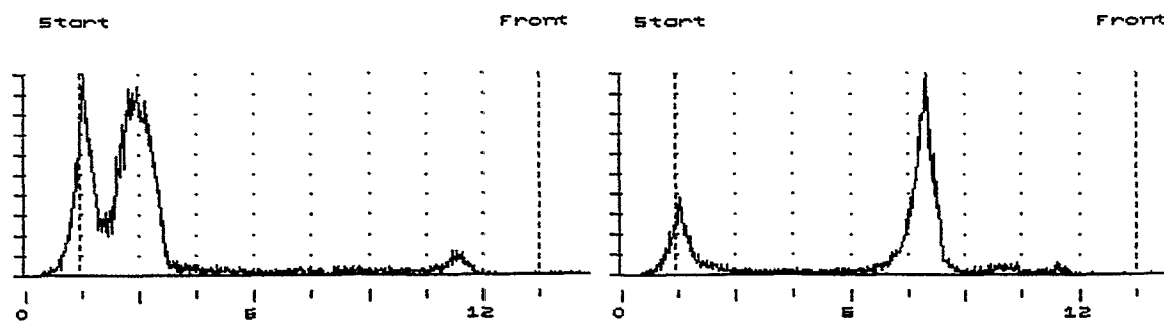


Fig. 2. TLC of the reaction of $^{99/99m}\text{Tc}$ gluconate with 1 before and after addition of HSSSH

The most convenient way of generating 1,4-dihydropyridines from pyridinium salts is reduction with sodium dithionite in alkaline solution [2, 3]. In this way we tried to reduce the complex 3 to the dihydropyridine 6. After addition of the reducing agent a brown discoloration of the yellow complex was observed and within three hours a brown precipitate appeared. TLC showed that after 15 minutes part of complex 3 was already decomposed and insoluble material was found at the start that did not run on the TLC mobile solvent (Fig. 3). Three hours later only the insoluble precipitate at the start was visible. It can be assumed that the brown insoluble compound is reduced hydrolyzed technetium. A reduction of the metal has obviously occurred. This competitive reaction is not surprising because the ligand 1 as well as the sodium dithionite have been used in great excess over the technetium.

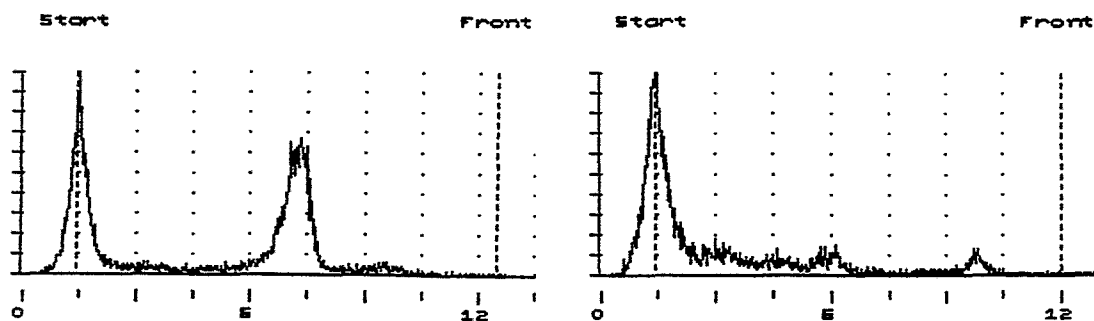


Fig. 3: TLC of 3 with $\text{Na}_2\text{S}_2\text{O}_4$ after 15 min and 180 min

To avoid reduction of the metal, the free dihydropyridine ligand 4 was prepared starting from 1 followed by complexation as an additional step. 1 was reduced with sodium dithionite within 15 minutes. Because of the sensitivity of 4 to air oxidation, the product was not isolated in substance. The solution containing freshly reduced 4 was analysed by UV-VIS spectrometry. A strong absorption at 361.8 nm was observed that disappeared within 45 minutes (Fig. 4). As the literature shows, a significant identifying mark of 1,4-dihydropyridines is their characteristic absorption in UV-VIS spectrometry at about 360 nm [4, 5].

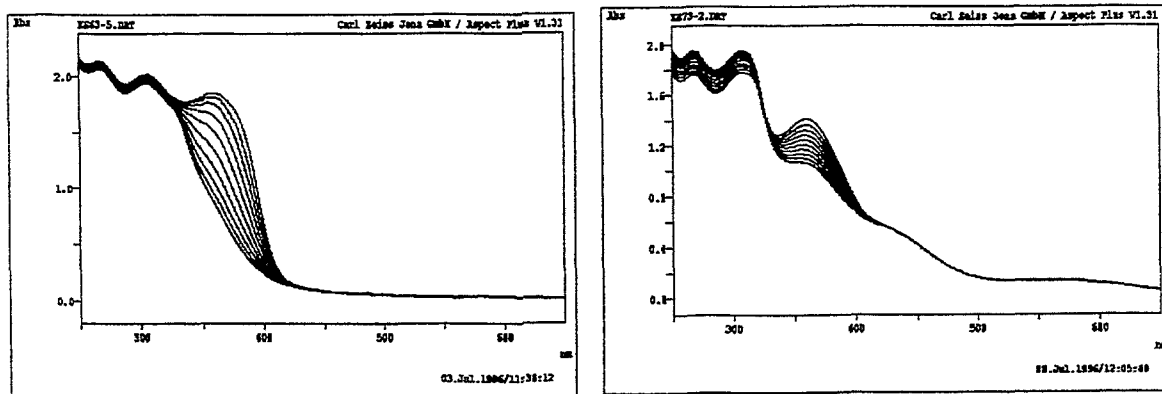


Fig. 4: UV-VIS spectrum of 4 and of 5 in water over 45 minutes

If a solution of freshly reduced dihydropyridine 4 is given to $^{99/99m}\text{Tc}$ gluconate, a complex of structure 5 is expected. The UV-VIS spectrum of 5 again showed a significant dihydropyridine absorption at 360.4 nm that disappeared over 45 minutes (Fig. 4). By immediate addition of tridentate ligand HSSH to 5, the desired dihydropyridine '3+1' complex 6 becomes available. In the UV-VIS spectrum of 6 a strong absorption at 365.6 nm was observed that did not change over two hours (Fig. 5). This band overlaid the dihydropyridine absorption so that no detailed statements can be made about the stability of 6. By analogy with 4 and 5 we assume that complex 6 is also stable for approximate 45 minutes.

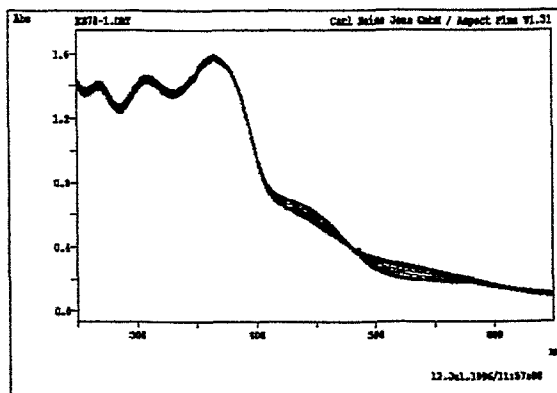


Fig. 5: UV-VIS spectrum of 6 in water over 120 minutes

Investigation of the stability of the dihydropyridines by UV-VIS spectrometry shows that decomposition occurs within a short time. Further efforts are needed to obtain complexes of a higher stability, suitable for in vivo tests. Improvements in the stability of the dihydropyridine complexes may be achieved by introduction of various substituents on the pyridinium ring and modification of the tridentate ligand. In addition the search for other ways of reduction by chemical, biochemical or electrochemical methods should be continued.

References

- [1] Kniess T. and Spies H. (1996) Nicotinamide-substituted rhenium(V) mixed-ligand complexes. *This report*, pp. 96 - 100.
- [2] Lovesey A. C. and Ross W. C., (1969) Potential coenzyme inhibitors. Reduction of 4-methylnicotinamide derivatives by sodium dithionite and sodium borohydride. *J. Chem. Soc. (B)*, 192 - 194.
- [3] Blankenhorn G. and Moore E. G. (1980) Sulfoxylate Ion, the hydride donor in dithionite-dependent reduction of NAD^+ analogues. *J. Am. Chem. Soc.* **102**, 1092 - 1098.
- [4] Bodor N. and Farag H. H. (1984) Brain specific, sustained delivery of testosterone, using a redox chemical delivery system. *J. Pharm. Sci.* **73**, 385 - 389.
- [5] Lehninger A. L., Nelson D. L. and Cox M. M. (1994) *Prinzipien der Biochemie*. 2nd edn., Spectrum Akadem. Verlag, Heidelberg, p. 458.

26. Note on the Fast Hydrolysis of the Methyl Ester of MAG₂ during Complexation with Tc/Re(V) gluconate

St. Noll, B. Noll, H. Spies

Introduction

We report on the ligand exchange of Tc gluconate with the methyl ester of mercaptoacetyl diglycine (MAG₂) in alkaline solution. The reaction involves an unexpectedly fast saponification of the ester group resulting in formation of the known 1:1 complexes of both Re and Tc with MAG₂ as the tetradentate ligand.

Experimental

Preparation of [ReO(MAG₂)] from Re gluconate and MAG₂ methyl ester

22 mg MAG₂ methyl ester (0.1 mmol) was dissolved in 2.0 ml water and added to 2.0 ml 0.05 M Re gluconate (0.1 mmol) solution under an inert gas (nitrogen) atmosphere while stirring. After adding 200 µl 1 N NaOH the reaction mixture was stirred for 30 minutes and then neutralized with 200 µl 1 N HCl. After addition of 48 mg Ph₄AsCl the solution was extracted with methylene chloride. The reddish-brown organic phase was dried over sodium sulphate, evaporated to dryness and the residue crystallized from ethanol. 49 mg (64 %) brown crystals, m.p. 201 - 202 °C.

Preparation of the ^{99m}Tc complex

1.0 mg MAG₂ methyl ester was dissolved in 120 µl methanol and added to 2.0 ml ^{99m}Tc gluconate solution containing 400 µl 0.1 M NaOH. After 20 minutes the mixture was neutralized with 380 µl 0.1 N HCl and analysed by HPLC on an RP 18 column (Eurosphere), eluent A: 0.05M phosphate buffer pH 5.8, eluent B: methanol; 3 min 100 % A, 15 min from 100 % A to 20 % A / 80 % B. R_t: 14.3 min;

The resulting preparation was compared with a reference ^{99m/99}Tc-MAG₂ complex prepared with MAG₂ as the ligand according to the above procedure.

Results and Discussion

Hydrolysis of the MAG₂ methyl ester under these conditions is nearly quantitative and the MAG₂ formed reacts immediately with Re gluconate to form the complex [ReO(MAG₂)]. The identity of the isolated complex (as Ph₄As salt) with the previously described Ph₄As[ReO(MAG₂)] [1] is confirmed by the identical retention time in HPLC, melting point and elemental composition.

Analogously to the studies with rhenium, MAG₂ methyl ester forms [TcO(MAG₂)] [2] when allowed to react with Tc gluconate as a precursor. It could also be proved that the saponification also takes place at the n.c.a. level so that attempts to label the MAG₂ methyl ester with ^{99m}Tc result in the ^{99m}Tc(V) MAG₂ complex. The R_t value in HPLC is the same both for the ^{99m}Tc labelled MAG₂ ester and MAG₂. A mixture of both reaction products shows only one peak at R_t 14.3 min in the HPLC analysis.

The results supply the evidence for hydrolysis of the MAG₂ ester both for the c.a. and the n.c.a. level under conditions normally used for complexation reaction. This behaviour enables us to use the ester as a protecting group in the ligand synthesis, when required. In complexation reactions, there is no need to split the protecting group prior to the reaction, a fact that could be benefit in sensitive labelling procedures at the n.c.a. level of ^{99m}Tc.

References

- [1] Johannsen B., Noll B., Leibnitz P., Reck G., Noll St. and Spies H. (1993) Technetium and rhenium complexes with mercapto-containing peptides 1. Tc(V) and Re(V) complexes with mercaptoacetyl diglycine (MAG₂) and X-ray structure of AsPh₄[TcO(MAG₂)] C₂H₅OH *Inorg. Chim. Acta* **210**, 209 - 214.
- [2] Noll B., Leibnitz P., Noll St., Reck G., Spies H. and Johannsen B. Synthesis and X-ray crystal structure of AsPh₄[ReO(MAG₂)]. *To be published*.

27. Synthesis of ^{186}Re Gluconate by Stannous Chloride Reduction of $^{186}\text{ReO}_4^-$

B. Noll, T. Kniess, H. Spies

Introduction

The radioactive isotopes of rhenium, ^{186}Re and ^{188}Re , are of interest in nuclear medicine for therapeutical use because of their nuclear properties and the chemical analogy with technetium-99m [1, 2]. The labelling of molecules with ^{99m}Tc is often advantageously done by means of precursors such as Tc(V) tartrate or Tc(V) gluconate. Such starting materials are also required for rhenium complexes. The ability to form Re(V) gluconate in depending on the rhenium concentration up to a molar concentration of 10^{-3} by stannous chloride reduction of perrhenate has already been described in [2]. Because of the different redox potentials of pertechnetate and perrhenate, the formation of Re gluconate requires an excess of stannous chloride and sufficient reaction time. The lower the rhenium concentration, the longer is the reaction time with a constant amount of stannous chloride. To establish the conditions at the ^{186}Re concentration level necessary for complete conversion of perrhenate into Re gluconate, experiments were carried out including variation of the amounts of the reactands and the reaction time.

Experimental

The samples are analysed by TLC on silica gel sheets (Kieselgel 60/Merck) and acetone as the eluent. The distribution of radioactivity is measured with a linear analyzer (Berthold). Polarographic measurements were carried out with a DC/AC polarograph (GWP 673).

^{186}Re activity was obtained from Mallinckrodt Medical as sodium perrhenate with a specific activity ≥ 29.6 GBq/mg and a radioactive concentration ≥ 8.5 GBq/ml. For better handling the stock solution was diluted with water 1:10, the total Re concentration amounts to $1.7 \cdot 10^{-4}$ mol/l. Depending on the age of the ^{186}Re stock solution, 5 - 10 μl are taken from this stock solution for the labelling experiments carried out in a volume of about 2 ml, the Re concentration amounted to $4.25 \cdot 10^{-7}$ - $8.5 \cdot 10^{-7}$ mol/l.

Preparation of ^{186}Re gluconate

5 μl of the ^{186}Re perrhenate stock solution are added to a mixture of 2.0 ml 0.5 M sodium gluconate and 0.5 M hydrochloric acid or 0.5 M sodium hydroxide. $^{186}\text{ReO}_4^-$ is reduced with 0.1 M stannous chloride at neutral pH, using stannous tartrate. The content of perrhenate was determined by thin layer chromatography. (R_f perrhenate 0.7; R_f Re gluconate 0.0 - 0.1)

Results and Discussion

The formation of Re gluconate depending on the stannous chloride content is shown in Figure 1. The yield of the Re gluconate has a maximum at about 60 min, after this time the complex decomposes into perrhenate at lower stannous chloride concentrations. In our investigations an amount of 200 μl 0.1 M stannous chloride was necessary to obtain an yield of nearly 100 %. The ^{186}Re gluconate prepared in this way is stable for up to two hours without cooling.

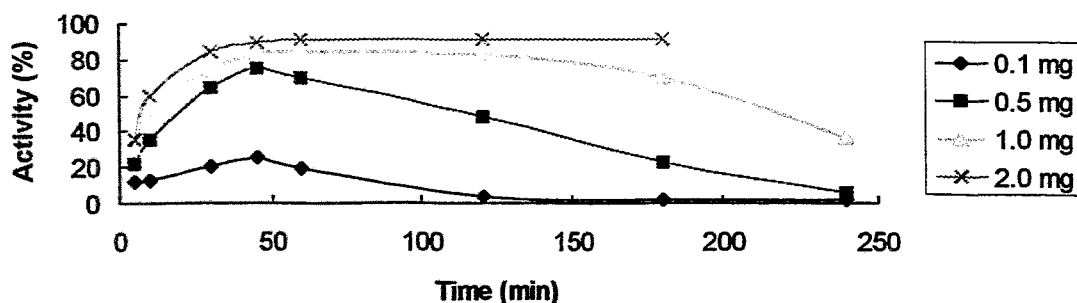


Fig.1: The formation of Re gluconate depending on the stannous chloride content and time by reduction of perrhenate at pH 4. The total Re concentration is about $4.3 \cdot 10^{-7}$ Mol/l.

Within the pH range from 4 to 7 there are no differences in the yield of Re gluconate. At low pH (<2) and high pH (>9) the yield of Re gluconate decreases drastically, only 20 - 30 % are found besides

unreacted perrhenate. The tin(II) content in the alkaline reaction mixture (pH 10) was controlled by means of dc polarographic measurements. A steady decrease in the cathodic wave of the stannous chloride as a function of time was observed after addition of the [$^{186}\text{ReO}_4$], even though the molar excess of stannous chloride is about 1000 times greater than the total content of rhenium. So, the decrease in the cathodic wave cannot have been caused by the presence of rhenium species. Instead, radiolytic processes should be taken into consideration. The corresponding measurement without addition of rhenium activity resulted in no decrease the cathodic wave and no stannous chloride was consumed. This behaviour may also be the reason for the instability of the ^{186}Re gluconate in time, and a slight excess of stannous chloride is obviously necessary to prevent a rapid oxidation to perrhenate. Optimum conditions for labelling gluconate with ^{186}Re at the concentration level from $4.25 \cdot 10^{-7}$ to $8.5 \cdot 10^{-7}$ mol/l were the pH range from 4 - 7, concentration of stannous chloride of 2.0 mg / ml and a reaction time of 45 - 60 min. The ^{186}Re gluconate solution prepared under this conditions is at least stable for two hours and can be successfully used for ligand exchange reactions with various ligands. A procedure that can be modified within the above defined conditions is given in the experimental part.

References

- [1] Weininger J., Ketring A. and Deutsch E. (1987) Rhenium-186-HEDP a bone therapeutic radiopharmaceutical. *Nucl. Med. Biol.* **14**, 223 - 232.
- [2] Hashimoto K., Bagiawati S., Izumo M. and Kobayashi K. (1996) Synthesis of ^{186}Re -MDP complex using carrier-free ^{186}Re . *Appl. Radiat. Isot.* **47**, 195 - 199.
- [3] Noll B., Kniess T., Friebe M., Spies H. and Johannsen B. (1996) Rhenium(V) gluconate, a suitable precursor for the preparation of rhenium(V) complexes; *Isotopes Environ. Health Stud.* **32**, 21 - 29.

8. Determination of Partition Coefficients for Coordination Compounds by Using the HPLC Column Nucleogel RP C₁₈ 80-10

R. Berger, T. Fietz, M. Glaser, H. Spies

Introduction

The transport and distribution processes within biological systems are to a large extent controlled by the lipophilicity of the system components. It is therefore not astonishing that the lipophilicity also plays a dominating role both during penetration of potential brain agents through the blood-brain barrier (BBB) and in the binding of potential ligand-like substances to certain receptors.

Lipophilicity is usually expressed by the partition coefficient (P or log P), a molecular parameter which describes the partitioning equilibrium of a solute molecule between a water-immiscible lipid-like organic solvent (e.g. octanol) and an aqueous phase [1 - 4]. As the determination of log P by the "shaking flask" procedure has some drawbacks, other simpler methods have been tested for their suitability. A promising method for assessing the lipophilicity of numerous interesting substances is the reversed-phase high-performance liquid chromatography (RP-HPLC). It represents a very comfortable and reliable method for determining partition coefficients [4, 5 - 8].

In order to obtain more insight into lipophilicity-dependent proceedings which play an important role during the passage of substances through membranes (e.g. BBB) as well as in binding to receptors, lipophilic numerical data of some rhenium complexes with the structures **1** and **2** (Fig. 1) synthesized by the (3+1) or (4+1) mixed-ligand procedure [9, 10] have been determined by using RP-HPLC

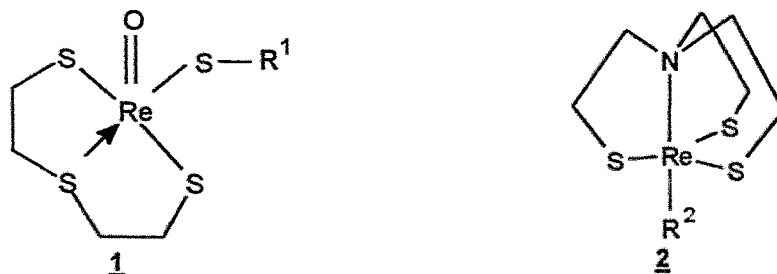


Fig. 1: General structure of the rhenium complexes **1** and **2**

columns with different stationary phases. Previous experiments made use of columns filled with octadecyl silica and poly(styrene-divinylbenzene) copolymer (RP 18 and PRP-1). For a better understanding of the behaviour of certain complexes with aliphatic and especially aryl residues on the aromatic PRP-1 column, an additional column based on a poly(styrene-divinylbenzene) copolymer modified by matrix-linked octadecyl chains is included in the studies. (Because of possible specific π - π interactions in the case of a pure aryl stationary phase, an influence on the retention of aryl solutes is expected [11, 12]).

Experimental

Before starting an HPLC run, a small quantity of the compounds selected was dissolved in a mixture of methanol and acetonitrile or dimethyl sulphoxide (about 2 mg/ml). (All reference chemicals were commercial products, and they were used without further purification.) Sample volumes of 5 - 10 μ l were injected into the Rheodyne valve 7125 connected with the Perkin Elmer Model 1020. A Perkin Elmer UV/VIS spectrophotometric detector LC 290 with an operating wavelength of mostly 254 nm and the recorder Kodak Diconix 150 Plus were used throughout the study. The experiments were carried out with the column NUCLEOGEL RP C₁₈ 80-10 (150 x 4.6 mm; PS/DVB/C₁₈, 10 μ m; MACHEREY-NAGEL) under isocratic elution conditions at room temperature and with a flow rate of 1.5 ml/min. For the buffer preparation reagent-grade chemicals were used. Water was prepared with an ion exchange unit. Acetonitrile from Baker, Roth, or Merck served as an eluent. For the mobile phase acetonitrile and 0.01 M KH₂PO₄/Na₂HPO₄ buffer in a volume ratio of 3:1 (pH 7.4) were used. (The experimental conditions for the RP 18 and PRP-1 columns are summarized in the last Annual Report [4]).

The capacity factors (k') were evaluated from the chromatograms by $k' = (t_R - t_0)/t_0$, where t_R and t_0 are the retention times of a retained and an unretained solute. Methanol was applied as the non-retained reference compound.

The capacity factors of the complexes of interest were changed to the corresponding log P values with the aid of the equation $\log P = a \log k' + b$. For a linear trend function the substances aniline (0.9), benzene (2.13), bromobenzene (2.99), and biphenyl (4.09) served as the log P references. Because these log P values depend on various unknown factors caused and influenced by the RP-HPLC system, the designation P_{HPLC} for an apparent constant was employed throughout this work.

Results and Discussion

P_{HPLC} values of Re complexes containing the structure form **1** are listed in Table 1. The preliminary P_{HPLC} values by using the NUCLEOGEL RP C₁₈ column (C) are compared with the corresponding values obtained by means of the RP 18 (A) and PRP-1 column (B) [4]. Quotients formed by P_{HPLC} value pairs (A/C) and (B/C) of the corresponding columns are demonstrated in addition.

Tab. 1: Partition coefficients (P_{HPLC} , $\log P_{\text{HPLC}}$) of various rhenium complexes **1** by using different chromatography columns [RP 18, PRP-1, NUCLEOGEL RP C₁₈] and their quotients formed by dividing the corresponding RP 18 and PRP-1 by NUCLEOGEL RP C₁₈ values

R ¹	RP 18 (A)		PRP-1 (B)		NUCLEOGEL RP C ₁₈ (C)		P _{HPLC}	
	P _{HPLC}	log P _{HPLC}	P _{HPLC}	log P _{HPLC}	P _{HPLC}	log P _{HPLC}	A/C	B/C
-CH ₂ -CO-OCH ₃	16	1.20	32	1.51	7.2 ± 0.9	0.86	2.2	4.4
-CH ₂ -CO-OC ₂ H ₅	39	1.59	74	1.87	13 ± 1.5	1.11	3.0	5.7
-CH ₂ -CO-O- <i>n</i> -C ₃ H ₇	132	2.12	173	2.24	26 ± 1.5	1.41	5.1	6.6
-CH ₂ -CO-O- <i>n</i> -C ₄ H ₉	455	2.66	398	2.60	55 ± 3	1.74	8.3	7.2
-CH ₃	25	1.40	146	2.16	51 ± 2	1.71	0.5	2.9
-C ₂ H ₅	62	1.79	244	2.39	157 ± 21	2.20	0.4	1.6
- <i>n</i> -C ₃ H ₇	222	2.35	598	2.78	354 ± 72	2.55	0.6	1.7
- <i>n</i> -C ₄ H ₉	763	2.88	1452	3.16	11740 ± 5390	4.07	0.06	0.1
- <i>n</i> -C ₈ H ₁₇	4754	3.68	4535	3.66	463886 ± 307000	5.67	0.01	0.01
-C ₆ H ₅	224	2.35	993	3.00	152 ± 20	2.18	1.5	6.5
-CH ₂ -C ₆ H ₅	610	2.79	1898	3.28	261 ± 46	2.42	2.3	7.3
-CH ₂ -CH ₂ -C ₆ H ₅	1784	3.25	4260	3.63	525 ± 123	2.72	3.4	8.1

For Re complexes with the structure form **2** preliminary P_{HPLC} values obtained by using the NUCLEOGEL RP C₁₈ column are summarized in Table 2. These values are compared with corresponding values obtained by using a PRP-1 column [4].

Tab. 2: Partition coefficients (P_{HPLC}) of various rhenium complexes **2** by using the columns PRP-1 and NUCLEOGEL RP C₁₈ and their quotients formed by dividing the corresponding PRP-1 by NUCLEOGEL RP C₁₈ values (eluent: acetonitrile/buffer = 3/1, pH 7.4)

R^2	PRP-1 (B)		NUCLEOGEL RP C ₁₈ (C)		P_{HPLC} B/C
	P_{HPLC}	$\log P_{\text{HPLC}}$	P_{HPLC}	$\log P_{\text{HPLC}}$	
-CN-CH ₂ -CO-OCH ₃	74	1.87	18 ± 1	1.26	4.1
-CN-CH ₂ -CO-OC ₂ H ₅	148	2.17	36 ± 1	1.56	4.1
-CN-(CH ₂) ₁₀ -CO-OC ₂ H ₅	177000	5.25	37200 ± 19000	4.57	4.8
-CN-C ₆ H ₅	4340	3.64	1100 ± 300	3.04	4.0
-CN-(CH ₂) ₂ -N[CH ₃]- (CH ₂) ₂ -C ₆ H ₅	2830	3.45	540 ± 120	2.73	5.2
-CN-(CH ₂) ₃ -CO-[p-F-C ₆ H ₄]	3340	3.52	540 ± 120	2.73	6.2
-CN-(CH ₂) ₃ -C[O-(CH ₂) ₂ -O]-[p-F-C ₆ H ₄]	5700	3.76	1015 ± 270	3.01	5.6
-CN-(CH ₂) ₂ -N[(CH ₂) ₂ -O-(CH ₂) ₂]	115	2.06	21 ± 1	1.32	5.5
-P[(CH ₃) ₂]-C ₆ H ₅	12000	4.08	4600 ± 1800	3.66	2.6

Considering the P_{HPLC} values determined by the NUCLEOGEL RP C₁₈ column in Tables 1 and 2, the rather high mean errors between about 2 and 60 per cent are remarkable. It can easily be recognized that with increasing P_{HPLC} values the mean errors also grow. This depends on the non-linear trend of the calibration substances aniline, benzene, bromobenzene, and biphenyl on NUCLEOGEL RP C₁₈. The retention behaviour expressed as capacity factors of these calibration substances on the columns NUCLEOGEL RP C₁₈ and PRP-1 is shown in Fig. 2. In comparison with the nearly linear trend on PRP-1 the curve for NUCLEOGEL RP C₁₈ is better described by a polynomial regression function.

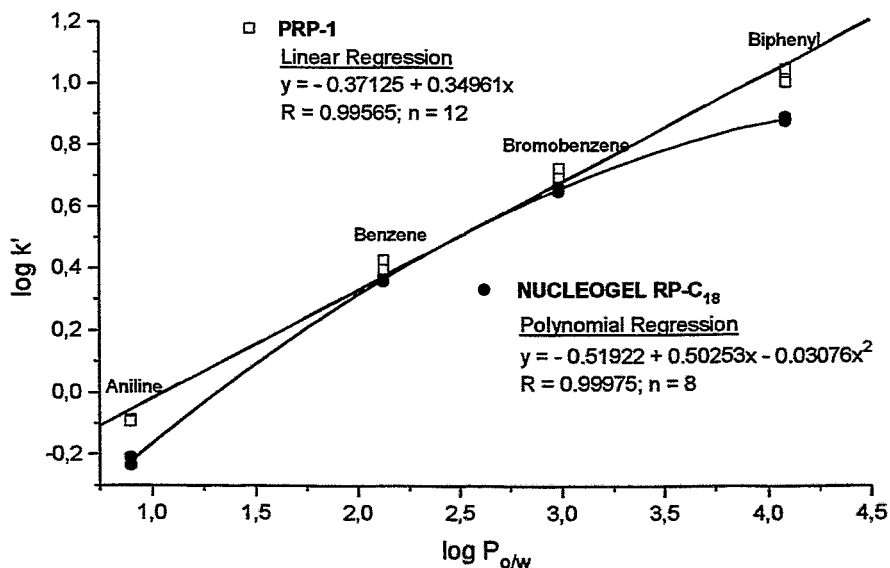


Fig. 2: Capacity factors ($\log k'$) in dependence on the octanol/water partition coefficients ($\log P_{\text{o/w}}$) of some benzene derivatives as calibration substances by using the columns PRP-1 and NUCLEOGEL RP C₁₈

Using the NUCLEOGEL RP C₁₈ column, the resulting P_{HPLC} values of several Re chelates correlate well with both the values of the PRP-1 and the RP 18 column. This includes such chelates which have either an ester group or a ring-like structure as benzene or morpholine in their monodentate ligand. That means that only log P_{HPLC} values of chelates with the P_{HPLC} ratio B/C of more than three are used for a linear correlation.

The corresponding value pairs obtained by using the PRP-1 and NUCLEOGEL RP C₁₈ column are plotted in Fig. 3. For better information an additional reference straight line ($y = x$) is outlined as well as the resulting linear regression function ($y = 1.00417x + 0.73691$; $R = 0.99499$; $n = 15$).

It is not quite clear why the log P_{HPLC} values of the residual complexes investigated are outside this correlation. In case of the Re complexes bearing monodentate ligands with more or less long hydrocarbon chains, hydrophobic (non-specific) interactions and surface effects between aliphatic residues of the Re complexes and octadecyl carbon chains of the stationary phase can probably be taken into account [11]. This is the case particularly when the carbon chain has more than three carbon atoms.

Using an RP 18 column consisting of silica-based reversed-phase packing bonded with *n*-octadecyl hydrocarbon chains a similar but not so pronounced appearance can be observed. In those cases, monodentate ligands with an aliphatic chain longer than C₄ result in much higher log P_{HPLC} values [4].

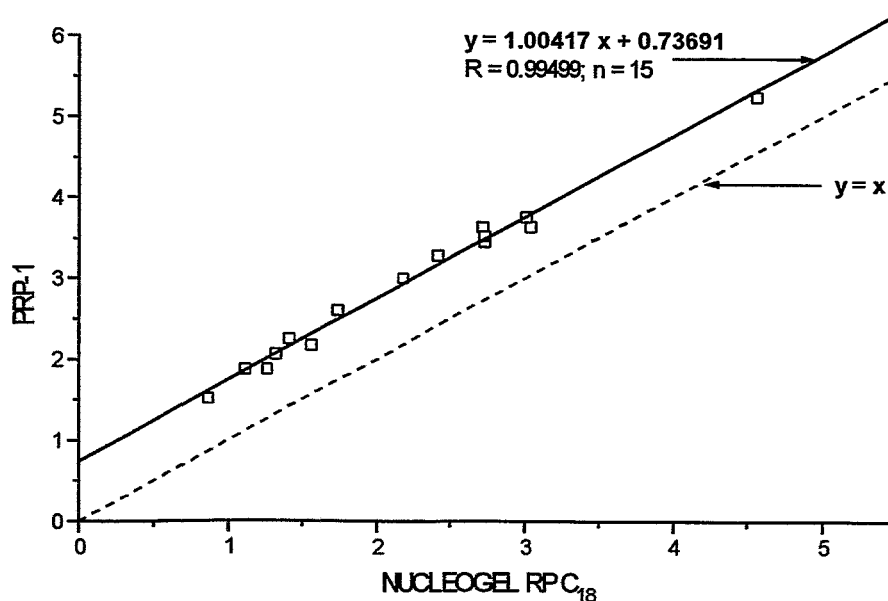


Fig. 3: Plot of log P_{HPLC} values of various rhenium complexes **1** and **2** by using both a PRP-1 and NUCLEOGEL RP C₁₈ column

Among the Re complexes with the structure form **2** only the substituted dimethyl-phenylphosphane shows a relative log P_{HPLC} value which is presumably too high by using the NUCLEOGEL RP C₁₈ column. In this example a more intensive interaction is supposed between the aliphatic column packing material and the two methyl residues linked to phosphorus.

A NUCLEOGEL RP C₁₈ column may also be used for assessment of the lipophilicity of coordination compounds. However, in this connection the restrictions concerning chelates with aliphatic ligand parts should be kept in mind. Analogous to the other columns tested, the lipophilic properties of substances are reflected by this column as relative partition coefficients. They are not expected to correlate closely with the octanol/water partition coefficients. For assessing the lipophilicity in a general way, an exclusive application of capacity factors without conversion into the apparent partition coefficients is recommended because by using the NUCLEOGEL RP C₁₈ column a linear

trend relating to the above mentioned aromatic calibration compounds is not described well. Otherwise, it should be tried to replace the aromatic compounds used until now by more aliphatic calibration compounds with known octanol/water partition coefficients.

References

- [1] Hansch C., Björkroth J. P. and Leo A.. (1987) Hydrophobicity and central nervous system agents: On the principle of minimal hydrophobicity in drug design. *J. Pharm. Sci.* **76**, 663 - 686.
- [2] Van de Waterbeemd H. and Testa B. (1987) The parametrization of lipophilicity and other structural properties in drug design. *Adv. Drug Res.* **16**, 85-225.
- [3] Berger R., Fietz T., Glaser M., Noll B. and Spies H. (1994) Octanol/water partition coefficients of some rhenium complexes. *Annual Report 1994*, Institute of Bioinorganic and Radiopharmaceutical Chemistry, FZR-73, pp. 52 - 55.
- [4] Berger R., Fietz T., Glaser M. and Spies H. (1995) Determination of partition coefficients for coordination compounds by using HPLC. *Annual Report 1995*, Institute of Bioinorganic and Radiopharmaceutical Chemistry, FZR-122, pp. 69 - 72.
- [5] Yamagami C., Yokota M. and Takao N. (1994) Hydrophobicity parameters determined by reversed-phase liquid chromatography. VIII. Hydrogen-bond effects of ester and amide groups in heteroaromatic compounds on the relationship between the capacity factor and the octanol water partition coefficient. *J. Chromatogr.* **662**, 49 - 60.
- [6] Pagliara A., Khamis E., Trinh A., Carrupt P.-A., Tsai R.-S. and Testa B. (1995) Structural properties governing retention mechanisms on RP-HPLC stationary phases used for lipophilicity measurements. *J. Liq. Chromatogr.* **18**, 1721 - 1745.
- [7] Pesek J. J. and Williamsen E. J. (1995) Comparison of novel stationary phases. In: *Retention and Selectivity in Liquid Chromatography* (R.M. Smith Ed.), *J. Chromatogr. Library* **57**, pp. 371 - 402.
- [8] Van de Waterbeemd H., Kansy, M., Wagner, B. and Fischer H. (1996) Lipophilicity measurement by reversed-phase high performance liquid chromatography (RP-HPLC). In: *Lipophilicity in Drug Action and Toxicology* (V. Pliška, B. Testa, H. van de Waterbeemd Eds.) Weinheim, pp. 73 - 87.
- [9] Fietz T. (1996) Oxorhenium(V)-Komplexe mit "3+1"-Gemischtligandkoordination, *PhD Thesis*, TU Dresden.
- [10] Glaser M. (1996) Tripodal-tetradentat/monodentat koordinierte Rheniumkomplexe mit Tris(2-thiolatoethyl)amin, *PhD Thesis*, TU Dresden.
- [11] Rudzinski W. E., Bennett D. and Garica V. (1982) Retention of ionized solutes in reversed-phase high performance liquid chromatography. *J. Liq. Chromatogr.* **5**, 1295 - 1312.
- [12] Thévenon-Emeric G., Tchaplá A. and Martin M. (1991) Role of π - π interactions in reversed-phase liquid chromatography. *J. Chromatogr.* **550**, 267 - 283.

29. Investigations into Serotonin Receptor Subtypes on the Blood-Brain Barrier

J. Wober, S. Matys, P. Brust

Introduction

Serotonin (5-HT) is a neurotransmitter involved in regulation processes of the cardiovascular, gastrointestinal, and central nervous systems, such as contraction [1] or relaxation [2] of vascular smooth muscle cells or contraction of the stomach fundus [3].

In the brain 5-HT is an mediator of important physiological processes, such as thermoregulation [4], sleep [5] or modulation of associative learning [6]. Dysfunction of the serotonergic system is involved in certain neurological and psychiatric diseases and mental abnormalities, for instance depression [7, 8], schizophrenia [9, 10], suicide [11], anxiety [12], and also Alzheimer's disease [13].

The diverse effects of 5-HT are mediated by several distinct 5-HT receptor subtypes [14, 15]. The 5-HT receptors have been classified into seven different families, from 5-HT₁ to 5-HT₇. All but the 5-HT₃ receptor are members of the superfamily of G protein-coupled receptors and transduce extracellular signals by activating GTP binding protein. Furthermore, 5-HT₁ receptors are subdivided into five subtypes, namely 5-HT_{1A}, 5-HT_{1B}, 5-HT_{1D}, 5-HT_{1E}, and 5-HT_{1F}. The 5-HT₂ receptor subclass is comprised of 5-HT_{2A}, 5-HT_{2B}, and 5-HT_{2C}. All 5-HT₁ receptors are linked to the adenylate cyclase/cAMP system, while 5-HT₂ receptors are linked to the phosphoinositide signalling system [16].

There is evidence that serotonin receptors may also exist at the BBB. The blood-brain barrier (BBB) forms an important part in brain physiology. It has three major functions: protection of the brain from the blood milieu, selective transport and metabolism or modification of blood- or brain-borne substances [13]. Neuropeptides like vasopressin and atriopeptin regulate the transport of substances through the BBB, possibly by receptor-mediated processes [17]. 5-HT may be involved in certain aspects of BBB dysfunction, like brain oedema and cerebral blood flow disturbances [18, 19]. However, the mechanism of the action of 5-HT on BBB permeability and endothelium-mediated changes of is unclear.

In this study we try to identify the type of 5-HT receptor(s) mediating the effects on the brain endothelium by different models of the BBB and various radioligands with selectivity for various 5-HT receptor subtypes.

Experimental

Preparation of rat cortex and hippocampus

Samples of the rat brain cortex and the hippocampus were homogenized in 10fold volumes of ice-cold Tris/HCl buffer (50 mM, pH 7.6) with an Ultra-Turrax T25. The homogenate was centrifuged at 20,000 g for 10 min. The resulting pellet was resuspended and centrifuged at 20,000 g for another 10 min. After repeating the same procedure, the pellet was resuspended in 10 volumes of buffer and stored at -70 °C until used in the binding studies.

Preparation of microvessels from porcine brain nucleus caudatus

Samples of the Nc. caudatus were isolated from porcine brains in a local slaughterhouse and were kept in ice-cold Tris/HCl buffer (50 mM, pH 7.4 with 120 mM NaCl and 5 mM KCl). After removing of the big blood vessels and the white matter, the tissue samples were macerated and filtrated through different nets of defined pore size (243 µm, 125 µm, 50 µm dia). The isolated microvessels were sampled in 30 ml ice-cold 0.25 M saccharose solution and washed twice in buffer (first centrifugation: 10 min, 800 g, 4 °C; second centrifugation: 10 min, 1000 g, 4 °C). The pellet was removed in 20 ml buffer and stored at -70 °C until used in the binding studies.

Preparation of choroid plexus from porcine and rat brain [method of Johnson et al., 1993 (20)]

Choroid plexus was isolated from porcine and rat brains and kept in ice-cold Tris/HCl buffer (50 mM, pH 7.4). After homogenization by sonification the homogenate was centrifuged (15 min, 40,000 g, 4 °C). The pellet was resuspended in buffer and incubated at 37 °C for 15 min. After incubation the homogenate was twice washed in buffer and stored at -70 °C until used in the binding studies.

Culture of porcine brain endothelial cells

Cryoconserved cells, isolated from porcine brain were used (21). Endothelial cells were grown on collagen-coated petri dishes in medium 199 containing 10 % FCS, 100 U/ml penicillin, 100 µg/ml streptomycin and 2.5 µg/ml amphotericin. The cells were incubated at 37 °C, with 95 % air and 5 % CO₂. On the fourth day in culture the cells formed monolayers. For experiments the cells were

removed by scraping, kept in Tris/HCl buffer of the appropriate binding assay and homogenized by short sonification.

Culture of RBE4 cells (immortalized rat brain endothelial cells)

Cells were grown on collagen-coated petri dishes in Alpha MEM/ Ham's F10 (1:1) containing 10 mM HEPES, 2 mM glutamine, 100 µl/ml gentamycin, 300 µg/ml geneticin, 10 % FCS and 10 ng/ml bFGF [22]. The cells were incubated at 37 °C, with 95 % air and 5 % CO₂. On the fourth day in culture the cells formed monolayers. For experiments the cells were removed by scraping, kept in Tris/HCl buffer of the appropriate binding assay and homogenized by short sonification.

Binding assays

The various binding assays followed the protocol outlined in Table 1. The binding assays were terminated by rapid filtration through GF/B glass fibre filters (Whatman). The filters were rapidly washed with four 4 ml portions of ice-cold buffer, transferred into 5 ml of scintillation fluid (Ultima-Gold, Packard) and analysed for radioactivity. The protein content of the membrane and cell suspensions was estimated according to the method of Lowry et al. [23].

Table 1: Protocols of the binding assays of the 5-HT_{2A}, 5-HT_{2C}, and 5-HT_{1A} receptors

Receptor	5-HT _{2A}	5-HT _{2C}	5-HT _{1A}
Ligand (conc. in displacer exp.)	[³ H]ketanserin (0.12 nM)	[³ H]mesulergin (1 nM)	[³ H]8-OH-DPAT (0.13 nM)
Unspecific binding	1 µM mianserin	10 µM mianserin	10 µM serotonin
Tris/HCl-buffer	50 mM, pH 7.6	50 mM, pH 7.4	50 mM, pH 7.4 0.1 % ascorbic acid 2 mM CaCl ₂
Duration of incub.	60 min	40 min	120 min
Incubation temp.	25 °C	25 °C	25 °C
Incubation vol.	5 ml	1 ml	5 ml
Tissue preparation	- microvessels of porcine brain nucleus caudatus - porcine brain endothelial cells - RBE4 cells - rat brain frontal cortex	- microvessels of porcine brain nucleus caudatus - porcine brain endothelial cells - RBE4 cells - rat and porcine brain choroid plexus	- microvessels of porcine brain nucleus caudatus - RBE4 cells - rat brain hippocampus
Reference	[24]	[25]	[26]

Results and Discussion

Up to now there has been no direct evidence that 5-HT_{1A} receptors are expressed on the BBB. But it is highly probable that the effects of 5-HT could be receptor-mediated processes. In this study we want to try to identify 5-HT receptors on the brain endothelium.

At present a great variety of selective agonists and antagonists of the several serotonin receptor subtypes are known. They are used in radioligand binding assays [see for review, 16]. Depending on the subtype studied, the type of radioligand had to be chosen and the tissue preparation used as standard or BBB model.

Sharma *et al.* [18] found, that 5-HT given by intravenous infusion markedly affect the cerebral circulation and the BBB permeability in rats. They established the hypothesis that 5-HT, when introduced into the circulation, binds on 5-HT₂ receptors and stimulates the prostaglandin synthesis in the cerebral vessels. These prostaglandins stimulate cAMP in the vessel causing an increased

vesicular transport in the endothelial cells resulting in extravasation of substances across the cerebral vessels. Following this hypothesis it is possible that 5-HT₂ receptor subtypes exist on the luminal side of the BBB.

From these facts and hypotheses we try to demonstrate the existence of receptors of this class on the BBB. Homogenate of porcine brain choroid plexus and homogenate of rat brain frontal cortex were used as standards for 5-HT_{2A} and 5-HT_{2C} receptors [24, 28].

Table 2 shows the results of our saturation experiments with [³H]ketanserin, a selective 5-HT₂ receptor ligand [24], on rat frontal cortex and [³H]mesulergine, a selective 5-HT_{2C} receptor ligand [25], on porcine choroid plexus. In both cases analysis of the binding data by a non-linear fitting routine (Fig. P, Biosoft, Cambridge, UK) revealed a significant fit for a model with one binding site. This is confirmed by the linear type of the Rosenthal-Scatchard plot.

Table 2. Results of the saturation analysis of the specific binding of radioligands on the 5-HT_{2A}, 5-HT_{2C} and 5-HT_{1A} receptor.

Receptor subtype	Radioligand	Brain region species	Non-linear plot		Linear plot	
			K _D [nM]	B _{max} [fmol/mg protein]	K _D [nM]	B _{max} [fmol/mg protein]
5-HT _{2A}	[³ H]ketanserin	frontal cortex rat	0.24 ± 0.03	890 ± 45	0.24 ± 0.02	891 ± 48
5-HT _{2C}	[³ H]mesulergine	choroid plexus pig	2.6 ± 0.3	306 ± 21	2.3 ± 0.4	298 ± 23
5-HT _{1A}	[³ H]8-OH-DPAT	hippocampus rat	0.32 ± 0.04	209 ± 14	0.33 ± 0.04	212 ± 15

The apparent dissociation constant K_D and the binding site density B_{max} were analysed by a non-linear fitting routine (Fig. P, Biosoft, Cambridge, UK) and by a linear Rosenthal-Scatchard plot. The binding parameters for 5-HT_{2A} and 5-HT_{2C} receptors were obtained from the plots of the single values of three experiments with ten concentrations of the radioligand. The binding parameters for the 5-HT_{1A} receptors were obtained from the plot of the single values of only one experiment with nine concentrations of the [³H]ligand.

In the frontal cortex 5-HT_{2A} receptors were found in the greatest density [29]. This receptor subtype was well characterized by radioligand binding studies, using [³H]ketanserin as the selective ligand [24, 30, 31]. The specific binding of ketanserin was measured at free [³H]ketanserin concentrations between 0.003 and 2 nM. The unspecific binding was estimated in the presence of 1 μM mianserin. The apparent dissociation constant (K_D) and the binding site density (B_{max}) of the 5-HT_{2A} of the rat frontal cortex, which we obtained by a non-linear plot, were 0.24 ± 0.03 nM and 890 ± 45 fmol/mg protein. The same binding parameters were obtained by the linear plot. The K_D values are comparable to data reported by others [24, 32]. However, the reported B_{max} values differ between 300 and 1000 fmol/mg protein [32, 24]. The values obtained by Mayeda *et al.* [32] are K_D 0.32 nM and B_{max} 10.3 pmol/g wet tissue. Leysen *et al.* [24] found a K_D of 0.42 nM and a B_{max} of 30.9 fmol/mg tissue.

But ketanserin has also an affinity to the 5-HT_{2C} receptor. The 5-HT_{2A} and the 5-HT_{2C} receptors are very similar in their structure and their pharmacological profile. [³H]mesulergine is also known to be an antagonist for the 5-HT_{2A} and 5-HT_{2C} receptors however with a higher affinity to 5-HT_{2C} than to 5-HT_{2A} [28]. It is known that only one binding site for this radioligand exists on human, rat and porcine choroid plexus, the 5-HT_{2C} receptor. The tight junctions of the choroid plexus epithelium represent the constitutive element of the blood-liquor barrier and could be used as a standard for the specific [³H]mesulergine binding on the 5-HT_{2C} receptor. For determination of the binding properties the specific binding was measured at free [³H]mesulergine concentrations between 0.05 and 6 nM. The unspecific binding was estimated in the presence of 10 μM mianserin. The K_D and B_{max} values obtained were 2.6 ± 0.3 nM and 306 ± 21 fmol/mg protein. These are also confirmed by the linear type of the Rosenthal-Scatchard plot with similar values. K_D was 2.3 ± 0.4 nM and B_{max} was 298 ± 23 fmol/mg protein. Pazos *et al.* [25] also found similar values, a K_D of 1.1 nM and a B_{max} of 300 fmol/mg protein.

In addition to 5-HT_{2A} and 5-HT_{2C} receptors we also studied 5-HT_{1A}. Two principal localizations of 5-HT_{1A} in the brain were described [27]. They are found on the cell bodies of the 5-HT neurones, in the midbrain raphe nuclei, where they function as autoreceptors to modulate the activity of these neurones, and also on postsynaptic membranes in many forebrain areas, notably in the hippocampus. The classical radioligand binding assays for 5-HT_{1A} receptors use [³H]8-OH-DPAT and homogenized preparations of cortex or hippocampus from rat, pig, or other species [33]. Other radioligands have been described for 5-HT_{1A} sites, but none has surpassed [³H]8-OH-DPAT in its overall usefulness (16). We determined the binding parameters of the specific 8-OH-DPAT binding on rat hippocampal homogenate (see Table 2). It was measured at free [³H]8-OH-DPAT concentrations between 0.05 and 1.5 nM. The unspecific binding was estimated in the presence of 10 μM serotonin. We found a K_D of 0.32 ± 0.04 nM and a B_{max} of 209 ± 14 fmol/mg protein by a non-linear plot of a one site model. The Scatchard transformation shows a linear regression. The values obtained were similar, K_D was 0.33 ± 0.04 nM and B_{max} was 212 ± 15 fmol/mg protein. It is, however, described that [³H]8-OH-DPAT labels two binding sites. On rat hippocampus Mongeau *et al.* [34] found a K_D of 0.51 ± 0.09 nM and a B_{max} of 182 ± 33 fmol/mg protein for the high-affinity binding site, and a K_D of 8.5 ± 2.4 nM and a B_{max} of 225 ± 34 fmol/mg protein for the low-affinity binding site. The second binding site was detectable because the free [³H]8-OH-DPAT concentrations used in the binding experiment were between 0.05 and 60 nM. In our experiments we used free [³H]8-OH-DPAT concentrations only up to 1.5 nM. That is to say, we determined only the high-affinity binding site representing the 5-HT_{1A} receptor [33]. The identity of the low-affinity binding site remains unknown [35]. We used the specific high-affinity [³H]8-OH-DPAT binding on rat hippocampus as the standard of the 5-HT_{1A} receptor binding under our experimental conditions.

After performing the standard binding assays we tried to determine the 5-HT receptor subtypes on the brain endothelial cells which form the BBB. We used different preparations of these cells: a) isolated microvessels from porcine brain caudate nucleus, b) cultured porcine brain endothelial cells, and c) an immortalized rat brain endothelial cell line (RBE4 cells). Isolated microvessels are still a relative complex system because the vessel preparations do not only contain endothelial cells but also some impurities of other cell types. There are astrocyte feed, pericytes, microglia and neuronal endings. Cultured endothelial cells are more homogeneous. They form monolayers and contain less than 5 % other cells. However, they already tend to dedifferentiate.

[³H]ketanserin (0.12 nM) was used for determination of 5-HT_{2A} binding sites. Total and unspecific binding to porcine brain microvessels, porcine brain endothelial cells and RBE4 cells is shown in Fig.1.

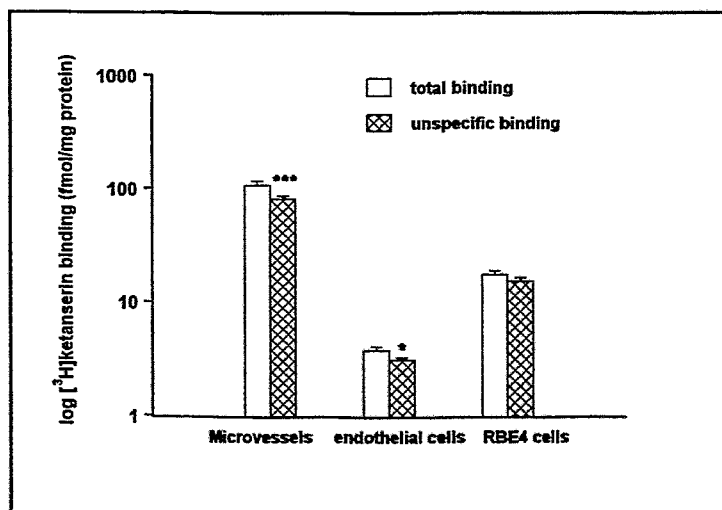


Fig. 1. [³H]ketanserin binding on porcine brain microvessels and endothelial cells and on RBE4 cells. Unspecific binding was determined with 1 μM mianserin. The [³H]ketanserin concentration was 0.12 nM. (* p < 0.05; *** p < 0.001)

The total [³H]ketanserin binding was inhibited by 1 μM mianserin, an antagonist of the 5-HT_{2A} receptor. Binding in the presence of this specific inhibitor is defined as unspecific binding. Specific binding of [³H]ketanserin, i.e. the difference between total and unspecific binding, was detectable on microvessels (27 fmol/mg protein; p < 0.001) and endothelial cells after 6 days in culture (0.6 fmol/mg protein; p < 0.05), but not on RBE4 cells.

It is known that ketanserin does not only bind on 5-HT_{2A} but also on 5-HT_{2C} receptors. The binding of mesulergine on microvessels and RBE4 cells was therefore determined because this ligand has a higher affinity to the 5-HT_{2C} than to the 5-HT_{2A} receptor. Fig. 2 shows the total and the unspecific [³H]mesulergine binding on homogenate of porcine caudate nucleus, on microvessels isolated from this brain region and on RBE4 cells, at a tracer concentration of 1 nM.

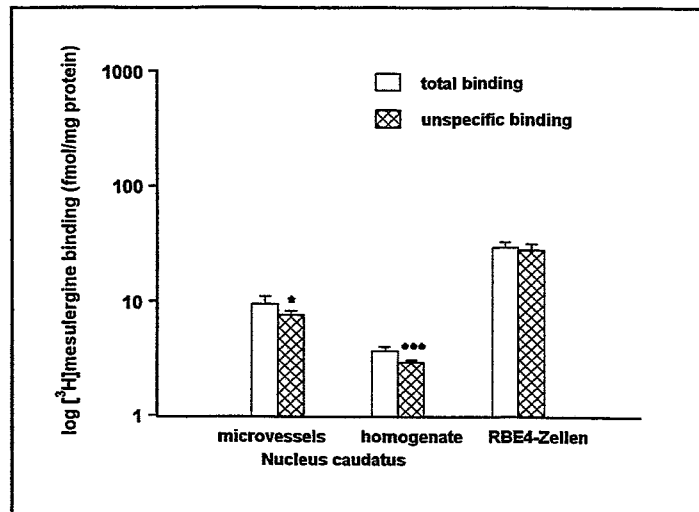


Fig. 2. [³H]mesulergine binding on microvessels and homogenate of porcine nucleus caudatus and on RBE4 cells. Unspecific binding was determined with 10 μM mianserin. The [³H]mesulergine concentration was 1 nM. (* p < 0.05; *** p < 0.001)

The unspecific binding was defined by addition of 10 μM mianserin. Specific binding of [³H]mesulergine was detectable on microvessels (1.85 fmol/mg protein; p < 0.05) and on homogenate (0.74 fmol/mg protein; p < 0.001). The increase in the specific binding on microvessels (about 2.5fold) supports the presumed endothelial localization of the receptors.

Again, no significant difference between total and unspecific binding was found on RBE4 cells, indicating that no 5-HT₂ receptors are expressed on these immortalized cells. On the other hand, specific binding of [³H]mesulergine was also determined on cultured primary endothelial cells of the porcine brain (61 ± 47 fmol/mg protein) (Fig. 3), indicating the existence of 5-HT_{2C} receptors on the BBB. The binding was about 30 times as high as on microvessels under the same experimental conditions. The reason for this discrepancy is unclear. It seems that the binding site densities estimated on microvessels and on endothelial cells using [³H]ketanserin and [³H]mesulergine as ligands are different. This could be explained by different affinity states of a 5-HT₂-like receptor on the two preparations.

To further characterize the [³H]mesulergine binding on endothelial cells, it was compared with the specific binding on the choroid plexus. In addition, 50 nM ketanserin and 20 nM serotonin were used as inhibitors. At the given concentrations these drugs were able to displace about 50 % of the specific binding of [³H]mesulergine on the choroid plexus [25]. In our study ketanserin inhibits the specific mesulergine binding on choroid plexus by 62 % (p < 0.05) and on endothelial cells by 30 %. Serotonin inhibits this binding by 80 % (p < 0.01) on plexus and by 45 % on endothelial cells (Fig. 3).

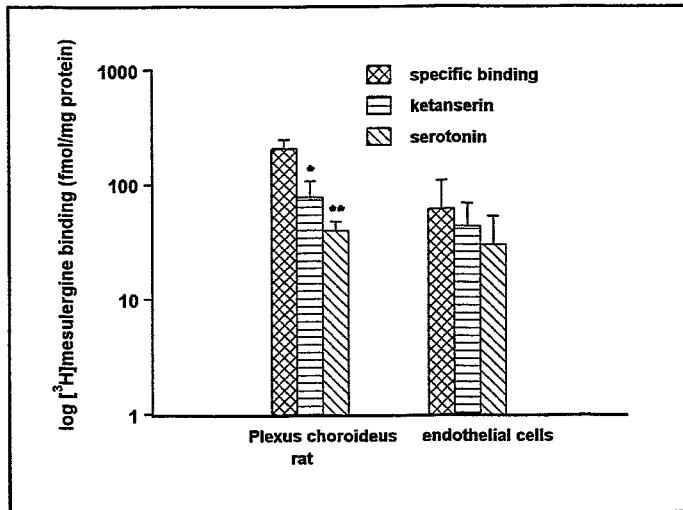


Fig. 3. Specific [^3H]mesulergine binding on rat choroid plexus and porcine endothelial cells. Unspecific binding was determined in the presence of 10 μM mianserin. The [^3H]mesulergine concentration was 1 nM. The concentrations of the displacers ketanserin and serotonin were 50 nM and 20 nM. (* $p < 0.05$; ** $p < 0.01$)

These results show that the inhibition profiles of the chosen inhibitors are similar. In both cases serotonin inhibits the mesulergine binding more than ketanserin. It is known that ketanserin has a higher affinity to 5-HT_{2A} than to 5-HT_{2C}, and serotonin has a higher affinity to the 5-HT_{2C} than to the 5-HT_{2A} receptor [16]. Therefore our data support the existence of the 5-HT_{2C} receptor subtype on porcine brain endothelial cells.

It is known that 5-HT₁-like receptors are present on the smooth muscle cells of cerebral blood vessels [16]. Considering the fact that the microvessel preparations from brain homogenate may contain some impurities deriving from these cells, we measured the total and the unspecific binding of the 5-HT_{1A} receptor ligand [^3H]8-OH-DPAT (0.13 nM) on homogenate of rat hippocampus, porcine brain microvessels and RBE4 cells (Fig. 4).

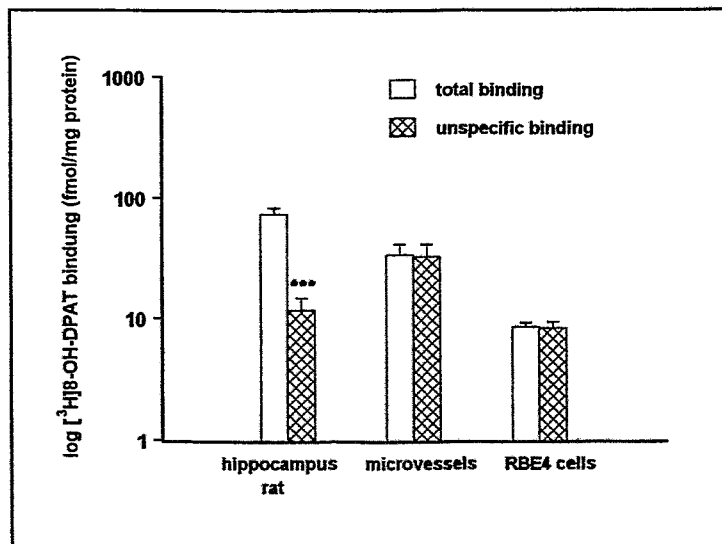


Fig. 4. [^3H]8-OH-DPAT binding on rat hippocampal homogenate, on porcine brain microvessels and on RBE4 cells. Unspecific binding was determined with 10 μM serotonin. The [^3H]8-OH-DPAT concentration was 0.13 nM. (***) $p < 0.001$)

The unspecific binding was defined by the presence of 10 μM serotonin in the binding assay. The specific binding of [^3H]8-OH-DPAT on rat hippocampal homogenate, a 5-HT_{1A} receptor-rich region, was 62 ± 10 fmol/mg protein ($p < 0.001$). No specific 5-HT_{1A} receptor binding was found on

microvessels and RBE4 cells, which indicates that no 5-HT_{1A} receptors are present on brain endothelial cells. Furthermore, we expect from these data that impurities by smooth muscle cells are low or absent in these preparations.

Summarizing, it can be said that there is clear evidence from our studies that serotonin receptors exist on the BBB. The significant [³H]ketanserin binding and [³H]mesulergine binding on isolated microvessels and cultured endothelial cells from porcine brain indicate that the receptor could belong to the 5-HT₂ subclass. A comparison of the inhibition profiles of some specific inhibitors on choroid plexus and on endothelial cells suggests that it may be the 5-HT_{2C} receptor subtype. However, the presence of 5-HT_{2A} receptors and of other subtypes of serotonin receptors, which we have not yet investigated, cannot be excluded.

The evidence of the existence of 5-HT receptors on the BBB, their localization and characterization, should make a contribution to a better understanding of the function of the BBB. It is known that 5-HT is involved in many physiological processes and neurological diseases in the brain. The effects of 5-HT could partly be mediated by 5-HT receptors on endothelial cells by activation or inhibition of second messenger systems, followed by changes in the cerebral blood flow and the permeability of the BBB. This may also be related to the function of the 5-HT_{2C} receptors on the choroid plexus where they are expected to regulate the composition and volume of the cerebrospinal fluid [36]. Knowing more about the 5-HT mediated processes on the luminal and/or abluminal side of the BBB may be of importance for a better understanding and perhaps treatment of certain brain diseases.

References

- [1] Frieden M. and Bény J.-L. (1995) Effects of 5-hydroxytryptamine on the membrane potential of endothelial and smooth muscle cells in the pig coronary artery. *Brit. J. Pharmacol.* **115**, 95 - 100.
- [2] Martin G. R., Leff P., Cambridge D. and Barrett V. J. (1987) Comparative analysis of two types of 5-hydroxytryptamine receptor mediating vasorelaxation: differential classification using tryptamines. *Naunyn-Schmiedeberg's Arch. Pharmacol.* **336**, 365 - 373.
- [3] Cohen M. L. and Fludzinski L. A. (1987) Contractile serotonergic receptor in rat stomach fundus. *J. Pharmacol. Exp. Ther.* **243**, 264 - 269.
- [4] Morishima Y. and Shibano T. (1995) Evidence that 5-HT_{2A} receptors are not involved in 5-HT-mediated thermoregulation in mice. *Pharmacol. Biochem. Behav.* **52**, 755 - 758.
- [5] Sharpley A. L., Elliott J. M., Attenburrow M.-J. and Cowen P. J. (1994) Slow wave sleep in humans: Role of 5-HT_{2A} and 5-HT_{2C} receptors. *Neuropharmacol.* **33**, 467 - 471.
- [6] Harvey J. A. (1996) Serotonergic regulation of associative learning. *Behav. Brain Res.* **73**, 47-50.
- [7] Eckert A., Gann H., Riemann D., Aldenhoff J. and Müller W. E. (1993) Elevated intracellular calcium levels after 5-HT₂ receptor stimulation in platelets of depressed patients. *Biol. Psychiatry* **34**, 565 - 568.
- [8] Stahl S. M., Hauger R. L., Rausch J. L., Fleishaker J. C. and Hubbell-Alberts E. (1993) Downregulation of serotonin receptor subtypes by nortryptiline and adinazolam in major depressive disorders: Neuroendocrine and platelet markers. *Clin. Neuropharmacol.* **16**, S19-S31.
- [9] Mita T., Hanada S., Nishino N., Kuno T., Nakai H., Yamadori T., Mizoi Y. and Tanaka C. (1986) Decreased serotonin S₂ and increased dopamine D₂ receptors in chronic schizophrenics. *Biol. Psychiatry* **21**, 1407 - 1414.
- [10] Laruelle M., Abi-Dargham A., Casanova M. F., Toti R., Weinberger D. R. and Kleinman J. E. (1993) Selective abnormalities of prefrontal serotonergic receptors in schizophrenia. *Arch. Gen. Psychiatry* **50**, 810 - 818.
- [11] McBride A. P., Brown R. P., DeMeo M., Keilp J., Mieczkowski T. and Mann J. J. (1994) The relationship of platelet 5-HT₂ receptor indices to major depressive disorder, personality traits, and suicidal behavior. *Biol. Psychiatry* **35**, 295 - 308.
- [12] Eison A. E. and Eison M. S. (1994) Serotonergic mechanisms in anxiety. *Prog. Neuropsychopharmacol. Biol. Psychiatry* **18**, 47 - 62.
- [13] Reynolds G. P., Arnold L., Rossor M. N., Iversen L. L., Mountjoy C. Q. and Roth M. (1984) Reduced binding of [³H]ketanserin to cortical 5-HT₂ receptor in senile dementia of the Alzheimer type. *Neurosci. Lett.* **44**, 47 - 51.
- [14] Hoyer D. and Schoeffter P. (1991) 5-HT receptors: subtypes and second messengers. *J. Receptor Res.* **11**, 197 - 214.
- [15] Julius D. (1991) Molecular biology of serotonin receptors. *Annu. Rev. Neurosci.* **14**, 335 - 360.
- [16] Hoyer D., Clarke D. E., Fozard J. R., Hartig P. R., Martin G. R., Mylecharane E. J., Saxena P. R., Humphrey P. P. A. (1994) VII. International Union of Pharmacology Classification of Receptors for 5-Hydroxytryptamine (Serotonin). *Pharmacol. Rev.* **46**, 157 - 203.
- [17] Ermisch A., Brust P., Kretzschmar R. and Rühle H.-J. (1993) Peptides and blood-brain barrier transport. *Physiol. Rev.* **73**, 489 - 527.

- [18] Sharma H. S., Olsson Y. and Dey P. K. (1990) Changes in blood-brain barrier and cerebral blood flow following evaluation of circulation serotonin level in anaesthetised rats. *Brain Res.* **517**, 215 - 223.
- [19] Sharma H. S., Westman J., Nyberg F., Cervos-Navarro J. and Dey P. K. (1994) Role of serotonin and prostaglandins in brain edema induced by heat stress. *Acta Neurochir. [Suppl.]* **60**, 65 - 70.
- [20] Johnson R. G., Fiorella D. and Rabin R. A. (1993) Effects of chronic cocaine administration on the serotonergic system in the rat brain. *Pharmacol. Biochem. Behav.* **46**, 289 - 293.
- [21] Mischek U., Meyer J. and Galla H. J. (1989) Characterisation of γ -glutamyl transpeptidase activity of cultured endothelial cells from porcine brain capillaries. *Cell. Tiss. Res.* **256**, 221 - 226.
- [22] Roux F., Durieu-Trautmann O., Chaverot N., Claire M., Mailly P., Bourre J. M., Strosberg A. D. and Couraud P. O. (1994) Regulation of γ -glutamyl transpeptidase and alkaline phosphatase activities in immortalised rat brain microvessel endothelial cells. *J. Cell. Physiol.* **159**, 101 - 113.
- [23] Lowry O. H., Rosebrough N. J., Farr A. L. and Randall R. J. (1951) Protein measurement with the Folin phenol reagent. *J. Biol. Chem.* **193**, 265 - 275.
- [24] Leysen J. E., Niemegeers C. J. E., Van Nueten J. M. and Laduron P. M. (1982) [3 H]ketanserin (R41468), a selective ligand for serotonin₂ receptor binding sites. Binding properties, brain distribution, and functional role. *Molec. Pharmacol.* **21**, 301 - 314.
- [25] Pazos A., Hoyer D. and Palacios J. M. (1985) The binding of serotonergic ligands to the porcine choroid plexus: characterisation of a new type of serotonin recognition site. *Eur. J. Pharmacol.* **106**, 539 - 546.
- [26] Hjorth S., Carlsson A., Lindberg P., Sanchez D., Wikström H., Arvidson L. E., Hacksell U. and Nilsson J. L. G. (1982) 8-Hydroxy-2-(di-n-propylamino)tetralin, 8-OH-DPAT, a potent and selective simplified ergot congener with central 5-HT receptor stimulating activity. *J. Neural. Transm.* **55**, 169 ff.
- [27] Bachy A., Steinberg R., Santucci V., Fournier M., Landi M., Hamon M., Manara L., Keane P. E., Soubrié P. and Le Fur G. (1993) Biochemical and electrophysiological properties of SR 57746A, a new, potent 5-HT_{1A} receptor agonist. *Fundam. Clin. Pharmacol.* **7**, 487 - 497.
- [28] Yagaloff K. A., Lozano G., Van Dyke T., Levine A. J. and Hartig P. R. (1986) Serotonin 5-HT_{1C} receptors are expressed at high density on choroid plexus tumours from transgenic mice. *Brain Res.* **385**, 389 - 394.
- [29] Laduron P. M., Janssen P. F. M. and Leysen J. E. (1982) *In vivo* binding of [3 H]ketanserin on serotonin S₂-receptors in rat brain. *Eur. J. Pharmacol.* **81**, 43 - 48.
- [30] Leysen J. E., Gommeren W. and Janssen P. A. J. (1991) Identification of non-serotonergic [3 H]ketanserin binding sites on the human platelets and their role in serotonin release. *Eur. J. Pharmacol. - Molec. Pharmacol. Section* **206**, 39 - 45.
- [31] Herndon J. L., Ismaiel A., Ingher S. P., Teitler M. and Glennon R. A. (1992) Ketanserin analogues: structure-affinity relationships for 5-HT₂ and 5-HT_{1C} serotonin receptor binding. *J. Med. Chem.* **35**, 4903 - 4910.
- [32] Mayeda A. R., Simon J. R., Hingtgen J. N., Hofstetter J. R. and Aprison M. H. (1989) Activity-wheel stress and serotonergic hypersensitivity in rats. *Pharmacol. Biochem. Behav.* **33**, 349 - 353.
- [33] Nénonéné E. K., Radja F., Carli M., Grondin L. and Reader T. A. (1994) Heterogeneity of cortical and hippocampal 5-HT_{1A} receptors: A reappraisal of homogenate binding with 8-[3 H]hydroxy-dipropylaminotetralin. *J. Neurochem.* **62**, 1822 - 1834.
- [34] Mongeau R., Weiner, S. A., Quirion R. and Suranyi-Cadotte B. E. (1992) Further evidence for differential affinity states of the serotonin_{1A} receptor in rat hippocampus. *Brain Res.* **590**, 229 - 238.
- [35] Nénonéné E. K., Radja F., Carli M., van Gelder N. M., Afkhami-Dastjerdian and Reader T. A. (1996) Alkylation of [3 H]8-OH-DPAT binding sites in rat cerebral cortex and hippocampus. *Neurochem. Res.* **21**, 167 - 176.
- [36] Catalán R. E., Martínez A. M., Aragonés M. D., Hernández F. and Díaz G. (1996) Endothelin stimulates protein phosphorylation in blood-brain barrier. *Biochem. Biophys. Res. Commun.* **219**, 366 - 369.

30. Comparison of a Microplate Assay with Conventional Binding Assay for the Screening of the Potential Receptor Ligands

J. Wober, P. Brust

Introduction

In the search of potential receptor-binding ligands the parameters, such as IC_{50} or K_i value, are conventionally used for selection [1, 2]. These parameters are usually determined with filtration manifolds combined with an analysis of the radioactive samples by conventional liquid scintillation counting (LSC). Recently it became possible to increase the efficiency of binding experiments by the use of a combination of a microplate cell harvester with a microplate scintillation counter (MSC), which allowed the analysis of the radioactive samples on microfilter plates to take place in a shorter time.

For evaluation of the potential receptor ligands the binding parameters obtained by both methods need to be comparable. Such a comparison of the two methods had not yet been performed. The inhibition of the binding of the specific 5-HT₂ receptor ligand [³H]ketanserin to homogenate of rat brain cortex by a potential serotonin (5-HT) receptor-binding ligand is used as an example. It will be demonstrated that the K_i values obtained by both methods are similar.

Experimental

Preparation of rat brain cortex

Samples of the rat brain cortex were homogenized in 10fold volumes of ice-cold Tris/HCl buffer (50 mM, pH 7.6) with an Ultra-Turrax T 25. The homogenate was centrifuged at 20,000 g for 10 min. The resulting pellet was resuspended and centrifuged at 20,000 g for another 10 min. After repeating the same procedure the pellet was resuspended in 10 volumes of buffer and stored at -70 °C until used in the binding studies.

Binding assay using a 30-port cell harvester combined with a conventional liquid scintillation counter (LSC) (conventional assay)

The incubation test contains 0.12 nM [³H]ketanserin, homogenate of membrane preparation (0.012 - 0.02 mg/ml protein), various concentrations of the displacer in Tris/HCl buffer (50 mM, pH 7.6) in a final volume of 5 ml. The unspecific binding was defined in the presence of 1 μM mianserin. A 30-port cell harvester (from Brandel) contains places for 30 single samples. Three samples were used to define the unspecific binding and three samples for each of seven concentrations of displacers and for noninhibited binding. The samples were incubated at 25 °C for 60 min in 8 ml test tubes. The GF/B glass fibre filter (Whatman) was incubated in 0.3 % polyethylene imine for 90 min before use. The binding assays were terminated by rapid filtration through this filter at 4 °C. The filter was rapidly washed with four 4 mL portions of ice-cold buffer, transferred into 5 ml scintillation fluid (Ultima-Gold, Packard) and analysed for radioactivity in a conventional LSC (Tricarb; Packard Instrument Company). Aliquots of incubation fluid were also measured in scintillation fluid for determination of the real concentration of [³H]ketanserin in the incubation tests. The protein content of the membrane suspension was estimated according to the method of Lowry *et al.* [3].

Binding assay using a microplate cell harvester combined with a microplate scintillation counter (MSC) (microplate assay)

The incubation test contains 0.36 nM [³H]ketanserin, homogenate of the membrane preparation (0.03-0.04 mg/mL protein, estimated according to the method of Lowry *et al.* [3]), various concentrations of the displacer in tris/HCl buffer (50 mM, pH 7.6) in a final volume of 1 ml. The unspecific binding was defined in the presence of 1 μM mianserin. A microplate cell harvester (Packard Instrument Company) has plates for 96 single samples. Thus 8 wells each were used to determine the unspecific and the noninhibited binding, and 4 wells for each of 18 concentrations of displacers. Eight places were reserved for standards (2 wells each for 4 radioligand concentrations with the same protein content as in the samples). The samples were incubated at 25 °C for 60 min in 1.5 ml-microtest tubes. The GF/B glass fibre filter plate (UniFilter, Packard) was incubated in 0.3 % polyethylene imine for 90 min before using. The binding assays were terminated by rapid filtration through this filter at 4 °C. The filter was washed rapidly with 400 ml ice-cold buffer. After drying, 50 μl scintillation fluid (Ultima-Gold, Packard) were added to each filter well and the plate was analysed for radioactivity by a microplate scintillation counter (Packard Instrument Company). Aliquots of incubation fluid and the standards were measured as well in 96-well plates in 200 μl of scintillation fluid to determine of the real concentration of [³H]ketanserin in the incubation tests.

Aliquots of the standards were also counted in 4 ml of scintillation fluid in a conventional LSC (Tricarb; Packard Instrument Company) to prepare a standard curve for converting cpm into dpm. Fig. 1 (A) shows that both relationships between the radioactivity concentration and the measured cpm values (MSC), on the one hand, and the measured dpm values (LSC), on the other, are described by linear regression. It is shown in Fig. 1 (B) that the relationship between the measured cpm and dpm is also described by linear regression. The dpm values necessary for quantitative evaluation are calculated from such a calibration curve for each filter plate.

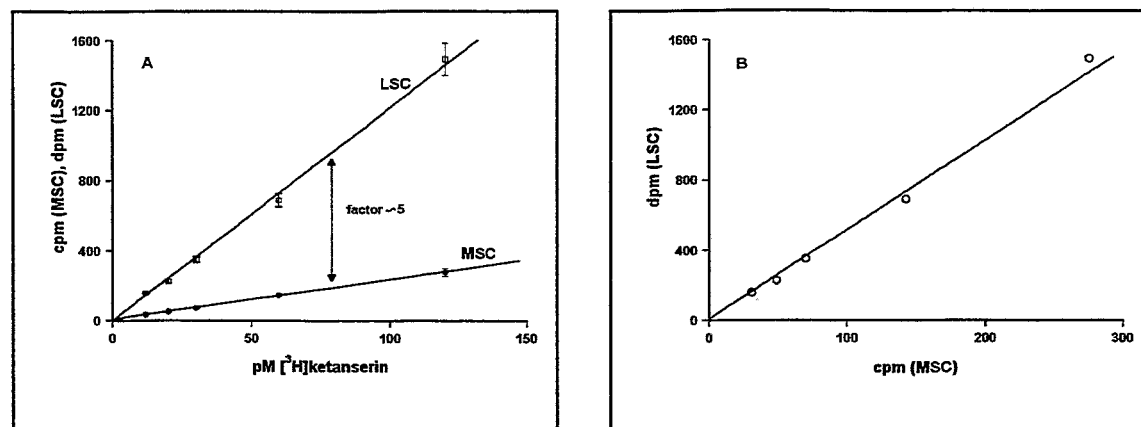


Fig. 1. Relationship of (A) measured cpm (circles) by Microplate Scintillation Counter (MSC) and dpm (squares) by conventional Liquid Scintillation Counter (LSC) at various concentrations of [³H]ketanserin and (B) between the measured cpm and dpm values. Aliquots of incubation fluid were measured in the same scintillation fluid. All points are means \pm SD, $n = 16$.

The total binding of [³H]ketanserin on homogenate of porcine *Nc. caudatus* was measured at various protein contents (0.02 - 0.18 mg/mL) and various radioligand concentrations (0.03 - 0.36 nM). As expected, in both cases the binding was increased with increasing protein content or [³H]ketanserin concentration, described by linear regression (data not shown). This applies to all of binding assays of which the experimental conditions will also be ranged in these linear areas.

Results and Discussion

In the search for potential receptor-binding compounds the equilibrium inhibition constant (K_i) is one of the parameters that will be used for selection. The K_i value indicates the molar concentration of the compound, which inhibits 50 % of the specific binding of the common radioligand, irrespective of the radioligand concentration in the incubation assay. In displacement experiments IC_{50} values of various compounds are obtained. The IC_{50} value represents the molar concentration of the tested compound, which under the particular experimental conditions can displace 50 % of the radioligand binding. The relation between IC_{50} and the K_i value is described by the following equation: $K_i = [IC_{50}]/[1 + C/K_D]$, with C the concentration and K_D the equilibrium dissociation constant of the radiolabelled ligand [4].

It is necessary to use a highly efficient screening method to select the potential receptor-binding compounds and determine their binding parameters. Up to now it has been usual to use filtration manifolds for 24, 30, or 40 samples [5 - 7] (conventional method). The radioactivity was counted in conventional LSC. Recently a microplate assay has been developed based on a cell harvester combined with a microplate scintillation counter (MSC). The new equipment allows more binding experiments to be carried out in minimized incubation volumes in a shorter time. The aim of the present study is to find out whether the same K_i will be obtained by both methods. The displacement of the specific [³H]ketanserin binding on rat brain cortex by a potential receptor-binding ligand is shown as an example.

In order to estimate K_i values, the K_D value of the radioligand has to be known (see above). It is obtained by saturation experiments. The specific [³H]ketanserin binding, the difference between the total and the unspecific binding, was estimated on rat brain cortex by various [³H]ketanserin concentrations ranging from 0.003 to 2 nM. The unspecific binding was determined by inhibition of the total binding with 1 μ M mianserin. The saturation curves and the Rosenthal-Scatchard plots, obtained by evaluation of the two methods, are shown in Fig. 2. The single values of all experiments were plotted in one curve.

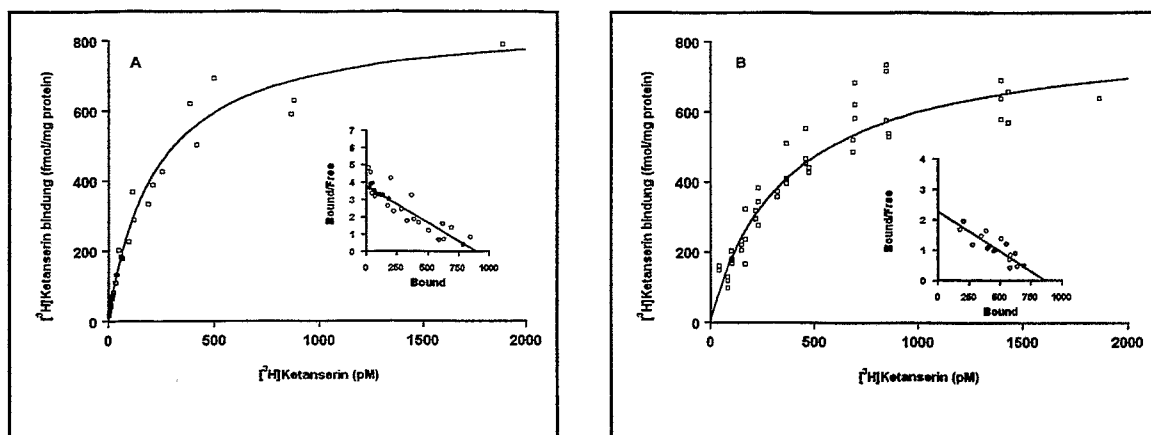


Fig. 2: Saturation curves and Rosenthal-Scatchard plots of specific [³H]ketanserin binding on rat brain cortex taken by (A) conventional assay and (B) microplate assay. Unspecific binding was determined with 1 μM mianserin. [³H]ketanserin concentration was between 0.003 and 2 nM. Single values of all experiments are shown. By conventional assay we found $K_D = 0.23 \pm 0.02$ nM and $B_{max} = 860 \pm 45$ fmol/mg protein and by microplate assay $K_D = 0.38 \pm 0.04$ nM and $B_{max} = 830 \pm 45$ fmol/mg protein.

The maximum number of binding sites B_{max} estimated by both methods is similar (conventional assay: $B_{max} = 860 \pm 45$ fmol/mg protein; microplate assay: $B_{max} = 830 \pm 45$ fmol/mg protein). However, the K_D values are slightly higher for the microplate assay (conventional assay: $K_D = 0.23 \pm 0.02$ nM; microplate assay: $K_D = 0.38 \pm 0.04$ nM). The Scatchard plots of the binding curves confirm these data (conventional assay: $K_D = 0.24$ nM; $B_{max} = 890$ fmol/mg protein; microplate assay: $K_D = 0.38$ nM; $B_{max} = 860$ fmol/mg protein). This difference between the K_D values is not significant, as shown by student's t-test.

The K_D values were used to calculate K_i values from the IC_{50} values of a potential serotonin receptor ligand (Table 1).

Table 1. Comparison of the binding parameters of [³H]ketanserin and a potential serotonin receptor ligand, using the conventional assay and the microplate assay

	Conventional assay	Microplate assay
Inhibition constant (IC_{50})	5.2 ± 0.9 nM	7.2 ± 0.6 nM
Equilibrium inhibition constant (K_i)	3.1 nM	3.4 nM
Equilibrium dissociation constant (K_D)	0.23 nM	0.38 nM
[³ H]Ligand concentration (C)	0.155 nM	0.418 nM
Number of single values (n)	3	4

As expected, the IC_{50} values are different because of the different [³H]ketanserin concentrations in the binding assays. The concentration of the [³H]ligand had to be increased 3fold in the microplate assay on account of the lower counting efficiency. The protein content was also raised by a factor of 3. Most important, the K_i values obtained by both methods are the same, allowing the comparison of binding data obtained with both methods.

The advantages of the new method are a higher time efficiency, a decrease in the consumption of chemicals, such as buffer, washing agents, radioligand, scintillation fluid, and also biological material. It follows that the amount of radioactive waste also decreases.

A disadvantage of the microplate assay is that the measured results obtained by MSC are given in cpm. This means that a standard curve has to be plotted for each filter plate in order to convert cpm into dpm for the following quantitative evaluation.

Summarizing, it can be said the microplate assay represents a new application method for carrying out binding experiments which produce more results in a shorter time. It is possible to compare the newly

obtained data with the former results by use of K_i values. The saving of materials and time and the avoidance of waste is not only an important economic aspect in scientific work but also an ecological one in view of the world around us.

References

- [1] Fukami T., Yamakawa T., Niiyama K., Kojima H., Amano Y., Kanda F., Ozaki S., Fukuroda T., Ihara M., Yano M. and Ishikawa K. (1996) Synthesis and structure relationships of 2-substituted D-tryptophan-containing peptidic endothelin receptor antagonists: Importance of the C-2 substituent of the D-tryptophan residue for endothelin A and B subtype selectivity. *J. Med. Chem.* **39**, 2313 - 2330.
- [2] Sonnesson C. and Boije M. (1993) Orally active central dopamine and serotonin receptor ligands: 5-, 6-, 7-, and 8-[[trifluoromethylsulphonyl]oxy]-2-(di-n-propylamino)tetralins and the formation of active metabolites *in vivo*. *J. Med. Chem.* **36**, 3409 - 3416.
- [3] Lowry O. H., Rosebrough N. J., Farr A. L. and Randall R. J. (1951) Protein measurement with the Folin phenol reagent. *J. Biol. Chem.* **193**, 265 - 275.
- [4] Cheng, Y.-C. and Prusoff, W. H. (1973) Relationship between the inhibition constant (K_i) and the concentration of inhibitor which causes 50 per cent inhibition (I_{50}) of an enzymatic reaction. *Biochem. Pharmacol.* **22**, 3099 - 3108.
- [5] Sprouse J. S., McCarty D. R. and Dudley M. W. (1993) Apparent regional differences in 5-HT_{1A} binding may reflect [³H]8-OH-DPAT labelling of serotonin uptake sites. *Brain Res.* **617**, 159 - 162.
- [6] Brust P., Bergmann R. and Johannsen B. (1996) High-affinity binding of [³H]paroxetine to caudate nucleus and microvessels from porcine brain. *NeuroReport* **7**, 1405 - 1408.
- [7] Leysen J. E., Gommeren W. and Janssen, P. A. J. (1991) Identification of non-serotonergic [³H]ketanserin binding sites on human platelets and their role in serotonin release. *Eur. J. Pharmacol. - Molec. Pharmacol. Sect.* **206**, 39 - 45.

31. Functional Expression of P-Glycoprotein in an Immortalized Rat Brain Endothelial Cell Line (RBE4) *in vitro*

R. Bergmann, S. Matys, P. Brust

Introduction

In a previous study we used the reverse transcription-polymerase chain reaction (RT-PCR) to examine an immortalized brain endothelial cell line (RBE4) [1] for expression of transport systems that may be important as conduits for drug delivery to the brain. We demonstrate that the RBE4 cell line [2] offers an *in vitro* system where the genes of multidrug resistance (mdr1a and mdr1b) are expressed. This gene family encodes an ~170 kDa integral membrane protein, the P-glycoprotein (PGP). A member of the ATP-binding cassette (ABC) transporter family, PGP is expressed in the plasma membrane and appears to function as an energy-dependent efflux pump for a broad spectrum of natural and synthetic drugs. RBE4 cells may therefore be regarded as an *in vitro* alternative for studying drug transport across the blood-brain barrier (BBB) [3]. This is of particular interest for our institute's attempts to design diagnostic ^{99m}Tc radiopharmaceuticals for functional imaging of the brain [4]. The uptake into the brain of such radioactive molecules requires that these compounds are transported through the brain capillary endothelial wall, which makes up the blood-brain barrier *in vivo*. However, the function of the PGP may restrict the blood-brain transfer. The functional expression and the specific inhibition of the PGP in RBE4 cells is therefore studied in the present paper. Using a multilabel tracer approach, we demonstrate that the inhibition of this transporter does not influence basic metabolic parameters of the cells. Such conditions are important for the future evaluation of new drugs with perhaps unknown cytotoxic properties.

Experimental

Reagents

L-glutamine, basic fibroblast growth factor (bFGF), rat tail collagen were from Boehringer Mannheim GmbH (Germany) and media were obtained from GIBCO-BRL Life Technologies. 24-well cell culture plates were from (Sarstedt). Fetal calf serum, sodium ortho-vanadate, dinitrophenol (DNP) and 2-deoxy-D-glucose were obtained from (Sigma, Deisenhofen, Germany). Stock solutions of verapamil,

vinblastine, colchicine (Sigma, Deisenhofen, Germany) were prepared with dimethyl sulphoxide (DMSO).

Tracers and radioactivity measurements

Various tracers with different isotopic labels were used for the studies. [³H]vinblastine (670 GBq/mmol) as PGP substrate [5], [³H]leucine (5.77 TBq/mmol) as a measure of the function of the L-type amino acid transporter and the protein synthesis [6], [³H]thymidine (962 GBq/mmol) as tracer of the DNA synthesis [7, 8] were purchased from Amersham. [³H]colchicine (2.73 TBq/mmol) from DuPont de Nemours (Germany) GmbH was used as PGP substrate [9]. [¹⁸F]fluoride labels the OH and Cl⁻ space. 2-[¹⁸F]fluoro-2-deoxy-D-glucose is transported into the cells via the glucose transport protein (GLUT). Then it can be phosphorylated by hexokinase(s). The 2-[¹⁸F]fluoro-2-deoxy-D-glucose-6-phosphate, however, is thought to be trapped intracellularly because it is a poor substrate for further metabolism. It cannot be converted to fructose-6-phosphate and degraded to CO₂ and H₂O, and it has low affinity to GLUT [10, 11]. The [¹⁸F]labelled tracers were prepared in the Rossendorf PET-centre [12]. The actual concentrations of the [¹⁸F]-labelled compounds were calculated from the absolute amount of tracer activity used and from the specific activities given by the manufacturers and were lower than 10 nM in the tests. [^{99m}Tc]sestamibi (Cardiolite, Du Pont Pharma GmbH, Germany), as a PGP substrate [13], and [^{99m}Tc]DTPA (ROTOP, VKTA Rossendorf, Germany) an extracellular tracer without any noticeable protein binding [14] were prepared from commercial kits according to the manufacturer's instructions and added to cell growth medium with a final concentration of 10 MBq/ml. Knowledge of the elution history of the ⁹⁹Mo/^{99m}Tc generator and of the activity of stock solutions than made it possible to use generator equilibrium equations to calculate the absolute concentration of total ^{99m}Tc in the incubation medium (<10 nM in all experiments) [15, 16, 17]. All samples were assayed for gamma activity in a multichannel well-type sodium iodine gamma counter (COBRA II, Packard). After a minimum of 10 half-lives of the short living isotopes used (¹⁸F, ^{99m}Tc) the count vials were assayed in a multichannel well-type beta counter (TRICARB, Packard) to determine the contents of ³H and ⁹⁹Tc in the samples. The results are expressed as an accumulation ratio calculated by dividing the total specific cell uptake, after subtracting the nonspecific binding (NSB), by the total radioactivity (supernatant and solubilized cells) per mg cell protein (%D/mg protein). The radioactivity recovery was calculated using appropriate incubation medium standards for control. The relation of the tracer content normalized to the protein mass in the test samples to that in the control samples, expressed as a percentage, was calculated to compare the influence of various drugs on the tracer accumulation in the cells. The remaining of supernatant liquid in the solubilized cells was assayed with [^{99m}Tc]DTPA. It was found to contribute <0.4 µl supernatant/well at a mean value of 80 µg cell protein/well. As a check on the specificity of drug accumulation under the conditions, control experiments were performed with [¹⁸F]fluoride or [^{99m}Tc]DTPA as additional labelled substances.

Cell culture

The RBE4 cells were a gift from F. Roux. The cells were seeded in a density of 10³ - 10⁴ cells/cm², either (a) in 24-well plates coated with either rat type 1 collagen or (b) in 24-well Cell⁺ plates ®. The cells were grown in culture medium consisting of a α-minimal essential medium (α-MEM)/Ham's : F10 (1:1 vol/vol), supplemented with 2 mM glutamine, 10 % heat-inactivated fetal calf serum, 1 ng/ml of basic fibroblast growth factor (bFGF), and 300 µg/ml of geneticin (G418) in humidified 5 % CO₂/95 % air at 37 °C. In the multiwell plates the cells reached confluence after 3 - 4 days. The accumulation studies with radioactively labelled compounds were conducted at cell densities between 10⁵ - 10⁶ cells per well (10⁶ cells were equivalent to 130 µg protein).

Drug uptake studies

In the common procedure tracer uptake and retention experiments were initiated by incubation of the confluent cells in 24-well plates with the complete growth medium supplemented by the appropriate tracers and modulators. This incubation was conducted at 37 °C in a 5 % CO₂/95 % air atmosphere or at 4 °C in a normal atmosphere. In previous experiments that were performed without equilibration of the cells with verapamil, a lag time of five minutes of the verapamil-induced enhanced tracer accumulation was detected. Hence, the experiments were started with a period of 60 min preincubation of the samples in growth medium with added test substances. In the experiments the appropriate amount of DMSO was added to the control samples, not exceeding 1 % (v/v) of the volume. Immediately after preincubation, the solution was aspirated from the wells and replaced by

0.5 ml per well of the incubation medium to initiate transport. The media contained up to three tracers (details are given in the figure and table legends) labelled with different isotopes (^{99m}Tc , ^{18}F , ^3H) and various drugs in concentrations ranging between 1 nM and 10 mM. At the end of incubation the well plates were transferred onto a cooling plate (4 °C). 100 μl of the medium from each well was used to assess the free tracer concentration in the supernatant. The remaining medium was then aspirated and the cells were carefully rinsed four times with 1 ml of ice-cold (4 °C) isotope-free phosphate buffered solution containing Mg^{++} (0.5 mM) and Ca^{++} (0.9 mM) for 8 s each column to clear the extracellular spaces. The remaining cells were solubilized with modified 500 μl Lowry reagent (see protein determination) during shaking of the plates for 30 min. Afterwards 350 μl aliquots were transferred into 4 ml scintillation cocktail (Ultima Gold, Packard) in PONY vials (Packard). Aliquots of the loading buffers and stock solutions were obtained for normalizing the cellular counts to the extracellular concentration of the studied tracers. Additional plates were incubated at 4 °C to determine the non-specific binding and accumulation (NSB) of the tracers in the cells. All data points were determined in quadruplicate from preparations obtained from the same culture. Statistical evaluation of the data was performed by Student's *t* test. Values of $p \leq 0.05$ were considered significant.

Protein determination

Aliquots of the solubilized cells were used to assay the protein by the method of Lowry et al. [18] (Protein determination Kit, SIGMA DIAGNOSTICS, Procedure No. P5656), using bovine serum albumin as the standard. The method was slightly modified to measure the samples in a 96-well plate. 50 μl of solubilized cells per sample were pipetted twice into the 96-well plate. 150 μl Lowry reagent was added and the plate was shaken for 10 min. Then 70 μl of Folin reagent was added to each well and the plate was again shaken for 20 min. Now the plate was measured using a microplate reader AT II (Anthos) at 605 nm. The calibration curve was fitted from 20 μg protein/ml up to 400 μg protein/ml and was used for protein mass determination in the samples.

Results and Discussion

The aim of the present paper is to study the functional expression of PGP at RBE4 cells and to demonstrate that the inhibition of this transporter does not influence basic metabolic parameters of the cells. In future experiments with various newly synthesized drugs we intend to study the cell transmembrane transport and the interactions of these drugs with the PGP. The unchanged cell metabolism is a prerequisite of such studies and should be used as a criterion for the selectivity of drug PGP interactions. This is expected to be important because cytotoxic effects of the drugs cannot be excluded at concentrations between 1 μM and 1 mM, which are normally involved in these studies. The PGP activity is proportional to the measured difference between the accumulation of a PGP substrate in the cells in the control experiment and the substrate amount in the cells by inhibition of the PGP. This is only true if the influx of the substrate used remains constant under both conditions. PGP has a broad substrate specificity. Drugs which may serve as substrates for the PGP include the antitumour alkaloids vinblastine, colchicine, and also the lipophilic organotechnetium cation [^{99m}Tc]sestamibi [19, 20, 21]. We used these substances to characterize the PGP function in the RBE4 cells. Fig. 1 shows the time dependency of the accumulation of [^3H]vinblastine, [^3H]colchicine and [^{99m}Tc]sestamibi, which occurs after inhibition of PGP with verapamil. A plateau was reached after about 60 min as had been previously shown with various tumour cell lines [22]. The development of plateau accumulation in the continued presence of extracellular [^{99m}Tc]sestamibi implied that a steady state or equilibrium condition had been achieved. This includes the possibility of saturation of the investigated system with the PGP substrates [23]. Therefore the incubation time of 60 min was chosen for further experiments.

Accumulation of PGP substrates in RBE4 cells

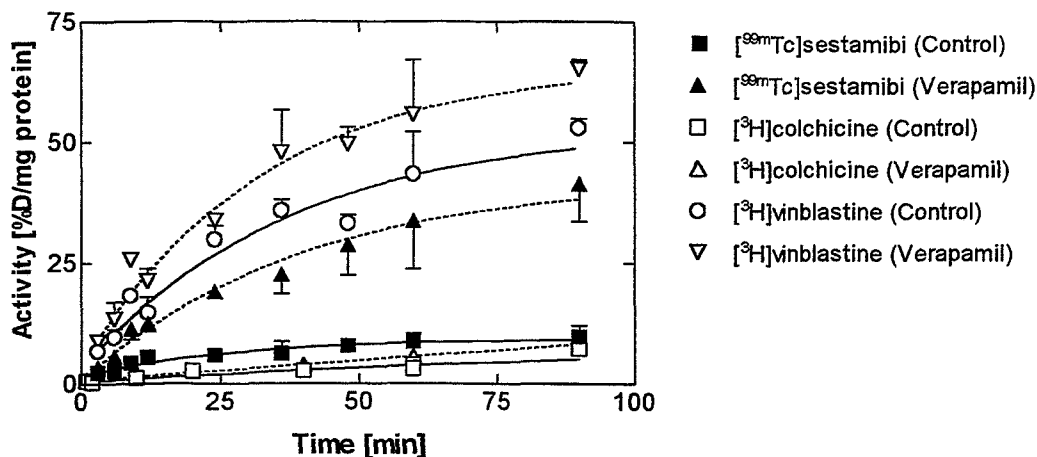


Fig. 1: Kinetics of [^{99m}Tc]sestamibi, [³H]vinblastine and [³H]colchicine accumulation in RBE4 cells. Cells were incubated in medium for various times in the absence of a drug (control) or in the presence of verapamil (10 μM). Each point represents the mean value of 4 determinations; bars represent ±SD.

The contribution of the extracellular radioactivity to the total accumulated activity of [^{99m}Tc]sestamibi was estimated from experiments with [^{99m}Tc]DTPA, a tracer with negligible protein binding known to be excluded from uptake by various cell types during short periods [24]. The recovery of the [^{99m}Tc]DTPA from the solubilized cells and supernatant normalized to the initial activity of each sample was 95.3 ± 5.0 % of the initial activity. The accumulation of [^{99m}Tc]DTPA was unchanged by inhibition of the PGP (the results with the highest inhibitor concentrations are shown in

Table 1). At a cell number of 6·10⁶ per well an extracellular volume of 0.07 μl was calculated. However, the remaining [^{99m}Tc]DTPA in the cell fraction was temperature dependent and 4.5 times lower at 4 °C.

Table 1: Extracellular volumes of [^{99m}Tc]DTPA in %D/mg protein determined by the common incubation procedure (60 min) at 37 °C and 4 °C. Each point represents the mean value of 4 determinations ± SD

	μM	37 °C		4 °C	
Control	0	0.226	0.038	0.050 ±	0.060
Verapamil	50	0.200 ±	0.059	0.079 ±	0.125
Colchicine	50	0.298 ±	0.141	0.042 ±	0.033
Vinblastine	50	0.199 ±	0.047	0.055 ±	0.088

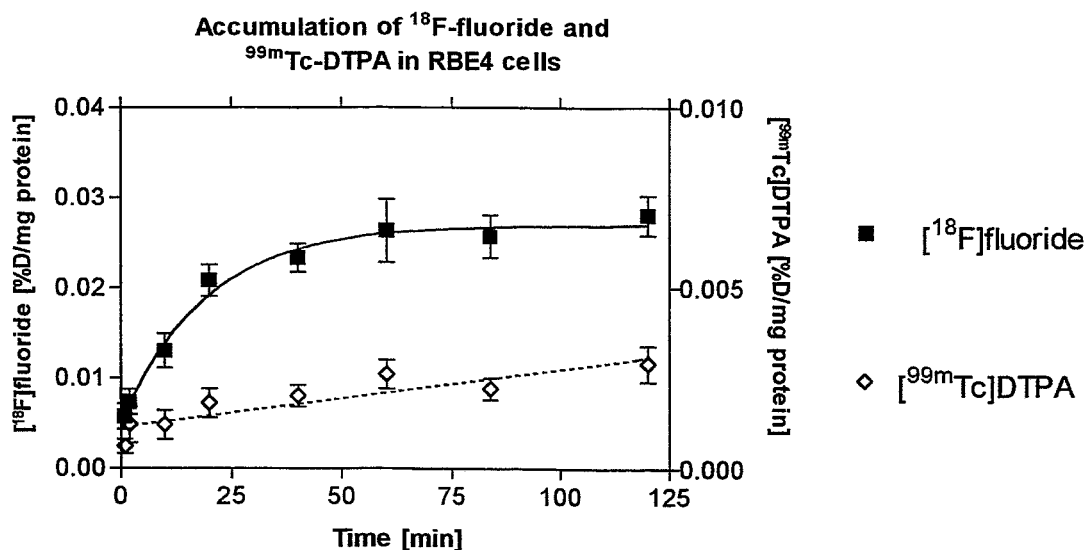


Fig. 2: Kinetics of $^{99\text{m}}\text{Tc}$ DTPA and ^{18}F fluoride accumulation in the cell fraction. Each point represents the mean value of 12 determinations; bars represent \pm SD; the linear regression results \pm SEM and the dotted lines are the 95 % confidence intervals.

But the linear time dependence of the $^{99\text{m}}\text{Tc}$ DTPA accumulation ($p < 0.01$). Fig. 2 may serve as an indicator of nonspecific binding and transport (e.g. vesicular transport) processes. Despite these considerations the following uptake data were calculated as the difference in tracer accumulation between 37 °C and 4 °C volume and normalized to the total radioactivity and to the protein amount, expressed as %D/mg protein, without correction for the extracellular compartment in each experiment.

Changes in cell volume may also result in unspecific changes in tracer uptake. Cell swelling is accompanied by an increased permeability for chloride [25, 26] thereby increasing the chloride space which represents a measure of the total extracellular space under normal conditions. Fluoride resembles OH^- and Cl^- in various physicochemical properties (Stokes radii, Pauling's crystal radii, binding orders to the carboxypeptidase or carbonic anhydrase) and may therefore imitate hydroxyl ions and chloride in biological systems. Bromide has been able to replace chloride in the measurement of chloride-dependent potassium transport [27]. We therefore used ^{18}F fluoride to check whether there are changes in cell volume during inhibition of PGP. The fluoride space (apparent cell volume) after 60 min of incubation was $0.97 \pm 0.042 \mu\text{l}$ (mean \pm S.E.M.) for controls. There were no significant differences to the samples in which the PGP was inhibited with verapamil, colchicine or vinblastine (all concentrations 10 μM). Fig. 2 shows the kinetics of ^{18}F fluoride accumulation in the cell fraction reaching a steady state after 50 min, probably because of specific transport mechanisms [28] and / or of exchange with OH^- in the cells or by binding to the zinc center of the carboxypeptidase [29].

**Temperature dependence of
[^{99m}Tc]sestamibi uptake**

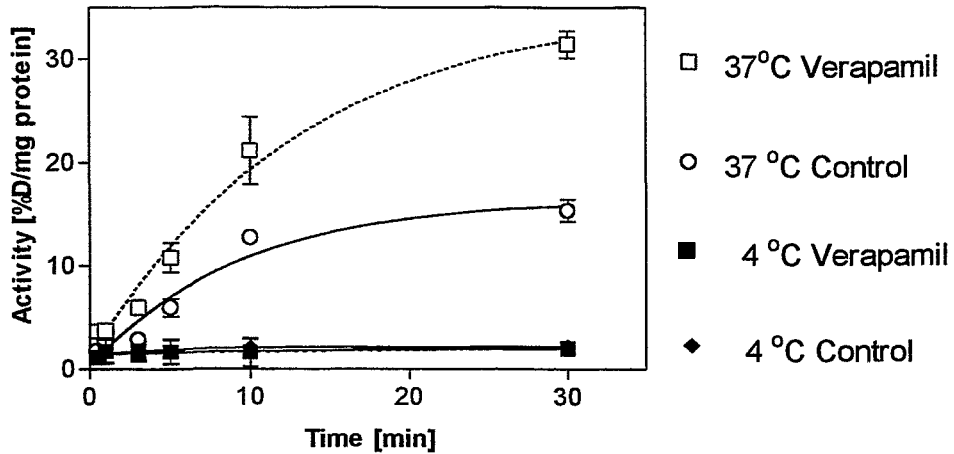


Fig. 3: Kinetics of [^{99m}Tc]sestamibi, accumulation in RBE4 cells at different incubation temperatures. Cells were incubated in medium for various times in the absence of drug (control) or in the presence of verapamil (10 μM). Each point represents the mean value of 4 determinations; bars represent ± SD.

The ^{99m}Tc-sestamibi accumulation was temperature dependent (Fig. 3). The large negative transmembrane potentials at the plasma and mitochondrial membrane, controlled by energy-dependent biochemical processes, are the driving force for the nonmediated [^{99m}Tc]sestamibi diffusion to the mitochondria [30]. The drastic decrease in tracer uptake at low temperature indicates the energy-dependency of the [^{99m}Tc]sestamibi accumulation process. A concentration-dependent increase in [^{99m}Tc]sestamibi accumulation was found when verapamil was added to in the incubation solution. This increase was absent at low temperature. Therefore the data from the 4 °C experiments were used to correct the uptake data at 37 °C for the nonspecific processes.

Furthermore, uptake experiments were simultaneously performed in the presence of other substrates of PGP, such as [³H]colchicine (Fig. 4) and [³H]vinblastine.

The accumulation of PGP substrates at steady state conditions depends on the substrate influx and on the activity of the PGP. It is therefore useful to measure the uptake of two PGP substrates with different accumulation and retention mechanisms at the same time. In the cells [^{99m}Tc]sestamibi is bound to the mitochondria [21], [³H]colchicine and [³H]vinblastine bind to the tubulin skeleton. The direct and linear correlation of the uptake of the two tracers at different levels of PGP inhibition may be interpreted as a sign of the main influence of the PGP on the drug accumulation process in the cells.

**Accumulation of [^{99m}Tc]sestamibi,
[³H]colchicine and [¹⁸F]FDG in RBE4
cells**

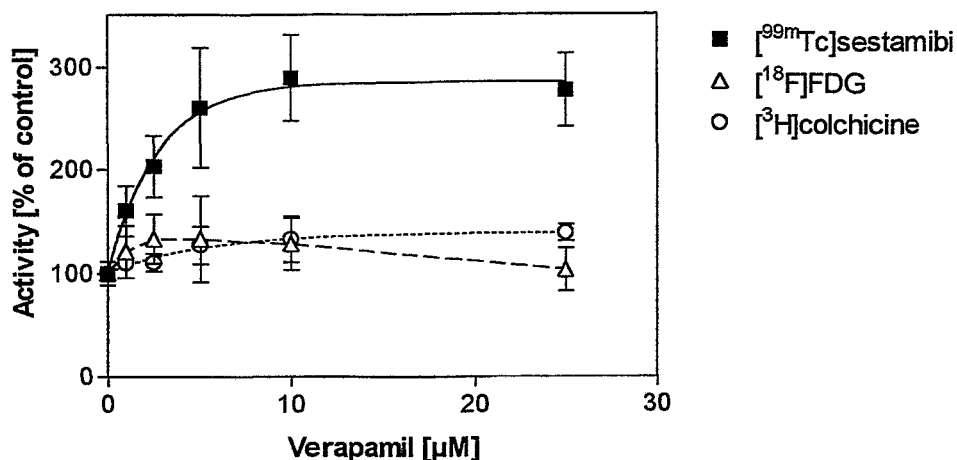


Fig. 4 Simultaneous measurement of the [^{99m}Tc]sestamibi, [³H]colchicine and [¹⁸F]FDG accumulation in RBE4 cells depending on various amounts of verapamil added (incubation at 37 °C; 60 min). Data expressed as a percentage of the accumulated activity in the control experiment without inhibitor.

Fig. 5 shows the linear correlation between [^{99m}Tc]sestamibi, [³H]vinblastine and [³H]colchicine accumulation under control conditions (r^2 : 0.9945, P value < 0.0001; r^2 : 0.9110, P value < 0.0001) and in the presence of 10 μM vinblastine (r^2 : 0.9977, P value < 0.0001; r^2 : 0.8005, P value < 0.0001). The accumulation of [^{99m}Tc]sestamibi during inhibition of the PGP with verapamil is relatively higher than that of [³H]vinblastine or [³H]colchicine, corresponding to the slopes 1.367 ± 0.026 , 0.450 ± 0.006 and 0.032 ± 0.003 , 0.017 ± 0.002 .

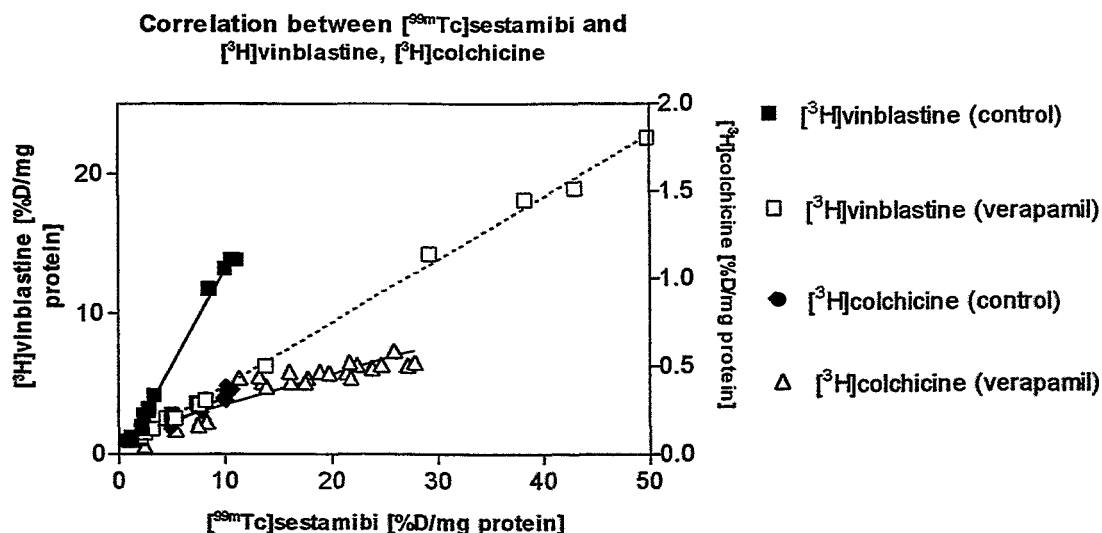


Fig. 5: Correlation between [^{99m}Tc]sestamibi and [³H]vinblastine, [³H]colchicine uptake. Each point represents one of four measurements at 5, 10, 20, 30, 60 min without (control) and with 10 μM verapamil.

Table 2: The influence of various drugs (10 μ M) on the accumulation of the PGP substrate in RBE4 cells after 60 min incubation at 37 $^{\circ}$ C, expressed as a percentage of control \pm SD. Each point represents the mean value of 8 determinations \pm SD.

Modulator	^{99m}Tc sestamibi		^3H colchicine		^3H vinblastine	
Control	100.00 \pm	21.29	100.00 \pm	10.99		
Verapamil	246.75 \pm	8.67	146.66 \pm	6.98	546.96 \pm	86.28
Amytal	104.86 \pm	7.11	96.01 \pm	3.43		
DNP	88.27 \pm	6.46	100.73 \pm	6.06	100.56 \pm	34.52
Rotenon	59.00 \pm	12.69	113.85 \pm	7.33		
Vinblastine	709.36 \pm	166.25	234.62 \pm	66.74		
Colchicine	112.12 \pm	6.09	106.09 \pm	14.41	165.89 \pm	2.30
Chlorpromacine	214.91 \pm	36.62	111.26 \pm	7.93		

The potential of various drugs to enhance the cellular accumulation of the PGP-substrate is shown in Table 2. Vinblastine has the greatest ability to inhibit the PGP, followed by verapamil chlorpromacine and colchicine. This is consistent with studies of the influence of the agents on the drug binding site of PGP and the transport function of the protein [31, 32, 33].

The L-amino acid transport system is symmetrically distributed between the luminal and abluminal membranes of brain endothelial cells [34]. It is therefore assumed that the distribution of the carrier system is also homogeneous in the monolayer cultures of the RBE4 cells. The function of the Na^+ independent neutral amino acid transport is a useful measure of the intact transport of leucine. Verapamil, colchicine and vinblastine had no effect on the L-leucine accumulation in the cells, indicating that the elevated accumulation of the PGP substrates is a specific inhibition of the PGP [35]. In addition, the accumulation of the neutral amino acid L- ^3H leucin and the nucleoside ^3H thymidine were measured under the same conditions. They provide information about possible changes in the rates of protein and/or DNA synthesis. No significant changes were observed during incubation with verapamil, colchicine, DMSO or DNP (Fig. 6).

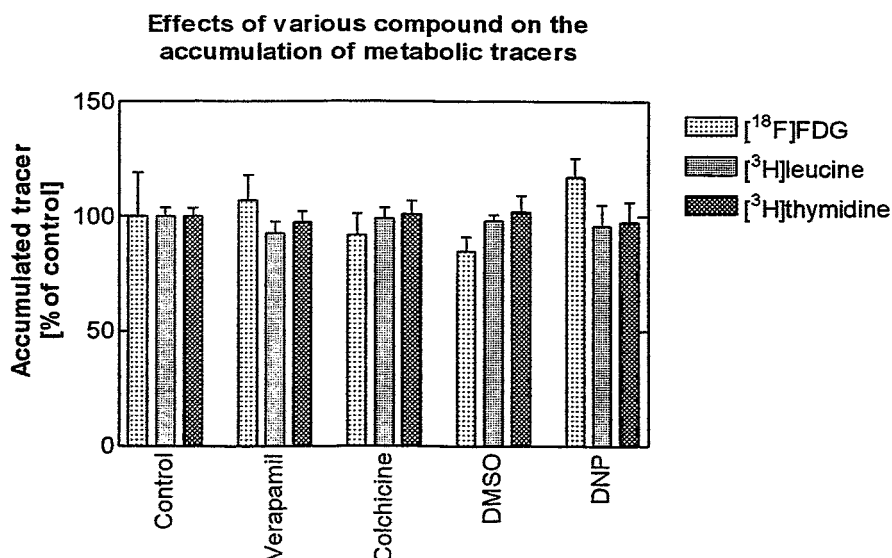


Fig. 6: Effect of various compounds on the ^{18}F FDG, ^3H leucine, ^3H thymidine uptake by RBE4 cells. The cells were incubated according to a common procedure for 60 min at 37 $^{\circ}$ C in the absence of drugs (control) and together with verapamil (10 μ M), colchicine (10 μ M), DMSO (1 % v/v) and DNP (10 μ M). Each value represents the mean \pm SD of 4 measurements.

Cordobes *et al.* [22] found a different uptake of [^{99m}Tc]sestamibi in various tumour cells, which the authors attributed to different levels of metabolic activity of the cells without having measured it. We therefore used [^{18}F]FDG to measure the glucose uptake and metabolism of the cells. [^{18}F]FDG is a glucose analogue which is expected to be transported into the cells by the glucose transporters GLUT1 and GLUT3. We previously showed that these transporters are expressed in RBE4 cells [1]. After 60 minutes mainly the phosphorylated compound, the product of the hexokinase reaction, is mainly found intracellularly [36]. Under normal conditions the accumulation of [^{18}F]FDG is strongly correlated with the cell number ($r = 0.9377$; $p < 0.001$).

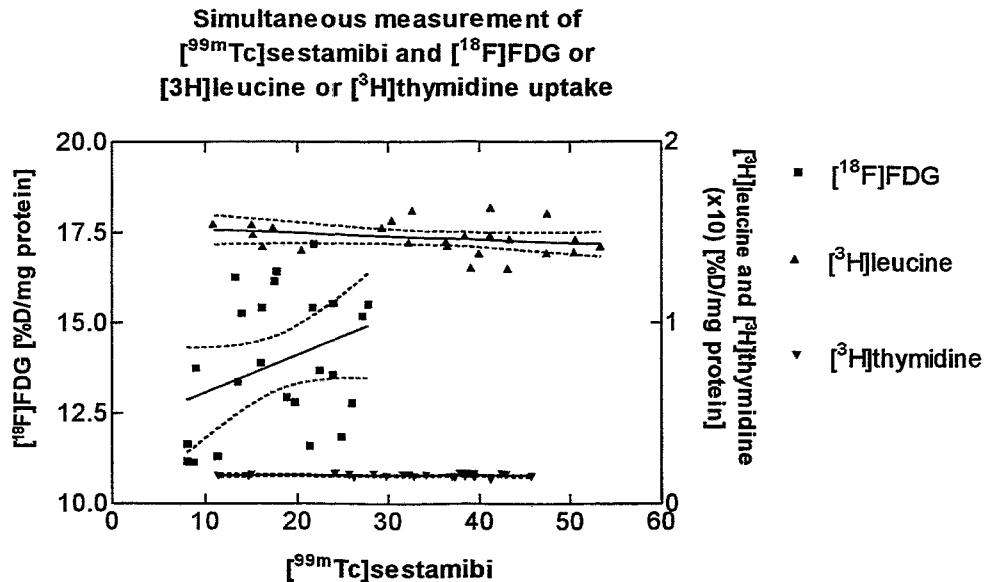


Fig. 7: Simultaneous measurement of [^{99m}Tc]sestamibi and [^{18}F]FDG or [^3H]leucine or [^3H]thymidine uptake in RBE4 cells. Each point represents one measurement in an uptake experiment with various verapamil concentrations (0, 1, 2.5, 5, 10, 25 μM ; incubation time 60 min; 37 $^{\circ}\text{C}$).

The uptake of [^{99m}Tc]sestamibi is not correlated with the uptake of [^{18}F]FDG ($r^2: 0.1204$) nor with the uptake of [^3H]leucine ($r^2: 0.07211$) nor with the uptake of [^3H]thymidine ($r^2: 0.01071$) in the RBE4 cells under normal conditions in the absence and presence of verapamil up to 25 μM (Fig. 4, Fig. 7). Also, the PGP inhibitors verapamil and colchicine have no influence on the accumulation of ^{18}F -FDG, and verapamil did not change the uptake of [^3H]leucine and [^3H]thymidine.

Taken together, our data show that the above system can be used to measure the functional characteristics of the PGP in the RBE4 cells, to study the interaction of various tracers and drugs with the PGP simultaneously with their influence on the cell metabolism. The system is therefore useful for identifying agents which underlie PGP-mediated drug transport or modulate it. The functional interactions, which may lead to information about the potential of the drugs to reverse PGP-mediated multidrug resistance and to freely pass cells expressing PGP, can be investigated. The system may be valuable in the design of new and more potent tracers passing the various barriers in the organism.

Acknowledgment: We are grateful to Dr. F. Roux (Laboratoire d'Immuno-Pharmacologie Moléculaire, CNRS UPR 0415, Université Paris, Paris, France) for supplying the RBE4 cells. The authors would like to thank G. Wunderlich (Clinics of Nuclear Medicine, University Hospital Dresden) for the supply of the [^{99m}Tc]sestamibi and J. Steinbach for the supply of the [^{18}F]FDG. Special thanks are due to Mrs. Herrlich for the technical assistance.

References

- [1] Bergmann R., Roux F., Drewes L.R., Brust P., Johannsen B. (1996) Expression spezifischer Transporter der Blut-Hirn Schranke, *Neuroforum* 2 (Supplement), 130.
- [2] Roux F., Durieu-Trautmann, Chaverot N., Claire M., Mailly P., Bourre J.-M., Strosberg A. D. and Couraud P. O. (1994) Regulation of gamma-glutamyl transpeptidase activities in immortalized rat brain microvessel endothelial cells. *J. Cell. Physiol.* 159, 101 - 113.
- [3] Begley D. J., Lechardeur D., Chen Z.-D., Rollinson C., Bardoul M., Roux F., Scherman D. and Abbott N. J. (1996) Functional expression of P-glycoprotein in an immortalised cell line of rat brain endothelial cells, RBE4. *J. Neurochem.* 67, 988 - 995.
- [4] Johannsen B.; Scheunemann M., Spies H., Brust P., Wober J., Syhre R. and Pietzsch H.-J. (1996) Technetium(V) and rhenium(V) complexes for 5-HT_{2A} serotonin receptor-binding: structure-affinity considerations. *Nucl. Med. Biol.* 23, 429 - 438.
- [5] Bellamy W. T. and Dalton W. S. (1994) Multidrug resistance in the laboratory and clinic. *Advances in Clinical Chemistry*, 31 1 - 61.
- [6] Brust P. (1986) Changes in regional blood-brain transfer of L-leucine elicited by arginine-vasopressin. *J. Neurochem.* 46, 534 - 541.
- [7] McAteer J. A. and Davis J. (1994) Basic cell culture technique and the maintenance of cell lines. In: Basic cell culture a practical approach. (Davis J.M. eds.) Oxford University Press, Oxford New York Tokyo, pp. 93 - 148.
- [8] Goethals P., Lameire N., van Eijkeren M., Kestloot D., Thierens H. and Dams R. (1996) [Methyl-carbon-11]thymidine for in vivo measurements of cell proliferation. *J. Nucl. Med.* 37, 1048-1052.
- [9] Gottesman M. M. and Pastan I. (1993) Biochemistry of multidrug resistance mediated by the multidrug transporter. *Annu. Rev. Biochem.* 62, 385 - 427.
- [10] Sokoloff L., Reivich M. and Kennedy C. (1977) The [¹⁴C]deoxyglucose method for the measurement of local cerebral glucose utilization: theory, procedure, and normal values in the conscious and anesthetized albino rat. *J. Neurochem.* 28, 897 - 916.
- [11] Nelson C. A., Wang J. Q., Leav I. and Crane P. D. (1996) The interaction among glucose transport, hexokinase, and glucose-6-phosphatase with respect to [³H]-3-deoxyglucose retention in murine tumor models. *Nucl. Med. Biol.* 23, 533 - 541.
- [12] Füchtner F., Steinbach J., Mäding P. and Johannsen B. (1996) Basic hydrolysis of 2-[¹⁸F]fluoro-1,3,4,6-tetra-O-acetyl-D-glucose in the preparation of 2-[¹⁸F]fluoro-2-deoxy-D-glucose. *Appl. Radiat. Isot.* 47, 61 - 66.
- [13] Herman L. W., Sharma V., Kronauge J. F., Barbarics E., Herman L. A. and Piwnica-Worms D. (1995) Novel hexakis(areneisonitrile)technetium(I) complexes as radioligands targeted to the multidrug resistance P-glycoprotein. *J. Med. Chem.* 38, 2955 - 2963.
- [14] Johannsen B., Berger R. and Schomäcker K. (1980) The binding of technetium compounds by human serum albumin. *Radiochem. Radioanal. Letters* 42, 177 - 188.
- [15] Lamson M. L., Kirschner A. S., Hotte C., Lipsitz E. L. and Ice R. D. (1975) Generator-produced ^{99m}TcO₄⁻: Carrier free? *J. Nucl. Med.* 16, 639 - 641.
- [16] Holland M. E., Deutsch E., Heinemann W. R. and Holland E. M. (1986) Studies on commercially available ⁹⁹Mo/^{99m}Tc radionuclide generators - I. Comparison of five analytical procedures for determination of total technetium in generator eluants. *Appl. Radiat. Isot.* 37, 165 - 171.
- [17] Goerner W., Noll B., Spies H. and Thieme K. (1988) Determination of technetium in ⁹⁹Mo/^{99m}Tc generators. *J. Radioanal. Nucl. Chem.* 122, 291 - 298.
- [18] Lowry O. H., Rosenbrough N. J., Farr A. L. and Randall, R. J. (1951) Protein measurement with the Folin phenol reagent. *J. Biol. Chem.* 193, 265 - 275.
- [19] Greenberger L. M., Cohen D. and Horwitz S. B. (1994) 5. In vitro model of multiple drug resistance. In: Anticancer drug resistance: Advances in Molecular and Clinical Research. (Goldstein L.J., Ozols R.F. eds), Kluwer Academic Publishers, pp. 69 - 106.
- [20] Jetté L., Murphy G., Leclerc J.-M. and Beliveau R. (1995) Interaction of drugs with P-glycoprotein in brain capillaries. *Biochem. Pharmacol.* 50, 1701 - 1709.
- [21] Piwnica-Worms D., Rao V. V., Kronauge J. F. and Croop J. M. (1995) Characterization of multidrug resistance P-glycoprotein transport function with an organotechnetium cation. *Biochem.* 34, 12210 - 12220.
- [22] Cordobes M. D., Starzec A., Delmon-Moingeon L., Blanchot C., Kouyoumdjian J.-C., Prévost G., Caglar M. and Moretti J.-L. (1996) Technetium-99m-sestamibi uptake by human benign and malignant breast tumor cells: correlation with *mdr* gene expression. *J. Nucl. Med.* 37, 286 - 289.
- [23] Miyamoto K.-I., Koga-Takeda K., Koga K., Ohshima T. and Nomura M. (1996) Saturable function of P-glycoprotein as a drug-efflux pump in multidrug-resistant tumor cells.

-
- J. Pharm. Pharmacol.* **48**, 522 - 525.
- [24] Ballinger J. R., Cowan D. S. M., Zhang Z. M. and Rauth A. M. (1993) Effect of hypoxia on the accumulation of technetium-99m-glucarate and technetium-99m-gluconate by chinese hamster ovary cells in vitro. *J. Nucl. Med.* **34**, 242 - 245.
- [25] Lauf P. K. (1985) On the relationship between volume- and thiol-stimulated K^+Cl^- fluxes in red cell membranes. *Molec. Physiol.* **8**, 215 - 234.
- [26] Hallows K. R. and Knauf P. A. (1994) Principles of cell volume regulation. In: *Cellular and Molecular Physiology of Cell Volume Regulation* (Strange K., ed.) CRC Press, Boca Raton, pp. 3 - 29.
- [27] Fujise F. and Lauf P. K. (1987) Swelling, NEM, and A23187 activate Cl^- -dependent K^+ transport in high- K^+ sheep red cells. *Am. J. Physiol.* **252**, C197 - C204.
- [28] Smith Q. R. and Rapoport S. I. (1984) Carrier-mediated transport of chloride across the blood-brain barrier. *J. Neurochem.* **42**, 754 - 763.
- [29] da Silva J. J. R. F. and Williams R. J. P. (1991) The biological chemistry of the elements the inorganic chemistry of the life. *Clarendon Press Oxford*, pp. 60 - 70.
- [30] Chiu M. L., Kronauge J. F. and Piwnica-Worms D. (1990) Effect of mitochondrial and plasma membrane potentials on accumulation of hexakis(2-methoxyisobutylisonitrile)technetium(I) in cultured mouse fibroblasts. *J. Nucl. Med.* **31**, 1646 - 1653.
- [31] Horio M., Lovelace E., Pastan I. and Gottesman M. M. (1991) Agents which reverse multidrug-resistance are inhibitors of [3H]vinblastine transport by isolated vesicles. *Biochem. Biophys. Acta* **1061**, 106 - 110.
- [32] Bruggemann E. P., Currier S. J., Gottesman M. M and Pastan I. (1992) Characterization of the azidopine and vinblastine binding site of P-glycoprotein. *J. Biol. Chem.* **267**, 21020 - 21026.
- [33] Boer R., Ulrich W.-R., Haas S., Borchers C., Gekeler V., Boss H., Przybylski M. and Schödl A. (1996) Interactions of cytostatics and chemosensitizers with the dextrin-glycoprotein binding site on P-glycoprotein. *Eur. J. Pharmacol.* **295**, 253 - 260.
- [34] del Pino M. M. S., Peterson D. R. and Hawkins R. A. (1995) Neutral amino acid transport characterization of isolated luminal and abluminal membranes of the blood-brain barrier. *J. Biol. Chem.* **270**, 14913 - 14918.
- [35] Horio M., Lovelace E., Pastan I. and Gottesman M. M (1990) Agents which reverse multidrug-resistance are inhibitors of [3H]vinblastine transport by isolated vesicles. *BBA*, **1061**, 106 - 110.
- [36] Crane P. D., Pardridge W. M., Braun L. D. and Oldendorf W. H. (1983) Kinetics of transport and phosphorylation of 2-fluoro-2-deoxy-D-glucose in rat brain. *J. Neurochem.* **40**, 160 - 167.

32. Different Response of Cerebral and Non Cerebral Endothelial Cells to Cytotoxic Hypoxia

B. Ahlemeyer, P. Brust, B. Johannsen

Introduction

The endothelial cells of cerebral capillaries play a crucial role in controlling the transfer of molecules from blood to brain and vice versa and they constitute the so called blood-brain barrier (BBB). Under normal conditions the integrity of the BBB is protected, which is essential for the correct function of the brain. Hypoxic brain injury - which is known to damage neurons and astrocytes - also affects the BBB e.g. leads to changes in the permeability [1 - 5] as well as to an increase in the expression of intercellular adhesions molecules [6 - 8] preceding the migration of leukocytes across the BBB. It has been shown that reactive oxygen species account for at least part of pathological damage [4, 5, 9]. Only a few data have been published concerning the effect of hypoxia on the BBB in vitro [4, 5, 10, 11]. In these studies, hypoxia was performed by exposure of cerebral endothelial cells to 95 % nitrogen and 5 % carbogen. Although hypoxic response of endothelial cells of peripheral tissue has already been studied [12 - 18] no direct comparison between cerebral and non cerebral endothelial cells under the same hypoxic conditions has been done. Therefore, it was the aim of the present study to find out whether the treatment with sodium cyanide is a suitable and practicable model to study hypoxic injury in cerebral endothelial cells, the major constituents of the blood-brain barrier, and to compare the cellular response between cerebral and non cerebral endothelial cells under the same hypoxic conditions.

Experimental

Materials

Medium 199, medium MCDB-131, fetal calf serum, collagen type I/III, dextran, Percoll, antibiotics, sodium fluorescein and the assay kits for the determination of lactate (735-10), lactate dehydrogenase (DG1340k) and protein (P5656) were purchased from Sigma (Deisenhofen Germany). L-glutamyl-a-methoxy-naphtylamide, dispase, collagenase/dispase, p-nitrophenylphosphate, IgG fractions of mouse anti-human factor VIII and sheep anti-mouse Ig-G fluorescein antibodies were from Boehringer Mannheim (Germany). Plastic cell culture dishes were from Becton Dickinson (Heidelberg, Germany) and all other chemicals were of the purest grade available from Merck (Darmstadt, Germany).

Cell cultures

Primary cultures of cerebral endothelial cells were prepared from adult porcine brain microvessels [19]. The cells were maintained in medium M199, supplemented with 10 % fetal calf serum and antibiotics, in a humidified atmosphere of 5 % CO₂ and 95 % air for 4 days before experiments. Immunohistochemical staining of the cultures using a mouse antibody to human Factor VIII-related antigen and a secondary fluorescein-labeled sheep anti-mouse F(ab')₂-fragment demonstrated that the cultures consisted of 95 % endothelial cells up to 5 days (data not shown). Human umbilical vein endothelial cells (non cerebral endothelial cells) were purchased from Promocell (Heidelberg, Germany) and were cultivated in medium MCDB-131 with 5 % fetal calf serum. Cell cultures of passage V were used for the experiments.

Hypoxia studies

Hypoxic injury was induced by adding sodium cyanide (NaCN) to the culture medium to give a final concentration of 1 mM for periods of 10, 30, 60, 120 and 180 min. Control experiments (normoxia) were performed by adding sodium chloride (NaCl) instead of NaCN. Hypoxia in the absence of glucose was performed by incubation of the cells with Hanks' Balanced salt solution (HBSS, 145 mM NaCl, 5.4 mM KCl, 0.4 mM KH₂PO₄, 3.2 mM Na₂HPO₄, 0.5 mM MgCl₂, 1 mM CaCl₂, 0.4 mM MgSO₄, 4.2 mM NaHCO₃, pH 7.4) without glucose and with 1 mM NaCN. The effect of glucose deprivation alone was also tested with HBSS without glucose and 1 mM NaCl.

Biochemical assays

We quantified cell damage by trypan blue exclusion method and we determined the protein content, the release of lactate as well as of lactate dehydrogenase (LDH, EC 1.1.1.27) using assay kits. The activities of alkaline phosphatase (ALP, EC 3.1.3.1) and γ -L-glutamyltranspeptidase (γ -GT, EC 2.3.2.1) were measured kinetically by the formation of p-nitrophenol at 420 nm and of 4-carboxyanilide at 410 nm, respectively as already described by Meyer *et al.* (1991).

Statistical analysis

Values are given as means \pm standard deviation (SD) of *n* experiments. The one-way analysis of variances (ANOVA-1) and Duncan-test were used for statistical analysis.

Results

The percentage of cell damage increased as a function of time during hypoxia in cerebral endothelial cells (Fig. 1), whereas there was no damage in non cerebral endothelial cells under the same hypoxic conditions (data not shown). The deprivation of glucose did not alter hypoxia induced changes in both cell types (data not shown). Similar results were found by measuring the release of LDH (Fig. 2) as an indication for membrane damage. In addition, we found an increase in the lactate release during hypoxia compared to controls in cerebral (Fig. 3) as well as in non cerebral endothelial cells (data not shown). Additional glucose deprivation reduced the release of lactate in both cell types (data not shown).

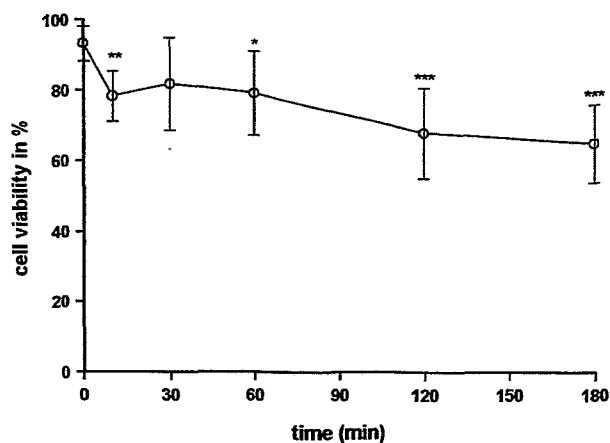


Fig. 1: The viability of cerebral endothelial cells after cytotoxic hypoxia with 1 mM NaCN compared to normoxic controls (time 0). Values are means \pm SD, *n* = 10; *** *P* < 0.001; ** *P* < 0.01; * *P* < 0.05 versus controls.

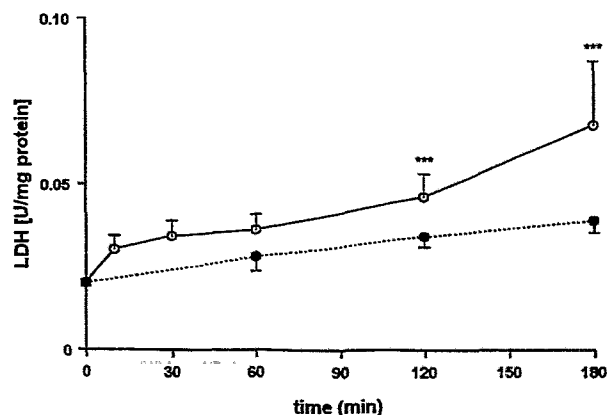


Fig. 2: The release of LDH of cerebral endothelial cells after cytotoxic hypoxia with 1 mM NaCN (open symbols) compared to normoxic controls (closed symbols). Values are means \pm SD, *n* = 5; *** *P* < 0.001 versus controls.

We also measured for the first time the activities of the marker enzymes of the BBB, ALP and γ -GT, during hypoxia in the presence and absence of glucose. The ALP activity of cerebral endothelial cells was 0.522 ± 0.017 U/mg protein after 4 days in culture with no change during hypoxia. In non cerebral endothelial cells the ALP activity was 10 times lower which was also unaffected during cytotoxic hypoxia.

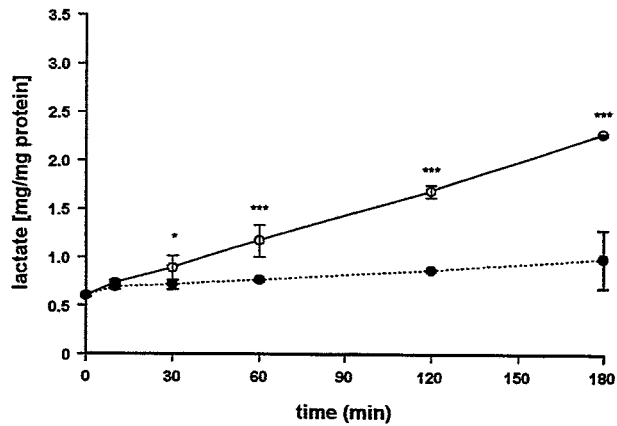


Fig. 3: The release of lactate of cerebral endothelial cells after cytotoxic hypoxia with 1 mM NaCN (open symbols) compared to normoxic controls (closed symbols). Values are means \pm SD, n = 5; *** P < 0.001; * P < 0.05; versus controls.

By measuring γ -GT activity in cerebral endothelial cells, we found a significant decrease from 3.8 ± 1.3 to 1.09 ± 0.3 after 3 hours of hypoxia in the presence and absence of glucose (Fig. 4), whereas the γ -GT activity in non cerebral endothelial cells was lower with 1.0 ± 0.3 U/mg protein under normoxic with no significant change under hypoxic conditions (data not shown).

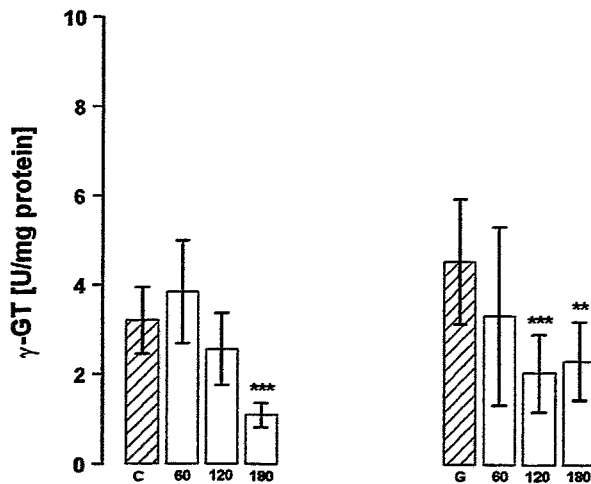


Fig. 4: The activity of γ -GT of cerebral endothelial cells after cytotoxic hypoxia with 1 mM NaCN (is given in min under the column) in the presence (left columns) and in the absence of glucose (right columns) compared to normoxic controls (in the presence of glucose = C; in the absence of glucose = G). Values are means \pm SD, n = 5; *** P < 0.001; ** P < 0.01 versus controls (C,G).

Discussion

The effect of hypoxia on cerebral endothelial cells

In our study, 2 hours of hypoxic injury to cerebral endothelial cells led to cell damage as revealed by a decrease in viability by 24 % and a 2.7-fold increase in LDH release as an indication for membrane damage. We found no significant differences in the response to hypoxia in the presence and in the absence of glucose. Only few data have already been published concerning the effect of hypoxia on the BBB *in vitro* [5, 9, 11] and the authors have used different cell cultures models (different culture conditions, species, cultivation time) and different experimental designs of hypoxia. Our results are comparable to those of Mertsch *et al.* [9] who measured in porcine brain endothelial cells after 10 days in culture a reduction in cell viability to 84 % and an increase in the release of LDH by 91 % after 2 hours of hypoxia in the absence of glucose compared to controls. Gobbel *et al.* [11] and Plateel *et al.* [5] investigated the response of cerebral endothelial cells to longer periods of 24 and 48 hours of hypoxia in the presence of glucose. Plateel *et al.* [5] have found in bovine brain endothelial cells, cocultured with astrocytes and astrocyte-conditioned medium for 12 days, a 50 % decrease in the ATP level and some apoptotic processes after 48 hours of hypoxia, but no increase in LDH release. Gobbel *et al.* [11] showed that rat brain endothelial cells after 5 - 9 days in culture remained viable with no release of LDH up to 24 hours of hypoxia in the presence of glucose, but this dramatically changed after 48 hours of hypoxia with 70 % non-viable of all the cells. The mentioned studies were performed either in the presence [5, 11] or in the absence of glucose [9]. Therefore we investigated both, the effect of hypoxia in the presence and in the absence of glucose and found no difference in the response of cerebral endothelial cells. We suggest that hypoxia itself is mainly responsible for the observed cell damage.

In addition, we found after 2 hours of hypoxia an increase in lactate release by 93 % in the presence and by 51 % in the absence of glucose. Consistently, Mertsch *et al.* [9] measured a 30 % increase in lactate release in porcine brain endothelial cells after 2 hours of hypoxia in the absence of glucose.

By measuring the activities of the marker enzymes of the BBB, ALP and γ -GT, only the γ -GT showed a significant decrease after 3 hours of hypoxia. In addition to our study, a decrease in the glutathione level has already been shown in cerebral endothelial cells after 12 hours of hypoxia [5]. Because γ -GT mediate the transfer of the γ -glutamyl residue from glutathione to amino acids, its activity may be reduced during the first time of hypoxia to maintain a sufficient level of glutathione as a protective mechanism. This would also explain why the two marker enzymes behave differently to hypoxia. However, further study have to clarify the importance of this finding.

The effect of hypoxia on non cerebral endothelial cells

In the present study, non cerebral endothelial cells remained viable with no significant increase in LDH release even after 3 hours of hypoxia in the presence and absence of glucose. Similarly, only a 2 - 5 % increase in LDH release was found in human umbilical vein endothelial cells [13] as well as in bovine aortic endothelial cells [16] and in rat coronary endothelial cells [14] after 2 hours of hypoxia in the presence and absence of glucose. It is suggested from these studies that endothelial cells of other organs than brain are relatively resistant to hypoxia regardless of the species and tissue origin of the vessel.

The same increase in lactate release as we measured in non cerebral endothelial cells were also found in rat coronary [14] and porcine aortic endothelial cells [12] after 2 hours of hypoxia in the presence and absence of glucose compared to controls.

We used sodium cyanide, an inhibitor of the respiratory chain, to study the effect of hypoxia in cerebral and non cerebral endothelial cells. Our results concerning the cellular damage are comparable with *in vitro* studies of other authors which were performed under conditions of low O₂ [9, 12 - 18]. We conclude that the incubation with sodium cyanide is a suitable and easy model to study hypoxic injury in cerebral endothelial cells as the major constituent of the blood-brain barrier. In addition, we found that cerebral endothelial cells are damaged during cytotoxic hypoxia as revealed by a decrease in cell viability and an increase in the release of LDH and lactate into the incubation medium. In contrast, non cerebral endothelial cells showed no significant changes in cell viability as well as in the release of lactate and LDH during hypoxia compared to controls. We therefore conclude that non cerebral endothelial are less sensitive to cytotoxic hypoxia than cerebral endothelial cells.

Acknowledgements

This work was supported in part by a research grant from the Saxon State Ministry of Science and Arts (Grant 7541.82-FZR/309).

References

- [1] Klatzo I. (1987) Pathophysiological aspects of brain edema. *Acta Neuropathol.* **72**, 236 - 239.
- [2] Betz A. L., Keep R. F., Beer M. E. and Ren X. (1994) Blood-brain barrier permeability and brain concentrations of sodium, potassium, and chloride during focal ischemia. *J. Cereb. Blood Flow Metab.* **14**, 29 - 37.
- [3] Pluta R., Lossinsky A. S., Wisniewski H. M. and Mossakowski M. J. (1994) Early blood-brain barrier changes in the rat following transient complete ischemia induced by cardiac arrest. *Brain Res.* **633**, 41 - 52.
- [4] Giese H., Mertsch K. and Blasig I. E. (1995) Effect of MK-801 and U83836E on a porcine brain capillary endothelial cell barrier during hypoxia. *Neurosci. Lett.* **191**, 169 - 172.
- [5] Plateel M., Dehouck M.-P., Torpier G., Cecchelli R. and Teissier, E. (1995) Hypoxia increases the susceptibility to oxidant stress and the permeability of the blood-brain barrier endothelial cell monolayer. *J. Neurochem.* **65**, 2138 - 2145.
- [6] Hess D. C., Zhao W. Z., Carroll J., McEachin M. and Buchanan K. (1994) Increased Expression of ICAM-1 during reoxygenation in brain endothelial cells. *Stroke* **25**, 1463 - 1468.
- [7] Okada Y., Copeland B. R., Mori E., Tung M.-M., Thomas W. S. and del Zoppo G. J. (1994) P-selectin and intercellular adhesion molecule-1 expression after focal ischemia ad reperfusion. *Stroke* **25**, 202 - 211.
- [8] Wang X., Siren A.-L., Liu Y., Yue Y. L., Barone F. C. and Feuerstein G. Z. (1994) Upregulation of intercellular adhesion molecule 1 (ICAM-1) on brain microvascular endothelial cells in rat ischemic cortex. *Mol. Brain Res.* **26**, 61 - 68.
- [9] Mertsch K., Grune T., Siems W. G., Ladhoff A., Saupe N. and Blasig I. E. (1995) Hypoxia and reoxygenation of brain endothelial cells in vitro: a comparison of biochemical and morphological response. *Cell Mol. Biol.* **41**, 243 - 253.
- [10] Grammas P., Liu G. J., Wood K. and Floyd R. A. (1993) Anoxia/reoxygenation induces hydroxyl free radical formation in brain microvessels. *Free Rad. Biol. Med.* **14**, 553 - 557.
- [11] Gobel G. T., Chan T. Y.-Y., Gregor G. A. and Chan P. H. (1994) Response of cerebral endothelial cells to hypoxia: modification by fructose-1,6-biphosphate but not glutamate receptor antagonists. *Brain Res.* **653**, 23 - 30.
- [12] Shyrook J. C., Rubio R. and Berne, R. (1988) Release of adenosine from aortic endothelial cells during hypoxia and metabolic inhibition. *Am. J. Physiol.* **254**, H223 - H229.
- [13] Hempel S. L., Haycraft D., Hoak J. and Spector A. (1990) Reduced prostacyclin formation after reoxygenation. *Am. J. Physiol.* **29**, C738 - C745.
- [14] Mertens S., Noll T., Spahr R., Krützfeld A. and Piper H. M. (1990) Energetic response of coronary endothelial cells to hypoxia. *Am. J. Physiol.* **258**, H689 - H694.
- [15] Ogawa S., Gerlach H., Esposito C., Pasagian-Macaulay A., Brett J. and Stern D. (1990) Hypoxia modulates the barrier and coagulant function of cultured bovine endothelium. *J. Clin. Invest.* **85**, 1090 - 1098.
- [16] Palluy O., Bonne C. and Modat G. (1991) Hypoxia/reoxygenation alters endothelial prostacyclin synthesis - protection by superoxide dismutase. *Free Rad. Biol. Med.* **11**, 269 - 275.
- [17] Mertsch K., Grune T., Ladhoff A. and Blasig, I. E. (1993) An *in vitro* model for hypoxia/reoxygenation with endothelial cells. *Neurobiol.* **1** (abstract).
- [18] Tretyakov A. V. and Faber H. W. (1995) Endothelial cell tolerance to hypoxia. *J. Clin. Invest.* **95**, 738 - 744.
- [19] Mischek U., Meyer J. and Galla H.-J. (1989) Characterization of g-GT activity of cultured endothelial cells from porcine brain capillaries. *Cell Tiss. Res.* **256**, 221 - 226.
- [20] Meyer J., Rauh J. and Galla H.-J. (1991) The susceptibility of cerebral endothelial cells to astroglial induction of blood-brain barrier enzymes depends on their proliferative state. *J. Neurochem.* **57**, 1971 - 1977.

33. Studies on an HPLC Method to Assay the Concentrations of Amines in Brain Microdialysis Perfusates Based on Naphthalene-2,3-Dicarbaldehyde Derivatization and Fluorescence Detection

G. Vorwieger, R. Bergmann, P. Brust, B. Johannsen

Introduction

The dopaminergic system in the immature brain is very sensitive to changes in tissue oxygen tension, as they occur under neonatal asphyxia. The pathogenesis of the resulting brain injury remains unclear. However, it is accepted that extracellular neurotransmitter concentrations and their metabolism change during asphyxia.

To study the dopamine metabolism under asphyxia we – together with the Institute of Pathophysiology in Jena – started PET experiments and brain microdialysis in newborn piglets. Brain microdialysis is expected to provide information about the changes in endogenous dopamine (DA), its metabolites and in excitatory amino acids as well. As a prerequisite, an ultrasensitive and reliable method for determination of these substances down to the subnanomolar range was to be established (Table 1).

Table 1: Reported brain microdialysis perfusate concentrations – in various animal species – of pertinent neurotransmitter candidates and some DA-metabolites, all accessible to naphthalene-2,3-dicarbaldehyde (NDA) derivatization (DA dopamine, NE norepinephrine, 5-HT serotonin, DOPA 3,4-dihydroxyphenylalanine, 3-MT 3-methoxytyramine, Asp aspartic acid, GABA γ -aminobutyric acid, Glu glutamic acid, Asn asparagine, Tau taurine, Gly glycine)

Substance	Brain region (various animal species)	Microdialysis perfusate concentration range
DA	striatum	1.5 - 13.6 nM
NE	various regions	0.7 - 3.43 nM
5-HT	cortex	1.8 nM
DOPA	various regions	0.4 - 0.75 nM
3-MT	striatum	4.3 nM
Asp	various regions	40 - 600 nM
GABA	various regions	9 - 750 nM
Glu	various regions	190 nM - 3 μ M
Asn	striatum	420 nM - 1 μ M
Tau	various regions	270 nM - 8.3 μ M
Gly	various regions	550 nM - 10 μ M

In the literature HPLC-based methods were used for this purpose, combined with electrochemical detection (ECD, for catechols, biogenic amines) or precolumn derivatization and subsequent fluorescence detection (for amino acids).

For precolumn derivatization, naphthalene-2,3-dicarbaldehyde (NDA) was developed as a rationally designed reagent for the derivatization of primary amines including amino acids to allow ultrasensitive fluorescence detection [1 - 3]. The reaction products are cyanobenzisoindole (CBI) derivatives (Fig. 1).

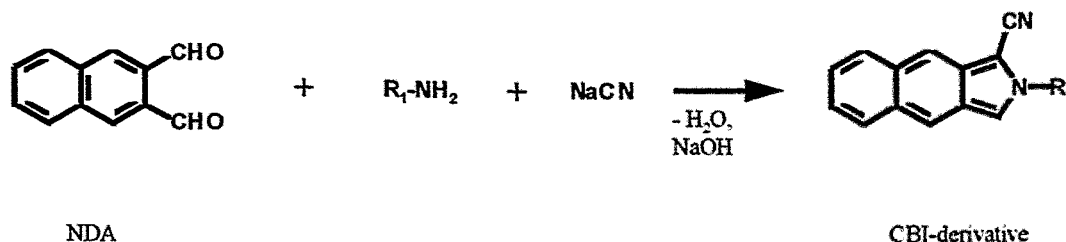


Fig. 1: Reaction scheme of the NDA derivatization.

Because of a number of advantages of this particular derivatization method, a procedure based on it should be established and adapted to our analytical tasks.

Thus, the aim of this work was to study the performance of NDA precolumn derivatization / HPLC analysis of primary amines at concentrations of 10 nM or less.

Experimental

All experiments were carried out with the Hewlett Packard HPLC system 1050 in the following configuration: pump 79852A, automatic liquid sampler 709855A, fluorescence detector (FLD) 1046A and variable wavelength detector (VWD) 79853C, the detectors coupled in the above-mentioned series.

As analytical column a 250x3 mm cartridge LiChroCART with LiChrospher 100 RP-18 (5 μ m) without precolumn was chosen. Various binary and ternary gradients (low pressure mixing) were applied, with a common phase A (20 nmol/l Na acetate, with acetic acid buffered to pH 7.2) and differing phases B (and C), consisting of Na acetate buffered solvents (MeOH, MeCN, THF).

The applied autosampler programs controlled mixing and reaction in three different enclosures: in the seat capillary (APS1), in the sample vial using sample transfer with the needle (APS2) and in the sample vial with indirect fluid movement (APS3). All derivatization experiments were carried out in Hewlett Packard 100 μ l microvial inserts (polypropylene or glass, HP 5182-0549 or 5181-1270). System control and chromatographic data analysis were accomplished with the software ChemStation 2D (Hewlett Packard).

For blank examinations, borate buffer (pH 9.3) was first mixed with cyanide and then with NDA solution. Deproteinized plasma (using deproteinization methods [4 - 6], separate or in combination) was vacuum-concentrated and dissolved in borate buffer. Stock standard solutions of amino acids were prepared by dissolving amino acids in diluted NaOH or HCl, respectively. Serial dilution's were then prepared in borate buffer. For precolumn derivatization, dissolved plasma concentrate and diluted standard solutions were treated as blanks.

Results and Discussion

Prior to HPLC separation and fluorescence detection amino acids were derivatized with naphthalene-2,3-dicarbaldehyde. Wishing to automate the procedure, an autosampler was used. Its use proved, however, to cause problems in the form of memory effects (peaks generated by contaminants) and insufficient reproducibility.

The method will be characterized by its background pattern (A) and reproducibility (C) under routine conditions. Calibration linearity will be verified and the detection limit will be estimated (B).

(A) Chromatographic background and memory effects under routine conditions

Practically, mixing in seat (APS1) and the two vial mixing programs (APS2 and APS3) were compared. Considerable memory effects occurred with the programs APS1 and APS2 (Fig. 2). Reasonable low background chromatograms were only achieved with the program APS3 (Fig. 2).

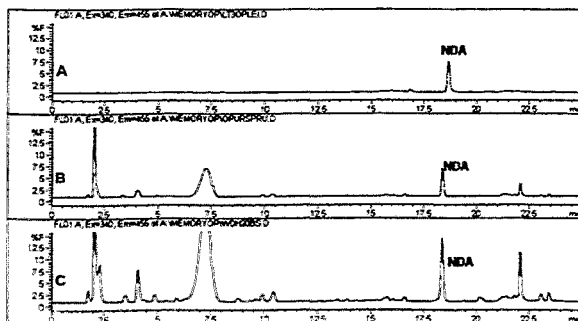


Fig. 2: Blank chromatograms after some each identically handled plasma sample runs, respectively: (A) with the autosampler program APS3 after 45 plasma runs (B) with APS2 after 3 plasma runs and (C) with APS1 after 3 plasma runs.

However, even such low background chromatograms exhibited characteristic peaks, which may result from reagent contamination's.

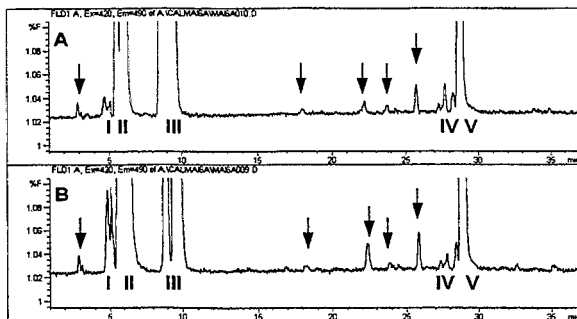


Fig. 3: Examples of calibration runs with different concentrations of substance pairs I - V, revealing a repetitive structure of the background peaks (indicated by arrows); zoomed baseline details. Standard substance pairs I - V were combined on the basis of their similar R_t values.

The zoomed baseline in Fig. 3 shows such peaks, indicated by arrows, together with five double peaks of five pairs of standard amino acids. Remarkably, the retention times of the background peaks and – to a limited extent – their peak heights are reproducible, thus leaving a structured background chromatogram. This structure pattern is most helpful in achieving a low detection limit, expressed as 3σ of the electronic noise. If they are subtracted with the *subtract chromatogram* function of the analysis software, these peaks can be at last ignored.

(B) Calibration curves and limit of detection

Calibration runs were performed with the autosampler program APS3 for most proteinogenic amino acids and some related compounds. Linear calibration curves were obtained for the concentration range from 1 - 70 μM ($r > 0.9999$).

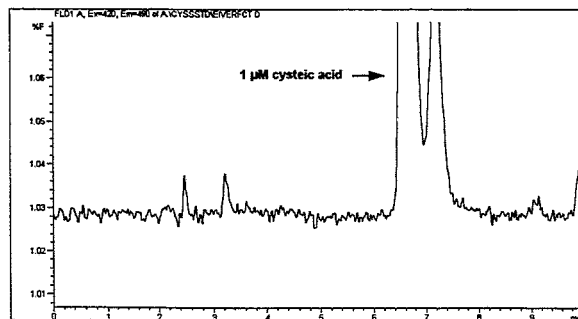


Fig. 4: Zoomed chromatogram detail for the estimation of the electronic noise amplitude σ and of the detection limit.

Fig. 4 was used for estimation of the electronic noise amplitude σ , which was determined to be $\sigma = 0.0036\% F$. With the slope of the calibration curve being $1.2\% F / 1\ \mu\text{M}$ for most substances, the detection limit (3σ) was found to be 9 nM.

The calculated detection limit is valid for a sample dilution factor of 1:4 in the derivatization mixture and corresponds to a total injected amount of 22 fmol. By lowering the dilution factor a mass-based detection limit of 10 fmol might be feasible.

(C) Method reproducibility with plasma samples

At this stage of the studies, amino acids (except proline and lysine) in the deproteinized plasma were separated and detected photometric absorption (VWD) and fluorescence (FLD) detection, as exemplified in Fig. 5. The reproducibility of the whole procedure, i.e. deproteinization, derivatization with the autosampler program APS3 and chromatographic separation, was determined.

The large number of peaks makes time-programmed sensitivity switches of the FLD undesirable due to baseline shifting. Nevertheless, analytes causing a signal overflow in the FLD may be integrated as VWD signal, as can be clearly seen from a comparison of the two chromatograms in Fig. 5. However, an upward extrapolation of the FLD calibration curves is impermissible because of the individual fluorescence quantum efficiencies of each single analyte. Separate calibration curves are therefore necessary for the VWD signals.

The peak areas of the CBI derivatives of Gln, Gly, Val, Leu (VWD) and of Glu, Asn, Carnosine, Met and Ile (FLD) were integrated with the software in the percent area mode. Then the relative standard deviations (RSD) of all runs were calculated (Table 2).

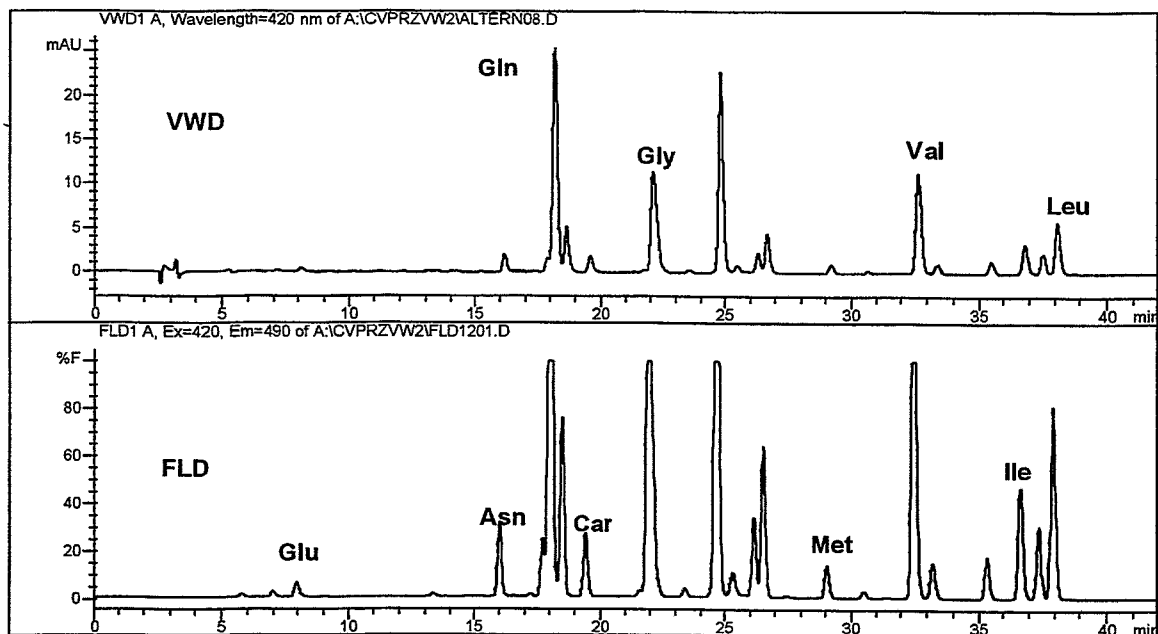


Fig. 5: Representative VWD (variable wavelength detector) and FLD (fluorescence detector) chromatograms of deproteinized plasma (NDA derivatization with autosampler program APS3) obtained with a LiChrospher RP-18 (5 μ M) 250x3 mm column. Only amino acids used for reproducibility studies are assigned.

Table 2: Reproducibility data obtained for the variable wavelength detector (VWD) and the fluorescence detector (FLD). VWD: n = 8; FLD: n = 11. RSD = relative standard deviation.

Detector	VWD signals				FLD signals					FLD signal ratios ("pseudo internal standard")				
	Gln	Gly	Val	Leu	Glu	Asn	Carno- sine	Met	Ile	Asn/ Glu	Carn/ Glu	Asn/ Carn	Carn/ Met	Ile/ Met
Peak area mean [area percent]	23.27	14.21	12.12	5.84	0.68	2.87	2.43	1.25	4.32	4.22	3.61	1.18	1.97	3.51
RSD [%]	1.70	1.40	1.40	1.60	17.56	17.35	12.30	16.92	8.10	0.97	7.23	7.36	12.75	10.40

More highly concentrated substances, as can be seen from Table 2, were analyzed with good reproducibility. Furthermore, this table shows the deterioration of reproducibility with decreasing analyte concentration, mainly due to limited chromatographic resolution. Better results were obtained by the use of internal standards within a given chromatogram region. This is also shown in Table 2 by declaring peak area ratios (pseudo internal standard).

In conclusion it can be said that the combination of precolumn derivatization of amines with naphthalene-2,3-dicarbaldehyde (NDA) in combination with HPLC separation and fluorescence detection proved to be a promising method if specific background problems are solved as proposed in this paper.

References

- [1] Carlson R. G., Srinivasachar K., Givens R. S. and Matuszewski B. K. (1986) New derivatizing agents for amino acids and peptides. 1. Facile synthesis of N-substituted 1-cyanobenz[f]isoindoles and their spectroscopic properties. *J. Org. Chem.* **51**, 3978 - 3983.
- [2] Matuszewski B. K., Givens R. S., Srinivasachar K., Carlson R. G. and Higuchi T. (1987) N-substituted 1-cyanobenz[f]isoindole: Evaluation of fluorescence efficiencies of a new fluorogenic label for primary amines and amino acids. *Anal. Chem.* **59**, 1102 - 1105.
- [3] Roach M. C. and Harmony M. D. (1987) Determination of amino acids at subfemtomole levels by high-performance liquid chromatography with laser-induced fluorescence detection. *Anal. Chem.* **59**, 411 - 415.
- [4] Begley D. J., Reichel A. and Ermisch A. (1994) Simple high-performance liquid chromatographic analysis of free primary amino acid concentrations in rat plasma and cisternal cerebrospinal fluid. *J. Chromatogr. B* **657**, 185 - 191.
- [5] Schuster R. (1988) Determination of amino acids in biological, pharmaceutical, plant and food samples by automated precolumn derivatization and high-performance liquid chromatography. *J. Chromatogr. Biomed. Appl.* **431**, 271 - 284.
- [6] Chromsystems (Instruments & Chemicals GmbH), Martinsried, Germany (Application): Serotonin im Serum/Plasma/Vollblut.

34. High-Affinity Binding of [³H]Paroxetine to Caudate Nucleus and Microvessels from Porcine Brain

P. Brust, R. Bergmann, B. Johannsen

Introduction

The indolamine serotonin (5-hydroxytryptamine, 5-HT) plays not only a role as neurotransmitter in the brain, it represents a signal molecule also in various peripheral organs. A plasma membrane transport system that is specific for this biogenic amine has been described in the brain as well as in a variety of other cell types including platelets, lymphocytes, placental epithelium and astrocytes [1]. It was also found on peripheral endothelial cells in particular in the lung [1]. Early evidence for the presence of a 5-HT transporter also on endothelial cells of the brain was obtained by studies of Spatz and co-workers who have demonstrated specific energy-dependent uptake of 5-HT into brain microvessels [2] and cultured endothelial cells [3]. However, the mechanisms of the 5-HT accumulation remained unclear. Active accumulation of 5-HT may also be mediated by the sodium-coupled noradrenaline transporter [1].

In a previous study, we have demonstrated that the tricyclic antidepressant [³H]imipramine binds specifically to endothelial cells of the porcine brain [4] indicating the presence of a 5-HT transporter with similarity to the neuronal transport system. However, binding studies in the brain have suggested that this ligand interacts with additional binding sites apart from labeling 5-HT uptake sites [5]. Imipramine exhibits significant affinity towards α_1 -adrenergic, histamine, and muscarinic receptors [6]. Recently, it was shown that the 5-HT transporter in brain membranes of humans, rats and mice can be labeled with the nontricyclic antidepressant [³H]paroxetine [1, 7 - 9]. This tracer is a more potent and more selective 5-HT uptake inhibitor which lacks the disadvantage of a complex binding behavior. Only a single class of high-affinity binding sites was demonstrated in both platelets and cerebral cortical membrane preparations from several mammalian species [1]. Recently, the kinetics of [³H]paroxetine in the rat brain was measured after i.v. injection [10]. From the data obtained it was suggested that the presence of a 5-HT transporter in the cerebral microvessels have reduced the effective permeability of [³H]paroxetine *in vivo*. In the present study, we have used [³H]paroxetine to characterize *in vitro* a specific 5-HT transport system on endothelial cells of porcine brain. In order to prove the similarity of the endothelial transport system with the neuronal transporter we have also used membranes of the porcine caudate nucleus, a region in which a high density of 5-HT transporters is expected.

Experimental

Radioligand binding assays were performed on brain membranes and microvessels from porcine brain. Samples of the caudate nucleus were obtained from a local slaughterhouse. Microvessels were prepared from the samples as previously described [4]. They were stored at -20 °C until use in the

binding studies. For membrane preparation the brain tissue was homogenized in 10 volumes of ice-cold buffer (Tris-HCl buffer, pH 7.4, containing 120 mM NaCl, 5 mM KCl) with an Ultra-Turrax T25. The homogenate was centrifuged at 20,000 g for 10 min. The resulting pellet was resuspended with the Ultra-Turrax and centrifuged again at 20,000 g for 10 min. After repeating the same procedure the pellet was resuspended in 10 volumes of buffer and stored at -20 °C until use in the binding studies. All samples were re-homogenized before use.

Binding of [phenyl-6³H]paroxetine (880.6 GBq/mmol, NEN) to the tissue preparations was performed according to published methods [11 - 14]. To study the time dependency of specific binding the samples (4 ml buffer, 0.5 ml isotope dilution, 0.5 ml microvessel suspension containing 0.05 mg protein) were incubated at 22 °C for nine different times (between 1 min and 120 min) with 0.5 nM [³H]paroxetine. An incubation time of 60 minutes was chosen for saturation and competition studies. Non-specific binding was determined in the presence of 1 μM fluoxetine. The binding assays were terminated by rapid filtration over GF/B glass fiber filters (Whatman, Maidstone, England) on the Brandel cell harvester. The filters were presoaked in 0.3 % polyethylenimine. Following four washes with 4-ml portions of ice-cold buffer (see above) the filter paper containing the membrane-bound [³H]paroxetine was transferred into 10 ml of liquid scintillation cocktail (Ultima-Gold, Packard), and the radioactivity on each filter was counted in a Canberra-Packard liquid scintillation counter. Aliquots of the incubation fluid were measured as well. Corrections were made for binding of [³H]paroxetine to the filters. Tracer concentrations between 0.07 and 1.6 nM were used to determine the binding parameters. The K_d and B_{max} values were estimated directly from the binding data by non-linear regression analysis using the program Fig. P (Biosoft, Cambridge, UK) and from the Rosenthal-Scatchard plots by linear regression analysis. Increasing concentrations (between 0.01 nM and 1 μM) of various unlabeled drugs (paroxetine, fluoxetine, citalopram, clomipramine, imipramine, nisoextine, protriptylin, desipramine, serotonin) were competed against a fixed concentration of the radiolabeled ligand (0.22 nM). From the competition curves IC_{50} values were calculated using the program Fig. P. From these data K_i values were calculated using the following equation: $K_i = IC_{50}/(1 + [L]/K_d)$, where [L] is the free tracer concentration. Hill coefficients were calculated after appropriate linear transformation of the data by regression analysis. Each experiment was repeated at least three times. The protein content of the membrane suspensions was measured according to Lowry. The enrichment of the capillary fraction determined by measurement of alkaline phosphatase activity [15] was about 100-fold.

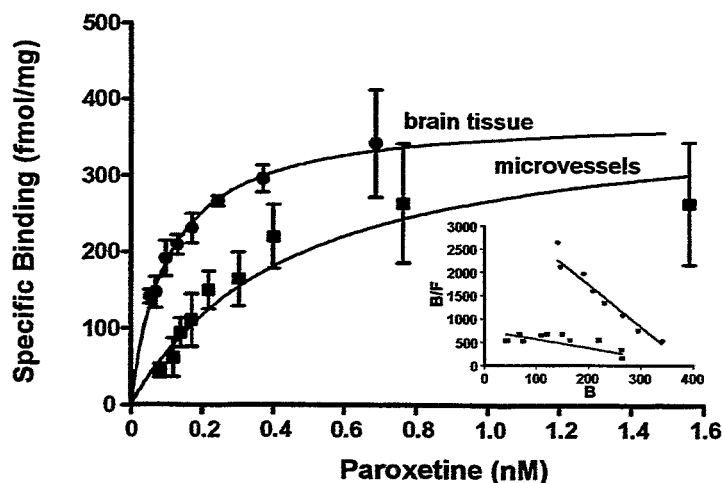


Fig. 1: Saturation analysis of [³H]paroxetine binding to membranes and microvessels prepared from porcine caudate nucleus. Filled squares represent the specific binding of [³H]paroxetine to brain microvessels at free paroxetine concentrations between 0.07 and 1.6 nM. Filled circles represent the specific binding of [³H]paroxetine on caudate nucleus membranes at free paroxetine concentrations between 0.05 and 0.7 nM. Data are means ± S.E.M. The curves were analyzed by a non-linear fitting routine (Fig. P, Biosoft, Cambridge, UK). Graphic analysis of the membrane binding data according to Rosenthal shows a linear plot (inset) in agreement with the existence of a single binding site. Linear regression was used to determine the best fit for the Rosenthal plot.

Results

Saturation studies

The equilibrium of specific [³H]paroxetine binding on porcine brain microvessels was reached after about 60 minutes (data not shown). Therefore, an incubation time of 60 minutes was chosen for saturation and competition studies of both preparations, i.e. membranes of the caudate nucleus and microvessels. Fig. 1 describes the influence of increasing concentrations of [³H]paroxetine (0.07 - 1.6 nM) on the specific binding of the tracer. Kinetic analysis of these binding data, as computed by linear regression analysis from Rosenthal-Scatchard plots, yielded a density of binding sites (B_{max}) of 392 fmol/mg and an equilibrium dissociation constant (K_d) of 0.11 nM in the caudate nucleus membranes and a B_{max} of 398 fmol/mg and a K_d of 0.53 nM in the microvessels. Moreover, the linearity of the plots indicate the presence of only a single binding site. The values obtained are similar to the values estimated from non-linear regression of the saturation curves (membranes: $B_{max} = 382 \pm 12$ fmol/mg, $K_d = 0.10 \pm 0.01$ nM; microvessel: $B_{max} = 392 \pm 59$ fmol/mg, $K_d = 0.47 \pm 0.12$ nM). Hence, the data consistently show that the transporter density in both preparations was similar. However, the affinity was about five-fold lower in the microvessels.

Drug inhibition studies

A wide range of monoamine uptake inhibitors (Table 1) was used to compete with the specific binding of [³H]paroxetine. In these experiments, the concentration of the drugs varied between 0.1 nM and 10 μ M. Inhibition of [³H]paroxetine binding to caudate nucleus membranes by these drugs revealed monophasic competition curves with Hill coefficients close to unity (Table 1), additionally indicating the presence of a uniform set of binding sites with no cooperativity in this preparation. Paroxetine, fluoxetine and clomipramine inhibited the binding with K_i values in the subnanomolar range. All these compounds are powerful inhibitors of the 5-HT transporter in brain, platelets and placenta. Surprisingly, another substance with high selectivity for the 5-HT transporter, citalopram ($K_i = 6.61$), was less potent than imipramine ($K_i = 2.90$). Nisoxetine, which is known to be a selective NE uptake inhibitor, was still rather potent at the [³H]paroxetine binding site ($K_i = 57.9$). This was also the case for other NE uptake inhibitors such as desipramine ($K_i = 36.1$) and protriptylin ($K_i = 35.9$).

Table 1: Inhibition of [³H]paroxetine binding on membranes and microvessels prepared from porcine caudate nucleus.

Compound	Caudate Nucleus		Microvessels	
	K_i	n_H	K_i	n_H
Paroxetine	0.19 ± 0.05	1.09	2.48 ± 0.89	0.71
Clomipramine	0.19 ± 0.04	0.62	n.d.	n.d.
Fluoxetine	0.89 ± 0.12	0.93	1.53 ± 0.48	0.66
Imipramine	2.90 ± 0.49	0.89	31.6 ± 12.3	0.48
Citalopram	6.61 ± 0.64	0.95	n.d.	n.d.
Protriptylin	35.9 ± 7.1	1.04	n.d.	n.d.
Desipramine	36.1 ± 3.1	1.16	205 ± 145	0.81
Nisoxetine	57.9 ± 14.0	0.96	n.d.	n.d.
Serotonin	592 ± 98	0.82	28.2 ± 1.8	0.31

Concentration-dependent inhibition of [³H]paroxetine binding to membranes of porcine caudate nucleus and microvessels was determined at a tracer concentration of 0.22 nM and competitor concentrations between 0.01 nM and 10 μ M. The concentration of drug required to inhibit binding of the radiolabelled ligand by 50 % (IC_{50}) was calculated using Fig. P (Biosoft). K_i values (means \pm S.E.M.) were subsequently calculated using the formula $K_i = IC_{50}/(1+[L]/K_d)$ where [L] is the concentration of the radioligand and K_d is the equilibrium dissociation constant for [³H]paroxetine binding (0.10 nM).

A smaller range of compounds was used to characterize the specific binding of [³H]paroxetine to isolated brain microvessels (Table 1). The data reveal obvious differences to those obtained on the caudate nucleus membranes. The K_i values of paroxetine ($K_i = 2.48$) and imipramine ($K_i = 31.6$) were 13-fold and 11-fold higher than those observed at the membrane preparation. However, the K_i value of fluoxetine ($K_i = 1.53$) was only by factor 1.7 higher than in the membranes. Most surprisingly,

despite the decrease of affinity towards all the selective uptake inhibitors the affinity for serotonin ($K_i = 28.2$) increased by a factor 21 in the microvessel preparation. The Hill coefficients are between 0.31 (serotonin) and 0.81 (desipramine) indicating negative cooperativity between the binding sites.

Discussion

This study has shown that the affinity, but not the density, of [3 H]paroxetine binding is diminished in brain microvessels as compared with membrane preparations from the porcine caudate nucleus. [3 H]paroxetine represents a highly selective 5-HT uptake inhibitor without the disadvantage of a complex binding kinetics as observed using [3 H]imipramine as ligand [4, 11 - 14]. In consideration of the 100-fold enrichment of the microvessel preparation the data clearly indicate the presence of a distinct 5-HT transporter-like protein on the brain endothelial cells.

There are only a few data describing the 5-HT transporter in pigs. Recently, Erreboe *et al.* have investigated [3 H]paroxetine binding in the brain of four different species [8]. The authors found a K_d of 0.11 nM for the pig, which is identical to our value obtained for the caudate nucleus membranes and close to the value calculated for the human brain, but about factor 10 higher than the values found for rat and mouse. Also the binding capacities and dissociation rates measured with different labeled 5-HT uptake inhibitors support the suggestion that there is a greater homology between human and pig than between rat and pig [9]. The human and rat transporter proteins are both 630-amino acid polypeptides, with 92 % overall sequence homology [16]. The sequence of the porcine transporter has not been evaluated yet.

The B_{max} value measured by Erreboe *et al.* was 108 fmol/mg. However, whole brain minus cerebellum was used for the binding studies. This explains the higher B_{max} values found in our study, because regional differences have to be considered. In human, B_{max} values varied among the various brain regions between 60 fmol/mg (cortical regions) and 250 fmol/mg (caudate nucleus) [7, 9].

There is a number of highly potent inhibitors of the 5-HT transporter such as paroxetine, fluoxetine, citalopram, clomipramine and imipramine [12 - 14, 17, 18]. The pharmacological profile of inhibition of high-affinity [3 H]paroxetine binding to platelets or brain membranes by these and other drugs was reported to correlate significantly with the rank order of potency of the drugs to inhibit 5-HT uptake [12]. Therefore, it is generally accepted that this binding site is associated with the sodium-dependent 5-HT transporter [11, 12, 20]. Only a single gene appears to encode 5-HT transporter proteins in brain and the periphery [16]. In our study, the K_i values obtained with the non-tricyclic antidepressants paroxetine and fluoxetine as competitors of [3 H]paroxetine binding were lower than the values of the tricyclic antidepressants imipramine and desipramine. This finding is in agreement with studies of the neuronal and placental 5-HT transporter [11 - 14, 19]. On the other hand, citalopram was less potent than imipramine which may be due to species differences. In our membrane preparation of porcine brain the rank order of potency found for various antagonists (clomipramine < fluoxetine < imipramine < citalopram) closely resembles that observed by others in cloned *human* 5-HT transporters (clomipramine < fluoxetine < citalopram = imipramine) [21] and is different from that found in cloned *rat* 5-HT transporters (clomipramine = citalopram < fluoxetine < imipramine) [14, 21]. Therefore, the pharmacological profile of various 5-HT uptake inhibitors supports the suggestion that the homology between the human and porcine transporter protein is greater than between the rat and pig.

In the microvessels, the affinity measured for [3 H]paroxetine was factor 5 less than in the caudate membranes. In a previous study, we have measured only a small difference of high-affinity [3 H]imipramine binding between brain tissue and microvessels (brain: $K_{d1} = 1.0$ nM, microvessels: $K_{d1} = 1.6$ nM) [4]. The binding capacities in the mentioned study differed by about factor two, whereas the present data reveal similar B_{max} values for [3 H]paroxetine binding. This indicates that paroxetine and imipramine bind, at least partly, to different protein domains as was already suggested by others [5, 8]. Also, the pharmacological profile of various 5-HT uptake inhibitors is different in caudate membranes and microvessels. All substances, with the notable exception of serotonin, expressed lower affinity towards the microvessel preparation. The decrease of affinity was smallest for fluoxetine (factor 1.7) and highest for paroxetine (factor 13). Although the Rosenthal-Scatchard plot was linear in both preparations the Hill coefficients were different. In caudate membranes all n_H values were close to unity while they were considerably smaller in the microvessels suggesting the presence of an additional allosteric binding site as proposed also in other models [7, 8, 21].

Altogether these findings suggest that the [3 H]paroxetine binding sites, expected to represent the transport protein for 5-HT, are different or differently regulated in brain tissue and brain microvessels. Interestingly, similar discrepancies were also found in humans. More than two-fold differences in the affinity of paroxetine binding were observed between various brain regions [7, 9]. The affinities of

fluoxetine and citalopram were much lower to brain tissue [7] than to HeLa cells transfected with cloned human transporters [21] or to placental tissue [19].

The finding that a 5-HT transporter is present in the brain endothelial cells is interesting and important for a number of reasons. The brain endothelial cells are the constitutive elements of the blood-brain barrier. Because of the presence of tight junctions the cells are polarized with two distinct plasma membrane regions, a luminal and a basolateral region. The only other polarized cell type in which a 5-HT transporter is present is the human placental syncytiotrophoblast [13]. The transporter has not been found in intestinal and renal tubular cells [13]. We do not know at this time the physiologic role of a 5-HT transport system in the endothelial cell membrane. Principally, brain endothelial cells may be targets of serotonergic innervation. But 5-HT may reach the endothelium also from the blood side where it is stored in platelets. Therefore, the important question arises whether the transporter is located at the luminal and/or abluminal part of the endothelial plasma membrane. At present, there is no data to support any of these possibilities. It has been suggested that the 5-HT uptake occurs on both sides of the brain endothelium [2]. Interestingly, there is also evidence that 5-HT is synthesized even by the endothelial cells themselves [3]. It may therefore act as an autocrine or endocrine substance on the endothelium being involved in the regulation of the blood-brain barrier permeability [22, 23] and/or the cerebral blood flow [24].

We conclude that in our preparation [³H]paroxetine labels 5-HT uptake sites localized on the brain microvessels. The transport protein has a similar density as in brain tissue. However, the binding affinities towards [³H]paroxetine and a number of other 5-HT uptake inhibitors are reduced while the affinity to serotonin is increased on brain microvessels compared to the brain tissue. Therefore, it is hypothesized that the 5-HT transporters in the brain and microvessels are different or differently regulated proteins.

Acknowledgements

The technical assistance of Mrs. Sonja Lehnert is gratefully acknowledged. This work was supported in part by a research grant from the Saxon State Ministry of Science and Arts (Grant 7541.82-FZR/309).

References

- [1] Graham D. and Langer S. Z. (1988) The neuronal sodium-dependent serotonin transporter: studies with [³H]imipramine and [³H]paroxetine. In: Osborne N. N., Hamon M., eds. *Neuronal Serotonin*. New York: Wiley: pp. 367 - 391.
- [2] Spatz M., Maruki C., Abe T., Rausch W.-D., Abe K. and Merkel N. (1981) The uptake and fate of the radiolabeled 5-hydroxytryptamine in isolated cerebral microvessels. *Brain Res.* **220**, 214 - 219.
- [3] Maruki C., Spatz M., Ueki Y., Nagatsu I. and Bembry, J. (1984) Cerebrovascular endothelial cell culture: metabolism and synthesis of 5-hydroxytryptamine, *J. Neurochem.* **43**, 316 - 319.
- [4] Brust P., Bergmann R. and Johannsen B. (1995) Specific binding of [³H]imipramine indicates the presence of a specific serotonin transport system on endothelial cells of porcine brain. *Neurosci. Lett.* **194**, 1 - 4.
- [5] Mellerup E. T. and Plenge P. (1986) High-affinity binding of [³H]paroxetine and [³H]imipramine to rat neuronal membranes. *Psychopharmacology* **89**, 436 - 439.
- [6] Rudorfer M. V. and Potter W. Z. (1989) Antidepressants: a comparative review of the clinical pharmacology and therapeutic use of the "newer" versus "older" drugs. *Drugs* **37**, 713 - 738.
- [7] Bäckström I., Bäckström M. and Marcusson J. (1989) High affinity [³H]paroxetine binding to serotonin uptake sites in human brain tissue. *Brain Res* **486**, 261 - 268.
- [8] Erreboe I., Plenge P. and Mellerup E. T. (1995) Differences in brain 5-HT transporter dissociation rates among animal species. *Toxicol.* **76**, 376 - 379.
- [9] Dean B., Opeskin K., Pavey G., Naylor L., Hill C., Keks N. and Copolov D.L. (1995) [³H]paroxetine binding is altered in the hippocampus but not the frontal cortex or caudate nucleus from subjects with schizophrenia. *J. Neurochem.* **64**, 1197 - 1202.
- [10] Cumming P. and Gjedde A. (1993) Kinetics of the uptake of [³H]paroxetine in the rat brain. *Synapse* **15**, 124 - 129.
- [11] Habert E., Graham D., Tahraoui L., Claustre Y. and Langer S. Z. (1985) Characterization of [³H]paroxetine binding to rat cortical membranes. *Eur. J. Pharmacol.* **118**, 107 - 114.
- [12] Graham D. and Langer S. Z. (1990) 5-Hydroxytryptamine transport systems. In: Saxena PR, Wallis DI, Wouters W et al., eds. *Cardiovascular Pharmacology of 5-Hydroxytryptamine*.

- Dordrecht: Kluwer Academic Publishers, pp. 15 - 30.
- [13] Cool D. R., Leibach F. H. and Ganapathy V. (1990) High-affinity paroxetine binding to the human placental serotonin transporter. *Am. J. Physiol.* **259**, C196 - C204..
- [14] Cheetham S. C., Viggers J. A., Slater N. A., Heal D. J. and Buckett W. R. (1993) [³H]paroxetine binding in rat frontal cortex strongly correlates with [³H]5-HT uptake - effect of administration of various antidepressant treatments, *Neuropharmacology* **32**, 737 - 743.
- [15] Brust P., Bech A., Kretzschmar R. and Bergmann R. (1994) Developmental changes of enzymes involved in peptide degradation in isolated rat brain microvessels. *Peptides* **15**, 1085 - 1088.
- [16] Lesch K. P., Wolozin B. L., Murphy D. L. and Riederer P. (1993) Primary structure of the human platelet serotonin uptake site - identity with the brain serotonin transporter
J. Neurochem. **60**, 2319 - 2322.
- [17] Langer S. Z., Moret C., Raisman R., Dubocovich M. L. and Briley M. (1980) High-affinity [³H]imipramine binding in rat hypothalamus: association with uptake of serotonin but not norepinephrine. *Science* **210**, 1133 - 1135.
- [18] Sette M., Briley M. S. and Langer S. Z. (1983) Complex inhibition of [³H]imipramine binding by serotonin and nontricyclic serotonin uptake blockers, *J. Neurochem.* **40**, 622 - 628.
- [19] Cool D. R., Leibach F. H. and Ganapathy V. (1990) Interaction of fluoxetine with the human placental serotonin transporter. *Biochem. Pharmacol.* **40**, 2161 - 2167.
- [20] Blakely R. D., Defelice L. J. and Hartzell H. C. (1994) Molecular physiology of norepinephrine and serotonin transporters, *J. Exp. Biol.* **196**, 263 - 281.
- [21] Barker E. L., Kimmel H. L. and Blakely R. D. (1994) Chimeric human and rat serotonin transporters reveal domains involved in recognition of transporter ligands.
Molec. Pharmacol. **46**, 799 - 807.
- [22] Crone C. and Olesen S. P. (1986) Autacoids and changes of capillary permeability.
Prog. Appl. Microcirc. **10**, 21 - 31.
- [23] Sharma H. S., Olsson Y. and Dey P.K. (1990) Changes in blood-brain barrier and cerebral blood flow following elevation of circulation serotonin level in anesthetized rats.
Brain Res. **517**, 215 - 223.
- [24] Miranda F. J., Torregrosa G., Salom J. B., Alabadi J. A., Jover T., Barbera M. D. and Alborch E. (1993) Endothelial modulation of 5-hydroxytryptamine-induced contraction in goat cerebral arteries. *Gen. Pharmacol.* **24**, 649 - 653.

35. Measurement of the Cerebral Uptake and Metabolism of L-6-[¹⁸F] Fluoro-3,4-Dihydroxy phenylalanine in Newborn Piglets

P. Brust, R. Bauer², R. Bergmann, B. Walter², J. Steinbach, F. Füchtner, E. Will, H. Linemann¹, M. Obert, U. Zwiener², B. Johannsen

¹Clinic of Nuclear Medicine, University Hospital Dresden

²Institute of Pathophysiology, Friedrich-Schiller-University Jena

Introduction

Dopamine is a major striatal neurotransmitter. Therefore, it has been given special attention in early brain disorders. Dopamine in immature brain plays an important role in the mechanisms of irreversible disturbances in neuronal metabolism due to moderate to severe brain hypoxia [1]. Age-related increases in the density of dopamine D₁ and dopamine D₂ receptors during human brain development has been described [2, 3]. Because the in vivo dopamine synthesis appears to be regulated by D₂ receptors [4] one may expect that changes of the rate of dopamine synthesis occur during brain development. Knowledge of these processes may be of importance for the understanding of the genesis of parkinsons disease and other brain disorders.

However, available information on the catecholamine metabolism in the immature brain is very fragmentary. L-6-[¹⁸F] fluoro-3,4-dihydroxyphenylalanine (FDOPA) has been used as a tracer to estimate the activity of the dopamine synthesizing enzyme DOPA-decarboxylase (DDC; EC 4.1.1.28) with positron emission tomography (PET) in human brain [5, 6]. The clinical significance of this method has been demonstrated [7, 8].

Data allowing insights in the regulation of dopamine synthesis during ontogenesis are difficult to obtain in humans. In order to find a useful model, we have performed PET experiments with newborn piglets using FDOPA as tracer.

Experimental

Six male newborn piglets in age from 2 to 6 days and weighing between 1,8 and 3,2 kg were anesthetized with 0.5 % isoflurane in a gas mixture of 70 % nitrous oxide and 30 % oxygen via endotracheal tube using a volume-controlled ventilator. Blood gases, blood glucose and lactate, blood pressure, EEG and ECG were monitored before and during the PET study. No statistically significant differences were found (data not shown).

Cerebral blood flow (CBF) was measured using the reference sample method with coloured microspheres and was calculated from the following formula: $CBF = (A_t \times Q_r) / (A_r \times W_t) \times 100$, where A_t , Q_r , A_r , W_t are tissue absorption, reference blood withdrawal rate, reference blood absorption and tissue weight.

Cerebral blood volume (CBV) was measured in separate animals of the same age after i.v. injection of 20 - 30 MBq $^{99m}\text{TcO}_4^-$ in saline under the same conditions as described. Euthanization by i.v. injection of saturated KCl occurred 5 min after injection. CBV was calculated from the following formula: $CBV = (A_t \times W_b) / (A_b \times W_t) \times 100$, where A_t , A_b , W_t , W_b are tissue activity, blood activity, tissue weight and blood weight.

PET studies were performed using the positron emission tomograph POSITOME IIIp (Montreal Neurological Institute). The 2-ring tomograph acquires three slices with an axial slice thickness (FWHM) of 15 mm, a spatial resolution (transaxial) of 11 mm and an axial field of view of 5 cm. Attenuation correction was performed using transmission scans with two rotating ^{68}Ge point sources. FDOPA was produced according to the destannylation method [9] by direct fluorination of the tin precursor with $^{18}\text{F}\text{F}_2$ simplifying the procedure (to be published). The process takes 40 min, the overall decay corrected yield is in the range of 16 to 20 %.

A total of 30 - 50 MBq FDOPA in 5-10 ml saline was injected into the lower caval vein over 1 min with an automated infusion pump. Emission scanning began simultaneously with the start of FDOPA injection. Dynamic scan data were acquired in list mode between 0 and 120 min with 35 frames between 30 and 600 s each. The time course of plasma ^{18}F radioactivity was determined by arterial blood sampling from the abdominal aorta. Twenty five 15 sec samples and fifteen 1 min samples were taken by a precision peristaltic pump. Nine discrete samples were taken during the remaining time period. The samples were stored on ice and centrifuged to obtain plasma. Plasma activity in 100 μl was measured in a well counter (COBRA II) cross-calibrated with the tomograph. In additional nine blood samples taken at 2, 4, 8, 12, 16, 25, 50, 90 and 120 min p.i. plasma metabolites of FDOPA were measured using HPLC with radiochemical detection.

The HPLC-system consisted of a Hewlett-Packard 1050 pump with autosampler (0.5 ml sample loop) and a flow-through radioactivity detector (Flow One Beta A 100, Caberra Packard) with high γ - γ coincidence detection efficiency. A C18 reverse-phase column (125 x 4 mm, LiChrospher 100, 5 μm) and a preguard column (4 x 4 mm, LiChrospher 100, 5 μm) were used for separation of metabolite peaks with the following eluents: A: H_2O (0.1 % acetic acid), B: Acetonitril: H_2O = 80:20 (0.1 % acetic acid) at a flow rate of 1 ml/min and a temperature of 30 $^\circ\text{C}$ (start: A:B = 100:0, end (15 min): A:B = 60:40).

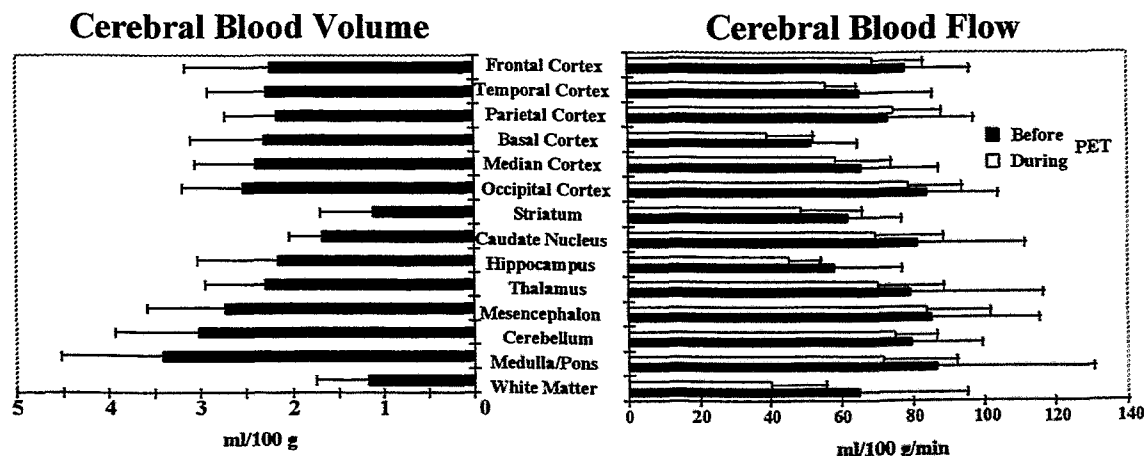


Fig. 1: Local cerebral blood volume and cerebral blood flow (CBF) in newborn piglets (means \pm S.D.). CBF was measured before and during the PET study. No significant differences were found.

Results

The values of CBV measured in separate animals are shown in Fig. 1. The data varied between 1.18 ml 100g⁻¹ (white matter) and 3.41 ml 100g⁻¹ (pons/medulla oblongata). They were given as a constant parameter in the fitting routine which was used to estimate the transfer coefficients of FDOPA. The CBF was measured before and simultaneously with the PET study (Fig. 1). No significant differences were found between these two measurements. The values during the PET study varied between 40 ml 100 g⁻¹ min⁻¹ (white matter) and 84 ml 100 g⁻¹ min⁻¹ (mesencephalon). The respective data were used to calculate the regional permeability-surface (*PS*) product of the blood-brain barrier for FDOPA (Table 1).

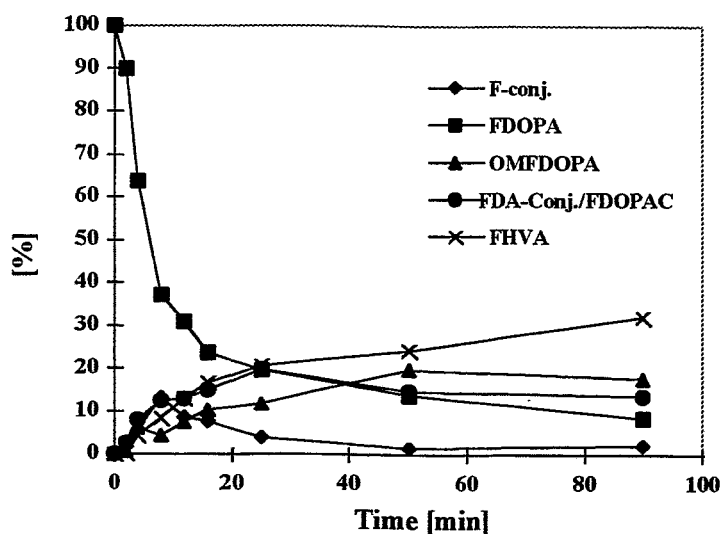


Fig. 2: Relative amounts of FDOPA metabolites in porcine plasma as function of time based on HPLC-determined plasma fractions of six piglets (means \pm S.D.).

The distribution of FDOPA metabolites in plasma was measured by HPLC (Fig. 2). From the plasma time-activity curves of FDOPA and OMe-FDOPA the rate constants of peripheral synthesis ($k_0^D = 0.0080 \pm 0.0014$ min⁻¹) and elimination ($k_1^M = 0.0009 \pm 0.0010$ min⁻¹) of OMe-FDOPA were calculated. The plasma input function for the estimation of FDOPA transfer coefficients was obtained by correction of the plasma time-activity curves of ¹⁸F with the fraction of metabolites calculated from the HPLC data.

The distribution of radioactivity occurs between the intravascular space, the extravascular precursor pool and the metabolite compartment and is described by nine transfer coefficients [5, 6]. This includes transfer coefficients for OMe-FDOPA since this compound is able to cross the blood-brain barrier. This complicates the estimation of separate rate constants for FDOPA. Our estimation of the parameters for blood-brain and brain-blood transfer, K_1 and k_2 (Table 1), includes both FDOPA and OMe-FDOPA which is expected to result in an overestimation of the FDOPA precursor pool and an underestimation of the decarboxylation rate of FDOPA k_3 .

Table 1: Kinetic transfer coefficients of ¹⁸F accumulation in the brain, partition volume (V_e) and *PS*-product of blood-brain transfer in newborn piglets

	Frontal Cortex	Striatum
K_1 (ml g ⁻¹ min ⁻¹)	0.057 \pm 0.017	0.068 \pm 0.021
k_2 (min ⁻¹)	0.056 \pm 0.022	0.081 \pm 0.033
k_3 (min ⁻¹)	0.026 \pm 0.016	0.038 \pm 0.017
k_4 (min ⁻¹)	0.038 \pm 0.019	0.035 \pm 0.007
V_e (ml ml ⁻¹)	1.1 \pm 0.2	0.9 \pm 0.1
<i>PS</i> (ml g ⁻¹ min ⁻¹)	0.060 \pm 0.019	0.072 \pm 0.024

Transfer coefficients of FDOPA were obtained from brain time-activity curves of six individual experiments (Fig. 3) and the respective plasma input functions. The values of K_1 , k_2 and k_3 estimated in the striatum are 19 %, 45 % and 46 % higher than in the frontal cortex. The rate constant k_4 , which accounts for the clearance of labelled metabolites from tissue, is similar in frontal cortex and striatum.

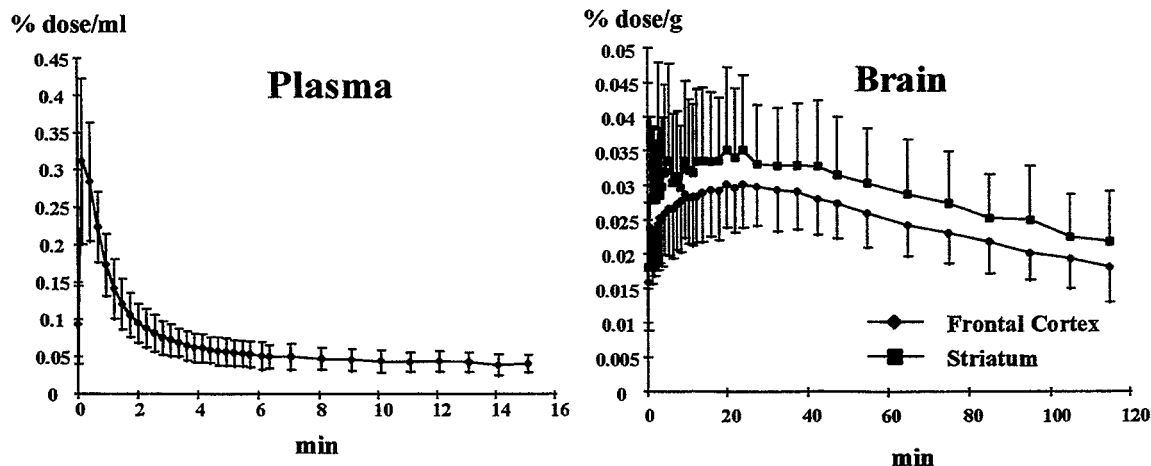


Fig. 3: Normalized time-activity curves ($n = 6$) of ^{18}F in plasma and brain of newborn piglets.

Discussion

We have measured the cerebral uptake and metabolism of FDOPA in newborn piglets in order to find a useful model to study the regulation of the dopamine synthesis during ontogenesis. There is a lack of data related to this aspect of dopamine synthesis. On the other hand, conflicting data regarding an influence of normal aging on the presynaptic nigrostriatal dopaminergic function exist [10].

FDOPA is a potential substrate for DDC the ultimate enzyme in dopamine synthesis in terminals of the dopaminergic nigrostriatal pathway [11, 12]. From *in vitro* data it is expected that DDC activity is in great excess with respect to the synthesis of dopamine and that tyrosine hydroxylase is the rate limiting enzyme because it is nearly saturated with tyrosine [for references see 12]. Despite this there is evidence that the activity of DDC is modulated by neuronal activity [13, 14] which may be related to the rate-limiting step in the synthesis of 2-phenylethylamine, a putative modulator of dopamine transmission.

Until now there were no data available about the FDOPA metabolism in pigs. Using HPLC we have identified in plasma the major metabolites of FDOPA. In rats and humans [11, 15, 16] FDOPA undergoes a rapid metabolism by *O*-methylation (k_0^D) which mainly reflects hepatic COMT activity. In our study a methylation rate was estimated which is 40 % and 90 % less than those observed in humans [5, 16] and rats [11], respectively. The rate constant of elimination of OMe-FDOPA (k_{-1}^M), which presumably is related to renal elimination, is about 50 % smaller than in rats but comparable to humans.

Our values for K_1 and k_2 are about 50 % - 80 % higher than those in rats and humans [6, 17] which may be due to the inclusion of OMe-FDOPA in our estimation. It is reported that the blood-brain transfer (K_1) and brain-blood transfer (k_2) of OMe-FDOPA is about twice of FDOPA [17]. The average value of the decarboxylation rate constant (k_3) in striatum was 0.036 min^{-1} which is close to values measured in the striatum of adult humans [5, 6, 18]. We expect our value to be underestimated from the reason mentioned above and because of the partial volume effect which is related to the rather low spatial resolution of the tomograph. This may also explain the low ratio of k_3 between striatum and frontal cortex. We have found about 50 % higher rate of decarboxylation in striatum than in frontal cortex. In humans a five-fold difference was found [5, 18].

We conclude that PET measurements with FDOPA may serve as a useful tool to estimate the activity of DDC in the immature porcine brain. Some of the limitations of the present study will be overcome by future use of a tomograph with a higher spatial resolution and by inclusion of separate input functions of FDOPA and OMe-FDOPA.

Acknowledgements

This work was supported in part by research grants from the Saxon State Ministry of Science and Arts (Grant 7541.82-FZR/309) and from the Thuringian State Ministry of Science, Research and Arts (Grant 3/95-13). The excellent technical assistance of Mrs. R. Scholz, Mrs. R. Herrlich and Mrs. U. Jaeger is gratefully acknowledged.

References

- [1] Huang C. C., Lajevardi N. S., Tammela O., Pastuszko A., Delivoria-Papadopoulos M. and Wilson D. F. (1994) Relationship of extracellular dopamine in striatum of newborn piglets to cortical oxygen pressure. *Neurochem. Res.* **19**, 649 - 655.
- [2] Srivastava L. K. and Mishra R. K. (1994) Dopamine receptor gene expression: effects of neuroleptics, denervation, and development. In: *Dopamine Receptors and Transporters* (H.B. Niznik, ed.) Marcel Dekker Inc., New York, pp. 437 - 457.
- [3] Unis A. S. (1994) Ontogeny of [H-3]-Sch23390 and [H-3]-YM09151-2 binding sites in human fetal forebrain. *Biol. Psychiat.* **35**, 562 - 569.
- [4] Richard M. G. and Bennett J. P. (1994) Regulation by D₂ dopamine receptors of *in vivo* dopamine synthesis in striata of rats and mice with experimental. *Exp. Neurol.* **129**, 57 - 63.
- [5] Gjedde A., Reith J., Dyve S., Leger G., Guttman M., Diksic M., Evans A. and Kuwabara, H. (1991) Dopa decarboxylase activity of the living human brain. *Proc. Natl. Acad. Sci.* **88**, 2721 - 2725.
- [6] Huang S.-C., Yu D.-C., Barrio J. R., Grafton S., Melega W. P., Hoffman J. M., Satyamurthy N., Mazziotta J. C. and Phelps M. E. (1991) Kinetics and modeling of L-6-[¹⁸F]fluoro-DOPA in human positron emission tomographic studies. *J. Cerebr. Blood Flow Metab.* **11**, 898 - 913.
- [7] Kuwabara H., Cumming P., Yasuhara Y., Leger G. C., Guttman M., Diksic M., Evans A. C. and Gjedde A. (1995) Regional striatal DOPA transport and decarboxylase activity in parkinson's disease. *J. Nucl. Med.* **36**, 1226 - 1231.
- [8] Ishikawa T., Dhawan V., Chaly T., Margoueff C., Robeson W., Dahl J. R., Mandel F., Spetsieris P. and Eidelberg D. (1996) Clinical significance of striatal DOPA decarboxylase activity in parkinson's disease. *J. Nucl. Med.* **37**, 216 - 222.
- [9] Namavari M., Bishop A., Satyamurthy N., Bida G. and Barrio J. R. (1992) *Appl. Radiat. Isot.* **43**, 989 - 996.
- [10] Eidelberg D., Takikawa S., Dhawan V., Chaly T., Robeson W., Dahl R., Margoueff D., Moeller J. R., Patlak C. S. and Fahn S. (1993) Striatal ¹⁸F-DOPA uptake: absence of an aging effect. *J. Cerebr. Blood Flow Metab.* **13**, 881 - 888.
- [11] Cumming P., Kuwabara H. and Gjedde A. (1994) A kinetic analysis of 6-[F-18]fluoro-L-dihydroxyphenylalanine metabolism in the rat. *J. Neurochem.* **63**, 1675 - 1682.
- [12] Cumming P., Kuwabara H., Ase A. and Gjedde A. (1995) Regulation of DOPA decarboxylase activity in brain of living rat. *J. Neurochem.* **65**, 1381 - 1390.
- [13] Rosetti Z., Krajnc D., Neff N. H. and Hadjiconstantinou M. (1989) Modulation of retinal aromatic L-amino acid decarboxylase via α₂ adrenoceptors. *J. Neurochem.* **52**, 647 - 652.
- [14] Zhu M. Y., Juorio A. V., Paterson I. A., Boulton A. A. (1992) Regulation of aromatic L-amino acid decarboxylase by dopamine receptors in the rat brain. *J. Neurochem.* **58**, 636 - 641.
- [15] Melega W. P., Luxen A., Perlmutter M. M., Nissenson C. H. K., Phelps M. E. and Barrio J. R. (1990) Comparative *in vivo* metabolism of 6-[¹⁸F]fluoro-L-DOPA and [³H]L-DOPA in rats. *Biochem. Pharmacol.* **39**, 1853 - 1860.
- [16] Cumming P., Léger G. C., Kuwabara H. and Gjedde A. (1993) Pharmacokinetics of plasma 6-[¹⁸F]fluoro-L-3,4-dihydroxyphenylalanine (¹⁸F)FDOPA) in humans. *J. Cerebr. Blood Flow Metab.* **13**, 668 - 675.
- [17] Reith J., Dyve S., Kuwabara H., Guttman M., Diksic M. and Gjedde A. (1990) Blood-brain transfer and metabolism of 6-[¹⁸F]fluoro-L-DOPA in rat. *J. Cerebr. Blood Flow Metab.* **10**, 707 - 719.
- [18] Dhawan V., Ishikawa T., Patlak C., Chaly T., Robeson W., Belakhlef A., Margoueff C., Mandel F. and Eidelberg D. (1996) Combined FDOPA and 30MFD PET studies in parkinson's disease. *J. Nucl. Med.* **37**, 209 - 216.

36. High Yield Preparation of 6- ^{18}F Fluoro-DOPA

F. Füchtner¹, K. Günther¹, J. Steinbach, R. Lücke, R. Scholz², R. Hüller

¹Gemeinschaftspraxis für Radiologie und Nuklearmedizin, Leipzig

²Technische Universität Dresden, Klinik für Nuklearmedizin

Introduction

Because of the usefulness of 6- ^{18}F fluoro-L-DOPA (^{18}F -DOPA) for assessing dopamine metabolism, ^{18}F -DOPA is one of the standard PET radiopharmaceuticals [1, 2]. But in contrast to ^{18}F -FDG, a method which yields large amounts of ^{18}F -DOPA is not yet available despite enormous efforts [3, 4].

Based on the regioselective destannylation method by Namavari *et al.* [3], we went to improving, simplifying the procedure and increasing the yield. Since 1994 we have been producing ^{18}F -DOPA for investigation of the effects of asphyxia and dopamine metabolism in newborn piglets.

Experimental

An apparatus for routine production based on electrophilic reaction was set up.

The schematic layout of the ^{18}F -DOPA preparation unit is shown in Fig. 1.

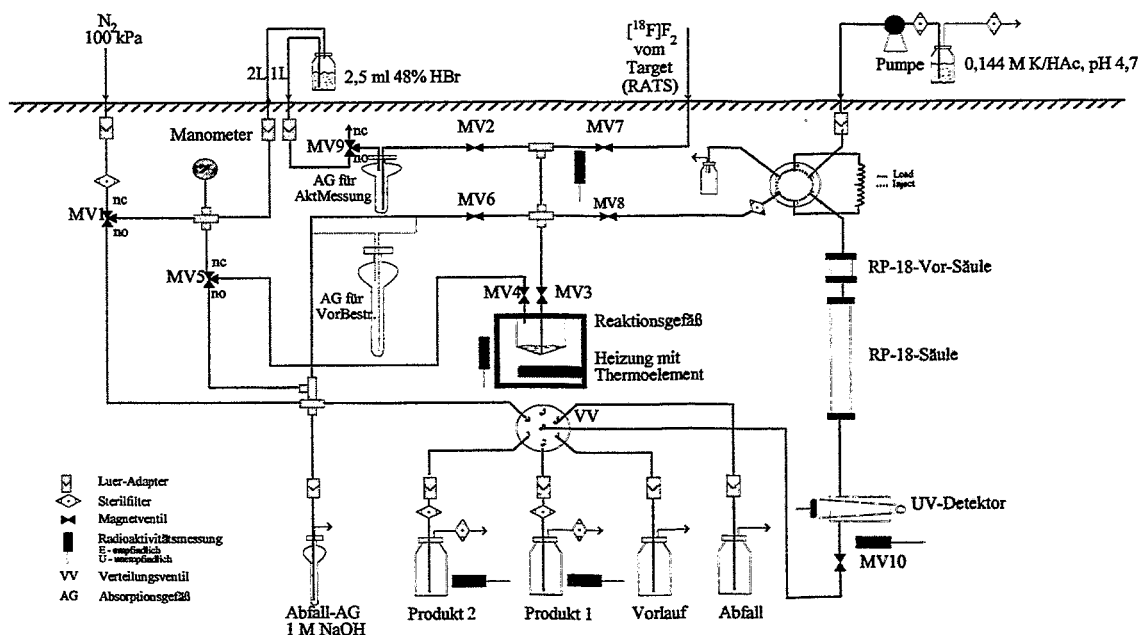


Fig. 1: Schematic presentation of the apparatus for routine production of ^{18}F -DOPA

The device consists of two main parts, the processing unit situated inside the hot cell and its control unit. A pump and radiation monitors are used in addition. All parts of the processing unit, such as the reaction vessel, purification columns, electro-magnetic and electric stream selection valves, fittings, tubes, a waste absorber, electrical and tube connectors, Geiger-Müller tubes and the manometer, are mounted on a stainless steel housing. The processing unit is remote controlled by the control unit. The PTFE tubes for the target gas, the compressed N_2 (for delivering the liquids), and the vessels containing the liquids needed for the synthesis are connected to the synthesis unit by Luer adapters.

^{18}F - F_2 is produced by the $^{20}\text{Ne}(d,\alpha)^{18}\text{F}$ reaction, using the 13.5 MeV deuterons of the Rossendorf cyclotron U-120 with $\text{Ne} + 0.2\% \text{F}_2$ (100 μmol) as target gas. The target gas is forced by its own pressure (2 MPa at the beginning) through the transporting copper tube (about 500 m). After being discharged from the target by its own pressure, the ^{18}F - F_2 is transported to the synthesis unit using N_2 as a carrier gas with a pressure of 0.5 MPa.

All parts of the equipment which come into contact with the precursors and the radiopharmaceutical are newly assembled for each production cycle from sterilized glassware and tubing. Before using the equipment, the liquid system and especially the chromatographic columns are cleaned by washing them with sterilized water to ensure that the system is free of endotoxins (apyrogenicity).

To increase the efficiency of absorption, the [^{18}F] F_2 is absorbed in a special Vigreux absorption column containing a precursor solution of 60 mg N-formyl-3,4-di-boc-6-(trimethylstannyl)-L-DOPA ethyl ester in 15 ml trichlorofluoromethane (CFCl_3 , freon 11). This arrangement also makes it possible to measure the starting activity by a dose calibrator. Under these conditions the reaction between the precursor and the gaseous [^{18}F] F_2 takes about 13 minutes. The volume of the solvent is reduced to about 5 ml by evaporation during absorption.

After absorption of [^{18}F] F_2 2.5 ml 48 % HBr are added and this mixture is transferred into the reaction vessel. The temperature is increased to 70 °C while the remaining solvent is evaporated by blowing in gaseous N_2 . After evaporation the temperature is increased to 130 °C for 5 minutes to reach the conditions for hydrolysis.

After hydrolysis the reaction mixture is directly transferred to the 5 ml loop by on-line filtration through a 0.22 μm filter without any treatment. After cooling down for 2 minutes the product is injected into the HPLC column.

Conditions for preparative HPLC:

- column: RP-18, LiChrosorb, 7 μm , 250 mm x 10 mm,
- guard column: LiChrospher RP-18, 5-20 μm , 30 mm x 9 mm,
- sample volume: 2.5 ml,
- injection loop: 5 ml,
- eluent: 105.6 mM of CH_3COONa and CH_3COOH , pH 4.7, isotonic, prepared with sterilized water, (aqua ad iniectionem),
- flow rate: 3 ml/min,
- pressure: about 6 MPa,
- detection: UV, 1 mm path length, 280 nm, radioactivity.

Fractionation of the eluent in the foreruns and [^{18}F]F-DOPA-fraction is carried out by monitoring radioactivity and the UV-signal on the outlet of the column and by switching the stream selection valve accordingly.

The main radioactive peak ([^{18}F]F-DOPA) is eluted after about 11 minutes. The sterilization of the final product is achieved by sterile filtration of the eluent.

According to the rules of good manufacturing practice (GMP), quality control of the final product is an essential part of the quality assurance of radiopharmaceutical production. The product has only been characterized by HPLC, GC/MS, pH and Osmometer, because of its use for animal experiments.

Results

The total preparation time of [^{18}F]F-DOPA after EOB, including the radionuclide transport, takes about 40 minutes. The total [^{18}F]F-DOPA yield is between 30 and 35 % (decay corrected) with good reproducibility. Starting from [^{18}F] F_2 a maximum yield of 50 % can be achieved due to the chemical background. Depending on the starting activity up to 1 GBq [^{18}F]F-DOPA is available.

The processing unit enables the [^{18}F]F-DOPA synthesis to be repeated twice without handling the processing unit in the hot cell. For an effective transport of the [^{18}F] F_2 over a distance of 500 m, the copper tube must be preconditioned with cold F_2 .

The in-line process control involved includes the monitoring of the reaction vessel temperature, of the radioactivity level on the transporting tube and of the reaction vessel as well as the pressure of the HPLC pump during the whole procedure. Fig. 2 shows the process data of the seven integrated sensors.

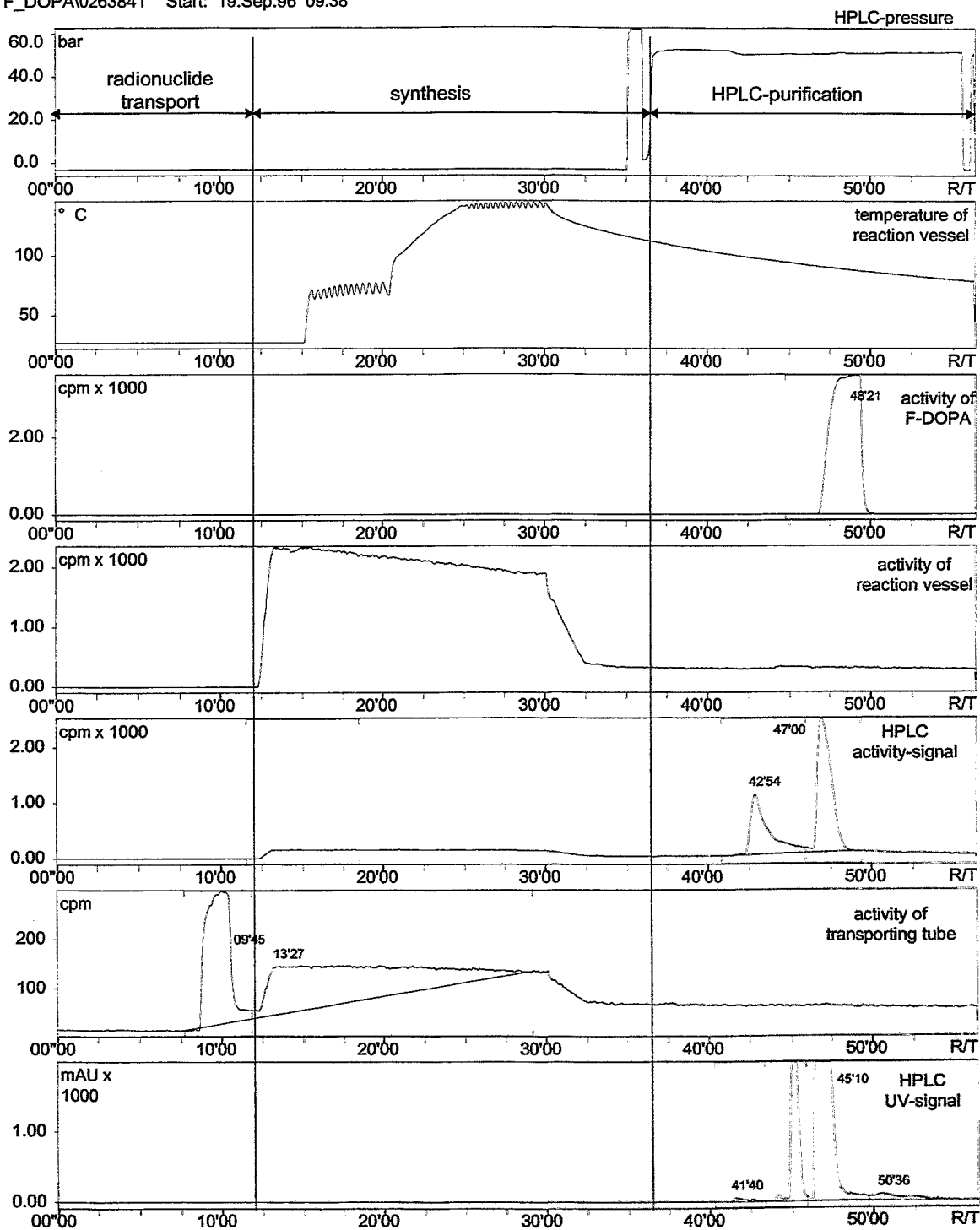


Fig. 2: Process data during [¹⁸F]F-DOPA preparation

The product is characterized by the following quality parameters:

Parameter	Method	Limit	Average value
- Radiochemical purity:	HPLC	> 95 %	> 98 %
- Chemical purity:	HPLC GC/MS	[F-DOPA] > 95 %	> 98 %
		[Freon 11] < 50 µg/ml	< 3 µg/ml
		[Ethanol] < 1 mg/ml	< 10 µg/ml
		[Acetonitrile] < 50 µg/ml	< 25 µg/ml
- Pharmaceutical parameters:	pH	4 - 5	4.7
	Osmolality	280 - 320 mOsmol/kg	304 mOsmol/kg

The pH value of the eluent plays an important role and should not exceed 5, otherwise the final product is not stable enough and the colour of the solution becomes light violet.

The F-DOPA concentration was found to be between 1.5 and 2.5 µg/ml depending on the cold F₂-concentration of the target gas.

We will shortly be setting up an automatically controlled synthesis unit for [¹⁸F]F-DOPA production.

References

- [1] Garnett E. S., Firnau G. and Namias C. (1983) Dopamine visualized in the basal ganglia of living man. *Nature* **305**, 137 - 138.
- [2] Meyer G.-J., Waters S. L. and Coenen, H. H. (1995) PET radiopharmaceuticals in Europe: current use and data relevant for the formulation of summaries of product characteristics (SPCs). *Eur. J. Nucl. Med.* **22**, 1420 - 1432.
- [3] Namavari M., Bishop A., Satyamurthy N., Bida G. and Barrio J. R. (1992) Regioselective radio-destannylation with [¹⁸F]F₂ and [¹⁸F]CH₃COOF: a high yield synthesis of 6-[¹⁸F]fluoro-L-dopa. *Appl. Radiat. Isot.* **43**, 989 - 996.
- [4] Bergman J., Haaparanta M. and Lehikoinen P. (1993) Electrophilic synthesis of 6-[¹⁸F]-fluoro-L-DOPA, starting from aqueous [¹⁸F]-fluoride, Tenth International Symposium on Radiopharmaceutical Chemistry, Kyoto, Japan, 25.-28. October, 476

37. Modified Access to the Thioester Precursor of [^{14}C](+)-McN-5652-Z

J. Zessin, J. Steinbach

Introduction

In the early eighties Maryanoff and co-workers [1-3] synthesized a number of hexahydro-6-arylpyrroloisoquinolines (**1**) as potential antidepressants. Some of them are potent inhibitors of the uptake sites of dopamine, norepinephrine or serotonin (5-HT) and regulate the concentration of these neurotransmitters in the synaptical cleft. Such compounds can therefore be used as antidepressants.

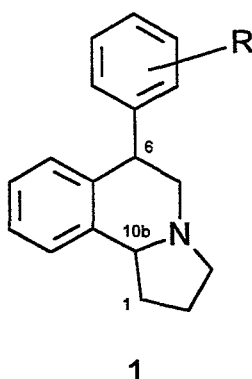


Fig. 1. General structure of pyrroloisoquinoline antidepressants

Especially the compound McN-5652-Z (**1**, R = 4-S-CH₃) was identified as a highly potent blocker of the 5-HT uptake site. This is reflected by a K_i value in the nanomolar range for inhibition of [^3H]5-HT binding to rat cerebral cortex. For example, K_i of the racemic trans compound is 0.6 nM [4]. This is a prerequisite for its use as an ^{14}C labelled radiotracer for positron emission tomography (PET) [5]. This radiotracer can be used for studies of the serotonergic neurons in the case of depressions, suicidality or drug abuse.

In comparison to other potential PET radioligands for imaging the 5-HT uptake sites, such as [^{14}C]citalopram or [^{14}C]fluoxetine, [^{14}C]McN-5652-Z (racemic mixture) shows a satisfactory ratio between hypothalamus and cerebellum. It reached 4.6 in the brain of mice after 90 min [6]. Consequently, [^{14}C]McN-5652-Z is known to be the most potent PET tracer for imaging the 5-HT transporter.

The selectivity of the inhibition of serotonin uptake sites is strongly dependent on the stereochemistry of McN-5652. Of the four diastereomers and enantiomers the trans-(+)-6S,10bR compound ((+)-McN-5652-Z) has the highest potency as a 5-HT transporter blocker [4,7]. In the case of injection of the radiolabelled enantiomerically pure [^{14}C](+)-McN-5652-Z into mice, the hypothalamus-to-cerebellum ratio increased to 6 [8]. In the human brain the midbrain-to-cerebellum ratio was 1.8 ((+)-enantiomer) after 115 min [9].

The radiotracer [^{14}C]McN-5652-Z was prepared by S-methylation of normethyl McN-5652-Z with [^{14}C]methyl iodide [5,10]. This precursor can be synthesized by demethylation of authentic McN-5652-Z with sodium thiomethoxide and subsequent esterification with acetyl chloride to stabilize it.

The demethylation reaction was carried out in dimethylformamide at 160 °C. Under these conditions this reaction was accompanied by a cis-trans isomerization. After 1 h, the time needed for complete cleavage of the thioether, a mixture of nearly 40 % trans diastereomer and 60 % cis diastereomer is obtained. This ratio represents the equilibrium concentrations and does not depend on the initial isomer ratio. In this way the yield of the biologically active diastereomer is remarkably reduced.

For this reason we developed an improved synthetic route based on the demethylation of McN-5652-Z with sodium amide (sodium in liquid ammonia). The isomerization reaction was strongly suppressed in this synthesis. Starting with the pure trans diastereomer of McN-5652-Z, the yield of the trans compound was increased up to about 80 %.

Experimental

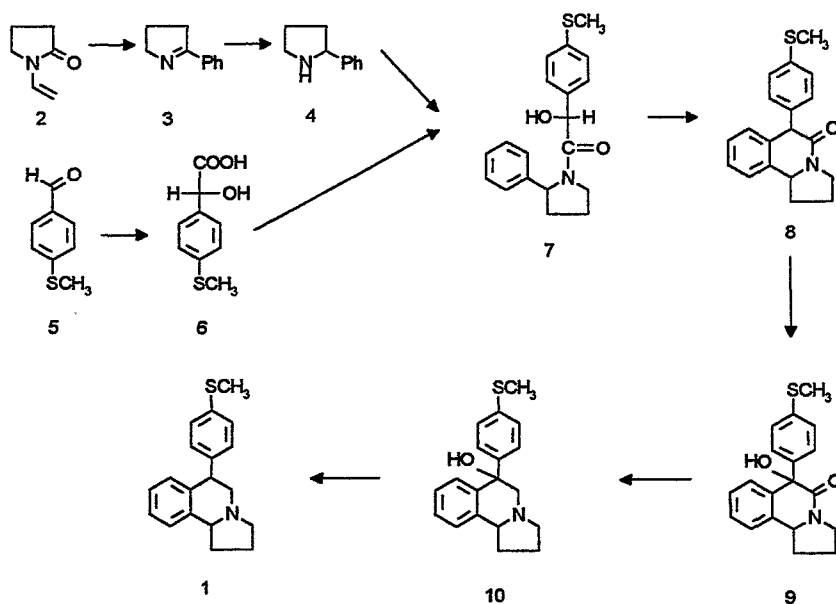
General

Reagents and solvents were obtained from Aldrich, Fluka and the BAYER AG. N-Vinyl-2-pyrrolidinone was freshly distilled before use. All other substances were used without further purification.

(+)-McN-5652-Z, general procedure

The authentic McN-5652-Z **1** was prepared in a nine-step synthesis as described by Maryanoff and co-workers [2, 13]. The synthetic route is represented in Scheme 1. 2-Phenylpyrroline (**4**) was synthesized according to Jacob [11]. 4-Methylthiomandelic acid (**6**) was prepared as described by Compere [12]. Most of the intermediate products in the following steps were used without further purification. Differences from this general synthetic route for **4**, **9** and **11** are described.

Scheme 1. Scheme of McN-5652-Z synthesis



2-Phenylpyrrolidine (4)

The hydrogenation of 2-phenylpyrroline was performed by dimethylamine borane, following the procedure of Billman *et al.* [15].

A solution of freshly distilled 2-phenylpyrroline (**3**) (0.37 mol, 54.2 g) in acetic acid (100 ml) was added to a solution of borane-dimethylamine complex (0.42 mol, 25 g) in acetic acid (100 ml) at 20 °C. This mixture was stirred for 4 h at room temperature.

Sodium hydroxide solution (4 M) was added to the cooled reaction mixture until a pH of 12 was reached. The temperature was not allowed to exceed 30 °C as 2-phenylpyrrolidine may react with acetic acid to the acetamide of **4**. The resulting suspension was extracted three times with ether, the combined organic extracts were dried with sodium sulphate and the solvent was removed in vacuo. The residue was distilled under vacuo.

Yield: 48.4 g (88 %) colourless liquid

Boiling point: 123 - 125 °C/ 3.5 kPa

Melting point of picrate: 149 - 150 °C (from EtOH)

(+)-McN-5652-Z

The hydroxy lactam **9** was purified by flash chromatography (silica gel 60, petroleum ether/ethyl acetate, 1:4). After the next two steps the final product **1** (R=4-SCH₃) was flash chromatographed (silica gel 60, petroleum ether/ethanol/ dichloromethane 22.5/15/5) to afford McN-5652-Z as a light brown viscous oil. The ratio between trans and cis isomer was 92:8 (determined by HPLC).

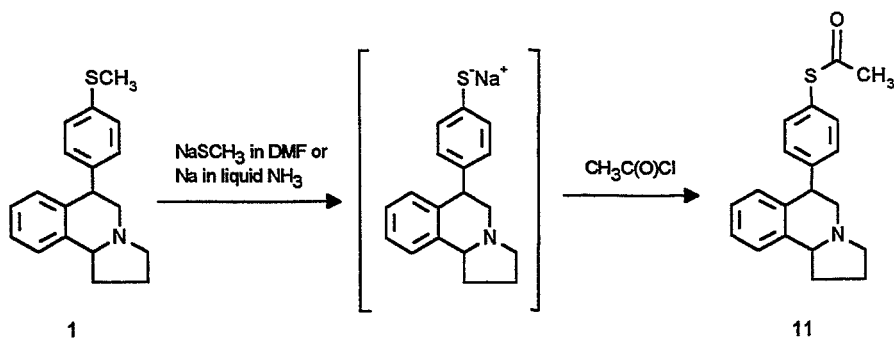
For resolution purposes purified McN-5652-Z and (+)-L-tartaric acid (molar ratios) were combined in hot acetonitrile and allowed to stand at ambient temperature for one week. The recovered solid was recrystallized two times from acetonitrile to give light brown needles. ¹H NMR of the free base with

Mosher's acid confirms the enantiomeric purity of the resulting (+)McN-5652-Z.

Thioester precursor 11 (sodium thiomethoxide route)

The synthesis pathway, which contains the demethylation of 1 and acetylation of the free thiol, is depicted in scheme 2.

Scheme 2. Synthesis of the thioester precursor



Purified McN-5652-Z (0.34 mmol, 100 mg), sodium methoxide (2.4 mmol, 170 mg) and dry DMF (1 ml) were combined in a reaction vessel, which was sealed and purged with argon. The reaction mixture was heated to 160 °C for 60 min and cooled to ambient temperature. A tenfold excess of acetyl chloride was added while cooling the solution with ice/water. The resulting suspension was stirred for some minutes at room temperature and then quenched by addition of water by cooling with ice/water. The thioester was extracted with dichloromethane, the combined organic phases were washed with water, dried with sodium sulphate and the solvent was removed under vacuo. The residue was purified according to Mathews [14] by means of semipreparative HPLC (Macherey&Nagel Nucleosil C18, 7 µm, 250 mm x 10 mm). The eluent consists of a mixture of acetonitrile and water (30/70) with 0.1 % trifluoroacetic acid. Because of this purification route, the thioester 11 was obtained in the form of the more stable ammonium trifluoroacetate.

Thioester precursor 11 (sodium-liquid ammonia route)

Sodium (1.7 mmol, 40 mg) was added to liquid ammonia (25 ml). (+)McN-5652-Z (0.5 mmol, 150 mg) was dissolved in 8 ml dry THF and was added to the sodium amide suspension. Two further portions of sodium (2 times 1 mmol, e. g. 23 mg) were added and the deep blue suspension was stirred for 10 min. When the colour was stable, the excess of sodium amide was discharged with a small amount of solid ammonium chloride and the ammonia was evaporated. Otherwise further addition of sodium was necessary.

An excess of acetyl chloride (40 mmol, 3.3 g) was added to the resulting solution of the free thiol while cooling with iced water. The suspension was stirred for 3 - 4 min at room temperature and then water (20 ml) was added. The thioester was isolated and purified as described above.

Yield: 80 mg (38 %) light brown, highly viscous oil

NMR data: δ_c (75.475 MHz; solvent: CDCl₃; internal standard: TMS) 21.62 CH₂ (C1 or C2), 30.25 CH₃ (Ac), 31.61 CH₂ (C2 or C1), 42.75 CH (C6), 53.31 CH₂ (C3 or C5), 55.86 CH₂ (C5 or C3), 62.22 CH (C10b) 126.60, 128.03, 128.08, 128.34, 128.88, 129.74, 131.15, 133.77, 135.17, 140.04 (aromatic carbons), 194.0 CO (Ac), a quadruplet between 110 and 121 ppm and a singlet at 161 ppm (broad signals) were assigned to the trifluoroacetic acid

McN-5652-Z from thioester 11

A small amount of the thioester (30 mg) was hydrolysed with tetrabutylammonium hydroxide (250 µl of a 1 M solution in methanol), dissolved in DMF after 10 min and methylated with methyl iodide (6 µl). The product was isolated by extraction with dichloromethane. The residue (18 mg) was used for ¹H NMR investigation of the enantiomeric purity.

Results and Discussion

In the synthesis of the thioester precursor **11** the compound McN-5652-Z **1** was demethylated with sodium amide in liquid ammonia. In contrast to the demethylation performed with sodium thiomethoxide, this new synthesis required very low reaction temperatures and shorter reaction times. These conditions suppressed the undesirable isomerization. As a result the share of the highly specific binding trans diastereomer was clearly increased. Instead of the nearly 40 % yield as obtained by the sodium thiomethoxide route, about 80 % were now reached. This is demonstrated in Fig. 2, which compares the HPLC chromatograms of the products of both reaction pathways.

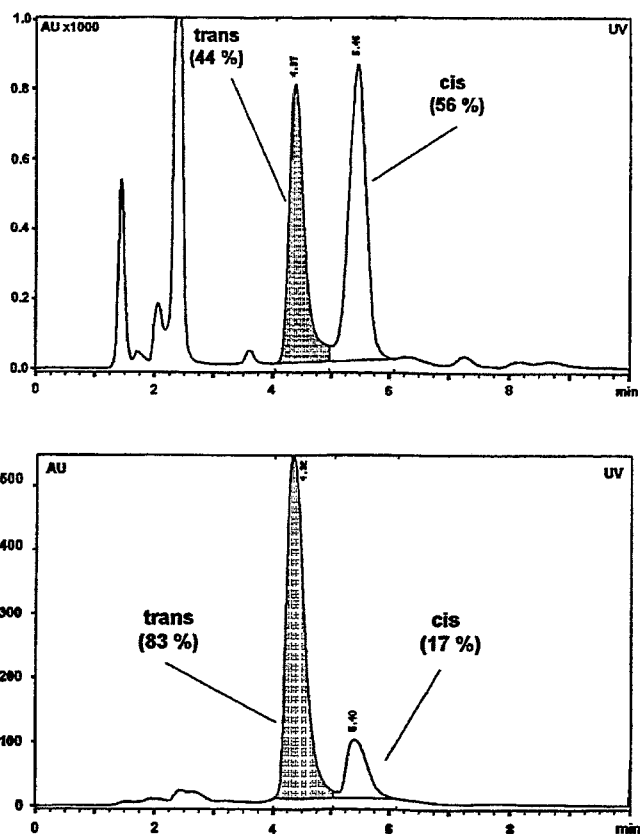


Fig. 2. HPLC chromatograms of normethyl McN-5652 obtained after demethylation with sodium methoxide (above) and with sodium in liquid ammonia (below)

The percentages of the diastereomers are strongly dependent on the implementation of the reaction. When the demethylation is not complete, the ratio of the diastereomers remains unchanged. After complete formation of the thiol, excess sodium amide causes isomerization. Consequently, demethylation and isomerization are consecutive reactions. For this reason sodium should preferably be added to the reaction mixture in portions. The end of demethylation can be recognized when the blue colour does not disappear within 10 to 15 min. Excess sodium amide must then be removed to avoid greater changes in the diastereomer ratio.

It is also possible that both reactions run as a competitive reaction. In this case the isomerization must be a very slow reaction in comparison with the cleavage of the thioether.

A small amount of the (+)thioester precursor **11** was hydrolysed by tetrabutylammonium hydroxide and the thiol generated in situ was methylated with methyl iodide. The ^1H NMR spectrum of the recovered McN-5652-Z with Mosher's acid indicates no racemization during the demethylation with sodium amide in liquid ammonia.

The thioester precursor obtained by the new synthetic route was also used in the synthesis of $[^{14}\text{C}]$ McN-5652-Z as described by Suehiro *et al.* [10] and gave comparable radiochemical yields of $[^{14}\text{C}]$ McN-5652-Z.

Acknowledgements

The authors thank Dr. D. Scheller and A. Rudolf of the Dresden University of Technology for recording the ^1H and ^{13}C NMR spectra.

References

- [1] Maryanoff B. E., McComsey D. F., Costanzo M. J., Settler P. E., Gardocki J. F., Shank R. P. and Schneider C. R. (1984) Pyrroloisoquinoline antidepressants. Potent, enantioselective inhibition of tetrabenazine-induced ptosis and neuronal uptake of norepinephrine, dopamine, and serotonin. *J. Med. Chem.* **27**, 943 - 947.
- [2] Maryanoff B. E., McComsey D. F., Gardocki J. F., Shank R. P., Costanzo M. J., Nortey S. O., Schneider C. R. and Settler P. E. (1987) Pyrroloisoquinoline antidepressants. 2. In-depth exploration of structure-activity relationship. *J. Med. Chem.* **30**, 1433 - 1454.
- [3] Maryanoff B. E., Vaught J. L., Shank R. P., McComsey D. F., Costanzo M. J. and Nortey S. O. (1990) Pyrroloisoquinoline antidepressants. 3. A focus to serotonin. *J. Med. Chem.* **33**, 2793 - 2797.
- [4] Shank R. P., Vaught J. L., Pelley K. A., Settler P. E., McComsey D. F. and Maryanoff B. E. (1988) McN-5652: A highly potent inhibitor of serotonin uptake. *J. Pharmacol. Exp. Ther.* **247**, 1032 - 1038.
- [5] Suehiro M., Ravert H. T., Dannals R. F., Scheffel U. and Wagner H. N. (1992) Synthesis of a radiotracer for studying serotonin uptake sites with positron emission tomography: [^{11}C]McN-5652-Z. *J. Labelled Compd. Radiopharm.* **31**, 841 - 848.
- [6] Suehiro M., Scheffel U., Dannals R. F., Ravert H. T., Ricaurte G. A. and Wagner H. N. (1993) A PET radiotracer for studying serotonin uptake sites: Carbon-11-McN-5652-Z. *J. Nucl. Med.* **34**, 120 - 127.
- [7] Smith D. F., Jensen P. N., Poulsen S. H., Mikkelsen E. O., Elbaz E. and Glaser R. (1991) Effects of pyrroloisoquinoline enantiomers ((+)- and (-)-McN5652-Z) on behavioral and pharmacological serotonergic mechanisms in rats. *Eur. J. Pharm.* **196**, 85 - 92.
- [8] Suehiro M., Scheffel U., Ravert H. T., Dannals R. F. and Wagner H. N. (1993) [^{11}C](+)McN-5652 as a radiotracer for imaging serotonin uptake sites with PET. *Life Sci.* **53**, 883 - 892.
- [9] Szabo Z., Pan Fu Kao, Scheffel U., Suehiro M., Mathwes W. B., Ravert H. T., Musachio J. L., Marengo S., Sang Eun Kim, Ricaurte G. A., Wong D. F., Wagner H. N. and Dannals R. F. (1995) Positron Emission tomography imaging of serotonin transporters in the human brain using [^{11}C](+)McN5625. *Synapse* **20**, 37 - 43.
- [10] Suehiro M., Musachio J. L., Dannals R. F., Matthews W. B., Ravert H. T., Scheffel U. and Wagner H. N. (1995) An improved method for the synthesis of radiolabeled McN5652 via thioester precursors. *Nucl. Med. Biol.* **22**, 543 - 545.
- [11] Jacob P. (1982) Resolution of (\pm)-5-bromonornicotine. Synthesis of (R)- and (S)-nornicotine of high enantiomeric purity. *J. Org. Chem.* **47**, 4165 - 4167.
- [12] Compere E. L. (1968) Synthesis of alpha-hydroxyarylacetic acids from bromoform, arylaldehydes, and potassium hydroxide, with lithium chloride catalyst. *J. Org. Chem.* **33**, 2565 - 2566.
- [13] Sorgi K. L., Maryanoff C. A., McComsey D. F., Graden D. W. and Maryanoff B. E. (1990) Asymmetric induction in an enammonium-iminium rearrangement. Mechanistic insight via NMR, deuterium labeling, and reaction rate studies. Application to the stereoselective synthesis of pyrroloisoquinoline antidepressants. *J. Am. Chem. Soc.* **112**, 3567 - 3579 and supplementary material.
- [14] Mathwes W. B. private communication.
- [15] Billman J. H. and McDowell J. W. (1961) Reduction of Schiff bases. III. Reduction with dimethylamine borane. *J. Org. Chem.* **26**, 1437 - 1440.

38. Substances Labelled in Metabolically Stable Positions:

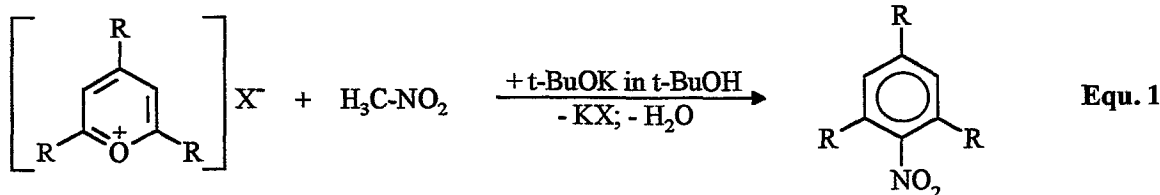
The Conversion of Pyrylium Salts with Nitro- ^{11}C methane - a New Method for the Synthesis of N.C.A. ^{11}C -Ring-Labelled Nitroaromatics

P. Mäding, J. Steinbach, H. Kasper

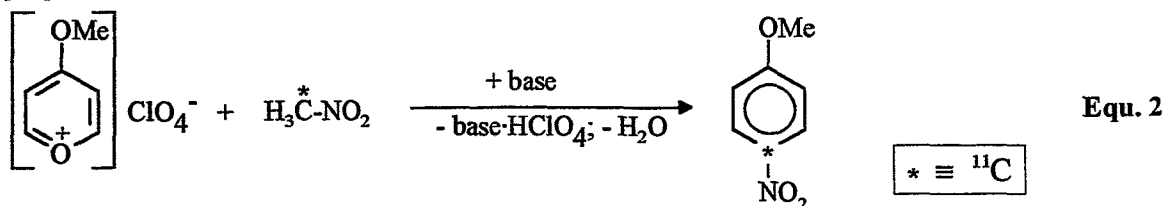
Introduction

In earlier papers we described the labelling of the following benzenoid compounds with ^{11}C in their rings by reaction of pentamethinium salts with nitro- ^{11}C methane: nitro- ^{11}C benzene [1], 3-nitro- ^{11}C anisole [2], 3-nitro- ^{11}C toluene and 4-nitro- ^{11}C toluene [3]. These syntheses are based on using the principle of the synchronous six-electron cyclization of hexatriene systems into aromatics. However, this reliable method has limitations due to the availability of the nonradioactive precursors [4].

We therefore investigated a new possibility of synthesizing substituted nitro- ^{11}C benzenes. The condensation of 2,4,6-trisubstituted pyrylium salts with nitromethane into many aromatic 2,4,6-trisubstituted nitro-compounds according to Equ. 1 has been known for a long time [5-8] but was not used for labelling with the carbon isotopes ^{11}C , ^{13}C or ^{14}C :



Although this method was not described for synthesizing *p*-substituted nitrobenzenes, we tried to apply it for preparing 4-nitro- ^{11}C anisole by condensation of 4-methoxy-pyrylium perchlorate [9] with nitro- ^{11}C methane according to Equ. 2:



In this way 4-nitro- ^{11}C anisole was surprisingly obtained by using reaction conditions which are not described in the literature. This was the reason for further investigations in view of the ^{11}C -ring labelling of two 2,4,6-trisubstituted nitrobenzenes.

Experimental

Materials

For identification of the labelled compounds by HPLC the following reference substances were used: nitromethane 99 %, 4-nitroanisole 97 % (Aldrich, Germany), 2-nitromesitylene 99 % (ABCR GmbH & Co., Germany) and 2,6-dimethyl-4-methoxy-nitrobenzene (synthesized according to [8]).

HMPT, *t*-BuOK and BuLi (1.6 M in hexane) were purchased from Merck, Germany and had for synthesis quality. $\text{Bu}_4\text{NF}\cdot 3\text{H}_2\text{O}$ (purum) and Bu_4NF on silica gel (1.1 mmol F/g resin) were obtained from FLUKA, Germany, *t*-BuOH (99.3 %) from Aldrich, Germany.

Analysis

To determine the extent of conversion and the radiochemical purity and to identify the products, an HPLC system (JASCO) was used, including a pump, a Rheodyne injector with a 20 μl loop, a LiChrospher 100 RP-18 endcapped column (5 μm , 150 mm x 3.3 mm, Merck) and a UV detector coupled in series with a radioactivity detector FLO-ONE/Beta 150TR (Canberra Packard). The HPLC analyses were carried out at a flow rate of 0.5 ml/min with the following linear gradient of the eluents: 0 min - 70 % buffer/ 30 % MeCN; 10 min - 0 % buffer/ 100 % MeCN; 20 min - 0 % buffer/ 100 % MeCN; buffer = phosphate buffer pH 7 ($\text{c}[\text{NaH}_2\text{PO}_4] = 0.26 \text{ mM}$; $\text{c}[\text{Na}_2\text{HPO}_4] = 0.51 \text{ mM}$).

Synthesis of reference substance

2,6-dimethyl-4-methoxy-nitrobenzene: A suspension of *t*-BuOK (0.946 g = 8.4 mmol) in *t*-BuOH (15 ml)

was slowly added to a solution of 2,6-dimethyl-4-methoxyppyrylium perchlorate (1 g = 4.2 mmol) in nitromethane (10 ml = 185 mmol) with an orange colour appearing. The reaction mixture was heated under reflux for 45 min. The potassium perchlorate separated in the reddish brown reaction mixture was then filtered through a frit glass filter. The filtrate was evaporated and the residue recrystallized from a mixture of methanol and water (2 : 1, 15 ml). Pale needles, yield: (0.3 g, 39.5 %).

Melting point: 47.6-50.6 °C (lit. m.p. 49.5-50.5 °C [8]).

NMR data: δ_H in ppm (200.13 MHz; solvent $CDCl_3$; standard $SiMe_4$) 2.24 (6 H, s, 2 CH_3), 3.73 (3 H, s, OCH_3), 6.52 (2 H, s, 2 CH)

δ_C in ppm (75.475 MHz; solvent $CDCl_3$; standard $SiMe_4$) 18.4 2- CH_3 and 6- CH_3 , 55.5 4- OCH_3 , 113.8 CH (C3), 132.4 C (C2), 145.5 C (C1), 160.0 C (C4)

¹¹C-ring labelling of the nitrobenzenes

The gaseous nitro-[¹¹C]methane produced according to [1] was introduced into a mixture of 250 μ l HMPT or t-BuOH and 8 - 9 mg (38 μ mol) pyrylium salt. The bases t-BuOK and Bu_4NF were added either before or after trapping the nitro-[¹¹C]methane (see Table 1 with the appropriate footnotes), whereupon the well sealed vessel was heated at 120 °C for 20 min.

Results and Discussion

The radiochemical yields (decay-corrected) of the substituted nitro-[1-¹¹C]benzenes synthesized according to Equ. 3 under various reaction conditions are listed in Table 1.

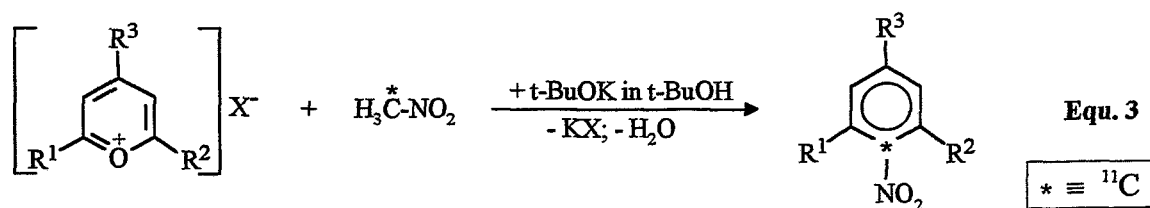


Table 1: Radiochemical yields of substituted nitro-[1-¹¹C]benzenes under various reaction conditions. General conditions: 38 μ mol pyrylium salts (8-9 mg) in a solvent (HMPT or t-BuOH), addition of a base (t-BuOK, $Bu_4NF \cdot 3H_2O$) either before or after trapping the nitro-[¹¹C]methane, reaction temperature: 120 °C, reaction time: 20 min

Amounts of solvents and bases				Radiochemical yields of the nitro-[1- ¹¹ C]benzenes (decay-corrected) [%]		
HMPT [μ l]	t-BuOH [μ l]	t-BuOK [μ mol]	Bu_4NF ($\cdot 3H_2O$) [μ mol]	$R^1, R^2=H$; $R^3=OMe$	$R^1, R^2, R^3=Me$	$R^1, R^2=Me$; $R^3=OMe$
-	250 ^{b)}	76 ^{b)}	-	8 ^{c)}	0 ^{c)}	-
-	250 ^{b)}	38 ^{b)}	38 ^{b)}	9	-	-
250 ^{b)}	250 ^{a)}	38 ^{a)}	38 ^{a)}	8	-	-
250 ^{b)}	38 ^{a), d)}	38 ^{a), d)}	38 ^{b)}	58	-	-
250 ^{b)}	250 ^{a)}	38 ^{a)}	38 ^{b)}	71 82	0	0
-	250 ^{b)}	38 ^{b)}	38 ^{b), e)}	-	21	-
-	250 ^{b)}	38 ^{a), d)}	38 ^{b)}	-	15 ^{g)}	-
-	250 ^{b)}	76 ^{b)}	38 ^{b)}	-	13 ^{g)}	-

^{a)} addition after trapping of nitro-[¹¹C]methane

^{b)} addition before trapping of nitro-[¹¹C]methane

^{c)} reaction temperature: 100 °C

^{d)} addition as 1 M solution in t-BuOH

^{e)} use of Bu_4NF on silica gel

^{g)} beside 57.7 % of [¹¹C]CH₃NO₂

^{h)} beside 57.3 % of [¹¹C]CH₃ONO

With 8 mg 4-methoxy-pyrylium perchlorate (38 μmol) in 250 μl HMPT and addition of 25 μl 1.6 M BuLi in hexane (40 μmol) before or after trapping the nitro- ^{11}C methane, 4-nitro- ^{11}C anisole was not obtained by heating this reaction mixture at 170 $^{\circ}\text{C}$ for 10 min.

Potassium tert-butyrate in tert-butanol proved to be necessary for this condensation reaction, and tetrabutylammonium fluoride is a suitable auxiliary base.

The best results in terms of extent of conversion were obtained by the synthesis of 4-nitro- ^{11}C anisole. It could be shown that the order of addition of the bases concerning the trapping of nitro- ^{11}C methane in a solvent/pyrylium salt mixture is of importance. The yields of 4-nitro- ^{11}C anisole increased considerably (about 58 %) when the following order was used: addition of 12 mg $\text{Bu}_4\text{NF}\cdot 3\text{H}_2\text{O}$ (38 μmol) to a mixture of 8 mg 4-methoxy-pyrylium perchlorate (38 μmol) in 250 μl HMPT, trapping of ^{11}C CH₃NO₂, addition of 38 μl 1 M t-BuOK in t-BuOH, and heating the reaction mixture at 120 $^{\circ}\text{C}$ for 20 min. A further increase of the yields of 4-nitro- ^{11}C anisole was achieved by using a greater amount of t-BuOH (250 μl). Thus, 4-nitro- ^{11}C anisole was prepared with a radiochemical purity of up to 82 %. Related to ^{11}C CH₃NO₂, the reproducible radiochemical yields of 4-nitro- ^{11}C anisole are in the range of 77 \pm 5 % (decay-corrected). An HPLC radiogram of unpurified 4-nitro- ^{11}C anisole is shown in Fig. 1.

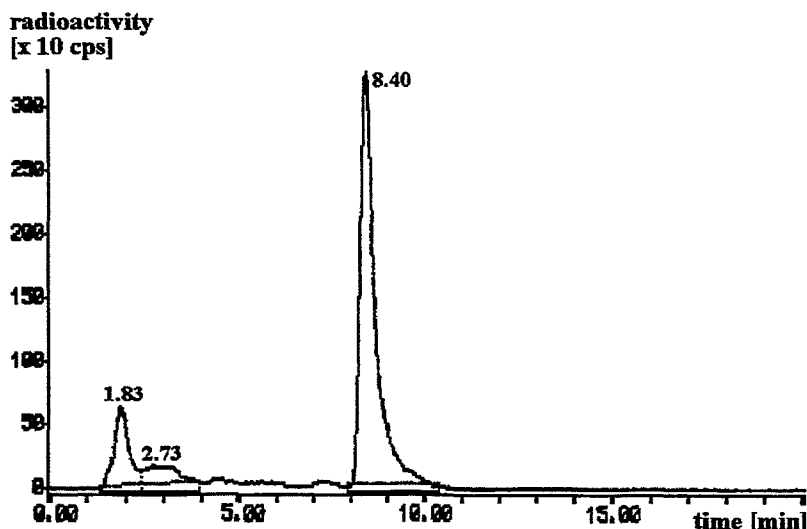


Fig. 1: HPLC radiogram obtained from the reaction mixture of the 4-nitro- ^{11}C anisole synthesis

1.83 min:	^{11}C CH ₃ ONO; 11.6 %
2.73 min:	^{11}C CH ₃ NO ₂ ; 6.5 %
8.40 min:	4-nitro- ^{11}C anisole; 81.9 %

The synthesis of 2-nitro- ^{11}C mesitylene and 2,6-dimethyl-4-methoxy-nitro- ^{11}C benzene from their appropriate pyrylium salts [9] was not possible under the above-described optimized reaction conditions. This phenomenon cannot be interpreted.

Other reaction conditions had therefore to be worked out. 2-Nitro- ^{11}C mesitylene was obtained in yields of about 21 % as follows: nitro- ^{11}C methane was trapped in a mixture of 250 μl t-BuOH, 8 mg 2,4,6-trimethylpyrylium tetrafluoroborate (38 μmol), 34.6 mg Bu_4NF on silica gel (1.1 mmol Bu_4NF /g resin Δ 38 μmol Bu_4NF) and 38 μl 1 M t-BuOK in t-BuOH. This reaction mixture was heated at 120 $^{\circ}\text{C}$ for 20 min. The yields of 2-nitro- ^{11}C mesitylene decreased when $\text{Bu}_4\text{NF}\cdot 3\text{H}_2\text{O}$ (38 μmol) was used without a carrier. An HPLC radiogram of unpurified 2-nitro- ^{11}C mesitylene is shown in Fig. 2.

These reaction conditions have yet to be tested for the synthesis of 2,6-dimethyl-4-methoxy-nitro- ^{11}C benzene.

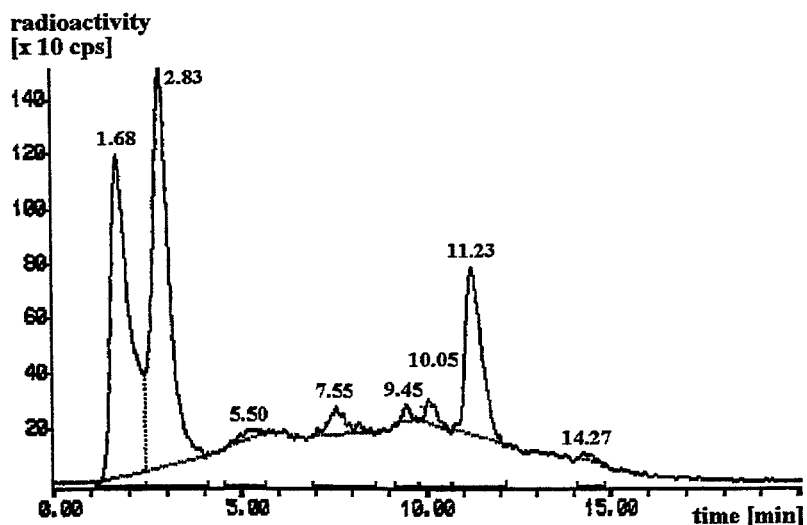


Fig. 2: HPLC radiogram obtained from the reaction mixture of the 2-nitro-[2- ^{11}C]mesitylene synthesis

- 1.68 min: $[^{11}\text{C}]\text{CH}_3\text{ONO}$; 32.2 %
 2.83 min: $[^{11}\text{C}]\text{CH}_3\text{NO}_2$; 38.4 %
 11.23 min: 2-nitro-[2- ^{11}C]mesitylene; 20.9 %

References

- [1] Steinbach J., Mäding P., Füchtner F. and Johannsen B. (1995) N.c.a. ^{11}C -labelling of benzenoid compounds in ring positions: synthesis of nitro-[1- ^{11}C]benzene and [1- ^{11}C]aniline. *J. Labelled Compd. Radiopharm.* **36**, 33 - 41.
- [2] Mäding P., Steinbach J. and Kasper H. (1994) Substances labelled in metabolically stable positions: 6. The synthesis of 3-nitro-[3- ^{11}C]anisole. *Annual Report 1994*, Institute of Bioinorganic and Radiopharmaceutical Chemistry FZR-73, pp. 100 - 104.
- [3] Mäding P., Steinbach J. and Kasper H. (1995) Substances labelled in metabolically stable positions: 11. The synthesis of 3-nitro-[3- ^{11}C]toluene and 4-nitro-[4- ^{11}C]toluene. *Annual Report 1995*, Institute of Bioinorganic and Radiopharmaceutical Chemistry FZR-122, pp. 6 - 8.
- [4] Mäding P. and Steinbach J. (1997) publication in preparation
- [5] Dimroth K. and Bräuninger G. (1956) Aromatische Nitroverbindungen aus Piryliumsalzen. *Angew. Chem.* **68**, 519.
- [6] Dimroth K., Bräuninger G. and Neubauer G. (1957) Über Reaktionen mit Piryliumsalzen, I. Die Nitrierung von symm. Triphenylbenzol. *Chem. Ber.* **90**, 1634 - 37.
- [7] Dimroth K., Neubauer G., Möllenkamp H. and Oosterloo G. (1957) Reaktionen mit Piryliumsalzen, II. Aromatische Nitroverbindungen aus Piryliumsalzen. *Chem. Ber.* **90**, 1668 - 72.
- [8] Dimroth K. (1960) Neuere Methoden der präparativen organischen Chemie III. 3. Aromatische Verbindungen aus Piryliumsalzen; *Angew. Chem.* **72**, 331 - 342.
- [9] Mäding P., Steinbach J. and Kasper H. (1996) Substances labelled in metabolically stable positions: The synthesis of pyrylium salts as precursors for ^{11}C -ring labelling of nitrobenzenes. *This report*, pp. 166 - 168.

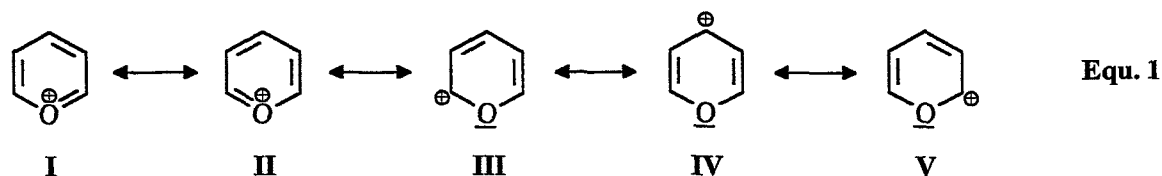
39. Substances Labelled in Metabolically Stable Positions:

The Synthesis of Pyrylium salts as Precursors for ^{13}C -Ring Labelling of Nitrobenzenes

P. Mäding, J. Steinbach, H. Kasper

Introduction

As defined, pyrylium salts consist of a cyclic-conjugated oxonium cation with a π -electron sextet and an anion such as perchlorate, tetrafluoroborate, tetrachloroferrate or chloride. The ground state of the pyrylium cation can be described by means of oxonium-Kekulé structures (I, II) and carbenium-pyran structures (III-V) according to Equ. 1 [1, 2]:



These resonance formulas express the two essential properties of the system: the aromaticity and the high reactivity against nucleophilic attack in positions 2, 4 and 6.

Pyrylium salts are "key" compounds in organic chemistry [1-3]. They can be converted into manifold compounds, mostly by an exchange of the oxygen atom.

In the foregoing paper [4] we described a new method for the synthesis of n.c.a. ^{13}C -ring-labelled nitroaromatics which is based on the condensation of pyrylium salts with nitro- ^{13}C methane. For this purpose the following three pyrylium salts had to be synthesized and characterized: 4-methoxypyrylium perchlorate, 2,6-dimethyl-4-methoxypyrylium perchlorate and 2,4,6-trimethylpyrylium tetrafluoroborate.

Experimental

Materials

γ -Pyrone (99 %) and 2,6-dimethyl- γ -pyrone (99 %) were purchased from Aldrich, Germany. Dimethyl sulphate (for synthesis) and perchloric acid (p.a., 70 %) were obtained from Laborchemie Apolda, Germany, acetanhydride (p.a.) from Feinchemie Sebnitz, Germany, and tetrafluoroboric acid (purum, 40 %) from Chemiewerk Nünchritz/ BT Dohna, Germany.

Synthesis

4-Methoxypyrylium perchlorate: A mixture of γ -pyrone (2.5 g = 26 mmol) and dimethyl sulphate (3.5 g = 28 mmol) was heated at 60 °C for 1 h with a brownish colour appearing. Then a solution of perchloric acid (60 %, 5 ml = 46 mmol), acetanhydride (15 ml) and diethyl ether (20 ml) was added at room temperature. After stirring for 30 minutes the crystalline solid separated, was filtered through a frit glass filter, washed with *n*-propanol and diethyl ether and dried. Pale crystals, yield: (2.0 g, 36.5 %). Melting point: 84-88 °C (lit. m.p. 76-77 °C [5]).

Elemental analysis: (Found: C, 33.8; H, 3.2; Cl, 16.2, $\text{C}_6\text{H}_7\text{ClO}_6$ requires C, 34.2; H, 3.3; Cl, 16.9 %).

NMR data: δ_{C} (75.475 MHz; solvent CD_3OD ; standard SiMe_4) 49.8 4-OCH₃, 102.7 CH (C3), 113.6 C (C4), 167.7 CH (C2)

2,6-Dimethyl-4-methoxypyrylium perchlorate: A mixture of 2,6-dimethyl- γ -pyrone (2.5 g = 20 mmol), dimethyl sulphate (4.0 g = 32 mmol) and methanol (0.25 ml) was heated at 50 °C for 1 h with a complete solution occurring and a yellow colour appearing. Perchloric acid (70 %, 9.5 g = 66 mmol) was added while cooling the solution with ice water. After stirring for 2 h at 0 °C, the crystalline solid separated, was filtered through a frit glass filter, washed with acetone and diethyl ether and dried. In this way only 0.7 g colourless crystals could be obtained. The yield of the pyrylium salt was increased by addition of diethyl ether to the solution sucked off, with grey crystals precipitating. The isolated crystals were purified by being dissolved in acetone and then precipitated with diethyl ether. Colourless crystals, total yield: (2.1 g, 43.7 %).

Melting point: 182-192 °C (lit. m.p. ~ 190 °C [6]).

Elemental analysis: (Found: C, 39.7; H, 4.7; Cl, 15.2, $\text{C}_8\text{H}_{11}\text{ClO}_6$ requires C, 40.2; H, 4.6; Cl, 14.9 %).

NMR data: δ_H in ppm (200.13 MHz; solvent CD_3CN ; standard $SiMe_4$) 2.73 (6 H, s, 2 CH_3), 4.24 (3 H, s, OCH_3), 7.32 (2 H, s, 2 CH)
 δ_C in ppm (75.475 MHz; solvent CD_3CN ; standard $SiMe_4$) 21.4 2- CH_3 and 6- CH_3 , 60.9 4- OCH_3 , 109.6 CH (C3), 179.3 C (C2), 180.5 C (C4)

2,4,6-Trimethylpyrylium tetrafluoroborate: Tetrafluoroboric acid (40 %, 7 ml = 39 mmol) was slowly added to a stirred mixture of acetic anhydride (50 ml = 530 mmol) and *t*-BuOH (4 ml = 42 mmol) at such a rate that the final temperature reached approximately 100 °C. The dark brown solution was allowed to cool spontaneously to 80 °C, and was then chilled to 5 °C in an ice bath. The separation of the salt began and was completed by addition of 100 ml diethyl ether. The crystalline solid was filtered through a frit glass filter, washed with 30 ml diethyl ether and dried. The pale yellow crystals (3.2 g) were recrystallized from a mixture of ethanol and methanol (1 : 1, 60 ml) containing 3 drops of tetrafluoroboric acid. Colourless crystals, yield: (2.0 g, 24.4 %). Melting point: 207-213 °C (lit. m.p. 224-226 °C [7]).

Elemental analysis: (Found: C, 45.7; H, 5.4, $C_8H_{11}BF_4O$ requires C, 45.8; H, 5.2 %).

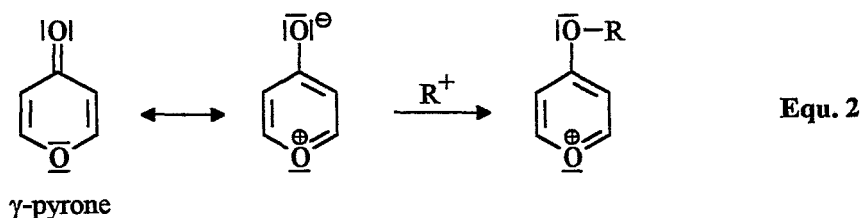
NMR data: δ_H in ppm (200.13 MHz; solvent CD_3CN ; standard $SiMe_4$) 2.78 (3 H, s, CH_3), 2.93 (6 H, s, 2 CH_3), 7.85 (2 H, s, 2 CH)

Results and Discussion

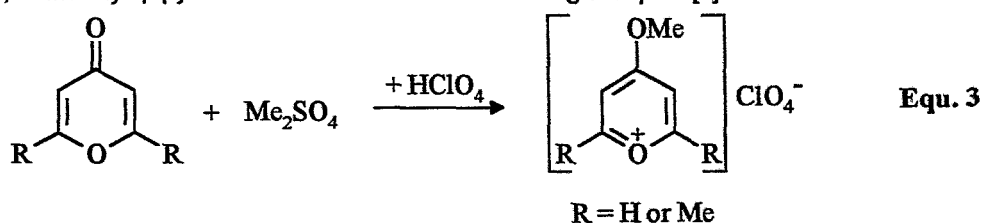
There are two synthetic principles to prepare pyrylium salts [2]:

- Syntheses starting from an existing heterocyclic compound;
- Syntheses using ring closure reactions.

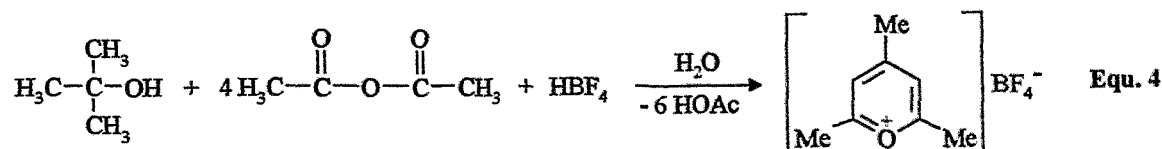
The electrophilic addition of alkylating agents to γ -pyrones is one method, starting from an existing heterocyclic compound. In this way many pyrylium salts can be synthesized. The possible electrophilic attack on the oxygen of the carbonyl group can be explained by the mesomeric structure of the γ -pyrone according to Equ. 2:



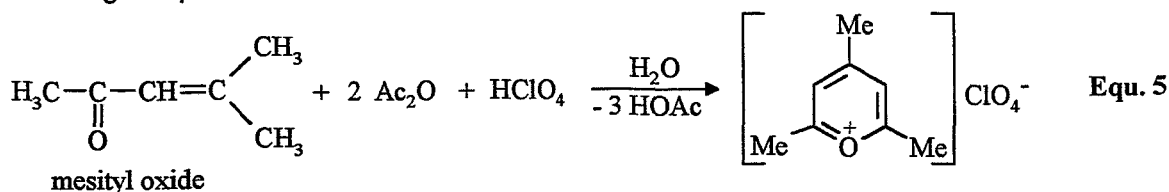
In this way we synthesized the 4-methoxypyrylium perchlorate (Equ. 3; R = H) from γ -pyrone (4H-pyran-4-one) using dimethyl sulphate as methylation agent, followed by addition of a mixture of perchloric acid, acetic anhydride and ether [5]. The 2,6-dimethyl-4-methoxypyrylium perchlorate (R = Me) was synthesized from 2,6-dimethyl- γ -pyrone in the same manner according to Equ. 3 [6]:



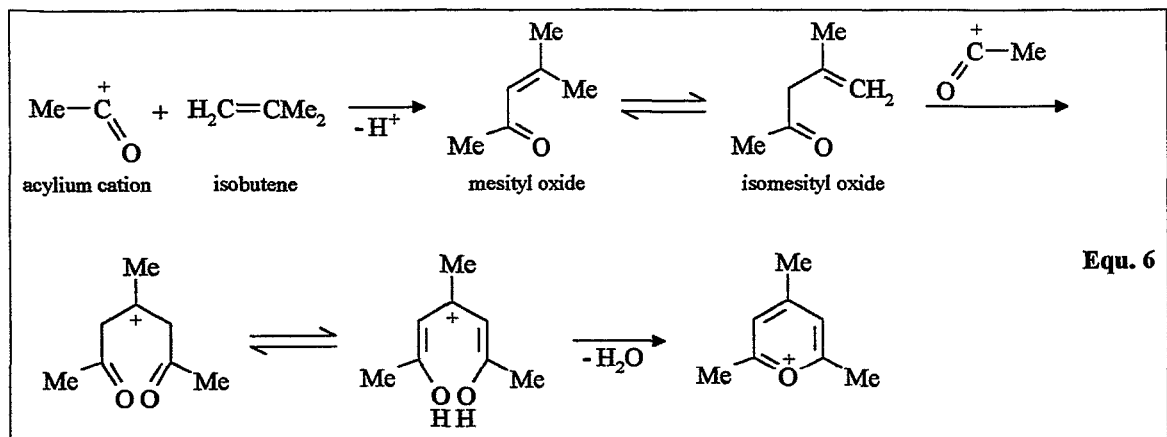
A third pyrylium compound, the 2,4,6-trimethylpyrylium tetrafluoroborate, was synthesized by a ring closure reaction. This synthesis is based on the diacetylation of isobutene, which is formed in situ by dehydration of *t*-butanol. In this case acetic anhydride, *t*-BuOH and tetrafluoroboric acid are converted according to Equ. 4 [7]:



A similar synthesis is based on the acetylation of mesityl oxide using acetic anhydride and perchloric acid. In this way the explosive 2,4,6-trimethylpyrylium perchlorate was synthesized by Hafner and Kaiser [8] according to Equ. 5:



In both reactions, isomesityl oxide is the actual intermediate. The reaction mechanism [2] based on the attack of the acylium cation is shown in Equ. 6:



References

- [1] Schroth W., Dölling W. and Balaban A.T. (1992) Pyrylium-Salze. *Houben-Weyl, Methoden der Organischen Chemie*, Georg Thieme Verlag Stuttgart, Vol. E 7b/2, p. 755 - 1004.
- [2] Schroth W. and Fischer G. (1964) Pyrylium-Synthesen, 65 Jahre Pyryliumsalze. *Z. Chem.* **4**, 281 - 292.
- [3] Dimroth K. (1960) Neuere Methoden der präparativen organischen Chemie III. 3. Aromatische Verbindungen aus Pyryliumsalzen; *Angew. Chem.* **72**, 331 - 342.
- [4] Mäding P., Steinbach J. and Kasper H. (1996) Substances labelled in metabolically stable positions: The conversion of pyrylium salts with nitro-[¹⁴C]methane - a new method for the synthesis of n.c.a. ¹⁴C-ring-labelled nitroaromatics. *This report*, pp. 162 - 165.
- [5] Hafner K. and Kaiser H. (1958) Eine einfache Synthese substituierter Azulene. *Justus Liebigs Ann. Chem.* **618** 140 - 152.
- [6] Baeyer A., Piccard J. and Gruber W. (1915) Untersuchungen über das Dimethylpyron. *Justus Liebigs Ann. Chem.* **407**, 332 - 369.
- [7] Balaban A.T. and Boulton A.J. (1973) 2,4,6-Trimethylpyrylium tetrafluoroborate. *Org. Synth., Coll. Vol. V*, 1112 - 13.
- [8] Hafner K. and Kaiser H. (1973) 2,4,6-Trimethylpyrylium perchlorate, Method II. *Org. Synth., Coll. Vol. V*, 1108 - 11.

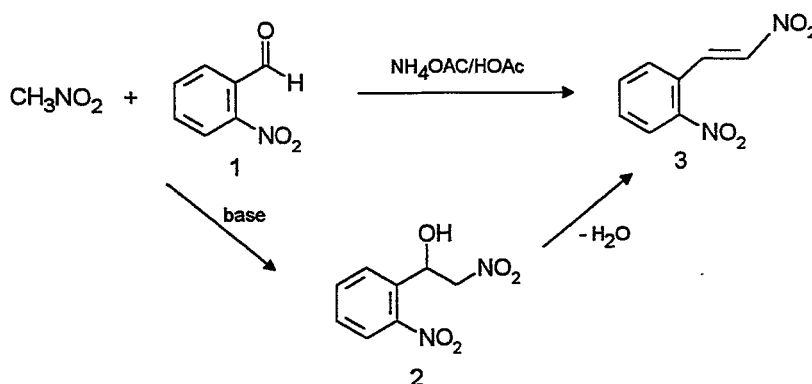
40. Substances Labelled in Metabolically Stable Positions: The Synthesis of [^{13}C]1-Hydroxy-2-nitro-1-(2-nitrophenyl)ethane and [$\beta\text{-}^{13}\text{C}$]2, β -Dinitrostyrene

J. Zessin, J. Steinbach

Introduction

In the synthesis of ^{13}C -ring-labelled heterocyclic compounds [$\beta\text{-}^{13}\text{C}$]2, β -dinitrostyrene (**3**) could be an intermediate of interest. Reduction of this substance may give access to [^{13}C]indole [1]. 2, β -Dinitrostyrene (**3**) can be prepared by condensation of nitromethane with o-nitrobenzaldehyde (**1**) [1]. This is illustrated in Scheme 1. This so-called Henry reaction can be carried out base-catalysed or in the presence of ammonium acetate in glacial acetic acid. The base-catalysed condensation leads to the intermediate 1-hydroxy-2-nitro-1-(2-nitrophenyl)ethane (**2**). Treatment with diluted hydrochloric acid yields **3**. The Henry reaction in the presence of ammonium acetate leads directly to the final product **3**.

Scheme 1. Synthesis routes of 2, β -dinitrostyrenes



Both routes were already adapted to the condensation of [^{13}C]nitromethane with various hydroxybenzaldehydes and protected hydroxybenzaldehydes [2-6]. On the basis of these results we tried to prepare [$\beta\text{-}^{13}\text{C}$]2, β -dinitrostyrene (**3**).

Experimental

General

Reagents and solvents were purchased from Aldrich and Fluka and used without further purification. HPLC measurements were performed by an HPLC system (JASCO) consisting of a pump with low pressure gradient system, injector with 20 μl loop, a LiChrospher 100 RP18 column (5 μm , 150 mm x 3.3 mm), a UV/VIS detector coupled in series with a radioactivity detector FLO-ONE/beta 150TR. A mixture of 50 % acetonitrile and 50 % water containing 0.1M ammonium formate was used as eluent. The HPLC was run with a flow of 0.5 ml/min in an isocratic mode.

[^{13}C]Nitromethane was prepared as described by Schoeps *et al.* [7] from [^{13}C]methyl iodide. This intermediate was synthesized according to Crouzel *et al.* [8].

The base-catalysed condensation of [^{13}C]nitromethane with **1** was carried out, using tetrabutylammonium fluoride (TBAF, method A) or sodium hydroxide (method B) as catalysts where as method C describes the condensation in the presence of ammonium acetate in glacial acetic acid.

TBAF catalysed condensation (method A)

The [^{13}C]nitromethane was trapped at 0 $^\circ\text{C}$ in a reaction vessel containing tetrahydrofuran (THF, 200 μl), o-nitrobenzaldehyde (50 μmol , 7.5 mg) and TBAF (as trihydrate, 65 μmol , 20 mg). After stirring at 0 $^\circ\text{C}$ for 2 min, a small sample of the reaction mixture was dissolved in the HPLC solvent and analysed.

The same procedure was repeated at -16 $^\circ\text{C}$ in a second experiment.

Sodium hydroxide catalysed condensation (method B)

Methanol (250 μl) and **1** (33 μmol , 5 mg) were placed in a reaction vessel and [^{13}C]nitromethane was trapped while cooling with acetone/dry ice. On reaching a constant radioactivity level, sodium hydroxide

(9 - 40 μmol , 0.36 - 1.6 mg) was added, dissolved either in water or in methanol. The reaction mixture was allowed to warm up to room temperature for 5 to 8 min. On finishing the reaction, a small sample was analysed by HPLC as described above.

For dehydration hydrochloric acid was added to the reaction mixture obtained from condensation. The hydrochloric acid was diluted either with water or methanol and the final concentration in the reaction mixture varied from $5 \cdot 10^{-6}\text{M}$ to 2.5M. The reaction was carried out at room temperature for 3 to 10 min.

For dehydration of **2**, phosphoric acid (85 %, 5 μl) or toluene-*p*-sulphonic acid (as monohydrate, 5 mg) were used in a similar manner. After the reaction at room temperature (10 min), the solution was heated to 130 °C for 10 min. The dehydration products were analysed by HPLC.

Condensation with ammonium acetate/glacial acetic acid (method C)

Glacial acetic acid (250 μl), **1** (70 μmol , 11 mg) and ammonium acetate (310 - 420 μmol , 24 - 32 mg) were placed in a reaction vessel. At 10 °C the [^{13}C]nitromethane was trapped in this solution, followed by heating of the sealed vessel to 145 °C for 7 to 10 min. The reaction products were determined as described above.

Results and Discussion

Three methods were tested for the condensation of [^{13}C]nitromethane with *o*-nitrobenzaldehyde (**1**). All results are summarized in Table 1.

When the condensation was carried out under basic conditions, the intermediate compound **2** was obtained. Method A using TBAF as a basic catalyst gave very low yields (7-9 %) of **2**. At 0 °C the main products were a highly polar substance (46 %), probably [^{13}C]methyl nitrite, and an unknown compound (23 %). In nonradioactive experiments the unknown substance was not obtained. It is therefore not possible to identify this substance.

Table 1. Radiochemical yields from condensation of *o*-nitrobenzaldehyde with [^{13}C]nitromethane by method A, B or C (related to [^{13}C]nitromethane, determined by HPLC, decay corrected)

Method	[^{13}C]methyl nitrite	[^{13}C]nitromethane	2	3
A	32 - 46 %	13 - 17 %	7 - 9 %	-
B	6 \pm 4 %	3 \pm 1 %	72 \pm 5 %	-
B ¹⁾	31 \pm 3 %	6 \pm 1 %	10 \pm 1 %	38 \pm 2 %
C	4 \pm 1 %	48 \pm 3 %	-	41 \pm 3 %

1) after dehydration with HCl (0.15 - 0.5 mol/l) in methanolic solution

When the reaction was carried out at -16 °C, the share of [^{13}C]methyl nitrite decreased to 32 %. The percentage of the unknown substance increased to 47 %.

In the sodium hydroxide catalyzed condensation the radiochemical yield of **2** increased remarkably to 68 - 77 % (Fig. 1a). Such high yields were only obtained, when the base was added after trapping the [^{13}C]nitromethane in the methanolic solution of the precursor **1**. Any other sequence leads to lower yields. [^{13}C]Methyl nitrite (2 - 10 %) was found as a side product. Its share was dependent on the reaction time. Shorter reaction times prevent the formation of [^{13}C]methyl nitrite. In the range from 9 to 40 μmol the concentration of the base has no influence on the product composition. The use of water or methanol as solvents of sodium hydroxide does not influence the composition.

The desired [β - ^{13}C]2, β -dinitrostyrene (**3**) is formed by dehydration of **2**. In the case of the isolated hydroxy compound **2**, sodium acetate and acetic acid anhydride can be used [1]. But this requires a time-consuming separation of the ^{13}C -labelled **2**. The similar compound 1-hydroxy-2-nitro-1-phenylethane was dehydrated in the presence of diluted hydrochloric acid [9]. This route was also used in the synthesis of [β - ^{13}C]2, β -dinitrostyrenes [2,3,6]. Following this procedure, the reaction solution resulting from condensation was treated with diluted hydrochloric acid. A product mixture containing [^{13}C]methyl nitrite, [^{13}C]nitromethane, unreacted **2** and [β - ^{13}C]2, β -dinitrostyrene (**3**) was produced. This was demonstrated by the HPLC radiogram in Fig. 1b. The highest yields of **3** were obtained with HCl concentrations between 0.15 and 0.5 mol/l and by dilution with methanol. After dehydration for 3 to 5 min at room temperature, 65 - 77 % of **2** were converted into **3**. During this reaction a decomposition of **2** was observed. When HCl was further

diluted with water, this competitive reaction increased.

Besides HCl, phosphoric acid (85 %) and toluene-p-sulphonic acid were also used to avoid the cleavage of ^{11}C -labelled 2. With these acids longer reaction times are necessary and the yields of 3 are lower compared with the dehydration by HCl.

By application of method C the condensation of ^{11}C nitromethane with 1 gave 3. After heating the reaction mixture to 150 °C for 7 min, only 38 - 44 % of ^{11}C nitromethane were converted into 3 (Fig. 2).

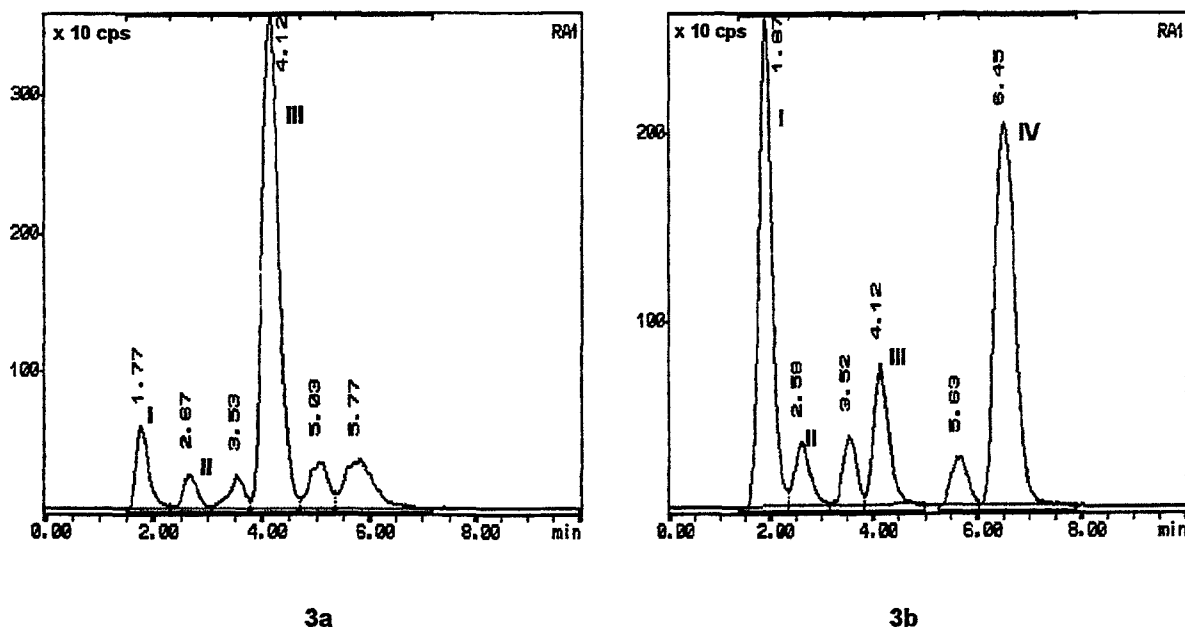


Fig. 1. HPLC radiograms obtained from condensation of ^{11}C nitromethane with *o*-nitrobenzaldehyde according to method B (1a) and from dehydration of 2 by treatment with hydrochloric acid (1b)
I: unknown compound, probably ^{11}C methyl nitrite; II: ^{11}C nitromethane; III: 2; IV: 3

Prolongation of the reaction time up to 10 min does not result in a higher degree of conversion. Also, higher reaction temperatures lead to decreasing yields of 3. The isomerization of ^{11}C nitromethane to ^{11}C methyl nitrite is of minor importance.

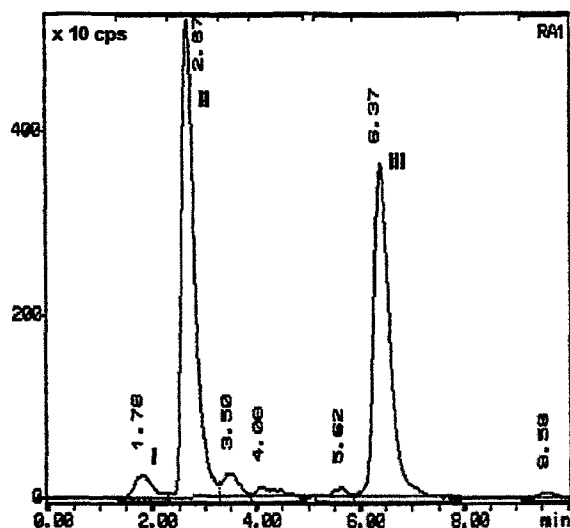


Fig. 2. HPLC radiogram after condensation of ^{11}C nitromethane with 1 (method C)
I: unknown compound, probably ^{11}C methyl nitrite; II: ^{11}C nitromethane; III: 3

Conclusions

Three methods were tested for condensation of [^{11}C]nitromethane with o-nitrobenzaldehyde. Satisfactory yields of **2** were obtained by using sodium hydroxide (method B) as a catalyst. Dehydration of this alcohol was carried out by treatment of the reaction mixture with hydrochloric acid. The radiochemical yield of **3** (related to [^{11}C]nitromethane) was in the order of 38 %.

Similar results were obtained by condensation under acidic conditions (method C).

The use of TBAF as a basic catalyst leads to a small amounts of **2** as well as to an unknown product. Method A is therefore unsuitable for obtaining **2**.

For preparation of **3** methods B or C are preferred, depending on further synthetic work.

References

- [1] Houlian W. H. (ed.) (1972) *Indoles*, vol. 1, p. 480 in: *The chemistry of heterocyclic compounds*, vol. 25. Wiley Interscience New York and references cited there.
- [2] Schoeps K.-O., Halldin C., Stone-Elander S., Langström B. and Greitz T. (1988) Preparation of ^{11}C -nitromethane and an example of its use as a radiolabelling precursor. *J. Labelled Compd. Radiopharm.* **25**, 749 - 758.
- [3] Schoeps K.-O., Halldin C., Nagren K., Swahn C.-G., Hall H. and Farde L. (1993) Preparation of [$1-^{11}\text{C}$]dopamine, [$1-^{11}\text{C}$]p-tyramine and [$1-^{11}\text{C}$]m-tyramine. Autoradiography and PET examination of [$1-^{11}\text{C}$]dopamine in primates. *Nucl. Med. Biol.* **20**, 669 - 678.
- [4] Nagren K., Halldin C., Swahn C.-G., Schoeps K.-O., Langer O., Mitterhauser M. and Zolle I. (1995) Some new methods for the synthesis of cardiac neurotransmission PET radiotracers. *Nucl. Med. Biol.* **22**, 1037 - 1043.
- [5] Nagren K., Schoeps K.-O., Halldin C., Swahn C.-G. and Farde L. (1994) Selective synthesis of racemic $1-^{11}\text{C}$ -labelled norepinephrine, octopamine, norphenylephrine and phenylethanolamine using [^{11}C]nitromethane. *Appl. Radiat. Isot.* **45**, 515 - 521.
- [6] Schoeps K.-O. and Halldin C. (1992) Synthesis of racemic [$\alpha-^{11}\text{C}$]amphetamine and [$\alpha-^{11}\text{C}$]phenylethylamine from [^{11}C]nitroalkanes. *J. Labelled Compd. Radiopharm.* **31**, 891 - 901.
- [7] Schoeps K.-O., Stone-Elander S. and Halldin C. (1989) On-line synthesis of [^{11}C]nitroalkanes. *Appl. Radiat. Isot.* **40**, 262 - 262.
- [8] Crouzel C., Langström B., Pike V. W. and Coenen H. H. (1987) Recommendations for a practical production of [^{11}C]methyl iodide. *Appl. Radiat. Isot.* **38**, 601 - 603.
- [9] Worall D. E. (1941) Nitrostyrene. *Org. Synth., Coll.* vol. 1, 413 - 415.

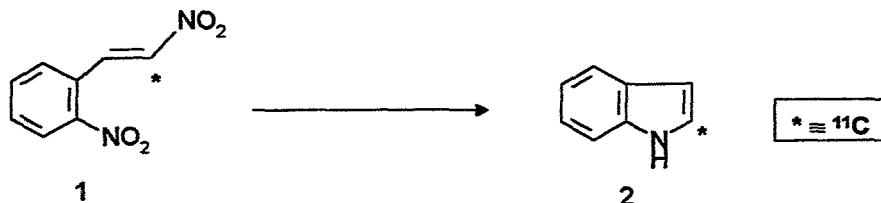
41. Substances Labelled in Metabolically Stable Positions: Synthesis of [$2-^{11}\text{C}$]Indole Starting with [$\beta-^{11}\text{C}$]2,β-Dinitrostyrene

J. Zessin, J. Steinbach

Introduction

[$\beta-^{11}\text{C}$]2,β-Dinitrostyrene (**1**) is the starting compound in the synthesis of ^{11}C -ring-labelled indole (**2**). After preparation of **1** by condensation of [^{11}C]nitromethane with o-nitrobenzaldehyde (**1**) we investigated the synthesis of **2** starting with **1** (scheme 1). This reaction involves the reduction of **1** and the cyclization of the intermediate 2,β-diaminostyrene accompanied by loss of ammonia.

Scheme 1. Synthesis of [$2-^{11}\text{C}$]indole by reduction of [$\beta-^{11}\text{C}$]2,β-dinitrostyrene



Various reduction agents can be used for this reduction. They are:

- molecular hydrogen with platinum or palladium catalysts (2),
- iron in acetic acid/ethanol (2),

- ammonium formate with palladium catalyst and (3)
- titanium (III) chloride (4,5)

With the exception of the latter, these reductants are not suitable for labelling with ^{11}C , because a high technical expenditure is required, heterogeneous catalysts are necessary or the reduction was accompanied by intensive foaming. By contrast, titanium (III) chloride allows a homogeneous reaction at room temperature with short reaction times. This agent is therefore most suitable for reduction of **1** and will be tested in the synthesis of $[2-^{11}\text{C}]$ indole (**2**).

Experimental

General

$[\beta-^{11}\text{C}]2,\beta$ -Dinitrostyrene (**1**) was synthesized by condensation of $[^{11}\text{C}]$ nitromethane with *o*-nitrobenzaldehyde in the presence of ammonium acetate in glacial acetic acid under conditions as previously described (1).

Titanium (III) chloride was used either in the form of the commercially available solution in hydrochloric acid (15 % TiCl_3 in HCl, 10 %, from Merck) or as a solid (Fluka).

The reactions were monitored by HPLC (HPLC pump with low pressure gradient system, injector with 20 μl sample loop, UV/VIS detector in series with a radioactivity detector) with an RP18-column (150 x 3.3 mm; LiChrospher 5 μm) and an eluent of water-acetonitrile (50:50) containing 0.1M ammonium formate (flow rate: 0.5 ml/min).

Separation of **1**

The dinitrostyrene **1** was separated after condensation by solid phase extraction with a C18-Sep-Pak Classical Cartridge from Waters. One part (120 μl) of the reaction mixture obtained from condensation was diluted with water (10 ml). The resulting solution was passed through the cartridge (prewashed with 5 ml methanol and 5 ml water), followed by washing with water (5 ml). The dinitrostyrene **1** was eluted either with acetic acid (1 ml) or methanol (1 ml). This eluate was used directly in the subsequent experiments.

Reduction of **1**

Titanium (III) chloride was placed in a sealed reaction vial and purged with nitrogen. The solution, which contained **1**, was added to the reduction agent. After 7 min at room temperature a sample of the reaction mixture was diluted with the HPLC solvent and analysed.

The conditions of the experiments are summarized in Table 1.

Table 1. Reduction of $[\beta-^{11}\text{C}]2,\beta$ -dinitrostyrene with titanium (III) chloride - reaction conditions

Method ¹⁾	Solvent	TiCl_3
A	reaction solution	110 μmol (as HCl solution)
B	1 ml acetic acid	110 μmol (as HCl solution)
A	reaction solution	100 μmol (as solid)
B	1 ml acetic acid	100 μmol (as solid)
B	0.5 ml methanol/ 0.2 ml acetic acid	300 μmol (as solid)

- 1) Method A: reduction as one-pot synthesis in reaction solution resulting from condensation
Method B: reduction after separation of **1** with solid phase extraction

Results and Discussion

Reduction of $[\beta-^{11}\text{C}]2,\beta$ -dinitrostyrene (**1**) with TiCl_3 was chosen as a way for synthesis of $[2-^{11}\text{C}]$ indole (**2**). At first this reaction was carried out by using of titanium (III) chloride in the form of a solution in diluted hydrochloric acid. When the reaction solution resulting from condensation of $[^{11}\text{C}]$ nitromethane with *o*-nitrobenzaldehyde was directly applied (method A), (**2**) was not formed. The main products were $[^{11}\text{C}]$ nitromethane and $[^{11}\text{C}]$ methyl nitrite.

After isolation by solid phase extraction, **1** was obtained as an acetic acid solution. When this solution was combined with TiCl_3 in diluted HCl, $[2\text{-}^{11}\text{C}]\text{indole}$ (**2**) was formed in yields of 7 %. Most of **1** was converted into an unknown polar compound. This indicates decomposition of **1** under the influence of hydrochloric acid (from TiCl_3). Similar effects were observed during the synthesis of **1** (**1**).

TiCl_3 was therefore applied as a solid in the solution yielded by condensation in the following experiments. Compared with the product distribution after condensation, reduction according to method A did not change the product composition. That means that TiCl_3 was consumed in side reactions.

Consequently, **1** was separated and the resulting acetic acid solution of **1** was mixed with solid TiCl_3 . A product mixture was obtained, which contained polar side products (57 %), **2** (19 %) and an unknown product (22 %) (see Fig. 1). This may be an intermediate compound, which would point to an incomplete reaction.

The formation of this intermediate was repressed by reduction of isolated **1** (method B) with greater amounts of TiCl_3 in an acetic acid/methanol mixture. The resulting product mixture contains polar side products and **2** in a percentage of 21 %. Only 1 % of the start substance **1** was detected. This indicates a nearly complete reaction.

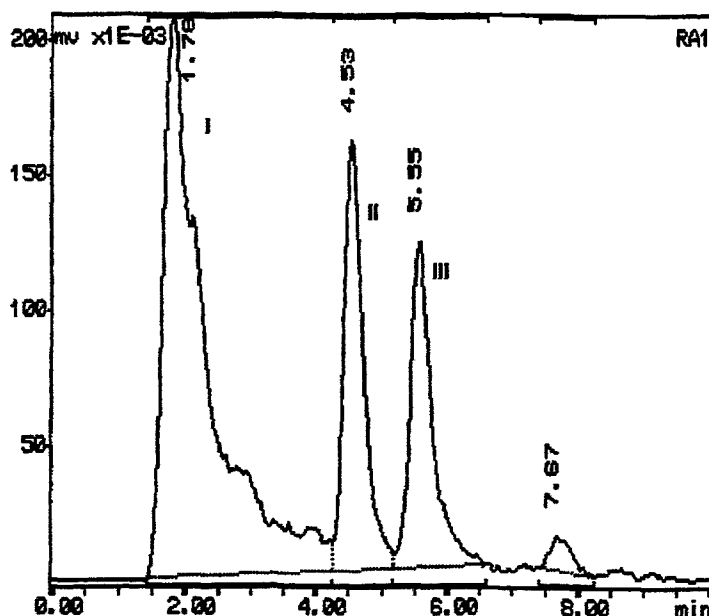


Fig. 1. HPLC radiogram after reduction (method B) of **1** with TiCl_3 in acetic acid
I: polar side products; II: unknown intermediate product, III: $[2\text{-}^{11}\text{C}]\text{indole}$ (**2**)

The radiochemical yield of **1** was 28 ± 5 % (related to $[^{11}\text{C}]\text{nitromethane}$, decay corrected) after separation by solid phase extraction. After reduction of isolated **1**, $[2\text{-}^{11}\text{C}]\text{indole}$ was obtained in radiochemical yields (related to $[^{11}\text{C}]\text{nitromethane}$, decay corrected) of 5 to 7 %. The overall decay corrected yield (related to $[^{11}\text{C}]\text{CO}_2$) of **2** was in the order of 3 %.

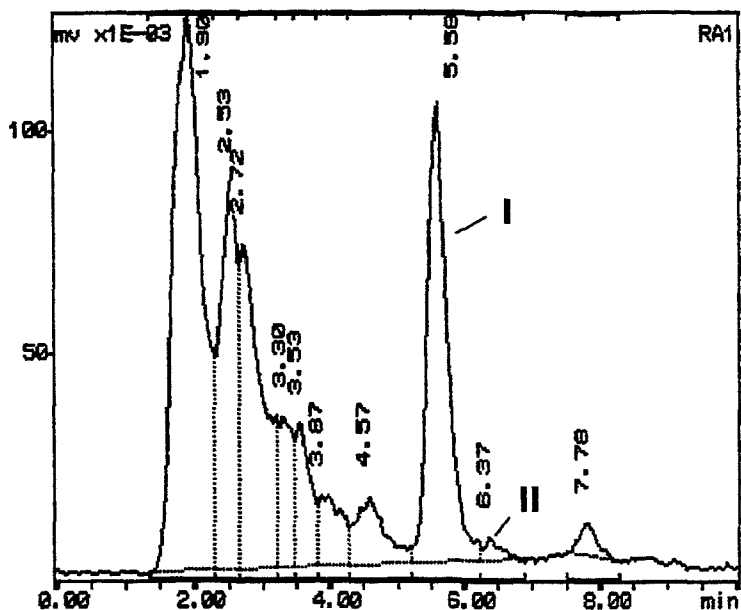


Fig. 2. HPLC radiogram after reduction (method B) of 1 with $TiCl_3$ in methanol/acetic acid
I: $[2-^{11}C]$ indole (2); II: $[\beta-^{11}C]2,\beta$ -dinitrostyrene (1)

Conclusions

The reduction of $[\beta-^{11}C]2,\beta$ -dinitrostyrene 1 by titanium (III) chloride was found to be the first synthetic approach to ^{11}C -ring-labelled indole 2. Besides the desired reaction, great amounts of 1 were decomposed, which decreases the radiochemical yield. Further work is necessary to increase the overall radiochemical yield of 2 by optimizing the reaction conditions.

References

- [1] Zessin J. and Steinbach J. (1996) The synthesis of $[2-^{11}C]1$ -hydroxy-2-nitro-1-(2-nitrophenyl)ethane and $[\beta-^{11}C]2,\beta$ -dinitrostyrene. *This report*, pp. 169 - 172.
- [2] Houlian W. H. (ed.) (1972) Indoles, vol. 1, p. 479ff in: *The chemistry of heterocyclic compounds*, vol. 25. Wiley Interscience New York and references cited there.
- [3] Rajeswari S., Drost K. J. and Cava M. P. (1989) A convenient reductive cyclization of 2, β -dinitrostyrenes to indoles. *Heterocycles* **29**(3), 415 - 418.
- [4] Ijaz A. S. and Parrick J. (1989) A convenient preparation of indole by the reductive cyclization of 2, β -dinitrostyrene. *Science International (Lahore)* **1**(6), 364 - 365.
- [5] Ijaz A. S., Parrick J. and Yahya A. (1990) The conversion of α,β -dinitrostyrene into indoles and the preparation of oxindole quinones. *J. Chem. Res. Synop.* **1990**(4), 116.

42. Electrophilic Fluorination: The Synthesis of [¹⁸F]Caesium Fluoroxysulfate - A New Reagent for Electrophilic Labelling

Chr. Fischer, K. Neubert, J. Steinbach

Introduction

The manifold reactivity and chemical characteristics of substances to be radio-fluorinated demand appropriate tailor-made fluorinating agents. Nucleophilic and electrophilic substitution are the two general ways for the introduction of fluorine into a molecule. Electrophilic introduction of the ¹⁸F radionuclide is of special interest in the case of activated aromatic compounds. Elemental [¹⁸F]fluorine and [¹⁸F]acetyl hypofluorite are the two well-known electrophilic fluorinating agents for radiolabelling. Both substances have a high reactivity and are in use for a wide application. In the case of highly reactive substances the fluorinating power of the reagent has to be adjusted.

In our search for new electrophilic reagents for ¹⁸F introduction we found caesium fluoroxysulfate to be a suitable compound for radiolabelling.

In 1979 Appelman [1] was the first to isolate fluoroxysulfate in form of its yellowish rubidium and caesium salts. Caesium fluoroxysulfate is the only known ionic hypofluorite. It is more powerfully oxidizing than peroxymonosulfate and decomposes in the course of a few hours. In this paper we are reporting on the synthesis of ¹⁸F-labelled caesium fluoroxysulfate (in figure 1), a new reagent for electrophilic labelling.

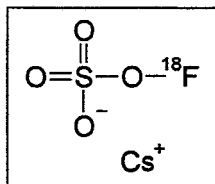


Fig. 1: [¹⁸F]caesium fluoroxysulfate

Experimental

[¹⁸F]CsSO₄F is synthesized by direct fluorination of Cs₂SO₄ with [¹⁸F]F₂ in aqueous solution. [¹⁸F]F₂ was produced by exploiting the ²⁰Ne(d,α)¹⁸F reaction by irradiation of a 0.2 % F₂/Ne mixture. After EOB the gas-mixture was passed through 0.1 ml of a 2 M Cs₂SO₄ solution in a quartz glass vial in the course of 20 min. The solution was kept at -5 °C. During the absorption procedure yellowish [¹⁸F]CsSO₄F precipitated. This crude product is ready for use without further purification. For absorption of non-reacted [¹⁸F]F₂ a trap filled with NaOH solution was connected to the reaction vial. Proof of the synthesis of [¹⁸F]CsSO₄F was given indirectly by reaction with N-formyl-3,4-diboc-6-trimethylstannyl-DOPA ethyl ester [2,3] and subsequent hydrolysis yielding 6-[¹⁸F]fluoro-DOPA, which was determined by HPLC [3].

Results and Discussion

The modified method by Appelman [1] is suitable for the synthesis of [¹⁸F]CsSO₄F in general. The method has to be optimized because of an inefficient [¹⁸F]F₂ absorption. Up to 65 % of the ¹⁸F were found in the NaOH solution. This result may be improved by increasing the volume of the absorption liquid and by an optimized geometric shape of the absorption vessel.

[¹⁸F]CsSO₄F might become a labelling reagent for special purposes, in the first place for highly reactive substrates.

References

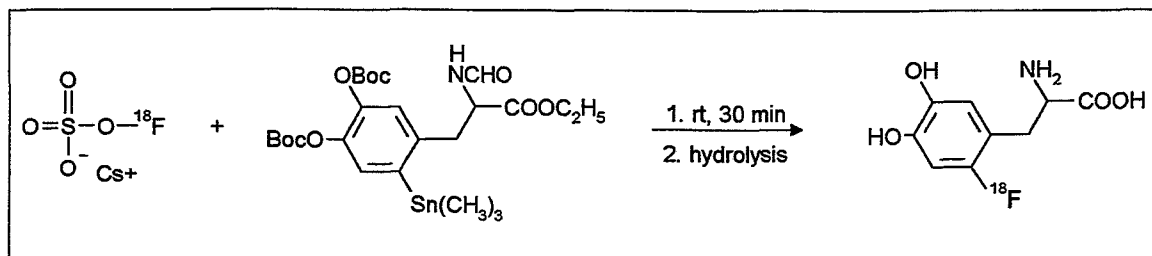
- [1] Appelman E.H, Basile L.J. and Thompson R.C. (1979) Fluoroxysulfate: a powerful new oxidant and fluorinating agent. *J. Am. Chem. Soc.* **101**, 3384 - 3385.
- [2] Namavari, M., Bishop, A., Satyamurthy, N., Bida, G. and Barrio, J.R. (1992) Regioselective radiofluorodestannylation with [¹⁸F]F₂ and [¹⁸F]CH₃COOF: a high yield synthesis of 6-[¹⁸F]fluoro-L-dopa. *Appl. Radiat. Isotop.* **43(8)** 989 - 996.
- [3] Fischer, Chr., Neubert, K., Scholz, R. and Steinbach, J., (1997) Electrophilic fluorination: a new route to ¹⁸F-labelled compounds by [¹⁸F]caesium fluoroxysulfate: 6-[¹⁸F]fluoro-DOPA as an example. *This report*, pp 177 - 178.

43. Electrophilic Fluorination: A New Route to ^{18}F -labelled Compounds by $[^{18}\text{F}]\text{Caesium Fluoroxysulfate}$: 6- $[^{18}\text{F}]\text{Fluoro-DOPA}$ as an Example

Chr. Fischer, K. Neubert, R. Scholz, J. Steinbach

Introduction

6- $[^{18}\text{F}]\text{fluoro-DOPA}$ is one of the routinely used PET-radiopharmaceuticals [1, 2, 3]. Initially it was synthesized by electrophilic attack of the versatile ^{18}F -labelled electrophilic fluorinating agents such as xenon difluoride, acetyl hypofluorite and elemental fluorine gas [4]. This is possible because of the highly reactive aromatic ring of the DOPA molecule. Beside the derived product, the other fluorinated isomers are also synthesized. In order to increase the radiochemical yield, precursor molecules with adjusted reactivity are used [5]. On the other hand, the reactivity of the fluorinating agent should also be adapted. In our search for new electrophilic labelling agents we found $[^{18}\text{F}]\text{caesium fluoroxysulfate}$ to be a useful compound for introduction of ^{18}F [6, 7]. As a model system we used N-formyl-3,4-diboc-6-trimethylstannyl-DOPA ethyl ester to generate 6- $[^{18}\text{F}]\text{fluoro-DOPA}$ (equation 1).



Eq. 1: ^{18}F -labelling with $[^{18}\text{F}]\text{caesium fluoroxysulfate}$

Experimental

$[^{18}\text{F}]\text{CsSO}_4\text{F}$ is produced by pushing 100 μmol $[^{18}\text{F}]\text{F}_2$ gas through an aqueous solution of 150 μl 2 M Cs_2SO_4 solution [7]. To this suspension of $[^{18}\text{F}]\text{CsSO}_4\text{F}$ 1.5 ml of 0.1 M N-formyl-3,4-diboc-6-trimethylstannyl-DOPA ethyl ester in CFC_3 are added and stirred vigorously at room temperature for 30 min. After the CFC_3 is evaporated, 1.0 ml of HBr (48 %) is added and refluxed for 5 min. This crude product can be handled as usual for further use. Analysis of the products was performed by HPLC (gradient: 0 min: 100 % H_2O + 0.1 % AcOH; 10 min: 100 % MeCN + 0.1 % AcOH; after 10 min: 100 % H_2O + 0.1 % AcOH; column: RP 18.5 μm , 240 x 2.1 mm (ODS, Hypersil) HP). The assignment of the chromatographic data was accomplished by reference substances.

Results and Discussion

An HPLC radiogram of the labelled products (equation 1) is shown in Fig. 1. Even though the decay-corrected radiochemical yield of 6- $[^{18}\text{F}]\text{fluoro-DOPA}$ is only 14 %, $[^{18}\text{F}]\text{CsSO}_4\text{F}$ proved to be a useful labelling agent. On the one hand, the reaction conditions are not optimized. On the other the reactivity of the N-formyl-3,4-diboc-6-trimethylstannyl-DOPA ethyl ester is adjusted to the $[^{18}\text{F}]\text{F}_2$ system. For substances of suitable reactivity to be electrophilically fluorinated with ^{18}F , $[^{18}\text{F}]\text{CsSO}_4\text{F}$ can become a suitable agent.

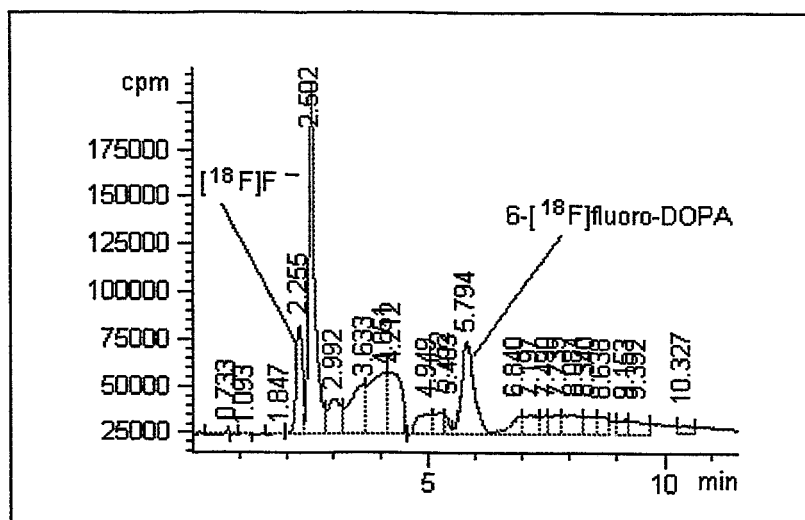


Fig.1: HPLC radiogram of the reaction of [^{18}F]caesium fluoroxysulfate with N-formyl-3,4-diboc-6-trimethylstannyl-DOPA ethyl ester.

References

- [1] Garnett E. S., Firnau G. and Namias C. (1983) Dopamine visualized in the basal ganglia of living man. *Nature* **305**, 137 - 138.
- [2] Bergman J., Haaparanta M. and Lejkoinen P. (1993) Electrophilic Synthesis of 6- ^{18}F Fluoro-L-DOPA, starting from aqueous ^{18}F fluoride, *Tenth International Symposium on Radiopharmaceutical Chemistry*, Kyoto, Japan. **476**.
- [3] Meyer G.-J., Waters S. L. and Coenen H. H. (1995) PET radiopharmaceuticals in Europe: current use and data relevant for the formulation of summaries of product characteristics (SPCs), *Eur. J. Nucl. Med.* **22**, 1420 - 1432.
- [4] Firnau G., Garnett E. S., Chirakal R., Sood S.; Nahmias C. and Schrobilgen G. (1986) ^{18}F Fluoro-L-dopa for the in vivo study of intracerebral dopamine. *Appl. Radiat. Isot.* **37(8)**, 669 - 675.
- [5] Namavari M., Bishop A., Satyamurthy N., Bida G. and Barrio J. R. (1992) Regioselective radiofluorodestannylation with ^{18}F F_2 and ^{18}F CH_3COOF : a high yield synthesis of 6- ^{18}F fluoro-L-dopa. *Appl. Radiat. Isot.* **43(8)**, 989 - 996.
- [6] Appelman E. H.; Basile L. J. and Thompson R. C. (1979) Fluoroxysulfate: a powerful new oxidant and fluorinating agent. *J. Am. Chem. Soc.* **101(12)**, 3384 - 3385.
- [7] Fischer Chr., Neubert K. and Steinbach J. (1997) Electrophilic fluorination: the synthesis of ^{18}F caesium fluoroxysulfate - a new reagent for electrophilic labelling. *This report*, p. 176.

44. Electrophilic Fluorination: A New Route to the Barnette Reagents - N-Fluorination with Perchloryl Fluoride

Chr. Fischer, J. Steinbach

Introduction

N-fluoro-N-alkylsulfonamides, known as Barnette reagents [1] (Fig. 1), are useful electrophilic fluorinating reagents for the selective fluorination of a broad variety of carbanions, amide enolates and alkyl and aryl organometallics under mild conditions. They are prepared from commercially available N-alkyl-

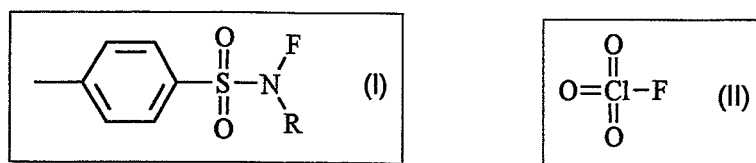
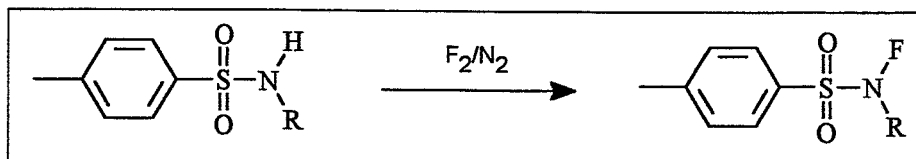
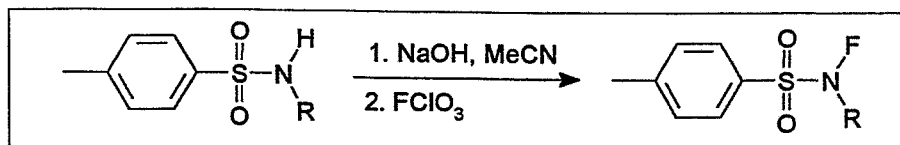


Fig. 1: Barnette-reagents (I), Perchloryl fluoride (II)



Eq. 1: Common synthesis of N-fluoro-N-alkylsulfonamides with fluorine gas

sulfonamides with elemental fluorine diluted in nitrogen [1] (equation 1). Perchloryl fluoride [2] (Fig. 1), also an electrophilic fluorinating agent but of a higher fluorinating power than the Barnette reagents, proved to be a N-fluorinating agent [3] and can be used to obtain N-fluoro derivatives. In this paper we are reporting about the new synthesis of some of the Barnette-reagents with perchloryl fluoride instead of diluted fluorine gas (equation 2).



Eq. 2: New synthesis of some Barnette-reagents with perchloryl fluoride

Experimental

Synthesis of perchloryl fluoride

2.0 g of dry crystalline potassium chlorate are placed in a column, kept between 50 °C and 60 °C and an F₂-stream (10 %) is passed through. The effluent gases were passed through a solution of aqueous 10 % sodium hydroxide containing sodium thiosulphate (5 %) and then over solid potassium hydroxide. Perchloryl fluoride was finally swept out of the system with nitrogen and passed through the reaction mixture, which contains the corresponding sulfonamides 1 - 4 as described in the following.

Fluorination of the sulfonamides

1.7 mmol of the sulfonamides 1 - 4 and carefully powdered NaOH (80 mg, 2 mmol) were stirred at room temperature in dry CH₃CN (10 ml) for 3 h until the dissolution of NaOH was complete. Perchloryl fluoride, which was synthesized as described by Engelbrecht *et al.* [2], is passed through the rapidly stirred suspension at 0 - 5 °C over the course of 30 min. The mixture was diluted with ether (15 ml) and the resultant precipitate was filtered off and washed with water (3 x 10 ml). The organic layer was dried over MgSO₄ and evaporated under reduced pressure. The residue was chromatographed (in hexane : ether 3:1) to afford the corresponding N-fluoro-sulfonamides.

N-fluoro-*N*-methyl-*p*-toluenesulfonamide **5** was determined by thin layer chromatography and by comparison with the corresponding standard compound.

N-fluoro-*N*-*t*-butyl-*p*-toluenesulfonamide **6** :

NMR data: δ_{H} (500 MHz; solvent CDCl_3 ; standard SiMe_4) 7.87 (2H, d, J 8 Hz, aromatic), 7.33 (2H, d, J 8 Hz, aromatic); 2.45 (3H, s, CH_3); 1.43 (9H, d, J 2.7 Hz, $\text{C}(\text{CH}_3)_3$)
 $\delta_{\text{N-F}}$ (400 MHz; standard CFCl_3 : -77) -62.78, see Fig. 2.

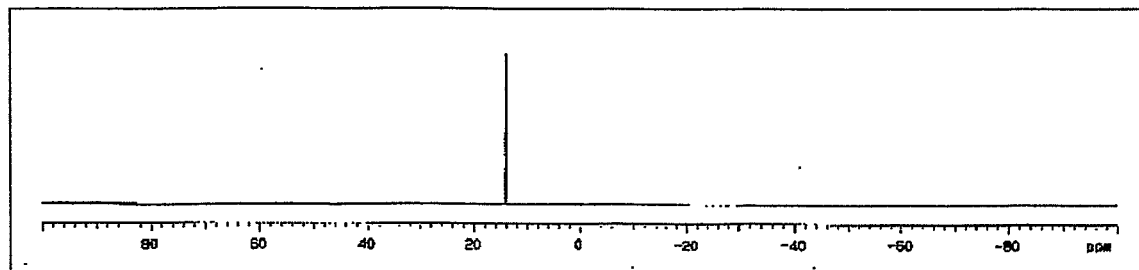


Fig. 2: ^{19}F NMR spectrum of *N*-fluoro-*N*-*t*-butyl-*p*-toluenesulfonamide

N-fluoro-*N*-cyclohexyl-*p*-toluenesulfonamide **7** :

NMR data: δ_{H} (500 MHz; solvent CDCl_3 ; standard SiMe_4) 7.82 (2H, d, J 8 Hz, aromatic), 7.31 (2H, d, J 8 Hz, aromatic), 3.63 (1H, dm, J 32 Hz, NCH), 2.40 (3H, s, CH_3), 0.75-2.30 (10H, m)
 $\delta_{\text{N-F}}$ (400 MHz; standard CFCl_3 : -77) -71.63, see Fig. 3.

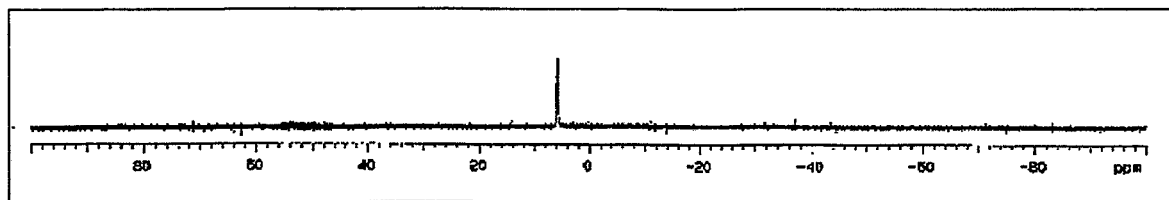


Fig. 3: ^{19}F NMR spectrum of *N*-fluoro-*N*-cyclohexyl-*p*-toluenesulfonamide

N-(2-fluorophenyl)-*p*-toluenesulfonamide **8** :

NMR data: δ_{H} (500 MHz; solvent CDCl_3 ; standard SiMe_4) 7.72 (2H, d, J 8 Hz, aromatic(-S)), 7.55 (1H, m, aromatic (-N)), 7.38 (2H, d, J 8 Hz, aromatic(-S)), 7.20 (2H, m, aromatic(-N)), 7.10 (1H, m, aromatic(-N)), 2.88 (1H, d, J 17 Hz, NH), 2.32 (3H, s, CH_3)
 $\delta_{\text{N-F}}$ (400 MHz; standard CFCl_3 : -77) -127.60, see Fig. 4.

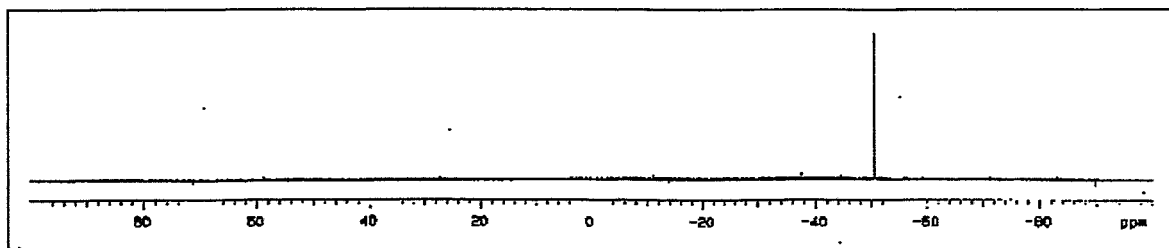


Fig. 4: ^{19}F NMR spectrum of *N*-(2-fluorophenyl)-*p*-toluenesulfonamide

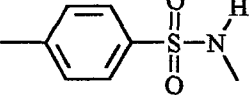
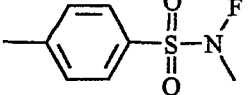
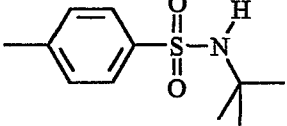
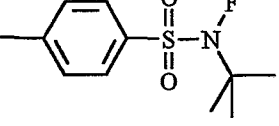
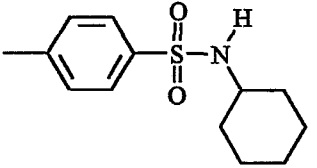
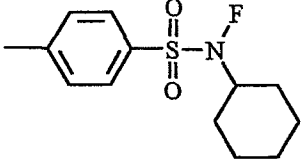
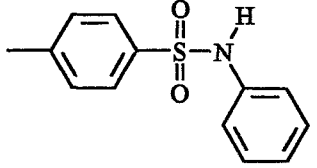
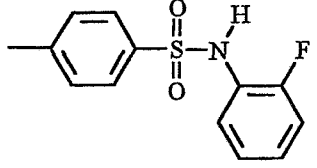
Results and Discussion

The yields of the *N*-methyl and the *N*-cyclohexyl derivatives **5** and **7** (Table 1) are lower than in procedures using fluorine gas as fluorinating agent. In the case of compound **2** perchloryl fluoride provides a higher yield of product **6**.

In contrast to the *N*-fluorination of the sulfonamides **5**, **6** and **7**, *N*-phenyl-*p*-toluenesulfonamide is fluorinated in the ortho position of the phenyl ring. This is obviously caused by the high basicity of the phenyl ring of the sodium salt and the high stability of the C-F bond.

To sum up, perchloryl fluoride provides an N-fluorinating agent and can be a useful reagent in the synthesis of Barnette reagents. It may be important in cases where elemental fluorine gas cannot be used.

Table 1: Yields of the reaction of perchloryl fluoride with the various sulfonamides 1 - 4 to the corresponding fluorine substituted compounds

 <p style="text-align: right;">1</p>	 <p style="text-align: right;">5</p>	Yield 23%
 <p style="text-align: right;">2</p>	 <p style="text-align: right;">6</p>	36%
 <p style="text-align: right;">3</p>	 <p style="text-align: right;">7</p>	8%
 <p style="text-align: right;">4</p>	 <p style="text-align: right;">8</p>	27%

References

- [1] Barnette W. E. (1984) N-Fluoro-N-alkylsulfonamides: Useful reagents for the fluorination of carbanions. *J. Am. Chem. Soc.* **106**, 452 - 454.
- [2] Engelbrecht A. and Atzwanger H. (1956) Perchloryl fluoride, ClO₃F - preparation and some physical and chemical properties. *J. Inorg. Nucl. Chem.* **2**, 348 - 357.
- [3] Barton D. H. R., Hesse R. H., Pechet M. M. and Toh H. T. (1974) Specific synthesis of N-Fluoro-compounds using perfluorofluoroxy reagents. *J. Chem. Soc., Perkin Trans.* 733 - 738.

45. Sulfamates of 3-Hydroxy-estra-1-3-5(10)-triene Derivatives

J. Römer, J. Steinbach, H. Kasch¹

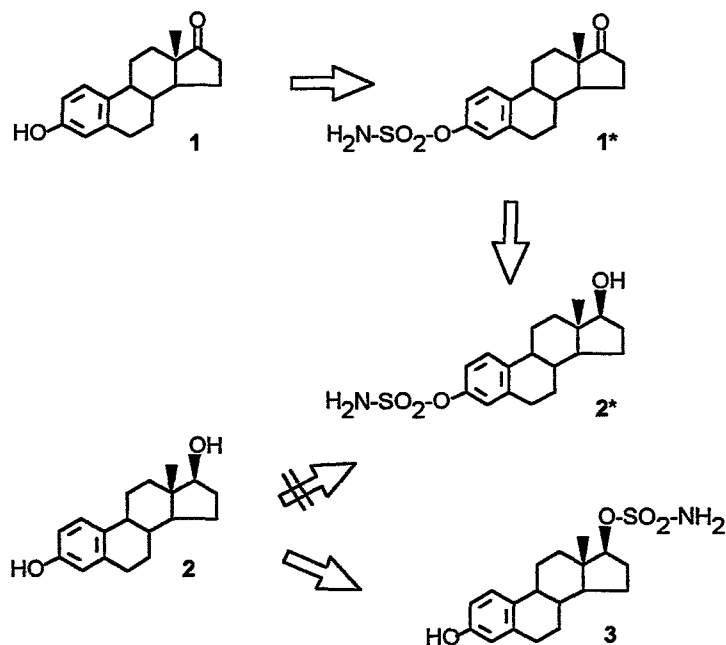
¹ Hans-Knöll-Institut Jena

Introduction

3-Sulfamate of estrogens were reported in the seventies for the first time [1 - 4]. In those days orally effective, synthetic contraceptive steroids were to be converted into sulfamates, which were supposed to be contraceptiva of a long lasting effect due to their lipophilic properties. Two findings of recent date caused estrogen sulfamates to be reinvestigated. Firstly, estrone-3-sulfamate was found to be the most potent estrone sulfatase inhibitor [5], and in this respect the compound may ultimately be of therapeutic utility. Secondly, the estrogenic sulfamates have an as yet unrecognized potential for overcoming the liver barrier without being metabolized, and thus they possess a potent systemic estrogenic activity [6].

The known procedures for synthesizing estrogen sulfamates differ widely. Schwarz *et al.* [3] prepared N,N-dialkylated estrogen-3-sulfamate using a phase-transfer catalyzed procedure which even made it possible to selectively obtain 3-sulfamates of polyhydroxy-estrogens. But it failed in the case of N-monoalkylated and unsubstituted sulfamoyl chloride as a reagent. An interesting procedure which was not previously used in the steroid field was introduced by Spillane *et al.* [7] who replaced the aqueous-alkaline phase by solid sodium carbonate and were able to obtain high yields of sulfamate alkyl esters and phenyl esters. Howarth *et al.* [5] who converted estrone to several 3-sulfamates, did not give any data about yield and reaction rate. After having deprotonated the estrone by NaH, they carried out the reaction at 0 °C in absolute DMF and used 2 equivalents of sulfamoyl chloride. Schwarz *et al.* [8] who tried to copy Howarth's procedure found only a low yield of estrone sulfamate and troublesome by-products. After comprehensive investigations they recommended CH₂Cl₂ as a solvent and 3 equivalents of sulfamoyl chloride in the presence of 2,6-di-tert.-butyl-4-methyl pyridine.

We are primarily interested in non-alkylated sulfamates of estradiol and estradiol derivatives. Therefore, we investigated the possibility of making good use of the recommended literature procedures to synthesize such sulfamates. The first preparative results are described here.



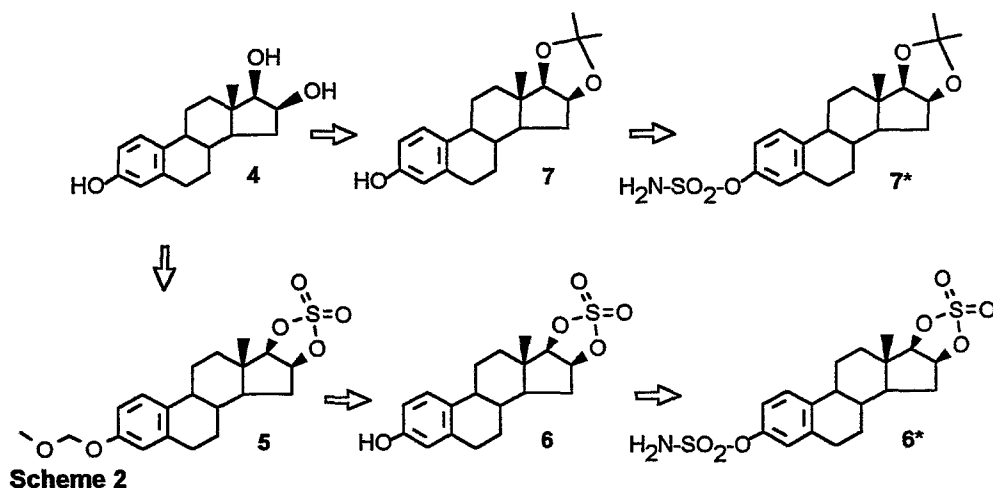
Scheme 1

Experimental

1. General procedure

By converting estrone (1) to estrone-3-sulfamate (1*), the most potent estrone sulfatase inhibitor is obtained [5,9]. This sulfamate 1* can be used as a reference compound for assessment of other estrogen-3-sulfamates as regards the estrone sulfatase inhibitory effect. Analogously to 1 → 1*, a second reference compound can be derived from estradiol (2), namely estradiol-3-sulfamate (2*). As 2 should also form estradiol-17β-sulfamate (3), we tried to prepare this compound as well (Scheme 1).

16-Epiestriol (4) is a hydroxy derivative of estradiol and was used for preparing 3-O-methoxymethyl-16,17-O-sulfuryl-16-epiestriol (5), which represents a suitable precursor for preparing 16α-fluoro-estradiol [10] and 16α-[¹⁸F]fluoroestradiol [11]. Subjecting 5 to acid hydrolysis, 16,17-O-sulfuryl-16-epiestriol (6) was formed which can be converted to 16,17-O-sulfuryl-16-epiestriol-3-sulfamate (6*). 16-Epiestriol (4) reacts with acetone to 16,17-O-isopropylene-16-epiestriol (7) which can be converted to 16,17-O-isopropylene-16-epiestriol-3-sulfamate (7*) (Scheme 2).



2. Materials and methods

Solvents and reagents were obtained from ALDRICH, FLUKA or SIGMA. Sulfamoyl chloride (SCI) was prepared according to Appel and Berger [12]. Melting points were recorded by a Thermogalen device and are uncorrected. The compounds were characterized by their ¹³C NMR spectra reported in the following paper [13] and by mass spectra which were recorded by a High Resolution Mass Spectrometer AMD 402 (AMD-Intra, Harpstedt) and by a VG Quattro device (VG Biotech, Altrincham). For the chromatographic investigations an HPLC system Merck-Hitachi was used, including gradient pump L-6200A, detector L-4500 DAD, a rheodyne injector with a 20-μl loop and an analytic RP column ET 125/8/4 Nucleosil 120-5C18 (Macherey & Nagel). In the case of preparative HPLC an RP column SP 250/10 Nucleosil 120-7C18 was used. Mixtures of MeCN and water or pure MeCN were used as the solvent. The analytic column was eluted at *v* = 0.5 ml/min, the preparative column at *v* = 2.2 ml/min. The UV absorption was recorded at 275 nm. TLC investigations were carried out with analytical TLC plates (MERCK, aluminium sheets, silica gel 60 F₂₅₄, 5x10 cm) and benzene/acetone(4:1) as the solvent. The spots were visualized under UV and after spraying with ethanolic vanillin-sulfuric acid and heating.

3. Syntheses

Estrone-3-sulfamate (1*) : In a little bulb estrone (1) (135 mg = 0.5 mmol) was dissolved in MeCN (abs., 15 ml). After cooling in an ice-bath, NaH (60%, 120 mg = 3 mmol) was added while stirring. Within 15 min SCI (solid, 175 mg = 1.5 mmol) was added and stirring was continued for 2 h. Although only in-complete conversion was registered, water was added and after acidification the batch was extracted with ether. After removing ether under reduced pressure, MeCN (5 ml) was added to the residue. Preparative HPLC was carried out (10 separations, 0.5 ml injection volume, pure MeCN as the solvent). 1* was eluted at *R_t* = 7.7 min. The peaks were cut and collected. The solvent was evaporated at room temperature to give white, fine crystals, yield: (92 mg, 53 %). Melting point: 203 - 207 °C (from MeCN).

MS: m/z 349.1351 (M^+), 270.1614 ($M^+ - \text{HNSO}_2$).

UV: $\lambda_{\text{max}}/\text{nm}$ 270.

Elemental analysis: (Found: C, 61.8; H, 6.8; N, 3.9; S, 9.0. $\text{C}_{18}\text{H}_{23}\text{O}_4\text{NS}$ requires C, 61.9; H, 6.6; N, 4.0; S, 9.2 %).

Estradiol-3-sulfamate (2*) : Estrone-3-sulfamate (1*) (70 mg = 0.2 mmol) was dissolved in THF (abs., 2 ml) and EtOH (99.9 %, 2 ml). After cooling in an ice-bath, NaBH_4 (solid, 20 mg = 0.54 mmol) was added while stirring. The batch was stirred for another 2 h at room temperature, acidified and worked up and chromatographed as described above. 2* was eluted at $R_t = 8.3$ min. After evaporating MeCN, the collected peaks gave a white product, yield: (37.8 mg, 54 %). Melting point: 175 - 182 °C (from MeCN). MS: m/z 351.1511 (M^+), 272.1769 ($M^+ - \text{HNSO}_2$), 213.1283 ($M^+ - \text{HNSO}_2 - \text{C}_3\text{H}_7\text{O}$).

UV: $\lambda_{\text{max}}/\text{nm}$ 270.

Elemental analysis: (Found: C, 59.5; H, 8.5; N, 3.9; S, 8.7. $\text{C}_{18}\text{H}_{25}\text{O}_4\text{NS}$ requires C, 61.5; H, 7.1; N, 4.0; S, 9.1 %).

Estradiol-17 β -sulfamate (3) : Estradiol (2) (120 mg = 0.45 mmol) was dissolved in MeCN (absolute, 10 ml) and after cooling in an ice-bath, NaH (60 %, 84 mg = 2.1 mmol) was added while stirring. Within 15 min SCl (solid, 70 mg = 0.6 mmol) was added and stirring was continued at room temperature. HPLC controls after 2 and 6 h showed 3 peaks and unreacted estradiol. The solvent was evaporated, the residue extracted with ether, and then the ether removed. After adding MeCN (5 ml), the solution was chromatographed (20 separations, 0.25 ml injection volume, pure MeCN as the solvent). 3 was eluted at $R_t = 7.5$ min. These peaks were cut and collected. Evaporation of solvent gave a white substance, yield: (21.5 mg, 13 %). Melting point: 158 - 161 °C (from MeCN).

MS: m/z 351.1539 (M^+), 333.1376 ($M^+ - \text{H}_2\text{O}$), 272.1769 ($M^+ - \text{HNSO}_2$), 254.1672 (100 %, $M^+ - \text{H}_2\text{O} - \text{HNSO}_2$).

UV absorption: $\lambda_{\text{max}}/\text{nm}$ 284.

Elemental analysis: (Found: C, 59.0; H, 6.6; N, 4.0; S, 8.6. $\text{C}_{18}\text{H}_{25}\text{O}_4\text{NS}$ requires C, 61.5; H, 7.1; N, 4.0; S, 9.1 %).

16,17-O-Sulfuryl-16-epiestriol-3-sulfamate (6*) : 3-O-Methoxymethyl-16,17-O-sulfuryl-16-epiestriol (5) [11] (147 mg = 0.373 mmol) was placed in a bulb. MeCN (5 ml) and HCl (1 M, 10 drops) were added and the batch was stirred in a bath (110 °C) for 10 min. After complete removal of the solvent in this bath, CH_2Cl_2 (abs., 6 ml), sodium carbonate (anhydrous, 700 mg) and SCl (solid, 180 mg = 1.56 mmol) were added. Then the batch was vigorously stirred. HPLC revealed 75 % conversion to 6* after 3 h and 94 % after 6 h. After adding water (150 ml), the steroids were extracted with ether (50 ml). After removing the ether, MeCN (6 ml) was added and preparative HPLC carried out (13 separations, 0.45 ml injection volume, pure MeCN as solvent). 6* was eluted at $R_t = 7.3$ min. After evaporating MeCN, the collected peaks gave a white, fine product, yield: (34.7 mg, 60 %). Melting point: 195 - 198 °C (from MeCN).

MS: m/z 429.0934 (M^+), 350.1180 (55 %, $M^+ - \text{NHSO}_2$), 270.1617 (50 %, $M^+ - \text{NHSO}_2 - \text{SO}_3$).

UV absorption: $\lambda_{\text{max}}/\text{nm}$ 270.

Elemental analysis: (Found: C, 49.3; H, 6.1; N, 3.5; S, 14.2. $\text{C}_{18}\text{H}_{23}\text{O}_7\text{NS}_2$ requires C, 50.4; H, 5.4; N, 3.3; S, 14.9 %).

16,17-O-Isopropylene-16-epiestriol (7) : 16-Epiestriol (4) (100 mg = 0.347 mmol) was placed in a bulb. CH_2Cl_2 (abs., 12 ml) and p-toluene sulfonic acid (20 mg) were added. Acetone (1 ml) was added while stirring. The solution, which was at first cloudy, became clear after about 30 min while stirring continued. After 2 h the clear solution was poured into NaHCO_3 solution. The CH_2Cl_2 extract was washed with water. Evaporation of the solvent gave white crystals, yield: (112 mg, 98.4 %). Melting point: 180 - 185 °C.

Elemental analysis: (Found: C, 76.7; H, 8.5. $\text{C}_{21}\text{H}_{28}\text{O}_3$ requires C, 76.8; H, 8.5 %).

16,17-O-Isopropylene-16-epiestriol-3-sulfamat (7*) : Sodium carbonate (anhydrous, 500 mg) and SCl (30 mg = 0.26 mmol) were added to 16,17-O-isopropylene-16-epiestriol (7) (75 mg = 0.228 mmol) dissolved in CH_2Cl_2 (absolute, 5 ml). The suspension was vigorously stirred for 60 h. From time to time small amounts of SCl (5 x 10 mg) were added. The batch was poured into NaHCO_3 solution and the steroids were extracted with ether (2 x 40 ml). After evaporating the ether and adding MeCN (4 ml), preparative HPLC (9 separations, 0.45 ml injection volume, pure MeCN as solvent) was carried out. 7* was eluted at $R_t = 8.7$ min. The solvent of the collected peaks was removed at room temperature. White crystals were obtained, yield: (26.3 mg, 28.4 %). Melting point: The crystals softened at about 190 °C.

from about 235 °C they turned brown while decomposing .

MS: m/z 407.1755 (M⁺), 392.1520 (M⁺ - CH₃), 313.1810 (M⁺ - CH₃ - NHSO₂);

UV: λ_{max}/nm 270.

Elemental analysis: (Found: C, 61.7; H, 7.1; N, 3.6; S, 7.9. C₂₁H₂₉O₅NS requires C, 61.9; H, 7.1; N, 3.4; S, 7.9 %).

Results and Discussion

As preparative aspects we will discuss i) the yield of the sulfamates, ii) the synthesis rate, and iii) the simplicity of the procedure. These points will be very important if the conditions are to be applied to the synthesis of an ¹⁸F labelled compound. Some chromatographic results will also be mentioned.

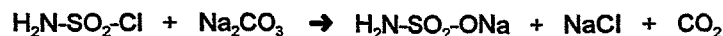
Estrone-3-sulfamate (1*) was prepared according to Howarth *et al.* [5]. But, because of its lower boiling point, MeCN was used instead of DMF. The reaction time was acceptable, the extent of conversion low. To prepare pure 1* preparative HPLC had to be applied with pure MeCN as a suitable HPLC solvent. In these attempts we found that λ_{max}(1*) = 270 nm whereas estrone (1) has λ_{max}(1) = 284 nm. λ_{max} = 270 nm was generally found for all the 3-sulfamates investigated.

The sulfamoylation of estradiol (2) according to Howarth's method did not result in estradiol-3-sulfamate (2*). Estradiol-17β-sulfamate (3) and some by-products were formed in low yields. 3 did not show 270 nm but 284 nm as the absorption maximum. Unequivocal evidence of the structure of 3 was presented by recording its ¹³C NMR spectrum [13].

In order to obtain estradiol-3-sulfamate (2*) we used the method proposed by Schwarz *et al.* [8] who were successful when subjecting estrone-3-sulfamate (1*) to NaBH₄ reduction. Ester cleavage did not occur during this treatment. We obtained 2* in about 80 % yield, after preparative HPLC in 54 %. As expected, the sulfamate 2* showed λ = 270 nm as the absorption maximum. Its structure was also confirmed by ¹³C NMR spectroscopy [13].

16,17-O-Sulfuryl-16-epiestriol-3-sulfamate (6*) was prepared from 3-O-methoxymethyl-16,17-O-sulfuryl-16-epiestriol (5) without isolating 16,17-O-sulfuryl-16-epiestriol (6). The fast and simple hydrolysis procedure 5 → 6 had been worked out previously [11]. However, there were some problems in the sulfamoylation reaction according to [5] and [8] which did not result in 6*. Only when taking advantage of a phase-transfer procedure with sodium carbonate and CH₂Cl₂ as solvent was 6* obtained in acceptable yields. We stated that the yield is the better, the more vigorously the reaction mixture is stirred and that about 5 equivalents of SCl should be used. Special attention must be paid to the fact that SCl is sensitive to humidity with sulfamic and hydrochloric acids being formed. But before neutralization by sodium carbonate, acids impair the procedure. Thus, we believe that even under the most favourable conditions the reaction 6 → 6* on the 100-mg scale will require a reaction time of several hours.

The sulfamoylation reaction 7 → 7* also caused problems as regards the yield of 7* and the reaction time. Here, the reaction rate is obviously much lower than in the foregoing example. In this manner the side reaction



begins to dominate and disturbs the reagent. We also found here that above all the acid medium due to excessive SCl is very disadvantageous. We tried to overcome this disadvantage by adding the reagent in small portions, of course at the expense of time. In spite of all that the yield of 7* did not exceed 30 %.

In order to characterize the new sulfamates ¹³C NMR spectroscopy, mass spectroscopy, UV absorption, elemental analysis and chromatographic procedures (HPLC, TLC) were used. The ¹³C NMR spectra are discussed in the following paper [13]. The UV absorption of 3-sulfamates at 270 nm was already mentioned. Now some interesting results of HPLC and TLC will be considered.

To prepare the new sulfamates in pure form, preparative RP-phased HPLC with MeCN as the solvent was used. Here it holds generally that the smaller the R_f value, the more polar is the compound. It can be seen from the R_f values listed in Table 1 that a sulfamate is basically more polar than the hydroxy compound from which it was prepared, in other words R_f (n*) < R_f (n). The same result is found for the compounds 3 and 2.

Table 1: Retention times R_t (in min) of some 3-hydroxy-estra-1,3,5(10)-triene derivatives (1, 2, 3, 6, 7) and some of their 3-sulfamates (1*, 2*, 6*, 7*)

Numbering	Steroid	R_t [min]
1	estrone	8.6
1*	estrone-3-sulfamate	7.7
2	estradiol	10.5
2*	estradiol-3-sulfamate	8.3
3	estradiol-17 β -sulfamate	7.5
6	16,17-O-sulfuryl-16-epiestriol	8.0
6*	16,17-O-sulfuryl-16-epiestriol-3-sulfamate	7.3
7	16,17-O-isopropylen-16-epiestriol	11.4
7*	16,17-O-isopropylen-16-epiestriol-3-sulfamate	8.7

Using TLC on silica plates, it is also valid that the smaller the R_f value, the more polar is the compound. All the R_f values found are listed in Table 2. Except for estrone, we can state that the rule $R_f(n^*) < R_f(n)$ is fulfilled. Some special features were furnished by colouring the spots with vanillin sulfuric acid the results of which are also summarized in Table 2. After spraying and heating the plate, the spots of the 3-sulfamates 1* and 2* turned brown and then green as it was cooled. But the spots of the 3-sulfamates 6* and 7* did not discolour at all whereas the corresponding 3-hydroxy derivatives 6 and 7 became at least a pale pink.

Table 2: TLC results of some 3-hydroxy-estra-1,3,5(10)-triene derivatives (1, 2, 3, 6, 7) and some of their 3-sulfamates (1*, 2*, 6*, 7*)

Numbering	R_f value	Colour of spots	
		hot	cold
1	0.50	purple	yellow
1*	0.66	brown	green
2	0.33	purple	yellow
2*	0.29	brown	green
3	0.22	brown	pink
6	0.50	pink	pink
6*	0.40	not detectable	not detectable
7	0.53	pink	pink
7*	0.46	not detectable	not detectable

In this paper, some first procedures for preparing estrogen sulfamates have been described. The procedures have still to be optimized. Further examples are under investigation with 3-sulfamates as the main objects.

Acknowledgement: We wish to express our gratitude to the Deutsche Forschungsgemeinschaft for its grant in support of this work.

References

- [1] Schwarz S., Weber G and Kühner F. (1970) Sulfamate des 17α -ethinylestradiols; *Z. Chem.* **10**, 299.
- [2] Schwarz S. and Weber G. (1974) Steroidsulfamate. *Z. Chem.* **14**, 15.
- [3] Schwarz S. and Weber G. (1975) Phasentransfer-katalysierte Veresterung von Estrogenen mit Sulfonylchloriden; *Z. Chem.* **15**, 270.
- [4] Schwarz S., Weber G. and Schreiber M. (1975) Sulfonyloxyderivate von Estrogenen; *Pharmazie* **30**, 17.
- [5] Howarth N. M., Purohit A., Reed M. J. and Potter B. V. L. (1994) Estrone sulfamates: Potent inhibitors of estrone sulfatase with therapeutical potential. *J. Med. Chem.* **37**, 219.
- [6] Elger W., Schwarz S., Hedden A., Reddersen G. and Schneider B. (1995) Sulfamates of various estrogens with increased systemic and reduced hepatic estrogenicity at oral application. *J. Steroid Biochem. Molec. Biol.* **55**, 395.
- [7] Spillane W. J., Taheny A. P. and Kearns M. M. (1982) Versatile synthesis of sulphamate esters by phase-transfer methods *J. Chem. Soc., Perkin I*, 677.
- [8] Schwarz S. and Elger W. (1996) Estrogen sulfamates, a novel approach to oral contraception and hormone replacement therapy. *Drugs Future* **21**, 49.
- [9] Purohit A., Williams G. J., Howarth N. M., Potter B. V. L. and Reed M. J. (1995) Inactivation of steroid sulfatase by an active site-directed inhibitor, estron-3-sulfamate. *Biochemistry* **34**, 11508.
- [10] Lim J. L., Lei Zheng, Berridge M. S. and Tewson T. J. (1996) The use of 3-methoxymethyl- 16β , 17β -epiestriol-O-cyclic sulfone as the precursor in the synthesis of F-18 16α -fluoroestradiol. *Nucl. Med. Biol.* **23**, 911.
- [11] Römer J., Steinbach J. and Kasch H. (1996) Studies on the synthesis of 16α - ^{18}F fluoroestradiol *Appl. Radiat. Isot.* **47**, 395.
- [12] Appel R. and Berger G. (1958) Über das Hydrazodisulfamid. *Chem. Ber.* **91**, 1339.
- [13] Römer J., Steinbach J. and Scheller D. (1996) ^{13}C NMR spectroscopic characterization of some sulfamates of 3-hydroxy-estzra-1,3,5(10)-triene derivatives. *This report*, pp. 188 - 189.

46. ^{13}C NMR Spectroscopic Characterization of Some Sulfamates of 3-Hydroxy-estra-1,3,5(10)-triene Derivatives

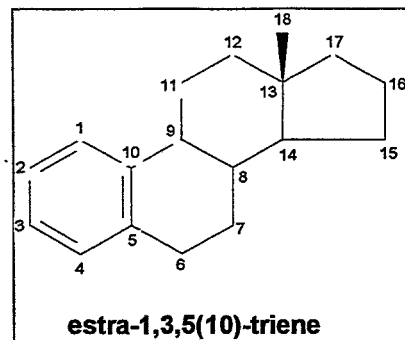
J. Römer, J. Steinbach, D. Scheller ¹

¹ Technische Universität Dresden

Introduction

In the foregoing paper [1] the syntheses of some sulfamates of 3-hydroxy-estra-1,3,5(10)-trienes were described. These sulfamates were characterized by the usual spectroscopic methods. As the ^{13}C NMR spectroscopy has been proved for years to be the most important method for characterizing new steroidal compounds, spectra of these sulfamates were recorded. The results are reported and discussed by comparing the spectra of the 3-hydroxy-1,3,5(10)-triene derivative and its corresponding sulfamate.

In the following list all the 3-hydroxy-1,3,5(10)-trienes and their sulfamates which were investigated are summarized. The steroid numbering was taken over from the foregoing paper.



Numbering	Trivial name (IUPAC name)
1	estrone (3-hydroxy-estra-1,3,5(10)-trien-17-one)
1*	estrone-3-sulfamate (3-amidosulfonyloxy-estra-1,3,5(10)-trien-17-one)
2	estradiol (estra-1,3,5(10)-triene-3,17 β -diol)
2*	estradiol-3-sulfamate (3-amidosulfonyloxy-estra-1,3,5(10)-trien-17 β -ol)
3	estradiol-17 β -sulfamate (17 β -amidosulfonyloxy-estra-1,3,5(10)-trien-3 β -ol)
4	16-epiestriol (estra-1,3,5(10)-triene-3,16 β ,17 β -triol)
6	16,17-O-sulfuryl-16-epiestriol (16,17-O-sulfuryl-estra-1,3,5(10)-triene-3,16 β ,17 β -triol)
6*	16,17-O-sulfuryl-16-epiestriol-3-sulfamate (3-amidosulfonyloxy-16,17-O-sulfuryl-estra-1,3,5(10)-triene-16 β ,17 β -diol)
7	16,17-O-isopropylene-16-epiestriol (16,17-O-isopropylene-estra-1,3,5(10)-triene-3,16 β ,17 β -triol)
7*	16,17-O-isopropylene-16-epiestriol-3-sulfamate (3-amidosulfonyloxy-16,17-O-isopropylene-estra-1,3,5(10)-triene-16 β ,17 β -diol)

Experimental

^{13}C NMR spectra were recorded at 75 MHz with a BRUKER MSL 300 spectrometer using BB decoupling and APT and DEPT methods for assignment. 30° pulses and repetition times of 2 s were applied, the digital resolution was 1.3 Hz. The spectra were calibrated indirectly to TMS as reference via solvent peaks (methanol- d_4 49.0 ppm, chloroform- d 77.0 ppm).

Results and Discussion

The chemical shifts of all the steroids measured are listed in Table 1. The usual numbering of the carbon atoms of the steroid skeleton is shown in the formula of estrane-1,3,5(10)-triene.

As was to be expected, all the signals of the ring A carbon atoms were affected by replacing a 3-OH proton with an amidosulfonyl group. We found a shielding effect on C(3), deshielding effects on C(2), C(4), and C(10), but very little effects on C(1) and C(5). These effects result in a close neighbouring position of the signals of C(5) and C(10) near about 138 ppm, a typical feature of all estrogen 3-sulfamates. By

contrast the spectrum of estradiol-17 β -sulfamate (3) did not show two neighbouring signals in this region.

Estradiol (2), 16-epiestriol (4) and 3-O-methoxymethyl-16,17-O-sulfuryl-16-epiestriol (compound 5 in [1]) were previously discussed [2]. Therefore, we will now concentrate on the compounds 6, 6*, 7, and 7* representing 16-epiestriol derivatives. Compared with 4, 16,17-O-sulfuryl-16-epiestriol (6) and its 3-sulfamate 6* reveal a great downfield shift of the signals of C(16) and C(17) and the same tendency is found at 16,17-O-isopropylene-16-epiestriol (7) and its 3-sulfamate 7*. This downfield shift is due to the fact that after substitution the free rotation of the two hydroxy groups no longer exists. The simultaneous deshielding effect on C(14) being notable cannot be explained. It seems to have to do with distortion of the ring D. As expected, the spectra of 7 and 7* contain three additional signals. One of these signals is found at 113.4 ppm. According to the DEPT spectrum, it represents the middle (hydrogen-free) carbon atom of the isopropylene group.

Table 1 : ^{13}C chemical shifts (in ppm) of some 3-hydroxy-estra-1,3,5(10)-triene derivatives and their 3-sulfamates

Carbon atom	1	1*	2	2*	3	4	6	6*	7	7*
1	126.1	126.7	126.1	126.9	127.2	125.4	127.2	127.1	126.4	126.8
2	112.7	119.1	112.5	119.5	113.8	112.1	113.9	120.0	112.7	118.9
3	154.3	148.1	154.0	148.7	156.0	153.9	156.2	149.3	153.6	147.9
4	115.1	122.0	115.0	122.4	116.1	114.5	116.1	122.7	115.2	121.9
5	137.5	138.8	137.8	139.6	138.7	137.1	138.5	138.7	138.0	138.8
6	29.3	29.3	29.4	29.9	30.6	28.9	30.4	29.7	29.5	29.4
7	26.3	26.2	27.1	27.4	28.4	26.8	28.7	27.8	27.4	27.2
8	38.2	37.9	38.7	39.0	40.2	37.8	39.5	38.3	38.2	37.9
9	43.7	44.1	43.7	44.6	45.2	43.6	44.9	44.3	43.6	43.9
10	130.8	138.6	131.6	139.0	132.3	131.0	131.6	138.4	132.2	139.5
11	25.7	25.7	26.1	26.7	27.4	25.5	27.2	26.5	26.3	26.2
12	31.3	31.4	36.5	37.1	37.7	36.8	37.9	37.4	37.9	37.8
13	48.0	47.9	43.0	43.6	44.4	42.1	44.7	44.2	42.3	42.2
14	50.2	50.3	49.8	50.5	50.5	46.0	48.3	47.9	51.5	51.5
15	21.3	21.5	22.8	23.4	24.0	33.9	31.6	31.3	31.0	31.0
16	35.7	35.8	29.7	30.1	28.9	69.0	83.6	82.8	79.5	79.4
17	222.3	221.1	81.3	81.7	90.2	80.1	92.1	91.3	88.7	88.7
18	13.6	13.8	10.8	11.3	12.2	11.0	13.2	13.0	13.9	13.9
CH ₃ -C-CH ₃	-	-	-	-	-	-	-	-	24.8	24.8
CH ₃ -C-CH ₃	-	-	-	-	-	-	-	-	25.6	25.6
CH ₃ -C-CH ₃	-	-	-	-	-	-	-	-	113.4	113.4

References

- [1] Römer J., Steinbach J. and Kasch H. (1996) Sulfamates of 3-hydroxy-estra-1,3,5(10)-triene derivatives. *This report*, pp. 182 - 187.
- [2] Römer J. and Scheller D. (1995) ^{13}C NMR spectroscopic characterization of estra-1,3,5(10)-triene-3,17 β -diol and 3,16,17-triols, and some of their 3-O-methoxymethyl and 16 α -fluoro derivatives. *Annual Report 1995*, Institute of Bioinorganic and Radiopharmaceutical Chemistry, FZR-122, p.27.

47. Synthesis of 16 β -Bromo-3-methoxy-estra-1,3,5(10)-trien-17 β -ol by a Novel One-Pot Reaction

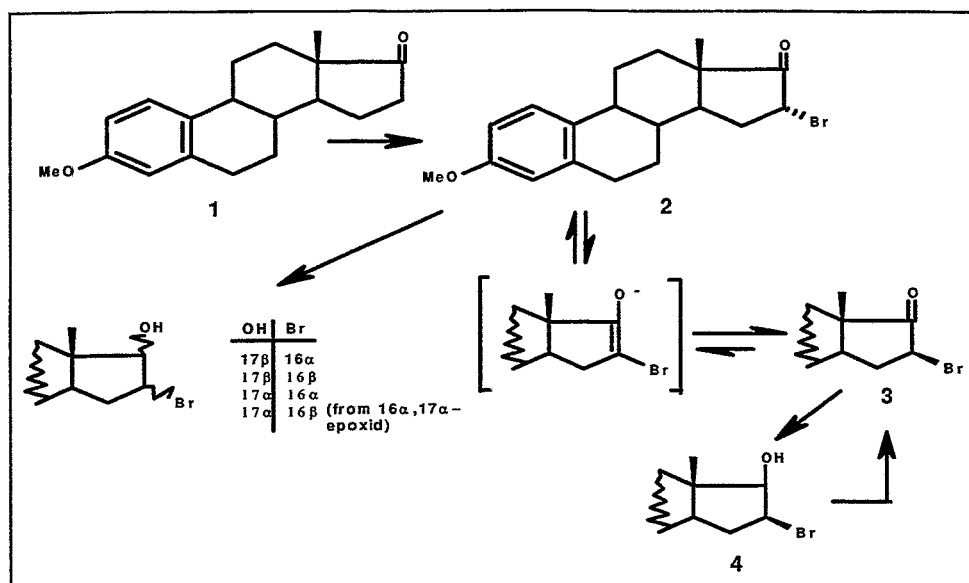
H. Kasch¹, U. Dintner¹, J. Römer, J. Steinbach

¹ Hans-Knöll-Institut Jena

Introduction

Estrogenic 16,17-bromohydrins are important starting compounds for 16,17-cis diols [1]. Except for 16 β -bromo-17 α -OH bromohydrin, all epimeric bromohydrins are available in two steps from 3-methoxy-estra-1,3,5(10)-trien-17-one (**1**) (see scheme) [2] with the CuBr₂ bromination according to Numazawa [3] being the first step to give pure 3-methoxy-16 α -bromo-estra-1,3,5(10)-trien-17-one (**2**). We were interested in particular in 3-methoxy-16 β -bromo-estra-1,3,5(10)-trien-17-one (**3**) and 3-methoxy-16 β -bromo-estra-1,3,5(10)-trien-17 β -ol (**4**).

Under alkaline conditions 3-methoxy-16 α -bromo-estra-1,3,5(10)-trien-17-one (**2**) isomerizes to a mixture of **2** and **3**. Pure **3** can be reduced by sodium borohydride to 3-methoxy-16 β -bromo-estra-1,3,5(10)-trien-17 β -ol (**4**). We were able to combine both processes in a one-pot reaction.



Experimental

3-Methoxy-16 β -bromo-estra-1,3,5(10)-trien-17 β -ol (**4**)

3-Methoxy-16 α -bromo-estra-1,3,5(10)-trien-17-one (**2**) (300 mg, 0.83 mmol) was dissolved in ethanol (15 ml), the solution was cooled to -5 °C and sodium hydroxide (14.6 mg, 0.384 mmol) was added while stirring. After 15 min a suspension of NaBH₄ (13.8 mg) in EtOH (0.5 ml) was added drop by drop. At the end excessive NaBH₄ was eliminated by adding a few drops of acetone and the reaction mixture was poured into ice water. The cis-bromohydrin **4** was separated by filtration and then recrystallized from methanol (85 % yield).

Melting point: 104 - 105 °C

TLC(R_f): 0.56 ; 0.34 (silica gel, toluene/ethylacetate = 5:1 ; 20:1); 0.62 (toluene/methanol=20:1).

IR absorption: ν_{\max} /cm⁻¹ 3544 (OH), 1605, 1570, 1497 (aromatic).

Mass spectrum: m/z 364.10510 (M⁺), calc. 364.1038 for C₁₉H₂₅O₂Br; 284.17718 (M⁺-HBr), calc. 284.1766 for C₁₉H₂₄O₂; 267.17569 (M⁺-H₂O-Br), calc. 267.1749 for C₁₉H₂₂O; 229.16020 (M⁺-C₃H₅OBr), calc. 229.159 for C₁₆H₂₁O.

¹³C NMR data: C(1) 126.3; C(2) 111.6; C(3) 157.6; C(4) 113.8; C(5) 137.6; C(6) 29.6; C(7) 27.3; C(8) 38.3; C(9) 43.9; C(10) 132.1; C(11) 25.8; C(12) 37.2; C(13) 43.6; C(14) 48.6; C(15) 37.3; C(16) 55.3; C(17) 79.5; C(18) 12.0; OCH₃ 55.2.

Results and Discussion

The chemistry of 16,17-substituted 14 α -steroids is extremely influenced by the steric hindrance of the β -face by the 13 β -methyl group and the 16 β -substituent, on the one side, and of the α -face by the 16 α -substituent, on the other.

Thermodynamic considerations (MM-2 calculations) of 16-bromoketones favour the 16 β -bromo compound. In practice, under basic and acidic isomerization conditions as well as on nucleophilic substitution by bromide in aprotic dipolar medium, a 60:40 percent mixture of 16 β -bromoketone **3** and 16 α -bromoketone **2** was obtained [5]. We found that a mixture of the bromoketones **2** and **3** formed by isomerization with catalytic amounts of sodium hydroxide in pyridine or DMF/ EtOH could be reduced to the cis- β -bromohydrin **4** in a substrate-specific manner. The α -bromoketone **2** was nearly untouched under the kinetically controlled reaction conditions.

This finding made it possible to combine the isomerization process and the reduction in a one-pot reaction. Using sodium borohydride at a low temperature, the reduction rate of the 16 α -bromoketone **2** decreased extremely in comparison with the 16 β -bromoketone **3**. The differences in reactivity attributed to a steric hindrance of the α -face by the 16 α -Br proved to be advantageous for a high yield of **4** because **3** consumed by reduction was formed gradually by alkaline isomerization of **2**. The low alkaline concentration as well as the low temperature were necessary in order to prevent that **4** was converted into estradiol- or estrone-3-methylether, respectively.

The one-pot reaction was carried out with an ethanolic 0.015 M solution of sodium hydroxide in DMF or ethanol at a temperature of -5 °C. When the isomerization equilibrium was reached, sodium borohydride was added in small portions (0.5 mol per mol steroid).

In this way the step by step isomerization, first by bromide [4] and then by alkali and reduction [5] could be simplified and replaced by a one-pot isomerization-reduction process. The cis-bromohydrin **4** was received in an overall yield of 85 %.

To obtain pure 3-methoxy-16 β -bromo-estra-1,3,5(10)-trien-17-one (**3**) Jones oxidation [6] of the cis-bromohydrin **4** can be used (see scheme).

Acknowledgement

This work was performed within a project conducted by the Institute of Bioinorganic and Radiopharmaceutical Chemistry (FZ Rossendorf e.V.), the Hans Knöll Institute of Natural Products Research Jena (Dir.: Prof. A. Hinnen) and the Clinic of Nuclear Medicine, University Hospital Dresden (Dir.: Prof. W.G.Franke).

References

- [1] Römer J., Steinbach J. and Kasch H. (1996) Studies on the synthesis of 16 α -[¹⁸F]fluoroestradiol, *Appl. Radiat. Isot.* **47**, 395.
- [2] Schönecker B. (1977) Beiträge zur Chemie und Stereochemie biologisch aktiver 16,17-substituierter Östra-1,3,5(10)-triene“ and literature cited there. *Dissertation B.*
- [3] Numazawa M. and Nagaoka M. (1982) Stereospezifische Synthese von 16 α -Hydroxy-17-Oxo-Steroiden durch kontrollierte alkalische Hydrolyse von entsprechenden 16-Bromo-17-Ketonen und ihr Reaktionsmechanismus. *J. Org. Chem.* **47**, 4024.
- [4] Schönecker B., Ponsold K. and Große P. (1974) Darstellung von 16-Brom-östradiolen und 16 β -Brom-östron-3-methylether. *Z. Chem.* **14**, 472.
- [5] Numazawa M. and Osawa Y. (1980) Controlled alkaline hydrolysis of 16-bromo-17-keto steroids without ketol rearrangement and its reaction mechanism. *J. Am. Chem. Soc.* **102**, 5404.
- [6] Bowden, K. Heilbron I. M., Jones E. R. H. and Weedon B. L. C. (1946) The preparation of acetylenic ketones by oxidation of acetylenic carbinols and glycols. *J. Chem. Soc.*, 39.

48. Further ^{13}C NMR Spectroscopic Proof of $16\alpha\text{-F}$ Configuration in $16\text{-Fluoroestradiol}$ Derivatives

J. Römer, J. Steinbach, D. Scheller ¹, H. Kasch ²

¹ Technische Universität Dresden

² Hans-Knöll-Institut Jena

Introduction

In earlier papers we reported on the synthesis [1] and the ^{13}C NMR spectroscopic characterization [2] of $16\text{-fluoroestradiol}$ derivatives. We found similar substituent effects for 16-F as for $16\alpha\text{-OH}$ and concluded that the fluorine atom was α -orientated in these 16-fluoro steroids. To prove the α -orientation of 16-F we now cite further NMR spectroscopic arguments which are based on coupling constants and chemical shifts.

Results and Discussion

In the ^{13}C NMR spectra of 16-fluoro steroids it was to be expected that the signals of the ring D carbon atoms are split in doublets. This splitting was found for C(16) ($^1J(\text{C},\text{F}) = -178.5$ Hz), for C(15) and C(17) ($^2J(\text{C},\text{F}) = 23.1$ Hz and 22.0 Hz) and for C(13) ($^3J(\text{C},\text{F}) = 7.4$ Hz) but it did not occur at C(14). This means that here $^3J(\text{C},\text{F}) = 0$ Hz and, due to KARPLUS equation [3], the dihedral angle $16\text{-F} - \text{C}(16) - \text{C}(15) - \text{C}(14)$ has to be about 90° . Molecular modelling (minimizing the binding energy by optimizing the geometry of $16\alpha\text{-fluoroestradiol}$, using the program MM-2 from Hyper-Chem) gave indeed 90° for this dihedral angle. All the torsion angles calculated are listed in Table 1. Similar dihedral angles were found for estradiol and other 16-fluoro steroids reported in [2]. But no useful values were obtained in the case of $16\beta\text{-fluoroestradiol}$.

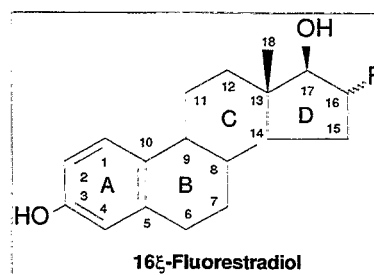


Table 1: Calculated torsion angles of ring D structure elements of $16\beta\text{-fluoroestradiol}$

No.	Structure element	Torsion angle	$^3J(\text{C},\text{F})$ [Hz]
1	$16\alpha\text{-F} - \text{C}(16) - \text{C}(15) - \text{C}(14)$	90.02	0
2	$16\alpha\text{-F} - \text{C}(16) - \text{C}(15) - 15\alpha\text{-H}$	31.18	-
3	$16\alpha\text{-F} - \text{C}(16) - \text{C}(15) - 15\beta\text{-H}$	151.28	-
4	$16\beta\text{-H} - \text{C}(16) - \text{C}(15) - \text{C}(14)$	147.34	-
5	$16\beta\text{-H} - \text{C}(16) - \text{C}(15) - 15\alpha\text{-H}$	91.46	-
6	$16\beta\text{-H} - \text{C}(16) - \text{C}(15) - 15\beta\text{-H}$	28.64	-
7	$16\alpha\text{-F} - \text{C}(16) - \text{C}(17) - \text{C}(13)$	121.95	7.4
8	$16\alpha\text{-F} - \text{C}(16) - \text{C}(17) - 17\beta\text{-OH}$	115.93	-
9	$16\beta\text{-H} - \text{C}(16) - \text{C}(17) - \text{C}(13)$	116.56	-
10	$16\beta\text{-H} - \text{C}(16) - \text{C}(17) - 17\beta\text{-OH}$	5.56	-

To understand the ^{13}C chemical shifts [2], these torsion angles are important. The DREIDING model shows that the bonds of C(15) and C(16) are arranged in an eclipsed form. Such a form is energetically less favourable than a staggered one. But, distorting the ring D in such a way that $16\alpha\text{-H} - \text{C}(16) - \text{C}(15) - \text{C}(14)$ form a dihedral angle of about 90° , this unfavourable eclipsed arrangement is eliminated and a practically syn-diaxial arrangement of $14\alpha\text{-H}$ and $16\alpha\text{-H}$ is developed. The H-H interaction of a syn-diaxial arrangement contributes to the high chemical shift of the C(14) atom in estradiol (49.8 ppm). According to Beierbeck et al. [4] elimination of an H-H interaction results in an upfield shift of the carbon atoms concerned. Consequently, 47.5 ppm and 47.7 ppm were found for C(14) in estriol and $16\alpha\text{-fluoroestradiol}$ [2].

The above-mentioned distortion of the ring D is energetically very advantageous although now the bonds of the atoms C(16) and C(17) form an eclipsed arrangement. Thus, substituents at C(16) are almost similarly directed to C(13) (see Table 1, nos.7 and 9). As γ_{anti} substituents they should have the same influence on C(13). The γ_{anti} effects of all the substituents measured at C(16) [2,5] were indeed of the same low level.

References

- [1] Römer J., Steinbach J. and Kasch H. (1995) Synthesis of 16- ^{18}F fluoroestradiol, *Annual Report 1995*, Institute of Bioinorganic and Radiopharmaceutical Chemistry, FZR-122, p.22.
- [2] Römer J. and Scheller D. (1995) ^{13}C NMR spectroscopic characterization of estra-1,3,5(10)-triene-3,17 β -diol and 3,16,17-triols, and some of their 3-O-methoxymethyl and 16 α -fluoro derivatives, *Annual Report 1995*, Institute of Bioinorganic and Radiopharmaceutical Chemistry, FZR-122, p.27.
- [3] Kalinowski H.-O., Berger S. und Braun S. (1984) ^{13}C -NMR-Spektroskopie, Georg-Thieme-Verlag Stuttgart, p. 520.
- [4] Beierbeck H., Saunders J. K. and ApSimon J. W. (1977) The semiempirical derivation of ^{13}C NMR chemical shifts. Hydrocarbons, alcohols, amines, ketones, and olefines, *Can. J. Chem.* **55**, 2813.
- [5] Engelhardt G., Zeigan D. und Schönecker, B. (1979) Substituenteneffekte an 16-mono- und 16,17-disubstituierten 3-Methoxy-estra-1,3,5(10)-trienen, *Org. Magn. Reson.* **12**, 628.

49. Improvements of the Rossendorf Radionuclide Transport System

St. Preusche, F. Füchtner, H. Krug¹, J. Steinbach

¹ Scientific Dept. "Experimental Facilities and Information Technology"

Introduction

The 500 m long Radionuclide Transport System (RATS) was designed to transport small volumes of the irradiated liquids ^{18}O H₂O/ ^{18}F F⁻ and H₂O/ ^{15}N NH₃ with a pneumatic post system and the radioactive gases within capillaries from the cyclotron to the radiochemistry laboratories due to special local features ([1], [2]).

Improvements of the gas transport system and the loading unit of the pneumatic post system concerning safe activity transport, higher reliability and higher specific activity have been carried out and are summarized in the present paper.

Gas Transport System: Peak Cutting by an Activity Dependent Control

Our ^{11}C target contains 20 ml of (N₂ + 5 % H₂) target gas at a pressure of (26 - 28) bars. During the unloading process after target irradiation the inactive gas which remains inside the 500 m long copper capillary (ca. 900 cm³) arrives at first at the hot cell 1 of the radiochemistry laboratory. In order to ensure high specific activity, this dead volume must not pass through the ^{11}C CO₂ trap and the ^{11}C HCN module. Inside the hot cell 1 an activity detector is mounted at the incoming capillary (comp. Fig. 1) near the distribution unit.

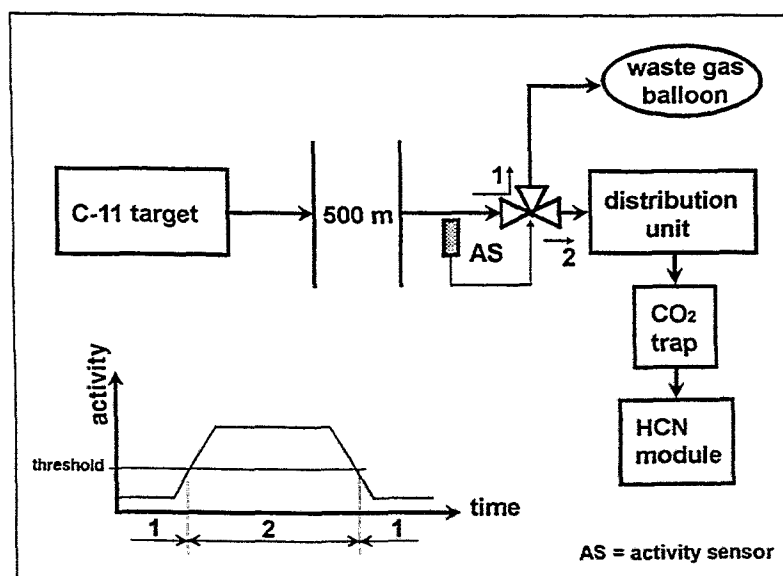


Fig. 1: Principle of ^{11}C transport

The detector controls a 3-way valve that is normally open to a waste gas balloon. If the measured activity is higher than a predicted value, the valve switches to the CO₂ trap and the HCN module and the radiochemical processes can be started. With (26 -28) bars of push gas we reach a transfer time of 4:30 minutes (EOB to BOS).

Pneumatic Post System: LASER Sensor for Improved Reliability

A LASER sensor mounted in the loading unit of the pneumatic post box detects the following failures and stops the loading process immediately if:

- there is no vial within the pneumatic post box
- there is no pneumatic post box inside the loading unit
- the lid of the filled pneumatic post box is not in the right position.

The LASER sensor prevents the unloading of an activated water target without the vial as the primary containment for the activity. Furthermore, it is not possible to transport the pneumatic post box with a not fully closed lid.

In all cases of failure the "AUTOMATIC MODE" of operation of the loading process will be stopped and switched to "MANUAL MODE". In this mode the operator can interrupt the process at any step and finish it step by step.

Pneumatic Post System: Pneumatic Post Box Running Time Measurement

For a safe activity transport the running time of the pneumatic post box within the polyethylene tube is measured and displayed both on the MASTER and the SLAVE terminal in the cyclotron building and the radiochemistry building. If the running time exceeds the predicted value of 200 s there is a message to the operator on the screens. The entrance of the transportation tube is blocked and it is not possible to use the tube for the next run. In that case we can use the second transportation tube.

For safety purposes there are special procedures for localizing the faulty pneumatic post box inside the tube and for removing it outwards.

References

- [1] Preusche, St. et. al., The new cyclotron of the Rossendorf PET Center, in "Cyclotrons and Their Applications", World Scientific Publishing C. Pte. Ltd., 1996
- [2] Preusche, St. et al., The Radionuclide Transport System of the Rossendorf PET Center, Poster at the XXX European Cyclotron Progress Meeting (ECPM), Catania, Italy, 04-06 Sept. 1996

50. Cerebral MRGlu and Perfusion Pattern of Patients with Myotonic Dystrophy

B. Beuthien-Baumann¹, B. Kunath², J. Pinkert¹, U. Reuner², H. Linemann¹, M. Obert, E. Will, F. Füchtner, J. Steinbach, B. Johannsen, W.-G. Franke¹.

¹Clinic of Nuclear Medicine, University Hospital Dresden, ²Clinic of Neurology, University Hospital Dresden

Introduction

Myotonic dystrophy (MD) is a multisystemic disease with autosomal dominant inheritance. The abnormal gene for this disorder has been localized on chromosome 19. It is the second most common inherited degenerative myopathy with a prevalence of between 1:10 000 and 2.4 - 5.5 per 100 000 [1]. Apart from muscular atrophy, myotonia and cataract, patients often suffer from an increased tendency to sleep and intellectual impairment of various degrees. Brain abnormalities such as white-matter lesions on magnetic resonance images [2] and decreased cerebral glucose utilization on positron emission tomographic (PET) scans [3] have been described.

The aim of this investigation was to address the question whether the anticipated impaired glucose utilization is reflected in an altered cerebral perfusion pattern.

Materials and Methods

Patients: 11 patients (8 female, 3 male), age 27 - 57 years (median 41 years) with genetically confirmed hereditary MD were investigated with Positron Emission Tomography (PET) and Single Photon Emission Tomography (SPECT). One female patient had a history of brain infarction 4 years previously, all other patients had no concomitant brain disease. None of the patients suffered from diabetes or abnormal fasting glucose levels.

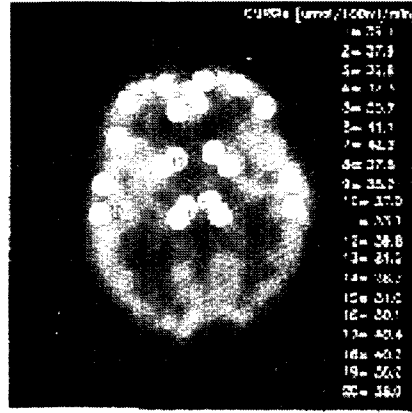
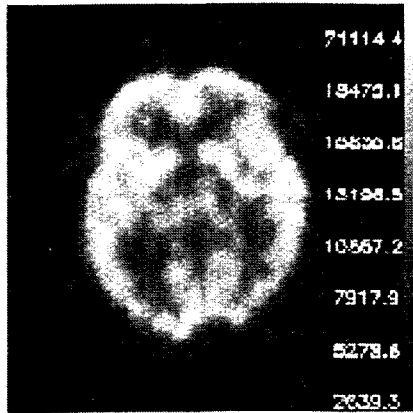
PET: The PET investigation to evaluate the metabolic rate of glucose consumption (MRGlu) was performed after an overnight fast. PET scans were performed on a two-ring, three-slice Positron Tomograph (Thompson, Montreal Neurological Institute [4]) with an image resolution of 10.9 mm (FWHM) and an axial resolution of 15.9 mm (FWHM). The distance between the slices was 18 mm. The patient's heads were positioned in a headholder with a laserlight, transaxial slices parallel to the orbitomeatal line (OM-line). One intravenous line was placed in each forearm, one for injection of the [¹⁸F]FDG, one to determine the blood glucose level and the [¹⁸F]FDG content of the blood during the study. After intravenous injection of 185 MBq [¹⁸F]FDG, pseudoarterial blood samples were withdrawn from the contralateral hand, which was heated by a heatcushion. To check for true pseudoarterial sampling, the oxygen saturation of the blood was measured prior to the start of the study. The oxygen saturation of the blood sample exceeded 80 %. Scans were performed for 75 min post injection (p.i.). The first set of slices was obtained during the first 60 min p.i. in the first position. To obtain a closer spacing between slices, a second set of slices, interleaving with the first set, was obtained 60 - 75 min p.i.. The cerebral metabolic rate of glucose in $\mu\text{mol}/100\text{ml}/\text{min}$ was calculated according to Sokoloff [5].

SPECT: The SPECT studies to evaluate the cerebral perfusion pattern were performed on a triple head gamma camera (Multi-SPECT 3, SIEMENS) equipped with fan beam collimators, starting 10 min after i.v. injection of 750 MBq [^{99m}Tc]HMPAO (CERETEC, Amersham). Images were obtained on a 128 x 128 matrix, 90 angles, 50 s per angle. After filtered backprojection, transaxial slices were reoriented parallel to the OM-line.

Quantification of regional glucose utilization and analysis of perfusion pattern was performed on two transaxial slices of each the PET and SPECT data sets. Level 1 included basal ganglia and thalamus (Figs. 1 + 3), the second level was placed approx. 3 cm above level 1 (Figs. 2 + 4).

On PET slices circular regions of interest (ROI) were placed on representative cortical and subcortical structures like frontal, temporal and parietal cortex, basal ganglia, thalamus and white matter (Figs. 1+2). Results were expressed in $\mu\text{mol}/100\text{ml}/\text{min}$.

On SPECT slices a semiautomated software for sector analysis, generating 12 regions per slice, was used (Figs. 3 + 4). The results were expressed in average counts per sector.



L

Fig. 1: PET transaxial slice level 1

R

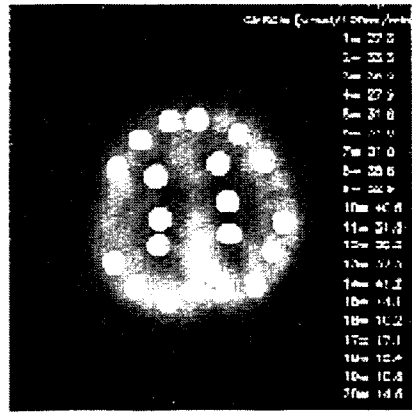
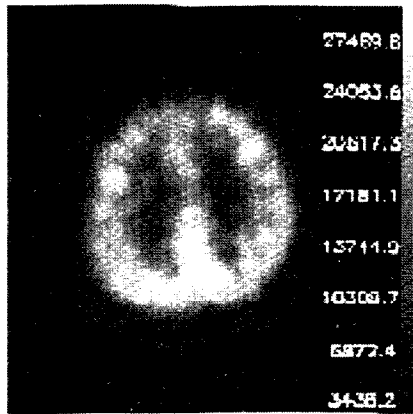
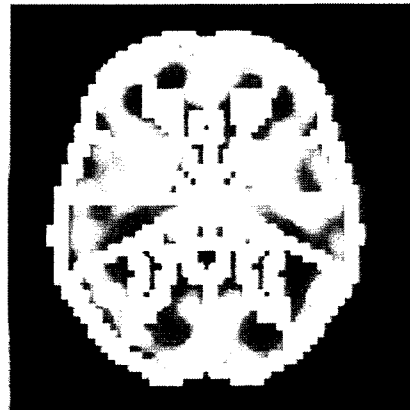
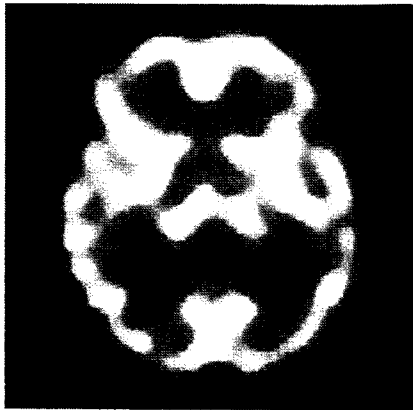


Fig. 2: PET transaxial slice level 2



R

Fig. 3: SPECT transaxial slice level 1

L

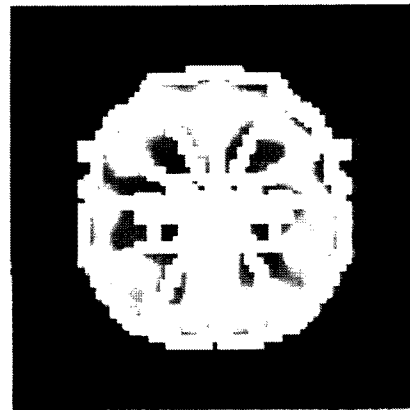
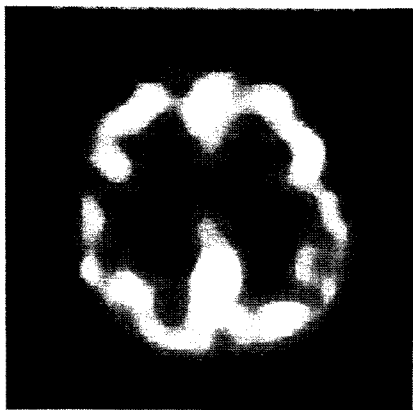


Fig. 4: SPECT transaxial slice level 2

Results and Discussion

9/11 patients showed no left to right asymmetry in PET. There was no gross regional deviation of MRGlu in different grey matter structures within the individual patient. Grey and white matter values revealed a broad range of MRGlu values (18-42 $\mu\text{mol}/100\text{ml}/\text{min}$ and 8-17 $\mu\text{mol}/100\text{ml}/\text{min}$) within

Table 1: Distribution of mean grey matter values

Grey matter $\mu\text{mol}/100 \text{ ml}/ \text{min}$	No. of patients
> 29 (29 - 42)*	4
26 - 28	3
23 - 25	3
18	1

Table 2: Distribution of mean white matter values

White matter $\mu\text{mol}/100 \text{ ml}/ \text{min}$	No. of patients
> 14 (14 - 17)	2
10 - 13	7
<10	2

this patient group (Table 1 + 2). Although all patients investigated suffered from genetically proved hereditary MD, 4/11 patients showed no reduced global MRGlu values. White matter values are to be regarded with caution, since they might include ventricular structures. When the MRGlu was impaired, no singular structure but the MRGlu of the whole brain seemed to be altered in most patients. Our PET results are in agreement with other publications, which describe a reduced MRGlu in patients with MD (3,7). In addition to a globally reduced MRGlu, Mielke *et al.* [7] found a marked decline in MRGlu in distinct cerebral structures, like frontal cortex and nucleus lentiformis, which was not noted in our patient group.

10/11 patients showed no left to right asymmetry in SPECT. There was no statistically significant regional deviation of average counts between sectors within the individual patient, therefore we found no evidence of local perfusion disturbances due to MD. Perfusion patterns were investigated by Chang *et al.* [8], who investigated the cerebral perfusion with ^{133}Xe and [$^{99\text{m}}\text{Tc}$]HMPAO-SPECT with SPECT. With ^{133}Xe , they found globally reduced cerebral blood flow (CBF) values with the lowest values in both temporal regions and, to a lesser extent, in the frontal region. With [$^{99\text{m}}\text{Tc}$]HMPAO, they found a different perfusion pattern with hypoperfusion in the temporoparietal, frontal or frontoparietal regions. Since we were not able to compare our patient group with a group of match normal controls, slight differences of the perfusion pattern within the group could have been missed. Normal values of MRGlu had to be taken from the literature. Nevertheless, the broad range of MRGlu values indicates that patients with hereditary MD are not a homogeneous entity concerning cerebral glucose consumption. In our study altered MRGlu values were not accompanied by an altered perfusion pattern in SPECT. The further correlation of our results with the intelligence score and hypersomnia as well as a comparison with clinically manifest, nonhereditary MD will be investigated.

References

- [1] Koch M. D., Grimm T., Harley H. G. and Harper P. S. (1991) Genetic risk for children of women with myotonic dystrophy. *Am J Hum Genet.* **48**, 1084 - 1091.
- [2] Glantz R. H., Wright R. B., Huckman M. S., Garron D. C. and Sigel I. M. (1988) Central nervous system magnetic resonance imaging findings in myotonic dystrophy. *Arch. Neurol.* **45**, 36 - 37.
- [3] Fiorelli M., Duboc D., Mazoyer B. M., Blin J., Eymard B., Fardeau M. and Samson Y. (1992) Decreased cerebral glucose utilization in myotonic dystrophy. *Neurology* **42**, 91 - 94.
- [4] Thompson C. J., Dagher A., Meyer E. and Evans A. C. (1986) Imaging performance of a dynamic positron emission tomograph: positome IIIp. *IEEE Trans Med Imag;MI-5* No.4:183.
- [5] Wienhard K., Wagner R. and Heiss W.-D. (1989) PET Grundlagen und Anwendungen der Positronen-Emissions-Tomographie. *Springer-Verlag Berlin Heidelberg New York* pp. 33 - 39.
- [6] Wang G. J., Volkow N. D., Wolf A. P., Brodie J. D. and Hitzemann R. J. (1994) Intersubject variability of brain glucose metabolic measurements in young normal males. *J. Nucl. Med.* **35**, 1457 - 1466.
- [7] Mielke R., Herholz K., Fink G., Ritter D. and Heiss W.-D. (1993) Positron emission tomography in myotonic dystrophy. *Psychiatry Research: Neuroimaging* **50**, 93 - 99.
- [8] Chang L., Anderson T., Migneco A., Boone K., Mehringer C. M., Villanueva-Meyer J., Berman N. and Mena I. (1993) *Arch. Neurol.* **50**, 917 - 923.

51. Three-Compartment Model Software Tools to Analyse and Synthesize PET Data

M. Obert, H. Linemann, E. Will

Introduction

The aim of this article is to give a short comprehensive summary of the kinetic equations which are defined by three-compartment models, since these models serve as the basic key in the interpretation of data obtained by positron emission tomography, PET. Furthermore, we present some results obtained by a computer simulation program, which analytically calculates time activity curves of such models. The simulation program was developed to facilitate the study of the highly complex interaction of up to twenty different parameters that affect the time activity curves. An understanding of such curves is fundamental to the understanding of PET.

We have written, implemented and tested some basic software programs for analysis of the data obtained with both our PET scanners. The aim was to develop software that is capable of describing the tracers that we use at the moment at the Forschungszentrum Rossendorf, which are [^{18}F]fluorodeoxyglucose, FDG, and 6- ^{18}F fluoro-DOPA, FDOPA. Such a description is basically possible with the aid of a three-compartment model [1, 2]: a three-compartment model is a simplified attempt to describe the biochemical behaviour of a radiotracer in the human body so that a mathematical estimation of kinetic parameters, k_i , is possible, see Fig. 1.

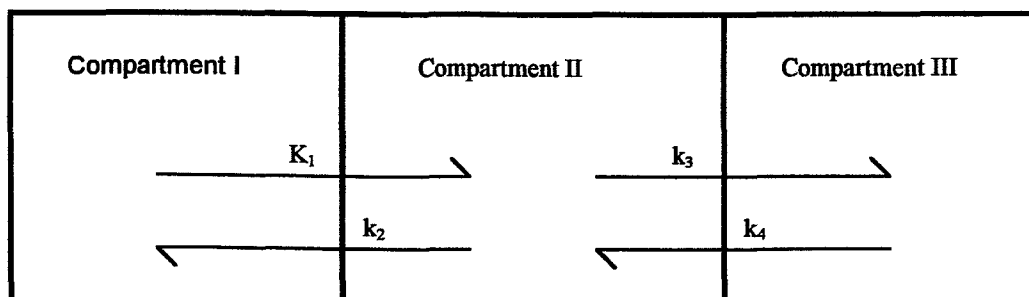


Fig.. 1: Compartment I is the vessel system, compartment II is the exchangeable tracer pool, and compartment III is a trapped tracer pool.

By definition, a compartment is a volume, real or kinetic, in which the concentration of a tracer or its derivatives remains the same everywhere [2]. In the case of FDG investigations we assume a k_4 of 0, which is due to the trapping of the tracer in the cell. For FDOPA investigations the model is a rough simplification of processes that are more complicated [1].

In addition we wanted to write a computer program that allows us to simulate the data of a PET investigation. This program enables us to study the complicated interaction of many parameters in a PET experiment in a numerically well-defined manner.

Data analysis

There are different levels of mathematical descriptions, established by various authors, to approximate a three-compartment model:

The Sokoloff approximation [3] allows determination of the turnover rate of the glucose metabolism, MRGL, for FDG investigations. It is often called the autoradiographic approach. It is based first on a single radioactivity measurement of a slice of interest with the PET scanner at a certain time, $C_{\text{PET}}(T)$, second on the determination of the blood glucose concentration, C_{Glucose} , and third on the dynamic measurement of the radioactivity of the blood plasma, $C_{\text{Plasma}}(T)$. The rate constants K_1 , k_2 , and k_3 , which are needed in the calculation of MRGL, must be known from other experiments. MRGL is defined as follows, Eq. (1), where LC is the Lumped constant, which eliminates the differences between FDG and glucose:

$$MRGI = \frac{C_{Glucose} \left[C_{PET}(T) - K_1 e^{-(k_2+k_3)T} \int_0^T C_{Plasma}(t) e^{(k_2+k_3)t} dt \right]}{LC \left[\int_0^T C_{Plasma}(t) dt - e^{-(k_2+k_3)T} \int_0^T C_{Plasma}(t) e^{(k_2+k_3)t} dt \right]} \quad (1).$$

All the following approaches to the three-compartment model are defined to approximate the rate constants K_i , or the term $K_1 k_3 / (k_2 + k_3)$ rather than MRGL.

Thus, it is possible to obtain MRGL for FDG investigations by the following relation, Eq. (2):

$$MRGI = \frac{C_{Glucose}}{LC} \frac{K_1 k_3}{k_2 + k_3} \quad (2).$$

The next approach defines the term $K_1 k_3 / (k_2 + k_3)$ as the slope of the plot $C_{PET}(T) / C_{Plasma}(T)$ versus $\int_0^T C_{Plasma}(t) dt / C_{Plasma}(T)$. It is often called Patlak plot [4, 5], Eq. (3).

$$\frac{C_{PET}(T)}{C_{Plasma}(T)} = \frac{K_1 k_3}{k_2 + k_3} \frac{\int_0^T C_{Plasma}(t) dt}{C_{Plasma}(T)} + \frac{K_1 k_2}{(k_2 + k_3)^2} \quad (3).$$

The approach defined by Blomqvist [6] allows an approximation of K_1 , k_2 , and k_3 , see Eq. (4). It is assumed that k_4 is equal to 0.

$$C_{PET}(T) = K_1 \int_0^T C_{Plasma}(t) dt + K_1 k_3 \int_0^T \int_0^t C_{Plasma}(u) du dt - (k_2 + k_3) \int_0^T C_{PET}(t) dt \quad (4).$$

We now express K_1 , k_2 , and k_3 of Eq. (4) in terms of parameters p_i , where the i goes from 0 to 2:

$$C_{PET}(T) = p_0 \int_0^T C_{Plasma}(t) dt + p_1 \int_0^T \int_0^t C_{Plasma}(u) du dt - p_2 \int_0^T C_{PET}(t) dt$$

In the Blomqvist approximation, we calculate the different integrals for different time intervals, T_i , and determine the coefficients p_i with the aid of multilinear regression [7] of an equation of the form $y = p_0 x_0 + p_1 x_1 + p_2 x_2$. We obtain the rate constants from $K_1 = p_0$, $k_2 = p_2 - p_1 / p_0$, and $k_3 = p_1 / p_0$.

Another setup by Evans [8] enables us to calculate the rate constants K_1 , k_2 , k_3 , and also k_4 , see Eq. (5).

$$C_{PET}(T) = K_1 (k_3 + k_4) \int_0^T \int_0^t C_{Plasma}(u) du dt - (k_2 + k_3 + k_4) \int_0^T C_{PET}(t) dt - k_2 k_4 \int_0^T \int_0^t C_{PET}(u) du dt + K_1 \int_0^T C_{Plasma}(t) dt \quad (5).$$

We now express K_1 , k_2 , k_3 , and k_4 of Eq. (5) in terms of the parameters p_i , where i goes from 0 to 3:

$$C_{PET}(T) = p_0 \int_0^T \int_0^t C_{Plasma}(u) du dt - p_1 \int_0^T C_{PET}(t) dt - p_2 \int_0^T \int_0^t C_{PET}(u) du dt + p_3 \int_0^T C_{Plasma}(t) dt$$

We determine the different integrals and double integrals for different time intervals, T_i , and calculate the p_i by multilinear regression [7]. Next, we describe the rate constants by the following relations:

$$K_1 = p_3$$

$$k_2 = p_1 - p_0 / p_3$$

$$k_3 = p_1 - (p_1 - p_0 / p_3) - p_2 / (p_1 - p_0 / p_3)$$

$$k_4 = p_2 / (p_1 - p_0 / p_3)$$

An attempt to describe the three-compartment model, which is most straightforward from a mathematical point of view, is given e.g. by Herholz [9]. The nonlinear approach is described in Eq. (6). This attempt also takes care of the fraction of blood, V_{Blood} , that is measured by the PET scanner within the slice of interest.

$$C_{PET}(T) = p_0 C_{Plasma}(T) + p_1 e^{-p_2 T} \int_0^T C_{Plasma}(t) e^{p_2 t} dt + p_3 e^{-p_4 T} \int_0^T C_{Plasma}(t) e^{p_4 t} dt \quad (6).$$

The different p_i are

$$\begin{aligned} p_0 &= V_{\text{Blood}}, \\ p_1 &= \frac{1}{2} K_1 ((k_2 - k_3 - k_4) / \sqrt{\beta} + 1), \\ p_2 &= \frac{1}{2} (k_2 + k_3 + k_4 + \sqrt{\beta}), \\ p_3 &= \frac{1}{2} K_1 ((-k_2 + k_3 + k_4) / \sqrt{\beta} + 1), \\ p_4 &= \frac{1}{2} (k_2 + k_3 + k_4 - \sqrt{\beta}), \text{ where} \\ \beta &= (k_2 + k_3 + k_4)^2 - 4k_2 k_4. \end{aligned}$$

In order to be able to calculate a nonlinear regression [7] we have to determine the derivatives with respect to the different p_i of Eq. (6). The partial derivatives are:

$$\begin{aligned} \frac{\partial}{\partial p_0} C_{PET}(T) &= C_{Plasma}(T), \\ \frac{\partial}{\partial p_1} C_{PET}(T) &= e^{-p_2 T} \int_0^T C_{Plasma}(t) e^{p_2 t} dt, \\ \frac{\partial}{\partial p_2} C_{PET}(T) &= \frac{p_1}{p_2} e^{-p_2 T} \int_0^T p_2 \cdot (t - T) \cdot C_{Plasma}(t) e^{p_2 t} dt, \\ \frac{\partial}{\partial p_3} C_{PET}(T) &= e^{-p_4 T} \int_0^T C_{Plasma}(t) e^{p_4 t} dt, \text{ and} \\ \frac{\partial}{\partial p_4} C_{PET}(T) &= \frac{p_3}{p_4} e^{-p_4 T} \int_0^T p_4 \cdot (t - T) \cdot C_{Plasma}(t) e^{p_4 t} dt. \end{aligned}$$

As initialization we now guess the parameters p_i and then calculate the nonlinear regression. The rate constants can be obtained from the different p_i as follows:

$$\begin{aligned} K_1 &= p_1 + p_3, \\ k_2 &= \frac{p_1(p_2 - p_4)}{p_1 + p_3} + p_4, \end{aligned}$$

$$k_3 = 2p_2 - \left(\frac{p_2 p_4 (p_1 + p_3)}{p_1 (p_2 - p_4) + p_4 (p_1 + p_3)} + (p_2 - p_4) \right) - \frac{p_1 (p_2 - p_4)}{p_1 + p_3} - p_4, \text{ and}$$

$$k_4 = \frac{p_2 p_4 (p_1 + p_3)}{p_1 (p_2 - p_4) + p_4 (p_1 + p_3)}.$$

For a detailed description of the various approximations of the compartment model and their constraints, see the given references.

The approaches given in Eq. (3) to (6) are implemented in IDL programs. Eq. (6) is the base for the nonlinear regression of a curve $C_{PET}(T)$. The program version realized so far has to be further modified in order to improve the robustness of the fit for practical applications.

We used the Patlak plot to calculate the metabolic rates of glucose of all patients investigated so far with the Positome IIIp scanner.

Data Simulation

The motivation for the simulation program is as follows: it enables us to study many questions that arise in a model which is affected by at least 20 different parameters. How reliable are the different mathematical approximations of the three-compartment model? How does the curve $C_{Plasma}(T)$ influence the curve $C_{PET}(T)$? How many data points have to be taken at the beginning of the function $C_{Plasma}(T)$?

We have therefore written a computer program that allows us to simulate a vector $C_{PET}(T)$ for arbitrary values of V_{Blood} , K_1 , k_2 , k_3 , and k_4 according to Eq. (6). There are three different options of how to generate a vector $C_{Plasma}(T)$, which must be known in Eq. (6) to be able to calculate the plasma integrals with the aid of numerical integration methods: First, experimental values of a plasma curve may be taken. Second, arbitrary values may be used. Third, we define a plasma curve, $C_{Plasma}(T)$, as follows, Eq. (7):

$$C_{Plasma}(t) = A(e^{-k_{out}t} - e^{-k_{in}t}) \quad (7).$$

In Eq. (7) A is a concentration, k_{out} , and k_{in} are rate constants. Eq. (7) allows us to simulate a function with a strong initial increase and then a more or less fast decrease. This is possible for a large range of properly chosen values of A , k_{out} and k_{in} , where $A > 0$, and $k_{in} > k_{out}$.

Further, the simulation program has an option to vary the time schedule so that the user may determine at what time t and how often a value of C_{Plasma} and C_{PET} is "measured" by Eqs. (6) and (7). This allows us to study the influence of a certain time schedule and the frequency of measurements on the estimation of V_{Blood} and the rate constants [10].

In addition, it is possible to put some "scattering" on either of the functions $C_{Plasma}(T)$ and / or $C_{PET}(T)$. This enables us to study the influence of error sources on our data.

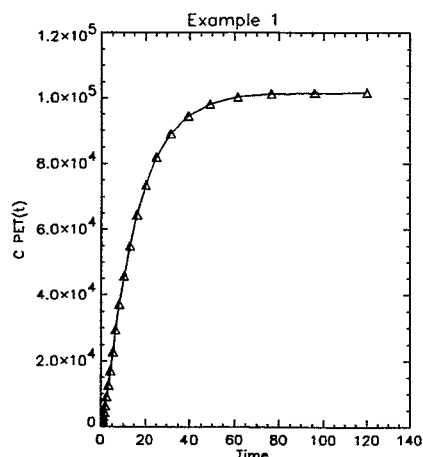
The units of the parameters in the simulation program are as follows: Plasma curve: A [concentration], k_{out} [1 / time unit], and k_{in} [1 / time unit]. PET-Curve: V_{Blood} [volume unit / weight unit of tissue], K_1 [volume unit / weight unit of tissue / time unit], k_2 [1 / time unit], k_3 [1 / time unit], and k_4 [1 / time unit].

A detailed description of the user friendly widget program, which is written in the computer language IDL, is given in ref. [11]. The reader who wants to develop a "numerical feeling" for Eqs. (3) to (7) is forced to work with this program package [11]: There are 14 parameters that can be modified in the simulation program. The analysis that follows Eq. (3) is affected by 3 parameters, the approximations given by Eqs. (4) and (5) are affected by 1 parameter, whereas 8 parameters must be properly chosen to enable a description of the data according to Eq. (6). The approximations by Eqs. (3) to (6) are called "Patlak plot", "Blomqvist analysis", "Evans analysis", and "nonlinear regression". We will now mention a few examples obtained with the aid of the simulation and analysis programs:

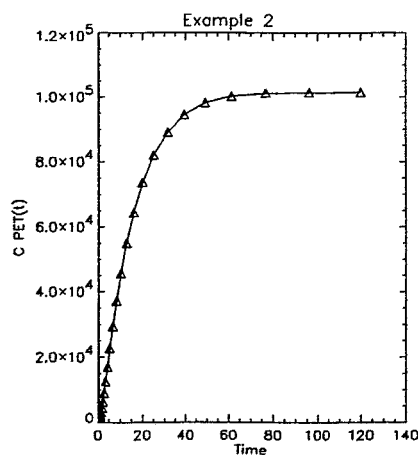
Results of the autoradiographic approach are not shown. A linear dependency exists between the measured value of the radioactivity and MRGL for a given function $C_{Plasma}(T)$ and $C_{Glucose}$, see Eq. (1). We therefore consider this approach as rather easy to understand.

We often find differences between the analytical term $K_1 k_3 / (k_2 + k_3)$ and the result obtained by the Patlak plot of this term that are in the range of $\pm 3.0\%$. This is sufficiently small.

Ex. 1 and 2 show the fit of a simulated PET curve, $C_{PET}(T)$, by the Blomqvist and the Evans analysis. The PET curve is simulated with the following parameter settings: $V_{Blood} = 0$, $K_1 = 0.0500$, $k_2 = 0.0400$, $k_3 = 0.0300$, and $k_4 = 0$.



Blomqvist Analysis:
 $K_1 = 0.0500$ $K_2 = 0.0400$ $K_3 = 0.0301$
 Chi-Square = 1.0000



Evans Analysis:
 $K_1 = 0.0500$ $K_2 = 0.0401$ $K_3 = 0.0302$ $K_4 = 0.0000$
 Chi-Square = 0.9997

The graphs in Ex. 1 and 2 show the simulated data as triangles and the fit result as solid line, the units are arbitrary. The sampling of the curve $C_{Plasma}(T)$ is identical to the sampling of the curve $C_{PET}(T)$. The fit results are given under each graph.

We find that both fit attempts in Ex. 1 and 2 lead to the expected results.

Acknowledgments

We thank B. Beuthien-Baumann and J. van den Hoff for their helpful suggestions during the program development.

References

- [1] Gjedde A. and Wong D. F. (1990) Modeling neuroreceptor binding of radioligands in vivo. In: Quantitative Imaging: Neuroreceptors, Neurotransmitters, and Enzymes, eds. J. J. Frost, H. N. Wagner, jr., Raven Press, New York, pp. 51 - 79.
- [2] Sheppard C. W. (1947) The theory of the study of transfers within a multi-compartment system using isotopic tracers. *J. Applied Physics* **19**, 70 - 76.
- [3] Sokoloff L. (1984) Modeling metabolic processes in the brain in vivo. *Annals of Neurology* **15**, S1 - S11.
- [4] Patlak C. S., Blasberg R. G. and Fenstermacher J. D. (1983) Graphical evaluation of blood-to-brain transfer constants from multiple-time uptake data. *J. Cerebr. Blood Flow and Metab.* **3**, 1 - 7.
- [5] Peters A. M. (1994) Graphical analysis of dynamic data: The Patlak-Ruthland plot. *Nucl. Med. Comm.* **15**, 669 - 672.
- [6] Blomqvist G. (1984) On the construction of functional maps in positron emission tomography. *J. Cerebr. Blood Flow and Metab.* **4**, 629 - 632.
- [7] Bevington P. R. (1969) Data reduction and error analysis for the physical sciences, McGraw-Hill, New York,.
- [8] Evans A. C. (1987) A double integral form of the three-compartmental, four-rate-constant model for faster generation of parameter maps. *J. Cerebr. Blood Flow and Metab.* **7**, S453

- [9] Herholz K. and Patlak C. S. (1987) The influence of tissue heterogeneity on results of fitting nonlinear model equations to regional tracer uptake curves with an application to compartmental models used in positron emission tomography. *J. Cerebr. Blood Flow and Metab.* 7, 214 - 229.
- [10] Feng D., Wang X. and Yan H. (1994) A computer simulation study on the input function sampling schedules in tracer kinetic modeling with positron emission tomography (PET). *Computer Methods and Programs in Biomedicine* 45, 175 - 186.
- [11] Obert M. (1996) Some PET fit programs - user information. *Manual*, Forschungszentrum Rossendorf, available upon request.

52. Application of the Fractal Concept of the Analysis of Positron Emission Tomography Investigations of Patients Suffering from Dystrophia Myotonia

M. Obert, B. Beuthien-Baumann, E. Will, H. Linemann, B. Kunath

Introduction

We earlier showed the possibility of describing a positron emission tomography (PET) image with the aid of the concept of fractal geometry [1 - 4]. Now we study the question whether it is possible to distinguish different grades of altered cerebral glucose metabolism in dystrophia myotonia, DM, [5] of 7 patients by this fractal concept. To do this, we investigated the numerical values defined either as global fractal dimension, D_g , or the distributions of the local fractal dimensions, D_l , or the multifractal description by the function $D(q)$. We analysed dynamic 3-dimensional brain images of [^{18}F]2-fluoro-2-deoxy-D-glucose investigations that were taken by the low resolution Positome IIIp PET scanner. The different grades of the disease ranged from slight muscle symptoms up to severe movement disabilities. The cerebral glucose metabolism ranged from normal rate values to a strong decrease in the overall cerebral metabolic rates. Thus, all different fractal investigations show identical results that vary only within the standard deviation of the numerical methods for all different grades of DM. We therefore conclude that these numerical fractal tools are without clinical relevance for the diagnosis or characterization of DM.

Methods

The protocol of the PET investigation is given in ref. [5]. See ref. [1] for a description of the PET scanner. The numerical method to determine the global fractal dimension, D_g , which is a measure of the global irregularity of a structure, is given in refs. [1, 4]. The way to calculate the local fractal dimension, D_l , which is a map of local dimension values, is shown in ref. [6]. The multifractal analysis, which describes the heterogeneity of a system by a function $D(q)$, is carried out as shown in refs. [7, 8].

Results

Table 1 shows the D_g values of the radioactivity distributions of 3 different representative transaxial sections through the brain. The cerebellar slice is positioned through the mid-cerebellum and the basal temporal lobes; the basal ganglia slice is drawn at the level of the basal ganglia and the thalamus; the cingulum slice shows the basal cingulum. We analysed the radioactivity measured by the PET scanner as a function of the spatial position of the 2-dimensional images. We assume a standard deviation of the D_g values of ± 0.05 , which is known from other experiments [6].

Table 1. D_g values of different sections of the brain

	Cerebellum	Basal Ganglia	Cingulum
Patients with severe symptoms:	2.02	2.27	2.05
	2.04	2.23	2.11
	2.01	2.24	2.03
	-	2.29	2.15
	-	2.25	2.16
weak symptoms:	2.06	2.22	2.11
	-	2.28	2.12

The results of Table 1 indicate different D_0 values for different sections: an average of 2.03 is found for the section that shows the cerebellum, whereas averages of 2.25 and 2.10 are found for the basal ganglia and for the cingular slice. No differences can be found between patients with normal or altered metabolic glucose rates.

Fig. 1 shows a map of D_i values for 9 different transaxial sections through a brain. The calculations of D_i were carried out on an affine 4-dimensional data set (position x , y , z , and radioactivity). It is not possible to find any correlation between the anatomical structure of the brain and the distribution of D_i . Furthermore, no differences in the structure of the different slices are visible. All positions in the brain that have a high D_i value are surrounded by small D_i s and vice versa. This leads to a granulated distribution of the D_i values in the brain, Fig. 1. The values of D_i are shown on the right margin of Fig. 1. No differences of such maps, Fig. 1, are visible among different patients.

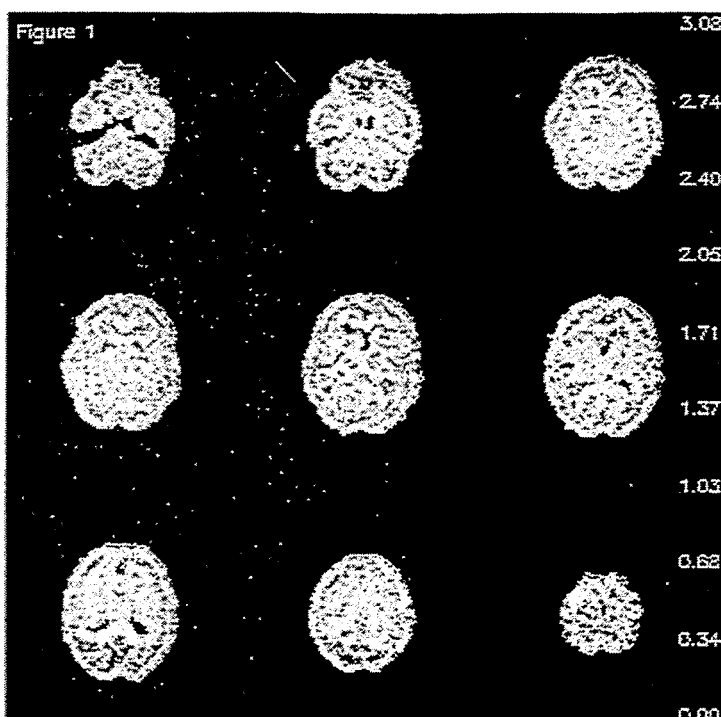


Fig. 1: Map of D_i values for 9 different transaxial brain sections.

The curves $D(q)$ versus q (not shown) are identical, within the standard deviations, for all patients regardless of the metabolic rate in DM.

Discussion

The application of the concept of fractal geometry is not fruitful if one wishes to describe differences between grades of DM.

The spatial resolution of the Positome IIIp PET scanner [1] is probably not sufficient to allow a reasonable investigation of fractal properties of these brain sets.

It remains to be explored whether this geometrical concept is able to describe the behaviour of receptor distributions in the brain and differences thereof between patients that suffer from other diseases.

References

- [1] Obert M., Bergmann R., Linemann H. and Brust P. (1995) Analysis of an image of the human brain obtained by positron emission tomography in terms of fractal geometry. *Fractal 95 - 3rd IFIP Conference on Fractals*, Chapman & Hall, London.

- [2] Obert M., Bergmann R., Linemann H. and Brust P. (1995) Analysis of an image of the human brain obtained by positron emission tomography in terms of fractal geometry. *Fractal 95 - 3rd International Working Conference*, Marseille.
- [3] Obert M., Brust P., Linemann H., Bergmann R. and Jestczemski F. (1994) Investigation of the distribution of a radiotracer in a human brain - a multifractal analysis of a positron emission tomography image. *International Workshop on Nonlinear Dynamics, Fractality, and Self-organization of Complex Systems*, Würzburg,.
- [4] Pfeifer P. and Obert M. (1989) *Fractals: Basic Concepts and Terminology*. D. Avnir (ed), *The Fractal Approach to Heterogeneous Chemistry: Surfaces, Colloids, Polymers*, Wiley, Chichester.
- [5] Beuthien-Baumann B. (1996) *Private communication*.
- [6] Obert M. (1993) Numerical estimates of the fractal dimension D and the lacunarity L by the mass radius relation. *Fractals 1*, 711.
- [7] Tel T. (1988) Fractals, multifractals and thermodynamics. *Z. Naturforsch.* **43a**, 1154.
- [8] Tel T., Fülöp A. and Vicsek T. (1989) Determination of fractal dimension for geometrical multifractals. *Physica A* **159**, 155.

II. PUBLICATIONS LECTURES AND TEACHING ACTIVITIES

PUBLICATIONS

Ahlemeyer B., Matys S., Brust P. (1996)

The effect of conditioned medium of porcine astrocytes and different cell lines on the activity of the marker enzymes ALP and γ -GT in endothelial cells of porcine brain microvessels.

In: *Biology and Physiology of the Blood-Brain Barrier: Transport, Cellular Interactions, and Brain Pathologies* (Couraud, P.O. and Scherman D., eds)

Plenum Adv. Exp. Med. Biol. **33**, 227-231.

Brust P., Bergmann R., Johannsen B. (1996)

High-affinity binding of [³H]paroxetine to caudate nucleus and microvessels from porcine brain. *NeuroReport* **7**, 1405-1408.

Brust P., Matys S., Wober J., Friedrich A., Bergmann R., Ahlemeyer B. (1996)

Blood-brain barrier properties *in vitro* as related to the neurotransmitter serotonin.

In: *Biology and Physiology of the Blood-Brain Barrier: Transport, Cellular Interactions, and Brain Pathologies* (Couraud, P.O. and Scherman D., eds)

Plenum Adv. Exp. Med. Biol. **33**, 107-113.

Fietz T., Spies H., Leibnitz P., Scheller D. (1996)

Mixed-ligand oxorhenium(V) complexes with rhenium-selenium bonds. Molecular structure of (3-oxapentane-1,5-dithiolato)(benzeneselenolato)oxorhenium(V).

J. Coord. Chem. **38**, 227-235.

Füchtner F., Steinbach J., Mäding P., Johannsen B. (1996)

Basic hydrolysis of 2-[¹⁸F]fluoro-1,3,4,6-tetra-O-acetyl-D-glucose in the preparation of 2-[¹⁸F]fluoro-2-deoxy-D-glucose.

Appl. Radiat. Isot. **47**, 61-66.

Hoepfing A., Spies H., Johannsen B. (1996)

Retropane - a new rhenium complex as a potential ligand of the dopamine transporter.

Bio. Med. Chem. Lett. **6**, 2871-2874.

Johannsen B., Scheunemann M., Spies H., Brust P., Wober J., Syhre R., Pietzsch H.-J. (1996)

Technetium(V) and rhenium(V) complexes for 5-HT_{2A} serotonin receptor binding: structure-affinity considerations.

Nucl. Med. Biol. **23**, 429-438.

Johannsen B., Spies H. (1996)

Chemistry of technetium(V) as relevant to nuclear medicine.

Topics Curr.Chem. **176**, 77-121.

Noll B., Knieß T., Friebe M., Spies H., Johannsen B. (1996)

Rhenium(V) gluconate, a suitable precursor for the preparation of rhenium(V) complexes.

Isotopes Environ. Health Stud. **32**, 21-29.

Preusche St., Steinbach J., Füchtner F., Krug H., De Leenheer M., Ghyoot M. (1996)

The new cyclotron of the Rossendorf PET center.

in: *Cyclotrons and their Applications* pp. 575-578.

Römer J., Steinbach J., Kasch H. (1996)

Studies on the synthesis of 16 α -[¹⁸F]fluoroestradiol.

Appl. Radiat. Isot. **47**, 395-399.

Schomäcker K., Wellner U., Scheidhauer K., Gabruk-Szostak B., Fischer T., Steinbach J., Füchtner F., Schicha H. (1996)

Zusammenhänge zwischen Eigenschaften von ¹³¹I-Therapiekapseln und der Radioiodkinetik.

Nuklearmedizin **35**, 175-180.

Uhlirova H., Matucha M., Kretzschmar M., Bubner M. (1996)
Aufnahme und Verteilung von Trichloressigsäure in Trieben Norwegischer Fichte.
Z. Umweltchem. Ökotox. **8**, 138-142.

Wüst F., Spies H., Johannsen B. (1996)
Synthesis of "3+1" mixed-ligand oxorhenium(V) complexes containing modified 3,17 β -estradiol.
Bio. Med. Chem. Lett. **6**, 2729-2734.

ABSTRACTS

Ahlemeyer B., Brust P., Syhre R., Matys S., Wober J., Pietzsch H.-J., Johannsen B. (1996)
Transport von Rezeptoraffinen $^{99m/99}\text{Tc}$ -Komplexen, ^{99m}Tc -HMPAO und ^{99m}Tc -Sestamibi durch
Himendothelzellkulturen als *in vitro* Modell der Blut-Hirn-Schranke.
Neuroforum **2** (Supplement), 130.

Bergmann R., Roux F., Drewes L.R., Brust P., Johannsen B. (1996)
Expression spezifischer Transporter der Blut-Hirn-Schranke.
Neuroforum **2** (Supplement), 130.

Beuthien-Baumann B., Kunath B., Pinkert J., Reuner U., Linemann H., Johannsen B.,
Franke W.-G. (1996)
FDG and HMPAO in myotonia dystrophica (MD).
Ann. Nucl. Med. **10**, S162.

Beuthien-Baumann B., Kunath B., Pinkert J., Reuner U., Linemann H., Obert M., Will E., Steinbach
J., Johannsen B., Franke W.-G. (1996)
Cerebral MRGluc and perfusion pattern of patients with myotonia dystrophica (MD).
Eur. J. Nucl. Med. **23**, 1197.

Brust P., Bauer R., Bergmann R., Walter B., Steinbach J., Füchtner F., Will E., Linnemann H., Obert
M., Johannsen B. (1996)
Measurement of the cerebral uptake and metabolism of L-6- ^{18}F Fluoro-3,4-dihydroxyphenylalanine
(^{18}F DOPA) in newborn piglets.
J. Neurochem. **66** (Suppl. 2) S69.

Brust P., Syhre R., Ahlemeyer B., Pietzsch H.-J., Scheunemann M., Schenker Ch., Spies H.,
Johannsen B. (1996)
Zum Transport von Rezeptoraffinen [$^{99m/99}\text{Tc}$]Oxotechnetium(V)-Komplexen durch die Blut-Hirn-
Schranke *in vivo* und *in vitro*.
Nucl.-Med. **35**, A38.

Füchtner F., Steinbach J., Mäding P., Johannsen B. (1996)
Basische Hydrolyse bei der Herstellung von [^{18}F]Fluor-2-Desoxy-D-Glucose ([^{18}F]FDG)
Nucl.-Med. **35**, A26.

Jankowski R., Noll B., Spies H., Johannsen B. (1996)
XAS investigations on Tc and Re complexes of oligoglycine ligands and Tc tartrate
HASYLAB-Jahresbericht 1996, im Druck.

Johannsen B. (1996)
Entwicklungen in der Technetium- und Rhenium-Chemie für die Nuklearmedizin
Nucl.-Med. **35**, A8.

Johannsen B., Pietzsch H.-J., Scheunemann M., Berger R., Spies H., Syhre R., Schenker Ch.,
Brust P. (1996)
Structural modification of serotonin receptor binding technetium and rhenium complexes in order to
improve receptor selectivity and blood-brain transfer.
J. Nucl. Med. **37**, 16P-17P.

Johannsen B., Pietzsch H.-J., Scheunemann M., Berger R., Spies H., Syhre R., Schenker Ch., Brust P. (1996)
Structural-affinity considerations for serotonin binding technetium and rhenium complexes.
Eur. J. Nucl. Med. **23**, 1140.

Johannsen B., Seifert S., Spies H., Syhre R. (1996)
Die enzymatische Hydrolyse koordinierter Estergruppen in Technetiumverbindungen.
Nucl.-Med. **35**, A99.

Kampf G., Franke W.-G., Knop G., Wunderlich G., Brust P., Johannsen B. (1996)
Studies on tumour cell-targeting with radiometals.
Eur. J. Nucl. Med. **23**, S24.

Kretzschmar M., Brust P., Syhre R., Wober J., Pietzsch H.-J., Scheunemann M., Spies H., Noll B., Noll S., Johannsen B. (1996)
Bindung von Oxorhenium (V)- und Oxotechnetium (V)- Komplexen an Serotonin (5-HT₂) Rezeptoren: Radioluminografische Untersuchungen am Rattenhirn.
Neuroforum **2** (Supplement), 229.

Mädig P., Steinbach J., Zessin J., Chebani K., Füchtner F., Johannsen B. (1996)
Möglichkeiten der ¹¹C-Kernmarkierung von Aromaten und Heteroaromaten
Nucl.-Med. **35**, A26.

Schenker Ch., Brust P., Johannsen B. (1996)
Ist der Serotonintransporter in den Transfer von rezeptorbindenden ^{99m}Tc-markierten Radiotraceren einbezogen?
Neuroforum **2** (Supplement), 133.

Wober J., Brust P., Johannsen B. (1996)
Untersuchungen zu Serotoninrezeptor-Subtypen an der Blut-Hirn- und der Blut-Liquor-Schranke mittels Ligand-Bindungsassays.
Neuroforum **2** (Supplement), 133.

LECTURES

Ahlemeyer B.
Die Nutzung von cerebralen Endothelzellen als *in vitro*-Modell der Blut-Hirn-Schranke für die Nuklearmedizin.
Symposium: "Die Zellkultur in der nuklearmedizinischen Forschung", Dresden, 26.10.1996.

Ahlemeyer B., Brust P., Johannsen B.
Different response of cerebral and non cerebral endothelial cells to cytotoxic hypoxia.
6th Int. Symposium on Pharmacology of Cerebral Ischemia, Marburg, 22.-24.7.1996.

Ahlemeyer B., Brust P., Syhre R., Matys S., Wober J., Pietzsch H.J., Johannsen B.
Transport von rezeptoraffinen ^{99m/99}Tc-Komplexen, ^{99m}Tc-HMPAO und ^{99m}Tc-Sestamibi durch Hirnendothelzellkulturen als *in vitro*-Modell der Blut-Hirn-Schranke.
1. Tagung der Neurowissenschaftlichen Gesellschaft, Berlin 24.-27.2.1996.

Brust P.
Modulation der Permeabilität der Blut-Hirn-Schranke durch vasoaktive Substanzen.
Institut für Molekulare Pharmakologie Berlin, 25.4.1996.

Brust P.
Measurement of DOPA decarboxylase activity in the brain of pigs using ¹⁸F-DOPA and PET.
PET-Center Aarhus, Denmark, 16.12.1996.

Brust P., Bauer R., Bergmann R., Walter B., Steinbach J., Füchtner F., Will E., Linemann H., Obert M., Johannsen B.

Measurement of the cerebral uptake and metabolism of L-6-[¹⁸F]fluoro-3,4-dihydroxyphenylalanine (¹⁸F-DOPA) in newborn piglets.

Conference on Preclinical Pharmacological Studies with and for Radiopharmaceuticals, Orsay, France, 24.-25.10.1996.

Brust P., Syhre R., Ahlemeyer B., Pietzsch H.-J., Scheunemann M., Schenker Ch., Spies H., Johannsen B.

Zum Transport von rezeptoraffinen [^{99m/99}Tc]Oxotechnetium(V)-Komplexen durch die Blut-Hirn-Schranke *in vivo* und *in vitro*.

DGN Jahrestagung, Münster, 17.-20.4.1996.

Füchtner F., Steinbach J., Mäding P., Johannsen B.

Basische Hydrolyse bei der Herstellung von [¹⁸F]Fluor-2-Desoxy-D-Glucose ([¹⁸F]FDG)

DGN Jahrestagung, Münster, 17.-20.4.1996

Hoepping A., Spies H., Johannsen B.

Rheniumkomplexe von Estern des Tropanols als potentielle Liganden für den Dopamintransporter.

4. Arbeitstagung AG Radiochemie/Radiopharmazie, Brielow, 18.10.1996.

Jankowsky R.

EXAFS measurements on Tc and Re peptides.

Eur. Nucl. Med. Congress. COST B3 workshop on development of new radiotracers and methods of quality assurance for nuclear medical application, Kopenhagen, Denmark, 16.9.1996.

Jankowsky R., Kirsch S., Noll B., Spies H., Johannsen B., Reich T., Dennecke M. A., Moll H., Bernhard G., Nitsche H.

Structural investigations of rhenium complexes by EXAFS

HASYLAB Nutzertreffen „Forschung mit Synchrotronstrahlung“, Hamburg, 6.1.1996.

Johannsen B.*

Entwicklungen in der Technetium- und Rheniumchemie für die Nuklearmedizin.

34. Intern. Jahrestagung Ges. für Nuklearmedizin, Münster, 17.-20.4.1996.

Johannsen B.*

Anwendungen kurzlebiger Isotope als Radiopharmaka. Gegenwärtiger Stand und Ausblick.

5. Arbeitstagung der IIS, Regionalgruppe Zentraleuropa, Bad Soden, 13.-14.6.1996.

Johannsen B.*

„Funktionalisierte“ Technetium(V)-Verbindungen.

Paul Scherrer Institut, Villingen, Schweiz, 27.6.1996.

Johannsen B.*

Technetium in der modernen Nuklearmedizin: Design von Tc(V)-Komplexen mit In-vivo-Reaktivität

Anorg. Institut, Universität Zürich, Schweiz, 28.6.1996

Johannsen B.*

Technetium in der modernen Nuklearmedizin: Design von in vivo reaktiven Tracern.

Institut für Interdisziplinäre Isotopenforschung, Leipzig, 4.12.1996

Johannsen B., Seifert S., Spies H., Syhre R.

Die enzymatische Hydrolyse koordinierter Estergruppen in Technetiumverbindungen

DGN Jahrestagung, Münster, 17.-20.4.1996.

Johannsen B., Pietzsch H.-J., Scheunemann M., Berger R., Spies H., Syhre R., Schenker Ch., Brust P.

Structure-affinity considerations for serotonin receptor binding technetium and rhenium complexes.

European Nuclear Medicine Congress 1996, Copenhagen, Denmark, 14.-18.9.1996.

Johannsen B., Pietzsch H.-J., Scheunemann M., Berger R., Spies H., Syhre R., Schenker Ch., Brust P.

Structural modification of serotonin receptor binding technetium and rhenium complexes in order to improve receptor selectivity and blood-brain transfer.

43rd Annual Meeting of the Society of Nuclear Medicine, Denver, Colorado, USA, 3.-5.6.1996.

Kretzschmar M.

New results: Radioluminography of technetium-labelled radiopharmaca in the brain.

Workshop: Radioluminography in Whole Body Radiography, Düsseldorf, 9.-10.6.1996.

Kretzschmar M., Brust P., Syhre R., Wober J., Pietzsch H.-J., Scheunemann M., Spies H., Noll B., Noll St., Johannsen B.

Bindung von Oxorhenium(V)- und Oxotechnetium(V)-Komplexen an Serotonin (5-HT₂) Rezeptoren: Radioluminografische Untersuchungen an Rattenhirnschnitten.

1. Kongreß der Neurowiss. Gesellschaft, Berlin, 24.-27.2.1996.

Mädig P., Steinbach J., Zessin J., Chebani K., Füchtner F., Johannsen B.

Möglichkeiten der ¹¹C-Kernmarkierung von Aromaten und Heteroaromaten

DGN Jahrestagung, Münster, 17.-20.4.1996

Pietzsch H.-J., Scheunemann M., Spies H., Brust P., Wober J., Johannsen B.

Potential receptor-binding technetium tracers: structure-affinity considerations for 5-HT₂ serotonin receptor binding technetium and rhenium complexes

31st International Conference on Coordination Chemistry, Vancouver, Canada, 18.-23.8.1996.

Preusche St., Steinbach J., Füchtner F., Krug H., Neumann W.

The radionuclide transport system of the Rossendorf PET Center

European Cyclotron Conference, Catania, Italy, 4.-6.9.1996

Römer J.

Synthese von 16-[¹⁸F]Fluorestradiol

5. Arbeitstagung der Regionalgruppe Europa der International Isotope Society, Bad Soden/Taunus, 13.-14.6.1996

Scheunemann M., Pietzsch H.-J., Brust P., Spies H., Berger R., Kretzschmar M., Seifert S., Syhre R., Wober J., Johannsen B.

Structural modification of serotonin receptor-binding technetium and rhenium complexes: influence on receptor selectivity and blood-brain transfer.

14. Symp. on Medicinal Chemistry, Maastricht, The Netherlands, 8.-12.9.1996.

Spies H., Berger R., Syhre R., Friebe M., Papadopoulos M., Chiotellis S., Johannsen B.

Lipophilicity and brain uptake of neutral technetium complexes with pendant amine groups

COST B3 Conference, Orsay, France, 24.-25.10.1996.

Wüst F., Spies H., Johannsen B.

Oxorhenium(V)-Komplexe mit funktionalisiertem 3,17β-Estradiol

4. Arbeitstagung AG Radiochemie/Radiopharmazie, Brielow, 17.-19.10.1996.

Zessin J., Steinbach J., Johannsen B.

Neue Aspekte zur Synthese von [¹¹C]McN 5652-z, einem Tracer zur Darstellung des Serotonin-transporters

4. Arbeitstagung AG Radiochemie/Radiopharmazie, Brielow, 17.-19.10.1996.

* invited lecture

TEACHING ACTIVITIES

Summer term 1996

B. Johannsen:

One-term course on **Metals in Biosystems**.

Introduction into Bioinorganic Chemistry, including aspects of medicine, nutrition and ecology.

Winter term 1996/1997

B. Johannsen:

Radiopharmaceutical Chemistry

Special readings and seminars on selected biochemical and radiopharmaceutical topics.
(for PhD students)

Postgraduate Education:

B. Johannsen:

Proposal on postgradual Education in Radiopharmaceutical Chemistry/ Radiopharmacy at the European School of Nuclear Medicine

B. Ahlemeyer

Guest lectures on physiology and pharmacology at the Philipps University Marburg, Faculty of Pharmacy.

PhD THESES

Matthias Glaser:

Tripodal-tetradentat/monodentat koordinierte Rheniumkomplexe mit Tris(2-thiolatoethyl)amin.
Dresden University of Technology, February 1996
Shaker Verlag Aachen 1996

Thomas Fietz:

Oxorhenium(V)-Komplexe mit „3+1“-Gemischtligandkoordination.
Dresden University of Technology, April 1996

Mohamad Khaled Chebani:

Synthese von ¹¹C-ringmarkiertem Pyridin und seiner Derivate.
Dresden University of Technology, October 1996

III. SCIENTIFIC COOPERATION

COOPERATIVE RELATIONS AND JOINT PROJECTS

In multidisciplinary research such as carried out by this Institute, collaboration, the sharing of advanced equipment, and above all, exchanges of ideas and information obviously play an important role. Effective collaboration has been established with colleagues at universities, in research centres and hospitals.

The *Technische Universität Dresden* (Dr. Scheller, Inst. of Analytical Chemistry) plays an essential part in SPECT tracer research by performing analytical characterization of new tracers and providing support with the synthesis of organic compounds (Dr. Habicher, Inst. of Organic Chemistry), as well as in biochemical research (Dr. Fischer, Dr. Kaspar, Institute of Pathology).

Common objects of radiopharmacological and medical research link the Institute with the *Universitätsklinikum "Carl Gustav Carus"*, above all with its Departments of Nuclear Medicine (Prof. Franke). A joint team of staff members from both the Institute and the Clinic of Nuclear Medicine are currently working at the Rossendorf PET Center.

Very effective cooperation also exists with the *Bundesanstalt für Materialforschung Berlin* (Dr. Reck, Mr. Leibnitz) who have carried out X-ray crystal structure analysis of new technetium and rhenium complexes.

Our long-standing cooperation with the *University of Padua* (Prof. Mazzi) and the "*Demokritos*" *National Research Centre for Physical Sciences* in Athens (Dr. Chiotellis) has been continued. The fruitful contacts to the *Paul Scherrer Institut*, Villigen, Switzerland, are very appreciated. The cooperation is part of the EU research programme COST-B3 with the working group on "New chelating systems for Tc and Re for medical application" (chaired by Dr. Spies, Rossendorf).

Cooperation on a special topic concerning bioinorganic chemistry is in progress with the *Arzneimittelwerk Dresden* (Dr. Unverferth).

Identification of common objects in PET radiopharmacy has led to collaborative research with the *Humboldt-Universität Berlin* and the *Universität Leipzig*.

In the field of PET tracers, cooperation exists with the *Montreal Neurological Institute* (Prof. Thompson), the *Turku Medical PET Centre* (Dr. Solin), and the *Hans-Knöll-Institut Jena* (Prof. Hinnen, Dr. Kasch). A fruitful cooperation in radiopharmaceutical application has been established with the *Private Institute of Radiology and Nuclear Medicine Wünsche MD, Neumann MD, Wehr MD*, Leipzig.

Cooperation on the biochemical aspects of radiotracer research exists with the *PET Centre Aarhus* (Prof. A. Gjedde), the *University of Minnesota* in Duluth (Prof. L.R. Drewes, Department of Biochemistry and Molecular Biology) and the *Friedrich-Schiller Universität Jena* (Dr. Bauer, Inst. of Pathophysiology).

In helpful discussions both abroad and at Rossendorf numerous colleagues have contributed to defining areas of cooperation and shaping projects.

Special thanks go to Dr. E. Chiotellis, National Research Centre, Athens, Greece, Dr. L. M. Dinkelborg, Schering AG Berlin, Dr. G. Ensing, Mallinckrodt Medical B. V., Petten, Netherlands, Dr. P.A. Schubiger, Paul-Scherrer-Institut, Villigen, Switzerland.

Within the scientific cooperation with the Arabic Republic Egypt, University of Assiut, Prof. R. M. Mahfouz started research on chemistry and radiopharmacology of technetium and rhenium.

LABORATORY VISITS

Brust P.
Kommune Hospital Aarhus, Denmark,
Dec. 9-21, 1996

Friebe M.
Institute of Radioisotopes and Radiodiagnostic Products of the National Center for Scientific
Research "Demokritos", Athens, Greece,
Sept. 14-28, 1996

Jankowski R.
Stanford Synchrotron Radiation Lab. at SLAC, Palo Alto, California, USA,
June 8-18, 1996

Jankowski R., Friebe M., Kirsch S.
HASYLAB at DESY, Hamburg, Germany,
July 29-Aug. 5, 1996 and Nov. 19-23, 1996

Johannsen B., Spies H.
Institute of Radioisotopes and Radiodiagnostic Products of the National Center for Scientific
Research "Demokritos", Athens, Greece,
Nov. 8-12, 1996

Johannsen B.
PSI Villigen, Switzerland,
June 27-29, 1996

Lehnert S.
Institut für Bioanalytik, Göttingen, Germany,
Dec. 15-17, 1996

Preusche S.
Herz- und Diabeteszentrum NRW, Bad Oeynhausen, Germany,
May 7-9 and Nov. 5-8, 1996

M. Reisgys
PSI Villigen, Switzerland,
Jan. 8-March 18, 1996

GUESTS

Dr. R. Alberto, PSI Villigen, Switzerland,
Nov. 4-7, 1996

Prof. R. M. Mahfouz, Assiut University, Dept. of Chemistry, Assiut, Egypt,
April 30-July 20, 1996

Dr. Th. Meina, Institute of Radioisotopes and Radiodiagnostic Products of the National Center for
Scientific Research "Demokritos", Athens, Greece,
Oct. 12-Nov. 3, 1996

Dr. B. Nock, Institute of Radioisotopes and Radiodiagnostic Products of the National Center for
Scientific Research "Demokritos", Athens, Greece,
Oct. 12-Nov. 3, 1996

R. Schibli, PSI Villigen, Switzerland,
March 10-29, 1996

MEETINGS ORGANIZED

1. Symposium on "Blood-Brain Barrier - Structure and Function" within the First Congress of the German Neuroscientific Soc., Berlin 24.-27.2.1996.
2. First International Workshop of the CYCLONE 18/9 User Community, Rossendorf, 10.-11.10.1996.
3. First IAEA Research Co-ordination Meeting of the Co-ordinated Research Programme on "Development of Agents for imaging Central Neural System Receptors based on Technetium-99m", Rossendorf, 4.- 7.11.1996.

OTHER ACTIVITIES

1. H. Spies:
Coordinator of Working Group 5 in the COST B3 program "New radiotracers and methods of quality assurance for nuclear medical application." (Coordinator: P. A. Schubiger)
2. B. Johannsen:
Chairman of the DGN Working Group on Radiochemistry and Radiopharmacy.
3. B. Johannsen:
Co-editor of the journal Nuclear Medicine and Biology.

IV. SEMINARS

TALKS OF VISITORS

Prof. A. Gjedde, Universität Aarhus, Dänemark
Dopaminergic neurotransmission with emphasis on regulation of neuronal excitability in the striatum
15. 03. 1996

Prof. G. Seidel, Wuppertal
Pharmaindustrie - Quo vadis?
21. 03. 1996

Dr. F. Oberdorfer, DKFZ Heidelberg
Neue Methoden zur Halogenierung und Radiohalogenierung von Hexopyranosen
12. 04. 1996

Prof. Dr. H. Schelbert, Universität Los Angeles, USA
PET in der Kardiologie
15. 04. 1996

Prof. W. Vaalburg, PET-Center Universitäts-Hospital Groningen, Niederlande
The Development, Evaluation and Clinical Application of PET-Radiopharmaceuticals
15. 05. 1996

Prof. W. Görner, BAM Berlin
Die Aktivierungsanalyse - ein Verfahren mit hohem dynamischen Bereich (Zentrumskolloquium)
21. 06. 1996

Frau Dr. A. B. Fischer, Hygiene-Institut, Universität Gießen
Chelatbildnertestung in vitro mit Säugerzellkulturen
30. 07. 1996

Prof. Dr. U. Hahn, Institut für Biochemie, Universität Leipzig
Protein Design
26. 09. 1996

Prof. Dr. C. Anderson, Washington University, Medical Center, St. Louis, USA
Copper-64-labeled Proteins and Peptides for PET Imaging and Therapy
09. 10. 1996

Dr. P. Elz, Institut für Pharmazie, FU Berlin
Ketanserin-analoge 5-HT_{2A}-Rezeptorliganden: Synthese, Pharmakologie und Struktur-Wirkungs-Bez.
25. 10. 1996

Dr. J. Kropp, Universitätsklinikum Dresden
Markierung und erste pharmakologische Untersuchungen von IQNP
14. 11. 1996

Prof. R. Beckert, Friedrich-Schiller-Universität Jena
Stickstoff- und schwefelhaltige Chelatkomplexbildner aus einfachen C₂-Bausteinen
22. 11. 1996

Prof. Cervos-Navarro, Institut für Neuropathologie der FU Berlin
Das Gehirn unter den Bedingungen einer chronischen Hypoxie
6. 12. 1996

Dr. Th. Arnold, AWD Dresden
Kombinatorische Chemie
12. 12. 1996

V. ACKNOWLEDGEMENTS

ACKNOWLEDGEMENTS FOR FINANCIAL AND MATERIAL SUPPORT

The Institute is part of the Research Center Rossendorf Inc., which is financed by the Federal Republic of Germany and the Free State of Saxony on a fifty-fifty basis.

Three research projects concerning technetium tracer design and PET radiochemistry were supported by the Deutsche Forschungsgemeinschaft (DFG):

- Development and characterization of mixed-ligand complexes of technetium and rhenium with multidentate chelating agents
Sp 401/2-4 (H. Spies)
- Technetium complexes with thioether ligands
Pi 255/1-1 (H.-J. Pietzsch)
- PET with steroids
Ste 601/3-2 (J. Steinbach)

One project was supported by commission of the European Communities:

- New chelating systems for technetium and rhenium for nuclear medical application
COST B3, working group 5
In collaboration with Greece, Italy and Switzerland

In addition, the Free State of Saxony provided support for a project covering the establishment of cell cultures:

- Characterization of transport of radiopharmaceuticals through the blood-brain barrier using a cultured cell model
7541.82-FZR/309 (P. Brust)

The Free State of Saxony and the Free State of Thuringia support PET studies on DOPA metabolism in brain. (P. Brust)

Supported by the "LIST" programme of the Free State of Saxonia studies on new ^{18}F -labelled tracers were started in cooperation with TU Dresden and Hans Knöll Institut, Jena. (Prof. W.-G. Franke)

Two projects were supported by cooperation with the pharmaceutical industry:

- Receptor-binding technetium tracers
Mallinckrodt Medical B.V.
- Cooperation in nuclear diagnostic
Schering AG Berlin

The project:

- Data processing
was supported by Siemens AG.